CRANFIELD INSTITUTE OF TECHNOLOGY

KHALAF HASSAN ALI

THE DESIGN AND PERFORMANCE OF GEAR PUMPS WITH PARTICULAR REFERENCE TO MARGINAL SUCTION CONDITION

SUPERVISOR:

Dr A M El-Zafrany

SCHOOL OF MECHANICAL ENGINEERING

TURBOMACHINERY AND ENGINEERING MECHANICS

Cranfield Institute of Technology
School of Mechanical Engineering

Ph.D Thesis

Academic Year 1988-89

KHALAF HASSAN ALI

THE DESIGN AND PERFORMANCE OF GEAR PUMPS WITH PARTICULAR REFERENCE TO MARGINAL SUCTION CONDITION

Supervisors:	Dr A M El-Zafrany
Internal Examiner:	Prof R L Elder
External Examiner:	Mr R A Heron
	BHRA

This Thesis is submitted in candidature for the Degree of Doctor of Philosophy.

December 1989

TO MY

PARENTS

ACKNOWLEDGEMENTS

The author is firstly, and mostly, indebted to the people of Iraq to whom education comes before all. The presence of the author, and many others like him, here in the UK and around the world, even in these troubled times, proves this point beyond doubt.

The author wishes to express his gratitude and thanks to Dr. Ali El-Zafrany for his valuable advice and unlimited help, without whom the present work could never have been realised. The author also wishes to express a special thankyou to Prof. Robin Elder, Head of the Department of Turbomachinery and Engineering Mechanics, with particular reference to his involvement during the final stages of this work.

The author is truly grateful to Mr. A.G. Salisbury for his guidance and valuable advice during the early stages of this work.

The author wishes to thank the staff and his colleagues in the Department of Turbomachinery and Engineering Mechanics, particularly Dr. Roy Bannister, Mr. Brian Reason, Mr. Brian Moffitt, Chris Evans, Mrs. E. Clark and S.Y. Kasim, who have provided valuable assistance and support. Thanks are also due to Mr. Brian Melon of Commercial Hydraulic Company of Bedford for the supply of some test parts and his co-operation.

I would like to express my appreciation to my wife for her encouragement and patience and to my children Noor and Zaid for giving up their father whilst he was studying and preparing the text of this thesis.

Finally, my thanks to Mrs. Howes who, with great patience, converted my handwritting into this neatly typed report.

SUMMARY

In this thesis an investigation for the identification, measurement and modelling of the gear pump performance under marginal suction condition, created in the suction line and resulting in cavitation at the suction port and cavitation erosion on the delivery side plate is introduced. A new technique for the detection of cavitation in gear pumps has been employed and proved to be more efficient and less expensive than other techniques available. The experimental study has been carried out by monitoring the pressure ripple at the pump inlet and outlet, as well as investigating the pressure distribution around the gear rotor under cavitating and non-cavitating conditions. It was found that the gear pump cavitation appeared in three distinct stages, these being cavitation-inception, discrete-cavitation and continuous-cavitation. These stages of cavit tion were investigated by means of pressure distribution around the gear rotor using a miniature pressure transducer positioned at a gear fillet. The experimental results demonstrate a drop in 'filling efficiency' of the tooth space due to cavitation, which provides a further understanding of the pump performance characteristics at different inlet conditions. An expression for the definition of transient pressure in the tooth space due to trapped volume has been derived for the first time and proved to give a good correlation with published experimental work. A surface analysis technique has been employed in this work to study the behaviour of the material erosion due to cavitation bubble collapse, using a 'Talysurf 4' instrumentation system, and the results obtained are in good agreement with those published by NEL.

CONTENTS

CHAPTER THREE - GEAR PUMP CHARACTERISTICS - THEORY

CHAPTER SIX - TEST RIG DESIGN AND INSTRUMENTATION

CHAPTER SEVEN

CHAPTER ONE

INTRODUCTION

1.1 General Background

Trends towards higher working pressure, pump speed, and oil velocities, act significantly to raise the noise level emitted by modern hydraulic control systems. However, in recent years, such rises in noise levels are not welcomed by customers due to the growing awareness of the hazards of industrial noise.

It is quite common these days to select a pump on the basis of its low noise-generating potential rather than on a marginal price difference. This is mainly a consequence of the action undertaken by most nations, and in particular industrial countries, to set maximum limits on noise levels acceptable in industrial environments. It is also a reflection of the wide usage of hydraulics in fields where low noise levels are very important, such as aircraft hydraulic control systems, submarines, etc. Thus, it is more desirable that the cause of hydraulic system noise be eliminated wherever possible.

In a great majority of systems, pumps and valves are considered the main components responsible for system noise. The pump normally exhibits a continuous noise, not only because of its noise in its own right (due to the motion of its elements) but also because of its capability to induce vibration in the whole system, through its pulsating flow rate which excites the whole structure. Such noises are commonly known as "fluid-borne noise" (FBN), "structure-borne noise" (SBN) and "air-borne noise" (ABN). As its name implies, the FBN can be defined as the noise which takes the form of pressure fluctuations or "pressure ripple" in the fluid. Although it is not directly damaging, it is a major cause of SBN, and hence ABN. However, SBN takes the form of the mechanical vibration of the circuit components, such as pipes and frames (where the vibrations can be transmitted). On the other hand, ABN is known as the noise which is propagated through the air and detected by the ear.

FBN can be propagated within great distances along hydraulic pipes. For example, the hydraulic circuits employed in submarines can generate low frequency noise which can be transmitted to great distances through the ocean and detected by hostile surveillance systems.

Current work (see Chapter 2) suggests that fluid-borne noise is responsible for the major portion of the total noise level emitted by many hydraulic control systems.

In hydraulic systems, gear pumps tend not to produce an absolutely steady flow rate, but a mean flow rate, on which a flow ripple is superimposed. The magnitude of this flow ripple is dependent upon the gear parameters and operating conditions. They have a periodic waveform at a frequency equal to the number of teeth multiplied by the rotational speed.

A large amount of work has been undertaken in the past [1.1 - 1.9] in order to devise a means for evaluating a pump FBN rating which is a function of the pump performance only and not of the circuit in which the measurements are made. However, due to the complex pump-circuit interaction, it is extremely difficult to measure the source flow ripple of a pump [10]. Most of the research work carried out [1.1 - 1.10] on the FBN has not considered the pressure waveform generated in the trapped space, which leads to a marginal suction pressure and then cavitation. This phenomenon causes serious damage to the gear pump side plate (such as surface pitting) which results in component failure. Cavitation might take place when the pump operates at a high speed (i.e. higher than the speed allowed by the pump designer and at which the oil cannot follow the speed of the moving part at the pump inlet). Therefore a part of the tooth cavity will be filled with oil and the rest will be filled with a mixture of released air and oil vapour. The size of the filled cavity to the total tooth space is called the "filling efficiency". As a result, lower flowrates are experienced.

When the filling efficiency is less than unity, part of the tooth cavity is filled with either air or oil vapour and the rest of the tooth is filled with a dense oil. However, when these cavities are shifted from the suction side of the pump to the pump discharge side such cavities will start to collapse. As it does so, a high energy is

concentrated into a microjet penetrating onto the surface. Moreover, its behaviour (i.e. cavity collapse) is very complex and despite extensive research the process is not fully understood. The collapse will generate a very high pressure which can damage both the hydraulic components (such as the side plate or the casing) and the hydraulic fluid.

Several theoretical and experimental research investigations have been carried out on the above subject, as summarised in Chapter 2. Most of the theoretical studies of fluid-borne noise in hydraulic systems have considered the hydraulic pump as a black box, measuring its impedance experimentally, and employing its outlet flow as an input to a mathematical model for the FBN characteristics of the hydraulic circuits. However, there are many drawbacks in such research, the pressure ripple generated due to the trapped volume has been ignored, which can create noise and damage to the gear pump parts, the effect of cavitation on the performance and mechanical integrity of gear pump has not been discussed in detail and the reasons for its onset need to be outlined. Finally an investigation on the rate and extent of cavitation damage is also needed as a result of cavitation in the pump.

1.2 Objectives of the Current Work

The principal aim of this project is to advance the understanding of the behaviour of fluid-borne noise in a gear pump, under critical marginal conditions, created in the suction line, and thus resulting in cavitation at the inlet of the pump. A further aim is to study the trapped oil and the pressure waveform generated in the tooth space. This is to entail the development of mathematical and experimental investigation to validate the mathematical derivation. In this current work, cavitation erosion is also reported.

A special test rig is to be designed to study the gear pump performance as well as the pump's transient pressure distribution around its gear rotor, under both normal and cavitating flow conditions. Additional facilities to monitor the delivery and suction dynamic pressures, shaft speed, oil temperature, pump oil flow rate and shaft input power are to be included. In order to determine the

extent of the damage due to cavitation a surface analysis technique is to be employed by using a stylus-based profilometer incorporating an in-house developed software to produce 2-D and 3-D colour representations of the surfaces under consideration.

1.3 Scope of the Thesis

The thesis is mainly divided into eight Chapters. This Chapter serves as an introduction and reviews the subjects related to the thesis.

Chapter 2 presents a survey of relevant literature and a summary of its results, highlighting their relevance to the current work.

Chapter 3 contains the theory related to the Gear Pump Characteristics. The gear tip losses, pressure distribution around the rotor, suction capability and trapped fluid are examined. A derivation of an expression to calculate the pressure waveform in tooth space is also presented.

Chapter 4 contains details on the structure of the computer programs for the design and performance of the gear pump and their predictions.

In Chapter 5 the experimental techniques employed in the current work are described together with the possibilities and limitations of such methods.

Chapter 6 presents the test rig design components and the instrumentation used to support the experimental programme.

Chapter 7 presents the experimental results for correlation with the theoretical predictions. A discussion of this correlation is also presented.

Conclusions and suggestions as to how this research could be continued are presented in the final Chapter (Chapter 8).

REFERENCES

[1.1] YUDIN E.M. 'Gear Pumps: Principal Parameers and their Calculation'
(Translation from Russian)
Pub. Nat. Lending Library for Science and Technology, 1967.

[1.2] BEYER, R. 'Noise Reduction in Gear Pumps'
Proc. Fluid Power International Conf., 1964, London, pp119-126.

[1.3] COLLINS, J.F. 'The Inter-ralationship of Air-borne and Fluid-borne Noise in Hydraulic Systems'
Proc. 20th Nat. Conf. on Fluid Power, 1966, pp84-92.

[1.4] BOWNS, D.E., and McCANDLISH, D. 'Pressure Ripple Propagation'
I.Mech.E. Conf. - Quite Oil Hydraulic Systems, London, Nov. 1977.

[1.5] TILLEY, D.G., and BUTLER, M.D. 'The Generation and Transmission of Fluid Borne Pressure Ripple in Hydraulic Systems'
I.Mech.E. Seminar - Quieter Oil Hydraulics, London, October 1980.

[1.6] FOSTER, K., and HANNAN, D. 'Fundamental Fluidborne and Airborne Noise Generation of Axial Piston Pumps'
I.Mech.E. conference - Quiet Oil Hydraulic Systems, London, Nov. 1977.

[1.7] BIHENDI, I.M., FOSTER, K., and TAYLOR, R. 'Computer Predictions of Cyclic Excitation Sources for an External Gear Pump'
I.Mech.E. Seminar - Computer Aided Design in High Pressure Hydraulic Systems, London, Nov. 1983.

[1.8] KOJIMA, E., and SHINADA, M. 'Characeristics of Fluid Borne Noise Generated by Fluid Power Pump (3rd Report, Discharge Pressure Pulsation of External Gear Pump)' Bulletin of J.S.M.E., vol. 27, no. 232, Oct. 1984

[1.9] MOLTON, G.R. 'Techniques for Reducing Fluid Borne Noise from Gear Pumps and their Circuits' 7th Int. Fluid Power symposium, Bath, England, Sept. 1986.

[1.10] JOHNSTON, D.N. 'Measurement and Prediction of the Fluid Borne Noise Characteristics of Hydraulic Components and Systems' PhD Thesis, University of Bath, 1987.

CHAPTER 2

LITERATURE SURVEY

2.1 Introduction

One of the major sources of noise in hydraulic systems is the flow ripple from pumps, especially gear pumps. It is therefore advantageous to provide a review of noise in hydraulic systems in general in the first section of this Chapter.

In an attempt to study the performance of the gear pump under cavitation and non-cavitation conditions, as well as the effect of this phenomenon on the performance and operation of the pump, a survey for the evaluation of concepts and ideas presented in the technical literature and an assessment of some of these concepts are introduced in the remaining sections of this Chapter. Gear pump design and performance in the presence of critical inlet conditions are discussed in the second section, with the influence of cavitation on the performance and operation of the pump and the life of its component parts being covered in the third and final section.

2.2 Noise in Hydraulic Systems

Engineers have been concerned for many years with the design and operation of gear pumps. In recent times there has also been a growing community awareness of the harmful effects which may result from over-exposure to high levels of noise.

As early as 1926, David Brown Limited [2.1], published an article concerning an improved gear design for pumps, and gave a simple equation by which the flowrate might be estimated.

In 1934, Bakewell [2.2] predicted, "In the future, pressures of 1000 lb or more will be successfully handled by rotary pumps." At the present time (1989), pumps which operate at between three to eight times this pressure level are common.

In Figs. (2.1, 2.2) the development of aircraft hydraulics since 1930 is illustrated. Until the second world war airborne hydraulic systems operated at around 1000 psi and were only used for operating the retractable landing gear.

Several authors [2.3, 2.4] have pointed out that increasing the power-to-weight ratio of hydraulic pumps also significantly raises the noise level emitted.

Noise control has been greatly accelerated by recent legislation affecting industry and its products [2.5]. Many papers have been published which deal with locating and eliminating sources of noise in hydraulic control systems. Drasfield, Stecki and Wilkins, [2.3] have reviewed a large number of such papers and prepared a comprehensive tabulation of their conclusions.

Several authors [for example 2.6,2.7,2.8 and 2.9] deal with aspects of pump design which can reduce the noise level of axial piston pumps. There is, however, very little information available regarding techniques for designing quiet gear pumps.

The major source of noise in the hydraulic system is the flow-ripple from a pump which itself can be considered to consist of two superimposed components. The 'Kinematic' ripple is a function of the pump geometry and is independent of pressure. The 'dynamic' ripple is pressure dependent and is commonly associated with fluid compressibility, leakage and inertia. These fluctuations result in fluid borne noise which has a fundamental frequency equal to the 'pumping frequency' given as:

Fundamental frequency = Shaft frequency x No. of teeth.

Several authors have studied the noise level generated by flow-ripple for different elements of the hydraulic system. In 1964 Beyer [2.10] reported noise levels measured in the vicinity of a hydraulic gear pump, when operating at several pressures and speeds. Elliott et al [2.11], concluded from his survey and tests of seventeen hydraulic

pumps, under sixty-two different operating conditions, that a more sensitive parameter to be considered during studies of system noise, is the fluid-borne noise (pressure fluctuation) produced by the pump.

Willekens [2.12] presents a diagram (Fig. 2.3) showing an analysis of the major parameters affecting air-borne noise emitted by a hydraulic system. In this diagram it can be seen that fluid pressure level fluctuation may interact with the system's components, causing structural borne-noise which in turn can cause air-borne noise.

In 1966, Collins [2.13], simultaneously measured the frequency spectrum of the fluid-borne and air-borne noise generated by an axial-piston pump. McCandlish and Linney in 1975 [2.14], expanded this work to gear pumps and measured and compared the frequency spectrum of air-borne noise, pump casing vibration, and discharge pressure ripple generated by several pumps. The results of this study showed that there was a good correlation between the discrete frequencies at which peaks occur in each of these spectra. McCandlish and Linney also found that the discharge pressure has only a small influence on the noise level of the gear pump. More recently, Crook and Heron [2.15] found that the pipe material and bore size has some effect on the air-borne noise level generated by the system. Rigid tubes and nylon hose produce a quieter circuit, but increase in the bore size of the rigid tube tends to increase the air-borne noise level of the system.

An increase of the bore size of the nylon hose decreased the air-borne noise, over a range (from the noisiest to the quietest pipe) of between 1Ø to 15 dB. Brown, Edge and Tilley [2.16] attempted to discover a standard method for assessing the fluid-borne noise generated by positive displacement pumps. They employed a high impedance pipe line method in order to measure the acoustic pressure signals from different pumps. This method is attractive because of its simplicity and apparent accuracy.

An attempt was made by Brown, Edge and McCandlish [2.17] to modify the above method for high impedance pumps, but they discovered that the technique does not work for such devices. A new method was therefore adopted by these authors whereby it is possible to change the length of pipe easily. This method gave good correlation with theory.

In 1977, McCandlish, Edge and Tilley [2.18] proposed a new method in order to find the source impedance which is generally difficult to measure. They began by working from the system load impedance from which the source impedance can be found. Attempts to find an accurate method to predict the delivery pressure ripple of positive displacement pumps continue to be sought as a completely satisfactory solution to this important problem has yet to be defined.

The National Engineering Laboratories has, for many years, been involved in the analysis of standing waves (in pumping systems). Early work by Henderson [2.19] and Whiston [2.20], on the measurement and design of hydraulic silencers, employed the National Engineering Laboratories silencer test facility which can provide the varying conditions necessary to characterise the pump's acoustic properties. The planewave transmission line theory has been used successfully to define the propagation of pressure ripples in simple systems. Butler and Tilley [2.21] developed an analytical model which depends upon the plane-wave transmission line theory in order to assess the pressure ripple level in more complex circuits.

Lindsay [2.22] in 1981 examined the behaviour of the pressure fluctuations in the suction line for an external gear pump. It was found that the behaviour of the suction line has a significant effect on the overall air-borne noise produced by the system. It was also found that the pressure fluctuation in the pump suction line varied in an unpredictable manner because of air released from the hydraulic oil.

Additional work was undertaken by Edge and Freitas [2.23] 1981, and 1985 [2.24], who studied both experimentally and theoretically the effect of mean boost (by an external gear pump) pressure on the piston pump discharge conditions. It was found that two superimposed wave forms in the boosted line were evident.

For the hydraulic units used in this study, the wave form generated by the gear pump was found to be dominant but highly dependent on the mean boost pressure. This effect was almost entirely due to the variation in the relief valve impedance with the mean pressure, which

was found to be a major factor in determining the boost system pressure fluctuation level. The application of plane-wave propagation theory has been shown to be consistent with experimental measurements. Similarly, it has been found that the inlet flow to such a system is unsteady and creates a standing pressure wave in the inlet line in the same manner as is found in high pressure lines. The inlet flow becomes small and unstable as the mean pressure in the suction pipe is reduced as a result of air release from the oil. Hence, to produce a quiet hydraulic system it is necessary to run the pump with a low suction line pressure beyond the cavitation condition.

Much work has previously been undertaken [2.25,26,27] with the aim of devising a means of evaluating the two fundamental pump properties which are used to compare or predict the pulsation characteristics of a pump, namely, the source flow ripples Q_s and the source impedance Z_s. Unfortunately, there is still not enough information available for this to be achieved. There is obviously a great need to study the characteristics of the pump in question, and those of the noise generator, as a function of the pump design parameters, so that the fluid-borne noise characteristics of a pump can be predicted.

2.3 Gear Pump

The principle of the gear pump was discovered by Serviere (France) about 1593 and has been employed since that date. Requirements for new machines, however, has led to rapid developement over recent years. As early as 1926 David Brown Limited published an article concerning their improved gear design for a gear pump, and gave a simple equation by which the flow-rate might be estimated. Not until 1933, however, did Darling, [2.28], Backewall, 1934 [2.29] and Humphrey, 1939 [2.30] attempt to establish theoretical and empirical relationships for determining the flow-rate and the nature of pulsation in gear pumps.

2.3.1 Gear Pump Performance

In 1939 Meldahi [2.31] used the geometrical properties of the involute geometry to derive a general expression for the ideal delivery volume of an involute profile external gear pump with backlash. This expression shows that the instantaneous swept-volume rate of the pump

and hence its discharge flow rate, is not steady. In fact the discharge flowrate is found to be the summation of a number of out-of-phase discrete discharges which are parabolic in shape. Meldahl also explained that when the gear contact ratio was greater than unity, trapped volumes occurred whenever two pairs of gear teeth meshed simultaneously. It was also shown that it is possible to relieve these trapped volumes by means of relief grooves in the side plate, in which case the mean flow-rate of the pump can be maximised.

In 1946 Exline [2.32] reported the theoretical analysis of leakage loss. This analysis showed that the leakage loss increases as the third power of the clearances. Such findings illustrated the necessity for maintaining close clearances and accurate tolerances in hydraulic machines.

Beacham in 1949 [2.33] also produced a useful explanation of the reduction in the volumetric efficiency caused by internal leakage. In the same work he mentioned that the percentage of slip, due to internal leakage, varies inversely with a factor produced as a product of the speed and the viscosity. He also wrote a general description of gear pumps, and their operation, and he estimated the flow variation (during cyclic operation) graphically.

Hadakel in 1951 [2.34] in his book published the mathematically derived equations for the instantaneous delivery, ripples and torque between the gears, but he did not consider the trapped volume or the internal leakage. In 1959, Ichikawa [2.35] developed the theory further and derived theoretical equations for the flowrate through an involute profile internal gear pump and specified the best position for relief grooves in a pump with backlash. Ichikawa concludes that internal gear pumps generate much less pressure and flow fluctuation than external gear pumps of comparable capacity. It follows that external gear pumps are more likely to produce higher levels of system noise than internal gear pumps.

The energy method, used by Ichickawa to analyse an internal gear pump, was also adopted by Paul, Muherjee and Bhattacharyya in 1972 [2.36] for the analysis of an external gear pump. They used the ideal equation for a gear pump to show graphically the relationship between

flow-ripple mean flow-rate, and pump parameter values. These curves showed that to achieve a large mean flow-rate accompanied by a low level of flow-ripple, involute profile external gear pumps should tend towards:-

i). large gear modules

ii). large number of teeth per gear

iii). wide gears

iv). large gear pressure angles.

Criteria such as size and weight usually tend to conflict with the above requirements. Limits will exist, therefore, beyond which pump parameter values cannot be altered in order to reduce the pump flow (and pressure) ripple of a pump and common external gear pumps cause flow pulsations which are approximately 15-20% of the mean discharge flow-rate of the pump.

Ichikawa and Yamaguchi [2.37] and Willekens [2.12] both published work concerned with the relationship between the pump flow fluctuation and the system pressure level fluctuation. In both papers mathematical models were presented which described this relationship for a simple hydraulic system consisting of an external gear pump, a straight pipe and a load valve. In both cases the accuracy of the model was checked experimentally. Ichikawa et al [2.37] derived their model by expanding the ideal flow-rate curve for a gear pump into a Fourier series and substituting its components into an expression for the frequency response of the system.

Willekens [2.12] in a related analysis assumed that the discharge line from the pump could be adequately modelled by the equations which describe the propagation of a one-dimensional wave through an ideal fluid. His model was based on the solution of these equations.

Both analyses provided good correlation between the predicted and the measure levels of system pressure fluctuation. During both investigations the mean system pressure did not exceed 7 MPa.

2.3.2 Distribution of Pressure around the Gear Pump

The evaluation of the pressure distribution around a gear pump has been attempted by many workers. In 1970 Singer [2.38] carried out experimental work to measure the pressure distribution around a gear pump manufactured by the Commercial Hydraulic Company, Bedford. Two pump models with standard parts were used. the pressure was measured through a hole in the gear fillet which extended through the shaft to a pressure sensor. The resulting pressure readings were not accurate because of the rapid variation in pressure ripple and the low response of the system, however, significant fluctuations in pressure were noted.

Egrton, in 1975 [2.39], made an initial analysis of the pressure distribution around the perimeter of a gear pump. He made this analysis both theoretically and experimentally, using a pressure transducer which measured the pressure around the pump casing at seven positions. The results appeared reasonable but a more detailed study is required. Using the same technique Fielding, et al [2.40] carried out an investigation on a gear pump which was fitted with seven transducers positioned around the pump casing on one side. A computer program was written in order to predict the pressure distribution around the gear, taking all leakages into consideration. He showed that correlation existed between the theoretical and the experimental results (for the test condition of 60 bar outlet pressure; 5 bar inlet pressure; 16 Hz shaft speed and 0.35 eccentricity ratio).

In 1981, Bidhendi et al [2.41] attempted to repeat the tests using a new measurement. In this technique a pressure transducer was mounted in the bottom of the tooth space of the gear and the signal was taken out through a slip-ring. Unfortunately, the transducer failed after only a limited number of results were obtained. The reason for the transducer failure is not mentioned in the paper but it could well be that it was damaged by the high pressure generated in the trapped volume. Kojima [2.42] in 1984 used the same technique to monitor the pressure transition in the tooth space during a gear revolution. It

was found experimentally that there was a large leakage through the relief grooves. Such leakage affected the fluctuation of the discharge flow (flow-ripple).

From the above review it will be noted that all of the experimental work was carried out in the absence of cavitation. Such studies, however, have been undertaken by Hassan [2.43] in 1986, who used the same technique to investigate the pressure distribution around gear pumps with and without cavitation, and good qualitative results were reported. However, he recommended that further work be carried out in order to produce quantitative results.

2.3.3 Trapped Fluid in a Gear Pump

Involute gears, which are those generally used in gear pumps, must have a contact ratio greater than one. This high contact ratio leads to periodic trapping of fluid in the space surrounded by the two pairs of contacting tooth surfaces of the driving and driven gears. The variation of the entrapped space was investigated mathematically by Yudin [2.44].

In order to avoid, or minimise, the pressue rise in the trapped fluid, relief grooves are provided on the side plates. Ickikawa [2.45] suggested two relief groove positions for the two cases, (a) where there is a relatively large backlash and (b) where there is no backlash. However, the accuracy, or otherwise, of his proposals in relation to the position of the relief groove have, to date,not been verified. Ishibashi and Muta [2.46] investigated the influence of the backlash size, and the relief groove position, on the overall efficiency of gear pump, and presented some interesting results. Their experiments were restricted to the low pressure range and the experimental results were not clearly explained. Interesting results were presented by Stupard Chernyshov [2.47], and by Stupa [2.48], on the analytical determination of the pressure in the inter-tooth space of a metering gear pump. They concluded that the pressure in the inter-tooth space reached significant level (greater than 5.5 (MPa) and exerted a large effect on the operating lifetime of pumps. Although the results presented by Chernyshov and Stupa may have been

valid, they did not present a clear explanation of their experimental techniques nor was there clear explanations to the experimental technique or graphical presentation of results to confirm these values.

A number of authors [2.31,2.35,2.37] refer to the need for correctly positioned relief grooves in external gear pumps. However, it would appear to the author of the present work that some clarification of the trapping phenomena itself is necessary before decisions can be made in relation to the optimal position of the relief groove. Any investigation of the trapping phenomenon would certainly include measurement of the fluid pressure in the trapped space and a study of the influence of the other salient parameters on the overall process.

In a recent publication, Yanada et al [2.49] described a very interesting study in which measurements of the pressure in the trapped space were made. In this investigation the pressure was measured by means of a miniature semiconductor pressure transducer which was installed in the casing. The resulting signals being taken out through pressure taps provided. Unfortunately, it was discovered that these pressure taps effectively damped the pressure signals and led to measurement errors.

2.4 Cavitation

When the pressure of a liquid is progressively reduced, cavity bubbles may form as a result of dissolved gases coming out of solution, or because the liquid vapourises. These phenomena are known respectively as gaseous, or vaporous, cavitation. When cavitation occurs in hydraulic equipment it can have three main adverse effects, (a) it usually results in noise, (b) erosion of the material can occur as a result of pitting, and (c) a combination of fully developed cavitation and erosion damage can lead to a loss of performance and a lower efficiency of plant.

The term cavitation was first used by R E Froude, S W Barnaby and Sir Charles Parson [2.50] in connection with propeller performance breakdown of early steamships. In 1895 Parson build the first water

tunnel in order to study cavitation, after 20 years of experiment he made the connection between cavitation and erosion of marine propellers.

The literature survey contained in this section will cover the general background of cavitation erosion and cavitation in positive displacement pumps.

2.4.1 General background of cavitation erosion

Cavitation damage has been important since the early 1890's, when in 1893 it was first observed on the propeller of the HMS destroyer Darling. This particular case arose because of the high propeller speeds resulting from turbine replacement of reciprocating engine drives and hence the involvement of Sir Charles Parson.

The undesirable nature of cavitation is not simply due to the presence of cavities but is related to their collapse or implosion.

As long ago as 1917, Lord Rayleigh [2.51] calculated the pressure developed in a liquid during the collapse of a spherical cavity. He assumed that a cavity was instantaneously introduced into a pressurised inviscid and incompressible fluid, and by considering the interchange of potential and kinetic energy was able to predict the life history of the cavity.

Knapp and Hollander [2.52] used a high speed camera to photograph the collapse of a cavity and measured collapse velocities of 250 m/s. As a result it is clear that large pressures will develop at the instant of a collapse and indeed pressures of the magnitude of 1000 MN/MPa/m^2 have been reported.

Later analysis, Knapp [2.53] Hammitt, [2.54] showed that the Rayleigh model (spherical collapse) is unlikely to occur in practice. A collapsing cavity is unstable and any slight disturbance will cause rapid distortion. In a subsequent paper Hammitt showed that a cavity moving into a region of higher pressure tends to distort into a toroidal or "doughnut" shape, while at the same time ejecting a high velocity micro jet, as shown in Fig. (2.3), at the instant of collapse.

It is generally agreed that the damage caused is due to both the liquid "microjet" impact, for non-symmetrical collapse, see Fig. (2.3, 2.4), and shock waves from so-called "rebounding" bubbles. It has been shown [2.55, 2.56] that these rebounding bubbles grow again after collapse due primarily to compressed internal gas and vapour. This occurrence does not conform with the Rayleigh model which predicts damage from shock waves from spherically-symmetric collapse. High-speed photography, Hammitt [2.57] has shown that spherical collapse does not occur near to surfaces. This discovery has been confirmed by computer study, Mitchell and Hammitt [2.58], Hicking and Presst [2.56]. The potential intensity of such mechanisms can explain damage for even the hardest and strongest materials as a result of cavitation.

2.4.2 Cavitation in hydraulic pumps

One of the most significant problems in the design and use of oil hydraulic equipment is that of cavitation, a phenomenon which takes place in oil hydraulic pumps as in all other pumps.

Cavitation occurs because dynamic losses in the pump suction line, including the pump inlet chamber, produces a very low absolute pressure in the suction inlet to the pump. It is accentuated by high pump speed, high oil velocity, high oil solubility and high pipe losses. Many workers have studied the effect of such parameters on cavitation inception [2.60, 2.61].

In 1970, Tsuji [2.62] introduced a modified nett positive suction head which depended upon the air separation pressure instead of the vapour pressure, and which was to be used for hydraulic oil rather than for water in calculating the cavitation index. Tsuji also proposed an empirical equation which could be used to assess the cavitation point in that a special drop in the flowrate of the pump was sufficient for cavitation inception, different sizes and models of gear pumps manufactured by the Commercial Hydraulic Company were tested. It was found that the critical pressure, required by the pump, increased as pump speed or viscosity. Similarly increasing the port size of the pump reduced the critical pressure required because this increased pump leakage.

In 1978, Jordan [2.65], gave a discussion concerning the difference between cavitation and aeration. He discussed methods for detecting and preventing hydraulic fluid cavitation. It would appear that aeration can be reduced by correct design of the reservoir, whilst cavitation can be prevented by correct design of the pump suction line and chamber so as to reduce the inlet dynamic losses.

Further work in this field was carried out by Zalka in 1971 [2.63]. He studied theoretically and experimentally, the effect of pump speed, suction pressure, suction chamber design, fluid viscosity, the gear module and the number of teeth, on the operating characteristics of a gear pump. Another aim of this work by Zalka was to determine the extent to which the speed ratio depends on the geometrical dimensions of the pump and the properties of the medium that is being transferred. It would appear from Zalka's results that the effect of speed was successfully clarified.

The above work was followed by a study made by Mason in 1976 [2.64]. In this study he investigated the effect of viscosity, air content of the oil, speed of rotation, oil temperature, and inlet port size of the gear pump, on the critical pressure required by the gear pump in order to prevent cavitation inception. By assuming, damage is identical (from both cases).

Budris, in 1980 [2.66], described the prevention of cavitation in rotary gear pumps by reducing the required net inlet pressure (RNIP). In this case the locations of the liquid source and suction lines must be so arranged as to ensure that the net-inlet-pressure available (NIPA) is greater than the required net inlet pressure (RNIP) of the pump.

The above work was follwed by that of Yamaguchi and Takab in 1983 [2.67], in which they discussed the cavitation mechanism, as well as its inception, in an axial piston pump whose main parts were made from transparent acrylic resin. They investigated the cavitation process in this pump as a function of operating conditions (speed, shape of valve plate, suction pressure) using a variety of hydraulic fluids. Hassan, in 1986 [2.43], explained the cavitation phenomenon in terms

of its inception in an external gear pump and the effect of pump speed and delivery line pressure. From the above review it is clear the majority of workers in this field have directed their investigations towards the parameters that affect cavitation, such as suction height, pump speed, oil viscosity and suction chamber design. Few have tried to explain the phenomena itself or to obtain a clear understanding of cavitation in positive displacement pumps. Similarly, there has been little effort expended in discovering how cavitation can affect hydraulic system performance or what damage it may do through the mechanism of erosion.

2.5 Conclusions

The conclusions which may be drawn from the literature review previously discussed can be summarised as follows:-

1. There is little information available on techniques for decreasing, by design, the noise-generating-potential of hydraulic gear pumps.

2. Suction chamber geometry and pump operating conditions can affect a gear pump's discharge flow rate and system pressure fluctuation.

3. The inlet conditions may have a considerable influence on a gear pump's performance and discharge flowrate.

4. There is hardly any information available on the trapped oil and the value of the pressure generated due to this phenomenon and its effect on the general performance of gear pumps.

5. Similarly, there has been less effort expended in discovering how cavitation can affect hydraulic system performance or what damage it may cause through the mechanism of erosion.

As a result of these findings, the present project has been aimed at investigating different parameters related to the cavitation phenomenon and its effect on the performance of, and damage to, gear pumps.

REFERENCES

[2.1] BROWN, D., 'Roloid pump gears, Mech.World. v80, p260, 1926, David Brown & Sons Ltd.

[2.2] BAKEWELL, W.E., 'Rotary Pumps. Their operation and application', Power 1934, Vol.78. No.11, pp602-603.

[2.3] DRANSFIELD, P., STECKI, J., and WILKINS, P., 'Noise in hydraulic control systems' Proc. Noise Shock and Vibration Conf.. 1974, Monash Univ., Melborne, pp 236-246.

[2.4] SKAISTIS, S.J., KENNAMER, D.E., and WALRAD, J.F., 'Quieting of high performance hydraulic systems', Proc. 20th Nat.Conf. on Fluid Power, 1964, pp51-60.

[2.5] BAXA, D.E., 'Noise legislation and its implication to industry', S.A.E., Earthmoving Industry Conf. 1974, Illinois.

[2.6] KELESY, J., and TAYLOR, R 'Optimised pintel valve timing for a radial piston pump', Seminar, Quieter Oil Hydraulics, I.Mech.E. 1980.

[2.7] KANE, J., RICHMOND, T.D., and ROBB, D.N., 'Noise in hydrastatic systems and its suppression', Proc.Inst.Mech.Engrs., 1965-66, Vol.180, Pt.3L, pp36-52.

[2.8] BASHTA, .M., 'Noise in machine hydraulic systems', Russian Engineering Journ., Vol.51, No.6.

[2.9] ZAICHENKO, I.Z., and BOLTYANSKII, A.D. 'Reducing noise level of axial-piston pumps', Russian Engineering Journ. Vol.49, No. 4.

[2.10] BEYER, R., 'Noise reduction in gear pumps', Proc. Fluid Power International Conf., 1964, London, pp119-126.

[2.11] ELLIOTT, L.R., MARONEY, G.E., and FITCH, E.C., 'An experimental survey of fluid power pump sound levels', Proc.29th Nat.Conf. of Fluid Power, 1973, Ohio.

[2.12] WILLEKENS, F.A.M. 'Fluid-borne noise in hydraulic systems', Proc. First European Fluid Power Conf., 1973, Paper No. 28, N.E.L., Glasgow.

[2.13] COLLINS, J.F., 'The inter-relationship of air-borne and fluid-borne noise in hydraulic systems', Proc.20th Nat.Conf. on Fluid Power, 1966, pp84-92.

[2.14] McCANDLISH, D., and LINNEY, G., 'Noise characteristics of gear pumps', Proc. 4th International Fluid Power Symposium, 1975, Paper G1, Sheffield.

[2.15] CROOK & HERON Air-borne noise from hydraulic lines due to liquid-borne noise, I.Mech.E. Conf. - Quiet Oil Hydraulic Systems, London, 1977.

[2.16] BOWNS, D.E., EDGE, K.A., and TILLEY, D.G., 'The assessment of pump fluid borne noise'. I.Mech.E. Conf. - Quiet Oil Hydraulics, London, Nov. 1977.

[2.17] BOWNS, D.E., EDGE, K.A., and McCANDLISH, D., 'Factors affecting the choice of a standard method for the determination of pump pressure ripple'. I.Mech.E. Conf. - Quiet Oil Hydraulics, London, Oct.1980.

[2.18] McCANDLISH, D., EDGE, K.A., and TILLEY, D.G. 'Fluid borne noise generated by positive displacement pumps'. I.Mech.E. Conf. - Quiet Oil Hydraulics, London, Nov. 1977.

[2.19] HENDERSON, A.R., 'Measuring the performance of fluid-borne noise attenuators, Research Projects Seminar on Quiet Oil Hydraulic Systems, London: I.Mech.E., 1977.

[2.20] WHISTON, R.J., 'The measured transmission loss characteristics of some hydraulic attenuators. Research Project Seminar on Quiet Oil Hydraulic, London, I.Mech.E., 1980.

[2.21] BUTLER, M.D., and TILLEY, D.G., 'The generation and transmission of fluid borne pressure ripple in hydraulic system'. I.Mech.E. Conf. - Quieter Oil Hydraulics, London, Oct. 29-30th, 1980.

[2.22] LINDSYA, I., 'The reduction of fluid borne noise in gear pump suction lines'. M.Sc. Thesis, University of Bath, 1981.

[2.23] EDGE, K.A., and FREITAS, F., 'Fluid borne pressure ripple in positive displacement pump suction lines'. 6th International Fluid Power Symposium, BHRA Fluid Engineering, Cranfield, Bedford, April 8-10th, 1981.

[2.24] EDGE, K.A., and FREITAS, F., 'A study of pressure fluctuations in the suction lines of positive displacement pumps'. Proc. of the Institution of Mechanical Engineers, Vol. 199, No. 134, 1985.

[2.25] HENDERSON, A.R., and WHITSON, R.J., 'The pulsation properties of positive displacement pumps, their measurement and application'. Gas and Liquid Pulsations in Piping Systems Prediction and Control, Seminar, I.Mech.E., 1988, pp31-39.

[2.26] JOHNSTON, D.N., and EDGE, K.A., 'Simulating of pressure ripple characteristics of hydraulic circuits'. Gas and Liquid Pulsations, Seminar, I.Mech.E., 1988, pp13-23.

[2.27] WHITSON, R.J., 'An 'in-line' method for measuring the transmission characteristics of pulsation dampers and attenuators'. Gas and Liquid Pulsations, Seminar, I.Mech.E., 1988.

[2.28] DARLING, C.S., 'Rotary displacement pumps', Industrial Pumping Practices, Mech. World, June, 1933.

[2.29] BACKEWALL, 'Rotary pumps'. Power, Vol.78, No.11, November, 1934.

[2.30] HUMPHREY, K.B., 'Rotary pumps - Their application and operation, Mill and Factory; Vol.24, No. 2, Feb. 1939.

[2.31] MELDAHL, A., 'Theory of gear pumps'. Brown Boveri Review, Vol.26, No.11/12, Nov-Dec. 1939, pp254-261.

[2.32] EXLINE, P.G., 'Leakage in capillary seals of hydraulic valves and pumps'. Production Eng. Vol.17. April 1946.

[2.33] BEACHAM, T.E., 'High pressure gear pumps,' Proc.I.Mech.E., Vol.154, 1949.

[2.34] HADEKEL, 'Displacement pumps and motors', Pitman and Son Publication, 1951, Chapter 11, p45.

[2.35] ICHIKAWA, T., 'Characteristics of internal gear pumps'. J.SME.Bulletin, Vol.2, No.5, Feb.1959, pp35-39.

[2.36] PAUL, A.K., MUKHERJEE, B.C., and BHATTACHARYYA, A. 'Analysis of gear pumps', Institution of Engineers (India) 1972, Vol.52, No.9, Part ME5, pp311-315.

[2.37] ICHIKAWA, T., and YAMAGUCHI, K., 'On pulsation of delivery pressure of delivery pressure of gear pump'. Bull.JSME, 1971, Vol.14, No.78, pp1304-1312.

[2.38] SINGER, C., 'Measurement of distribution pressure around external gear pump'. Commercial Hydraulic Company, 1970.

[2.39] EGRTON, P., 'Gear pump, and introduction'. B.Sc. Thesis, Birmingham University, 1975.

[2.40] FIELDING, D., FOSTER, K., HOOK, C.J., and MARTIN, M.J. 'Sources of pressure pulsation from a gear pump'. I.Mech.E. Conf. - Quiet Oil Hydraulics, London, Nov. 1977.

[2.41] BIDHENDI, I.M., FOSTER, K., and TAYLOR, R. 'Computer predictions of cyclic excitation source for an external gear pump'. Computer Aided Design in High Pressure Hydraulic Systems, I.Mech.E., 1083.

[2.42] KOJIMA, E., 'Characteristic of fluid borne noise generated by fluid power pump'. 3rd Report, Bulletin of JSME, Vl.27, No.23, Oct. 1984, pp2188-2195.

[2.43] HASSAN, A.M., 'Cavitation effects in hydraulic fluid power control systems'. Ph.D. Thesis, SME, Cranfield, Dec. 1986.

[2.44] YUDIN, E.M., 'Gear pumps. Principal parameters and their calculation'. Translation from Russian by E Harres, Ed. Joseph Luces Ltd. (National Lending Library for S.C. and Tech.Yorkshire).

[2.45] ICHIKAWA, T., 'Gear pump', 1962, (Nickkan Kogyo) "in Japanese".

[2.46] ISHIBASHI, A., and MUTA, R., 'The effects of relief groove position and backlash size on the efficiency and pressure fluctuation ratio of a gear pump. Trans. Soc. Mech.Engrs. 1967, pp33-251, 1155.

[2.47] STUPA, V.I., CHERNYSHOV, 'Analytical determination of the pressure inter-tooth space of metering gear pump'. Translated from Khimicheskie Volokna, No.5, pp478-48, Oct.1982.

[2.48] STUPA, N.I., 'Analytical determination of the pressure in the inter-tooth space of a metering gear pump'. Translated from Khimicheski Volokna, No.2, pp53-55, March-April, 1984.

[2.49] YANADA, H ICHIKAWA, T., and ITSUJI, Y. 'A study of the trapping of fluid in a gear pump'. Proc.Inst.Mech.E. vol.201, No.A1, 1987.

[2.50] PEARSALL, I.S., 'Cavitation'. Mills & Boon Ltd, 1972.

[2.51] RAYLEIGH, Lord 'On the pressure developed in a liquid during the collapse of spherical cavity'. Phil.Mag., Vol.34, 1917, pp94-98.

[2.52] KNAPP, R.T., and 'Laboratory investigations of the mechanism of cavitation'. Trans. ASME, 1948, 70, 419-35.

[2.53] KNAPP, R.T., 'Cavitation and nuclei'. Trans.ASME, 1958, 80, pp1315-24.

[2.54] HAMMITT, F.G., 'Damage due to cavitation and subcooled boiling bubble collapse'. Proc.Inst.Mech.Eng. 1968, 183, Pt.2.

[2.55] HAMMITT, F.G., 'Cavitation and multiphase flow phenomena', McGraw-Hill, 19809.

[2.56] HICKLING, R., and PLESST, M.S., 'Collapse and rebound of spherical bubble in water', Phys.Fluids, Vol.7, 1964, pp7-14.

[2.57 KLING, C.L., and HAMMITT, F.G., 'A photographic study of spark induced cavitation bubble collapse'. Trans. ASME, J. Basic.Engr. Vol.94, No.4, 1972, pp825-83.

[2.58] MITCHELL, T.M., and HAMMITT, F.G., 'Asymmetric cavitation bubble collpse', Trans ASME, J.Fluid Eng., Vol.95, No.1, March 1973, pp29-37.

[2.58] HICKLING, R., and PLESSET, M.S., 'Collapse and rebounded of a spherical bubble in water' Phys.Fluid, Vol.7 (1964) pp7-14.

[2.60] ACOSTA, A.J., and PARKIN, B.R., 'Cavitation inception - a selected review'. J.Ship Res, Vol.19,(1975), pp193-205.

[2.61] McNULTY, P.J., and PEARSALL, I.S., 'Cavitation inception in pumps'. International Symposium on Cavitation Inception, New York, ASME, 1968, pp6-7.

[2.62] TSUJI, S., 'Cavitation criteria for hydraulic pumps'. The 1970 Fluid Power International Conference, Day 2, Paper 3, 1970.

[2.63] ZALKA, A., 'Suction capability and cavitation of gear pumps', Second Fluid Power Symposium, BHRA Fluid Engineering, Guildford, January 4-7, 1971, Paper H3.

[2.64] MASON, D., 'Cavitation in gear pump'. Commercial Hydaulic Company, 1976.

[2.65] JORDEN, G.R., 'How to detect and prevent Hydraulic Fluid Cavitation'. Hydraulic and Pneumatic, October, 1978.

[2.66] BUDRIS, A.R., 'Preventing cavitation in rotary gear pumps'. Chemical Engineering, May, 1980.

[2.67] YAMAGUCHI, A. and TAKABE, T. 'Cavitation in an axial piston pump'. Bulletin of the JSME, Vol. 26, No. 211, Paper 211-12, January 1983.

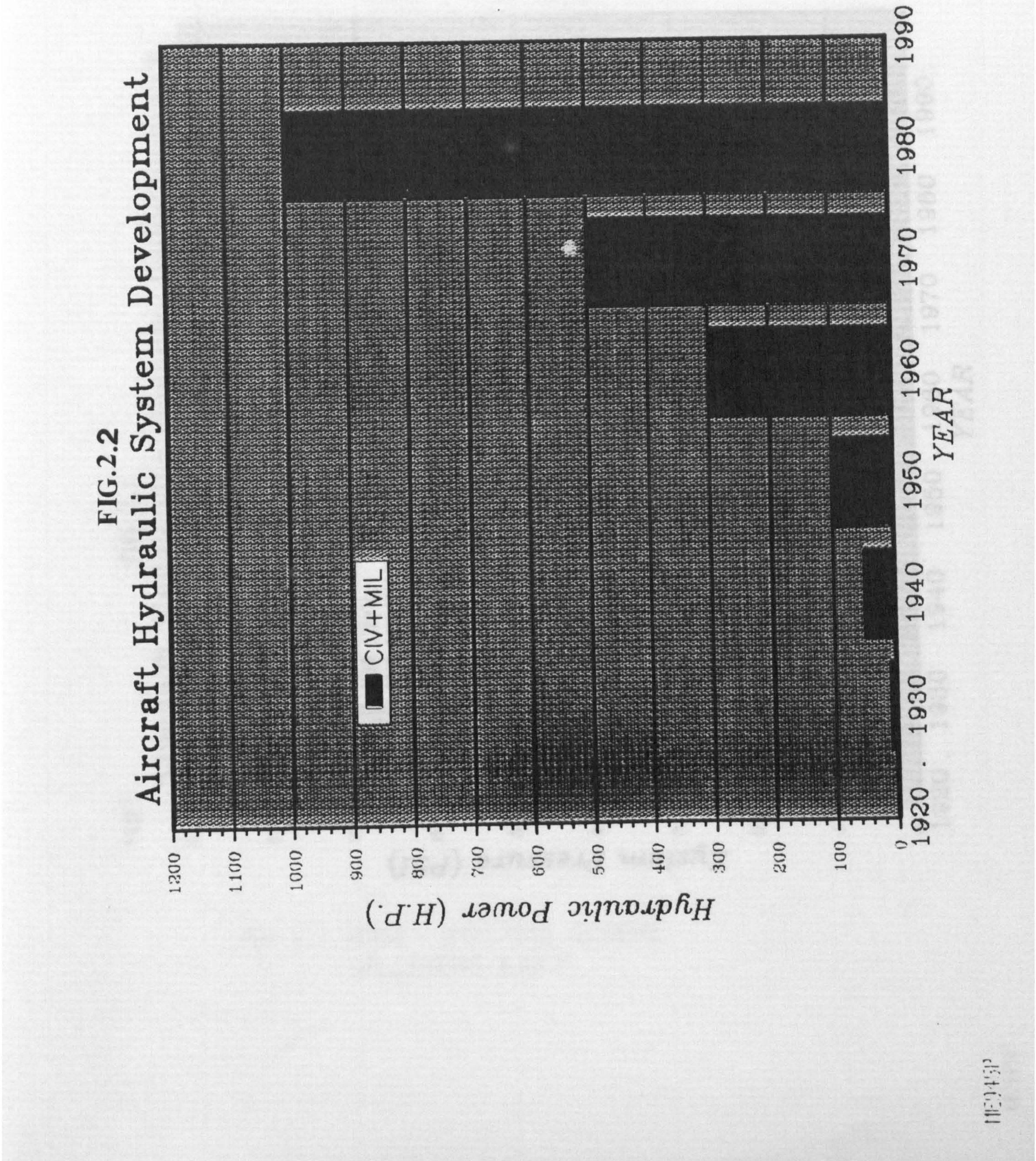
Aircraft Hydraulic System Development
CIV+MIL
Hydraulic Power (H.P.)
YEAR
1200
1100
1000
900
800
700
600
500
400
300
200
100
0
1920
1930
1940
1950
1960
1970
1980

FIG.2.2

FIG.2.1

Aircraft Hydraulic System Development

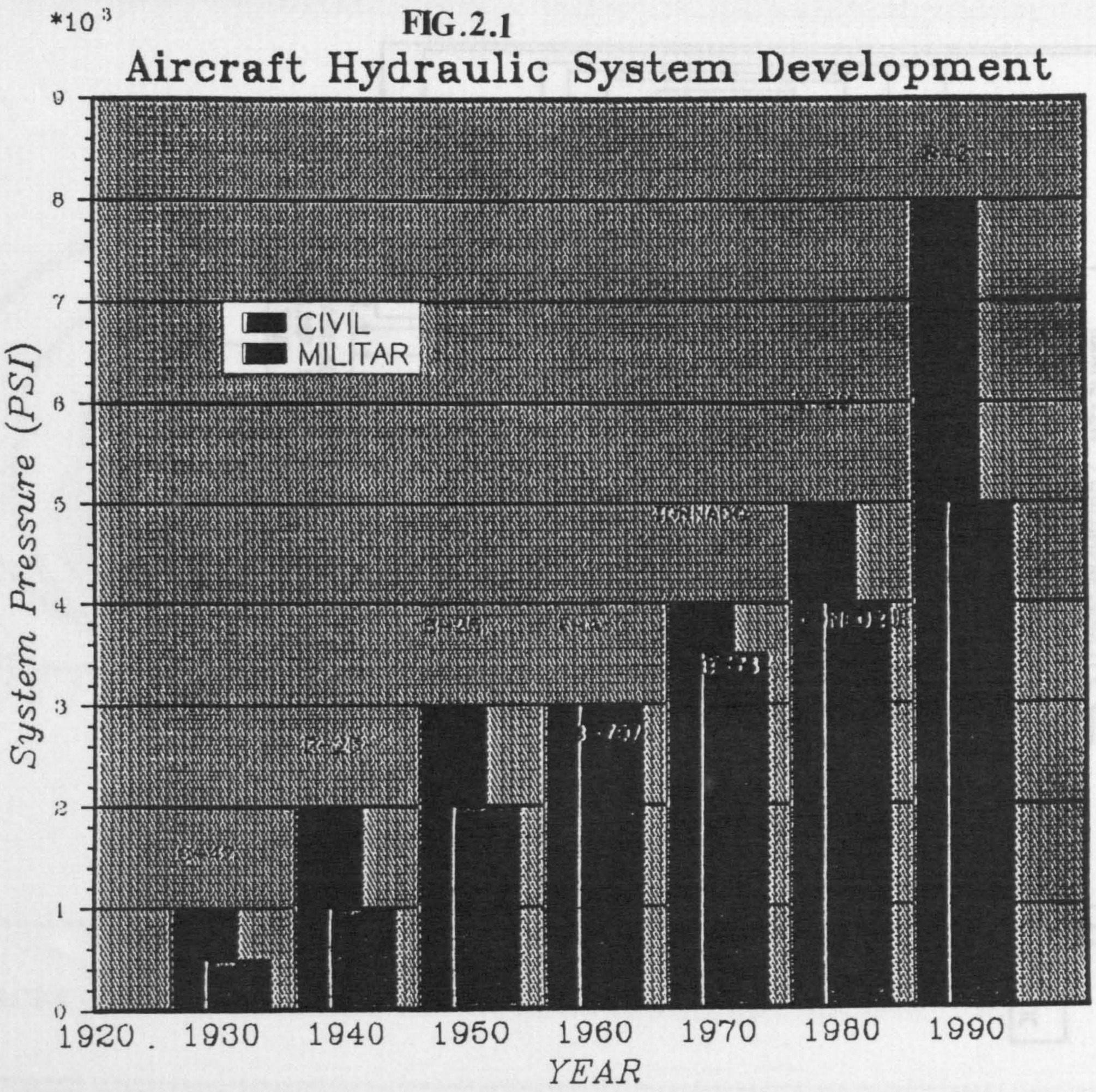

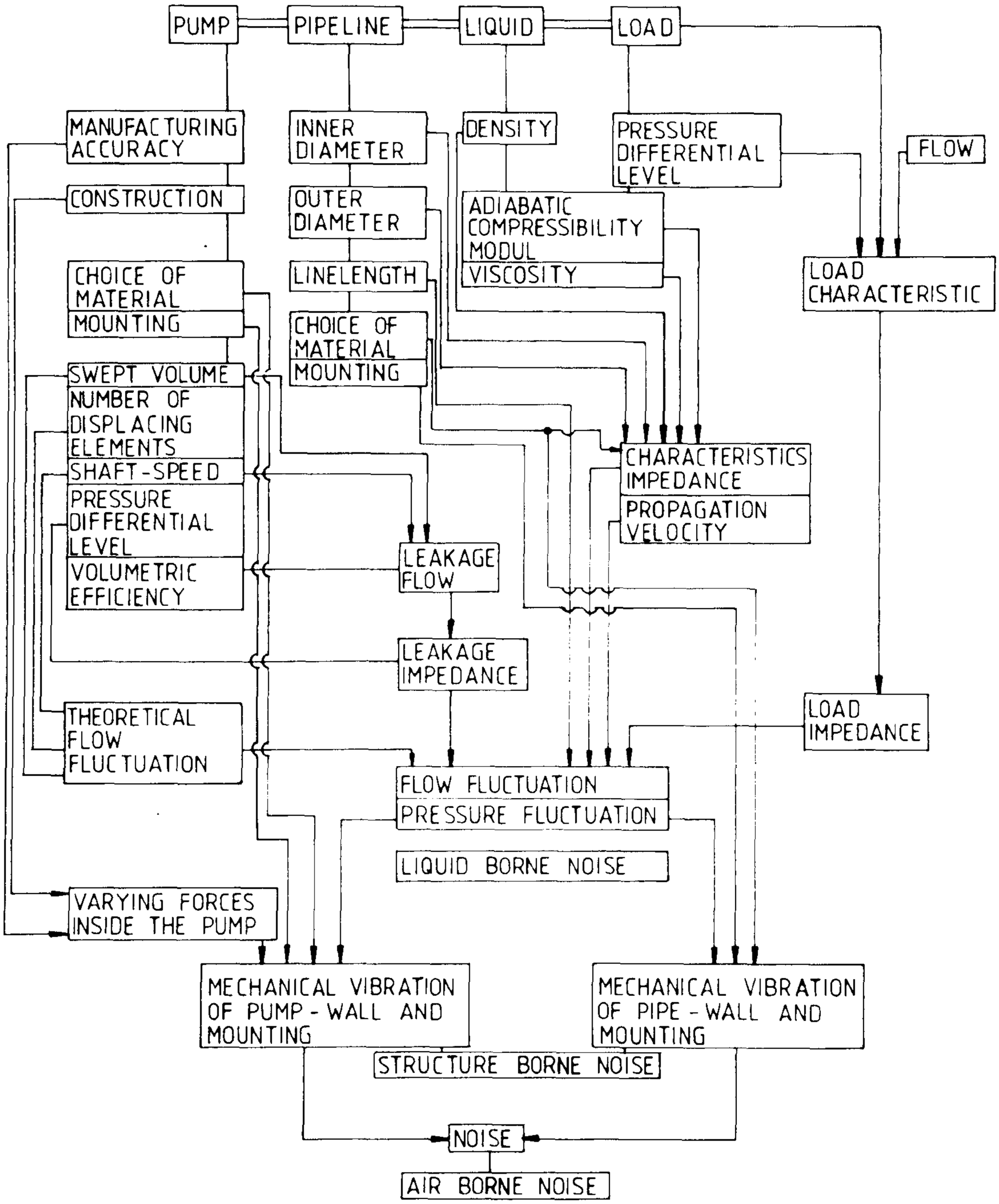

FIG. 2.3 NOISE - ANALYSIS SCHEME
(WILLEKENS **2.12**)

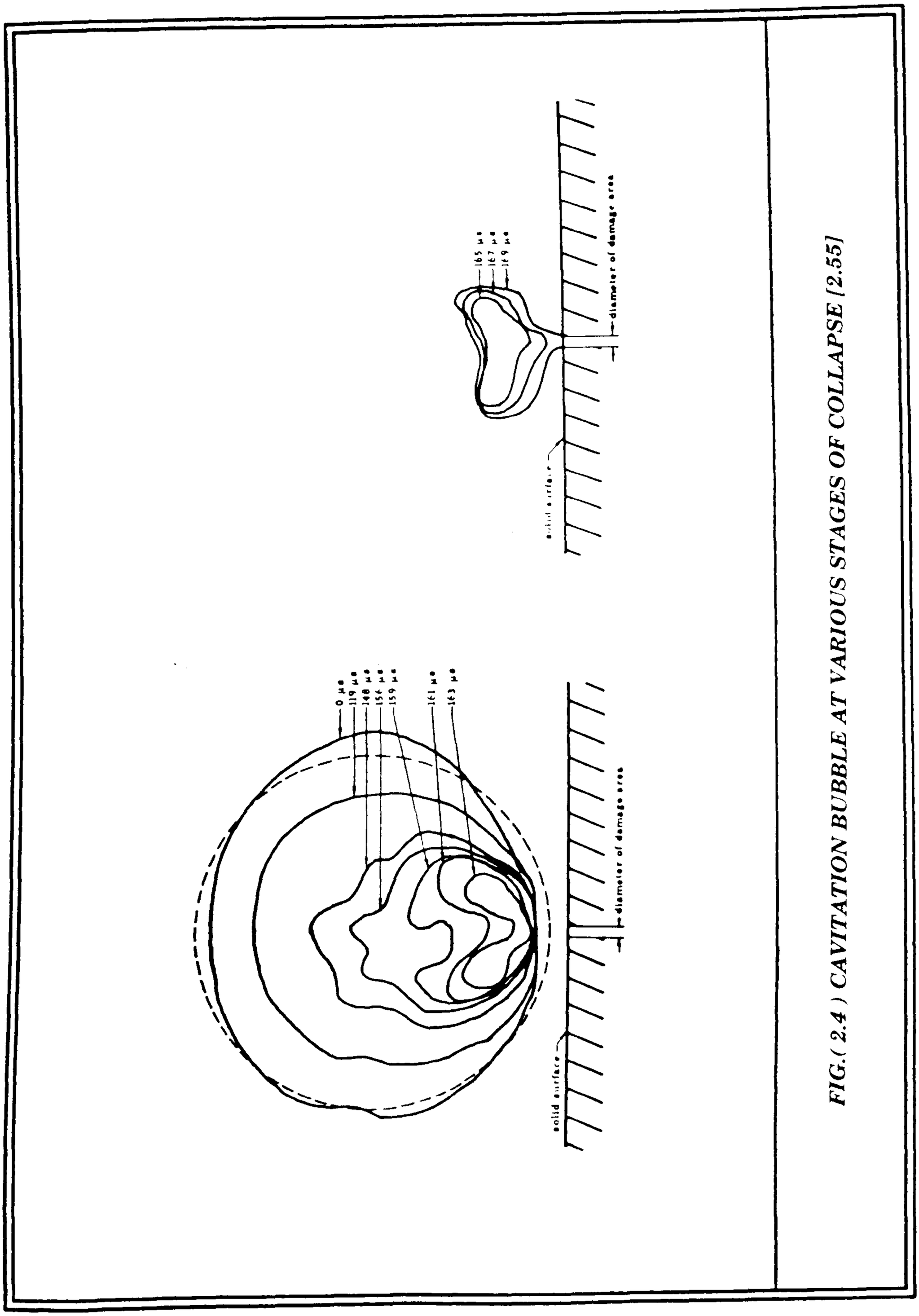

FIG.(2.4) CAVITATION BUBBLE AT VARIOUS STAGES OF COLLAPSE [2.55]

CHAPTER THREE

GEAR PUMP CHARACTERISTICS - THEORY

3.1 Introduction

Gear pumps have been used in very large numbers for various hydraulic services. Their general principles are well known. The meshing gears run in a casing which is a close fit at the sides and around the periphery except near the intersection of the casing bores and the relief grooves. Fig. 3.1 shows a solid model for a typical cross section through an external gear pump.

In this chapter the ideal flow from a gear pump, together with the trapped volume and internal leakage will be analysed in relation to pressure fluctuation generated in the hydraulic system circuit.

Fluid is carried around from the suction to the delivery by the teeth space. When the teeth engage with each other the oil is displaced through the pressure line and due to the continuous rotation of the gears, a continuous pumping action takes place.

Due to the intermittent meshing of gears the pumping action causes pulsating flow even though the pump is driven at constant speed. Due to the high working pressure the liquid leaks from the pressure to the suction side around the circumference (over the tips of the teeth), and across the flat end faces of the gears and between the individual tooth spaces. These internal leakages, as indicated in Fig. 3.2, affect the pumping efficiency.

Within a hydraulic system, fluctuations in flow and pressure are related, therefore, before attempting to reduce the level of pressure fluctuation, it is advantageous to know the magnitudes and the effect of the gear geometric properties, internal leakages and trapped volume.

In the literature, two different methods for calculating the pump flow have been presented. The first is based on the geometry of the gear (e.g., tooth and space areas). This method states that the two gear

cross-section areas are subtracted from the area built up by the addendum circle radius and the base circle [3.1,3.2,3.3]. The second method is based on the energy supplied which involves the concept of an ideal torque defined as the torque required to derive the pump when frictionless fluid flows through it, and that there is no mechanical losses, Paul et al [3.4].

3.2 Determination of the Area of the Tooth and Tooth Space

It is thought that the scientist Euler was the first to recognise that the involute profile form of the gear tooth provides a constant angular velocity. However, it was not until the beginning of this century that this tooth form became widely used. This delay was due to the difficulty in accurately manufacturing its form.

The involute profile has two particular properties of interest:

1. Involute angular function:

$$\text{Inv } \alpha = \tan(\alpha) - \alpha \qquad (3.1)$$

2. Second law of involutes which gives the area A bounded by two involutes:

$$A = \frac{\theta}{2}(R^2 - r^2) \qquad (3.2)$$

where θ = angle between radii OA and OD (Fig.3.3)

R = radius of the addendum circle

r = radius of the base circle.

By using the two properties we can derive that the area of the working part of the teeth bounded by the two involute profile and the base circle is:

$$A_T = r^2 \left[\frac{(\alpha - \text{inv}\alpha)^3}{3} - \left(\frac{\theta}{2} + \text{inv } \gamma \right) + R^2 \left(\frac{\theta}{2} + \text{inv } \gamma - \text{inv } \alpha \right) \right] \qquad (3.3)$$

The total area of the tooth A_{total} can be found as follows:

$$A_{total} = A_T + \Delta A_T$$

where ΔA_T is the area between the base circle and the root circle of the tooth (Fig. 3.4) without considering the fillets, i.e.,

$$\Delta A_T = (r^2 - r_i^2)\left(\frac{\theta}{2} + \text{inv } \gamma\right) \qquad (3.4)$$

Similarly the area of the tooth space can be calculated as:

$$A_s = R^2\left(\frac{\pi}{Z} - \frac{\theta}{2} + \text{inv } \alpha - \text{inv } \gamma\right) - r^2\left(\frac{(\alpha + \text{inv } \alpha^3)}{3}\right) - r_1^2$$

$$\left[\frac{\pi}{2} - \left(\frac{\theta}{2} + \text{inv } \gamma\right)\right] \qquad (3.5)$$

Equations (3.3) and (3.5) are used for both determining the theoretical delivery of the pump and calculating the geometric parameters of gears. The details of the derivation of equations (3.3) and (3.5) are presented in Appendix A.

3.3 Pump Flow Equation

3.3.1 Ideal Flow Equation

An external gear pump consists basically of two meshing spurs, helical or herringbone fashion. Helical gears are limited in use because of the tendency to develop end thrust under high pressure. The most widely used are spur gears with an equal number of teeth of involute profile and externally meshing.

Engineers have been concerned for many years with the design and operation of gear pumps. As early as 1926 David Brown Limited [3.1] published an article concerning their improved gear design for pumps and gave a simple equation by which the flowrate might be estimated. The equation is:

Delivery Q = KC^2bN [cubic inch]

where: K = delivery coefficient, depending upon the number of teeth

c = centre distance (inches)

b = face width of gear (inch)

N = number of revolution (rev/min).

In 1938 the following equations used for caluclating the delivery of gear pumps had been presented by Menshikov [3.2].

1. $Q = 2A_T ZbN$ (cm^3/min)

2. $Q = 2A_S ZbN$ (cm^3/min).

3. $Q = 0.0047 (D_e^2 - D_i^2) bN$ (/h)

4. $Q = 0.0525 (D_e^2 - D_i^2) bN$ (/h)

where A_T = area of the tooth (cm^2)

A_S = area of the tooth space (cm^2)

Z = number of teeth

b = gear width (cm)

N = speed (r.p.m.)

D_e = addendum diameter

D_i = root circle diameter

In the above equations, the first is most widely used for approximate calculations but is inaccurate and demands the calculation of the

cross section area of the tooth. The second equation differs from the first by using the volume of the tooth space in the calculation, the third and the fourth equations do not take into account the volume of fluid which is carried back to the suction line. None of these equations take into consideration the contact ratio, defined as: the ratio of the contact length to the base pitch), which influences the small volume trapped during the meshing action.

3.3.2 Gear Pump Mesh Flow Rate

The instantaneous delivery may be calculated by making use of the diagram given in Fig. 3.5. The output at any instant is the rate of decrease of the space above the line ROPQT. Taking two fixed reference lines OU,QV, the delivery is the rate of change of the segments ROU,TQV plus that of the volume UWVQPO, which is in turn equal to that of volume OPQO. Hence the delivery is equal to the difference between the volume swept by the arms OR and QT and that swept by the arms OP and QP. When the driving gear rotates $d\theta$ and correspondingly driven gear rotates by $d\Phi$ variation in the control volume will sweep out an area:

$$\frac{1}{2}(OR)^2\, d\theta \text{ from the driving gear}$$

$$\frac{1}{2}(QT)^2\, d\Phi \text{ from the driven gear.}$$

but the control volume OPQO will sweep out an area whose magnitude is decided by the point of contact P, and this area is

$$\frac{1}{2}(PQ)^2\, d\theta \text{ from the driving gear}$$

and

$$\frac{1}{2}(PQ)^2\, d\Phi \text{ from the driven gear}$$

then the total rate of change of area is:

$$dA = \frac{1}{2}\left[(OR^2 - OP^2)\, d\theta + (QT^2 - QP^2)\, d\Phi\right]$$

$$\therefore \qquad dV = \frac{1}{2} b \{(OR^2 - OP^2)\, d\theta + (QT^2 - QP^2)\, d\Phi\}$$

where b is the width of the gears.

For equal gears the angle $d\theta = d\Phi$ and $OR = QT = R$ where R is the addendum radius,

then

$$dV = \frac{1}{2} b \{(R^2 - OP^2)\, d\theta + (R^2 - QP^2)\, d\theta\}$$

$$= \frac{1}{2} b\, (2R^2 - OP^2 - QP^2)\, d\theta \qquad (3.6)$$

From equation (3.6), Hadekel [3.21] derived that:

$$\frac{1}{b}\frac{dV}{d\theta} = R^2 - \left(\frac{OP^2 + QP^2}{2}\right)$$

Since S is the pitch point on OQ then

$$OS = SQ = r$$

where r is the pitch radius and by Apollonius's thorem;

$$\frac{OP^2 + OQ^2}{2} = OS^2 + PS^2 = r^2 + PS^2$$

then:

$$\frac{1}{b}\frac{dV}{d\theta} = R^2 - r^2 - PS^2 \qquad (3.7)$$

where R,r are the radii of the addendum and pitch circles respectively.

PS is the contact length which is function of θ.

i.e., $PS = r\theta \cos \Psi$

where r = pitch circle

θ = angle of the rotation of the gears.

Substituting PS into equation (3.7), then it can be deduced that:

$$\frac{1}{d}\frac{dV}{d\theta} = R^2 - r^2 - r^2\,\theta^2\,\cos^2\Psi \qquad (3.8)$$

and we have $R = r + A$ where A is the addendum

then equation (3.8) becomes:

$$\frac{1}{d}\frac{dV}{d\theta} = 2ra + a^2 - r2\theta^2\,\cos^2\Psi$$

$$= r^2\left[\frac{2a}{r} + \left(\frac{a}{r}\right)^2 - \theta\,\cos^2\alpha\right]$$

Defining the module $m = \frac{2r}{z}$

and let $K = \frac{a}{m}$, $a = Km$

then $r = \frac{mz}{2}$, $\frac{a}{r} = \frac{2K}{z}$

$$\therefore \quad \frac{dV}{d\theta} = 4r^2 b\left(\frac{K}{z} + \frac{K^2}{z^2} - \frac{\theta^2}{4}\cos^2\Psi\right)$$

where K = the ratio of addendum to module

z = number of teeth

The effective limit of θ corresponding to $\pm\frac{\theta_o}{2}$

where $\theta_o = \frac{2\pi}{z}$ or $\frac{-\pi}{z} \leq \theta \leq \frac{\pi}{z}$

and the average value of θ^2 over a cycle is

$$\theta^2 = \frac{1}{3}\left(\frac{\pi}{z}\right)^2 \quad \text{Hence}$$

the average delivery per radian is

$$\frac{dV}{d\theta} = 4.r^2.b\left(\frac{K}{z} + \frac{K^2}{z^2} - \frac{\pi^2}{12z^2}\cos^2\Psi\right)$$

The expression for instantaneous delivery can be integrated and the bulk flowrate of the pump per revolution is

$$Q = 8\pi r^2 b \left(\frac{K}{z} + \frac{K^2}{z^2} - \frac{\pi^2}{12z^2} \cos^2 \Psi \right)$$

where

K = is the ratio of addendum to module
z = number of teeth
Ψ = pressure angle
r = pitch circle
b = gear width

Paul and Makherje [3.4] derived an equation specifying the ideal flow of a "spur" gear with identical involute profile which is given by:

$$Q = 2\pi b m^2 \left[z + \left\{ 1 + \frac{\pi^2 \cos^2 \Psi}{12} \right\} \right]$$

A number of authors (3.5, 3.6, 3.7) have derived equations specifying the ideal instanteneous delivery from an involute profile gear pump. All these and the above equations are comparable.

These equations are based on the following assumptions:

(1) The gears have a contact ratio greater than one.
(2) Leakage inside the pump casing is ignored.
(3) Backlash between gears is sufficient to allow fluid to move freely between the trapped volumes.
(4) Relief grooves are positioned on the side plates of the pump such that average discharge rate is a maximum to the pump.

Now it can be shown that the ideal flowrate Q from an involute profile external gear pump having two identical involute profile is given by:

$$Q = \omega . b . m^2 . \left[1 + z \left(1 - z . \cos^2 \Psi \frac{\theta^2}{4} \right) \right] \quad \text{for} \quad -\frac{\pi}{z} \leq \theta \leq \pi \frac{\pi}{z}$$

where

ω = angular velocity of the gears (rad/sec)

b = width of the geras

m = module of the gears

n = number of teeth per gear

Ψ = pressure angle of the gear

θ = an angle of th position of the contact point of the gears along the line of action.

3.4 Gear Pump Internal Leakage

Liquid leaks from pressure to suction side around the circumference (over the tips of the teeth) and across the flat end faces of the gears, as well as beteen the meshing teeth trapped volumes. The leakage (slip) will affect the volumetric efficiency of the gear delivery and depends on the clearances between the gears and the housing gear geometry, the pressure diffierence, as well as the type of fluid being pumped.

3.4.1 Gear Tip Leakage

Consider a tooth on the driving gear of the pump, (Fig. 3.6). The leakage across the tip of the tooth Q_L is given by:

$$Q_L = Q_1 - Q_2$$

where Q_1 is the flowrate produced by the pressure drop across the tooth tip which is against the direction of motion, and Q_2 is the flowrate produced by the moment of the tooth, toward the discharge port.

The pressure around the casing of gear pumps is generally assumed to rise in a linear manner across each tooth tip, Ernst [3.8], and for a gear with a number of teeth n adjacent to the casing then the pressure drop across the tip of each of these teeth will be:-

$$\Delta P = \frac{P}{n} \text{ where P is the pressure rise across the pump}$$

The leakage due to this pressure difference ΔP and clearance h between the tooth and the casing can be represented as flow between two parallel plates, the value of Q_1 is given by:

$$Q_1 = \Delta P\ h^3\ b/12\mu$$

where h = is the clearance between the tooth and casing
b = is the width of gears
μ = is the hydraulic oil absolute viscosity.

The gear tooth tip speed has some effect on the tip leakage because it is against the direction of motion, therefore the value of Q_2 depends on the gear tip velocity u and Q_2 is given as:

$$Q_2 = bhu/2$$

where u is the velocity of the the tooth tip

hence the total leakage flowrate, Q_L, is given by:

$$Q_L = b\ \{(Ph^3/12\mu\ n) - (hu/2)\}$$

As $U = \omega R = \omega(r + a)$

where: ω is angular velocity
a is the gear addendum
r is the pitch circle.

The total leakage flowrate, Q_L, will be:

$$Q_L = b \left\{(ph^3/12\mu\ n)) - \frac{\omega rh}{2}\left(1 + \frac{a}{r}\right)\right\} \qquad (3.4.1)$$

3.4.2 Gear Tip Power Losses

The total power loss W to occur at the tip of the teeth of an external gear pump is the sum of the leaking power loss, W_1, and the viscous drag power loss, W_2, Abdallah [3.9].

The leakage power loss, W_1, per tooth space, associated with this leakage flowrate is given by:

$$w_1 = p.Q_1/n$$

Using equation (3.4.1), this may be rewritten as:

$$W_1 = \frac{bp^2 r^2}{12\mu ln^2}\left(\bar{h}^3 - \frac{6\mu\omega\, hn(1 + \bar{a})}{p}\right) \qquad (3.4.2)$$

where:

$$\bar{a} = a/r$$

$$\bar{h} = h/r$$

$$= \quad /r$$

The equation for the viscous drag force on the moving tooth tip include two terms, one is due to the pressure gradient across the tip, and the other due to the motion of the tooth tip.

As a result, the force, F, opposite the motion of the tooth tip is given by:

$$F = (bph/2n) + (b\mu u\ /h)$$

This force is moving with velocity u, therefore the viscous drag power loss, W_2, will be:

$$W_2 = \omega br^2(1+\bar{a})\left\{\frac{p\bar{h}}{2n} + \frac{\mu l\omega(1 + \bar{a}}{\bar{h}}\right\}) \qquad (3.4.3)$$

Therefore, the total power loss, W, at a tooth tip is given by $W = W_1 + W_2$, and introducing a Sommerfield number, S_o, and after simplification, the total power loss equation reduced to this form:

$$W = \frac{\omega r^2 pb}{2n} \left\{ \frac{\bar{h}^3}{6zS_o} + 2zS_o \quad (1 + \bar{a})^2 / \bar{h} \right\} \qquad (3.4.4)$$

where;

$\bar{a} = \frac{a}{R}$ = addendum of gear tooth/pitch circle radius of gear

$\bar{h} = h/R$ = clearance between tooth tip and adjacent pump casing/pitch Radius

S_o = Sommerfield number, $\mu\omega/P$

$\bar{l} = l/R$ = circumferential length of tooth tip/pitch circle Radius

The results may be presented in the form of expressing the efficiency loss of the machine as a function of both the fluid film thickness (clearance) between the casing of the machine and the tips of the gear teeth and an operating parameter which is a modified form of the Sommerfield number. As well as this power loss at each tooth tip occurs during the time at which the tooth is adjacent to the casing and the ratio of this time to the total time of operation, and it may be given approximately by n/Z where Z is the total number of teeth on one gear. Hence the mean total power loss, Wm, per tooth tip is given as:

$$W_m = \frac{b\omega PR^2 \bar{a}}{2n} \{\bar{h}^3/3S) + S\ [1 + 1/\bar{a}]^2/\bar{h}\}$$

where S = pump operating parameter $2nS_o\ \bar{a}$

It has been shown in [3.4,3.10] that the ideal mean flow, Qm, is given as:

$$Q_m = \omega.b.m.^2\ \{Z + 1 - (\pi^2 .\ \cos^2\beta)/12\}$$

Hence the power delivered per tooth space, W_T, at a speed of ω is given by:

$$W_T = PQ_m/2n \qquad (3.4.5)$$

The efficiency loss, η_L, due to the tooth tip leakage and drag losses will be given by the ratio of equation (3.8) and (3.9) multiplied by 100 and after simplification this becomes:

$$\eta_L = \frac{50Z\ \{(\bar{h}^3/35) + S\left(1 + \frac{Z}{2}\right)^2/\bar{h}\}}{\{Z + 1 - (\pi^2.\cos^2\beta)/12\}} \qquad (3.4.6)$$

In practice it will be impossible to ensure that the exact value of the tooth tip clearance giving minimum loss will be maintained during the gear operation due to production tolerance, condition of operations (speeds, pressures, oil temperature) to those prescribed. As a result it is of interest to examine the effects of changes of both $\bar{h}$ and S on the value of efficiency losses, η_L, which can help in the design calculation of the gear and its required power. This is shown in Figs.(3.7a, b) for the pump employed in this study, and for a range of values of $\bar{h}$, with specified values of η_L.

3.4.3 Side Plate Leakage

The leakage between the ends of the gears and the side plates is generally considered to form the largest proportion of the total internal leakage in the high pressure gear pumps.

According to the design the side plates are classified into three groups:

(i) fixed side plate
(ii) floating side plate
(iii) bush design side plate

First, fixed side plate designs in which the clearance between the side plate and the gear face is constant, therefore leakage proportional to pressure and for high pressure there will be more leakage and vice versa. For this kind of side plate the pump volumetric efficiency as low as 75-85% and works with maximum pressure

of 50 - 100 bar. Second, floating side plate designs in which the clearance between the side plate and the gear face is changeable and depends on the pressure load applied on the back end of the plate. The design problem is to maintain an adequate film thickness (clearance) under all conditions without the plate becoming unstable and tilting or lifting off. Pumps with this kind of design have higher volumetric efficiency (88 - 93%) than the first type of side plate.

Third, bush designs where the side plates are free slide axially but are normally prevented from tilting and it has the same design problems as in floating end plates.

The leakage flowrate can be calculated using this equation, Keller [3.11],

$$Q = \frac{\pi d b^3 \Delta P}{12 \mu L}$$

To predict this leakage flowrate, it is important to know the clearance between the side plate and the gear face. Experimental data published by Hook [3.12], for fixed and floated side plate, Fig. (3.8) is used in the program to predict the side plate leakage flowrate.

3.5 Gear Rotor Internal Performance

3.5.1 Suction Capability of Gear Pump

The suction cycle in a gear pump starts as the two gear teeth come out of mesh and ends when the tips of the following teeth come into contact with the outer body casing wall Fig.(3.6). The volumetric displacement on the inlet of the pump is a mirror image of the outlet flow of the pump, as shown in Fig. (3.9).

The agreement between the actual displacement and the theoretical prediction depends upon whether the spaces in between teeth are completely filled with fluid or not.

The difference between the theoretical and the actual delivery is called 'suction loss'.

If an atmospheric pressure is acting on the fluid, then the pressure in the suction-chamber is:

$$p_s = p_o + p_1 - p_2 - p_3 \qquad (3.5.1)$$

where:

$p_1 = \pm \rho g h$ (oil tank head)

$$p_2 = \frac{1}{2} \rho v^2 \left(\frac{\lambda}{d} + \gamma \right) \text{ (hydraulic losses)}$$

$$p_3 = \frac{\rho v^2}{2} \text{ (suction-chamber loss)}$$

The pressure available for filling-up the tooth space is:

$$p_a = p_s - p_v \qquad (3.5.2)$$

Due to centrifugal forces, the roots of the teeth are the zones of lowest pressure. The equation defining the pressure loss due to the centrifugal forces is, Hibi [3.13].

$$p_c = [1 - (R/r_i^{\,2})]\ \rho .\ (u_a)^2/2$$

where

R = radius of addendum,

r_i = radius of dedendum,

u_a = tangent velocity-measured at addendum

ρ = diameter fluid density.

If the pressure, due to centrifugal forces, (p_c) is greater than that available (p_a) in the suction chamber, then it will not be possible for the tooth space to be completely filled. This will encourage cavitation to exist in the system.

On the other hand, when a pair of teeth come out of mesh and are ready for induction of fluid, the space between the teeth and the following pair is in contact with the inlet line over a limited angle. This could be as little as 30°. For a pump speed of 2500 rpm, the corresponding time for this space to open is 2 ms, which may be insufficient for the complete filling. For that, the time τ required for covering an arc length s, greater than the time τ_o required by the fluid for filling-up the tooth space is:

$$\tau \geq \tau_o$$

$$\frac{s}{u_a} \geq \frac{h}{u} = \frac{2m}{u} \qquad (3.5.3)$$

where

m = module

v = average speed of fluid

u_a = peripheral speed at addendum ($=\omega R$)

Zalka etal [3.14] demonstrated that the inlet chamber of a gear pump could be change in order to extend the angle of entry which would improve the pump suction performance considerably. However, such an approach seems to have been ignored by pump manufacturers because of production difficulties.

The speed of the fluid at which the tooth groove gets fitted is given by, [3.14].

$$v = \sqrt{\rho p_a - \frac{2}{3} R\omega^2 X + \frac{1}{4} \omega^2 X^2} \qquad \text{for } 0 \leq X \leq 2m \qquad (3.5.4)$$

From this brief explanation it is easy to understand that the suction of a gear pump should have better performance when the suction chamber is modified to allow more time for the tooth groove to get filled.

3.5.2 Calculation of the Distribution of Pressure Around the Gear Pump Casing

The distribution of pressure is calculated in two stages. Firstly, by calculating the values of the instantaneous pressure in each gear tooth, and secondly by using these values as starting values for itreative techniques to find the actual pressure in each point around the pump.

The first stage of calculation is carried out under the assumption that the hydraulic oil is incompressible and there is no slip between the gear face and the side plate. The other assumption means that the hydraulic oil passing across the leading tooth space gear tip is equal to the oil flow across the rear tooth space gear tip. This slip is the net of the slip due to the pressure difference between the gear tooth spaces and the entrained slip due to the fluid which adhers to a moving tooth tip. The flow passing the gear tip is treated as a flow between parallel plates. If h is the clearance between the gear tip casing at an angle of rotation, and a particular gear tooth, z, a pressure difference, Δp, the slip is given by:

$$Q_1 = \frac{h^3 . \Delta p . b}{12 \mu L} \qquad (3.5.5)$$

The entrained leakage for the same tooth is given by:

$$Q_e = \frac{h.u.b}{2} \qquad \text{where } u = \text{gear tip velocity}$$

The net flow is:

$$Q = \frac{h^3 . \Delta p . b}{12 \mu L} - \frac{h.u.b}{2} \qquad (3.5.6)$$

From the above equations:

$$\Delta p = \left[\frac{Q}{b} + \frac{hu}{2} \right] \frac{12 \mu L}{h^3} \qquad (3.5.7)$$

The total pressure drop is the summation of the pressure drop for each gear tip

$$p_{out} - p_{in} = \sum_{n=1}^{n=z} \Delta p_n \qquad (3.5.8)$$

where

z = the number of teeth is sealing with the pump casing.

$$\sum_{n=1}^{n=z} \Delta p_n = \frac{Q}{b} 12\mu L \sum_{n=1}^{n=z} \frac{1}{h^3} + 6u\mu L \sum_{n=1}^{n=z} \frac{1}{h^2} \qquad (3.5.9)$$

then:

$$Q = \frac{b}{12\mu L} \left\{ \frac{(P_{out} - p_{in}) - 6u\mu L \sum_{n=1}^{n=z} \left(\frac{1}{h^2} \right)}{\sum_{n=1}^{n=z} (1/h^3)} \right\} \qquad (3.5.10)$$

and, Δp will be:

$$\Delta p = \left\{ \frac{(P_{out} - p_{in}) - 6u\mu L \sum_{n=1}^{n=z} \left(\frac{1}{h^2} \right)}{h^3 \sum_{n=1}^{n=z} (1/h^3)} \right\} + \frac{6n\mu L}{h^2} \qquad (3.5.11)$$

with the values of p_n for each gear tip and the values of inlet and outlet presures, the pressure in each space can be determined.

3.5.3 Pressure Pulsation in the Delivery Line

The pump in a circuit generates a complex but a period ripple in its flow output. This flow ripple then reacts with the circuit to produce a pressure ripple whose magnitude and distribution, is dependent on the acoustic impedance of all the components in the system. The mathematical model used to describe the relationship between pressure and flow is based on a solution of the wave equations for one dimensional ideal flow. These equations are, [3.15], :-

$$c^2 \frac{\partial^2 p(x,t)}{\partial x^2} = \frac{\partial^2 p(x,t)}{\partial t^2} \qquad (3.5.12)$$

$$c^2 \frac{\partial^2 q(x,t)}{\partial x^2} = \frac{\partial^2 q(x,t)}{\partial t^2} \qquad (3.5.12)$$

where c = wave propagation velocity in the system

$p(x,t)$ = pressure in the system as a function of position and time.

$q(x,t)$ = flow in system as a function of position and time

x = distance along pump's delivery line

t = time after commencement of flow.

The solution adopted was in the form of a converging series. The general form of this model is:

$$p(x,t) = \frac{z_s . z_o .}{z_s + z_o} \Big\{ q_o\ [t-x/c] + \rho_s q_o\ [t-(2L-x)/c]$$

$$+ \rho_s . \rho_T . q_o\ [t-(2L+x)/c] + \rho_s / \rho_T^2 . q_o\ [t-(4L-x)/c]$$

$$+ \rho_s^2 . \rho_T^2 . q_o\ [t-(4L+x)/c] + \rho_s / \rho_T^2 . q_o\ [t-(6L-x)/c]$$

$$+ \rho_s^3 . \rho_T^3 . q_o\ [t-(6L+x)/c] + --- \Big\} \qquad (3.5.14)$$

In idealised circuits, Bows and McCandlish [3.16], shows an equation based on that model which calculates the pressure, p, at any point, x, along a pipeline connected to a positive displacement pump as:

$$p = \frac{Q_s z_s z_o}{z_s + z_o} \cdot \left(\frac{e^{-\alpha x} e^{-jwx/c} + \rho_T e^{-\alpha(2L-x)} e^{-jw/c(2-x)}}{1 - \rho_s \rho_T e^{-2\alpha L} e^{\frac{-j2wL}{c}}} \right) \qquad (3.5.15)$$

The equation for the acoustic pressure, p, at the pump outlet (i.e., x=0) becomes as:

$$p = \frac{Q_s z_s}{1 + \frac{z_s}{z_o}} \qquad (3.5.16)$$

where:

$$\rho_s = \frac{z_s - z_o}{z_s + z_o}$$

$$\rho_T = \frac{z_T - z_o}{z_T + z_o}$$

$$z_o = (4.\rho.c) / (\pi.d^2)$$

z_s = source impedance

z_T = impedance of the system's load valve

ρ = fluid density

c = sound velocity

ρ_s = source reflection coefficient

ρ_T = termination reflection coefficient.

3.6 Trapping Fluid in a Gear Pump

3.6.1 Introduction

Gear pumps, which are generally used as a power source in hydraulic systems, usually have a contact ratio greater than one. This leads to a periodic trapping of fluid in the space enclosed by the contacting teeth surfaces of the driving and driven gears, as seen in Fig. (3.10).

The volume trapped between the gear teeth gradually reduced as the gear rotates, hence pressurising the oil in this space, sometimes as high as 6-8 times the working pressure, Stupa (3.17). This high

pressure in the inter-tooth space can, on occasion, cause failure of some of the pump components, for example, the bearing. Such failure can result from the application of this high pressure load as a periodic load. Similarly, this very high pressure generates vibration and noise.

In order to avoid, or minimise, the pressure rise in the trapped volume, relief grooves are provided in the side plates. The design and position of these relief grooves has a great influence on the performance of the gear pump. For example, they can increase the leakage which in turn decreases the volumetric efficiency of the gear pump.

At the present time there is no unique design to define the position, or geometry, of the relief groove. In order to decide the optimal position of the relief grooves it is necessary to study and clarify the pnenomenon by which the volume of working fluid is trapped. For such a study it will obviously be necessary to measure the pressure in the trapped space, and to examine the effect of the experimental variables on the trapping phenomenon.

3.6.2 Trapped Volume Analysis

Previous analytical studies conducted with the objective of determining the maximum pressure developed in the tooth space, were based on the assumption that the liquid in the trapped volume is not forced out through the clearances, but only compressed under the action of external forces. However, in practice the oil is partially compressed, and partially forced out through any clearance existing around the trapped volume.

Therefore, the pressure in the trapped volume can be determined by calculating the rate of change of the trapped volume, with allowance for the clearance flowrate. The variation of the trapped volume can be determined as a function of the contact condition of the two gears. There are two cases of contact condition depending upon the position of the contact point on the contact line. These contacting conditions, as shown in Fig. 3.10, are repeated every $(2\pi/z)$ of the shaft position. Since there are ten gear teeth in the present case, each contacting condition is repeated every 36°.

3.6.2.1 Single Point Contact (No backlash)

When a single pair of teeth are in contact, as shown in Fig. 3.11, a semi-trapped volume will exist between the points A and B, and the restriction (backlash) formed by the back face of the gears. This semi-trapped volume will be separated into two volumes V_1 and V_2 for a zero, or very small, backlash.

The magnitude of these semi-trapped volumes V_1 and V_2 are a function of gear position, and the variation in this magnitude is expressed by the following equations, due to Ichikawa, (3.18):-

$$V_1 = V_{01} + 0.25b\, P_n^2 \left(\frac{z}{\pi}\right) \left(\theta - \frac{0.5\pi}{z}\right)^2 \quad \theta_{s1} \leq \theta \leq \theta_{f1} \qquad (3.6.1)$$

$$V_2 = V_{02} + 0.25b\, P_n^2 \left(\frac{z}{\pi}\right) \left(\theta + \frac{0.5\pi}{z}\right)^2 \quad \theta_{s2} \leq \theta \leq \theta_{f2} \qquad (3.6.2)$$

where

V_{01}, V_{02}	are the minimum volumes of each trapped space respectively
P_n	is the normal pitch of the gears
$\theta_{s1,2}$	are the starting angular points of trapping
$\theta_{f1,2}$	are the finishing angular points of trapping

Equations (3.5.1), (3.5.2) are shown graphically in Fig. 3.12 and 3.13 respectively by solid curves.

When the pump is operating, a high and low level of pressure may be generated inside this space unless it is adequately relieved.

3.6.2.2 Double Tooth Contact

In gears generally, in order to ensure a positive drive between meshing gears, a gear contact ratio grater than unity is required. Such a case exists in the gear pump when both teeth are contacting each other at the two points A, B. Fig. 3.14 shows the gear configuration during double contact. It can be seen from Fig. 3.14

that during double contact two semi-trapped volumes are formed between A and B. In practice, backlash between the gears allows fluid to move relatively freely between these volumes and these two volumes V_1, V_2 function as one full-trapped volume $V(=V_1 + V_2)$.

The variation in the trapped space is expressed by the following equation (3.19):

$$V = V_0 + 0.5b\ P_n^2 \left(\frac{z}{\pi}\right)\left(\theta - \frac{0.5\pi}{z}\right)^2 \quad \theta_s < \theta \leq \theta_f \qquad (3.6.3)$$

This variation in the trapped volume is shown in Fig. 3.15 and it is clear that the periods when double contact and a fully-trapped volume exist, are shorter and the volume compressed is smaller than for single contact (Fig. 3.16).

3.6.3 Measuring of v_o, v_{o1}, v_{o2}

The minimum volumes v_o, v_{o1}, v_{o2}, of each trapped space are difficult to evaluate analytically as no equation to describe such a volume exists. these volumes depend on the cutting process, the cutter shape and the gear-tooth form. Historically they were measured using an enlarged drawing and a planimeter. However, this method is not accurate enough as it needs a precise drawing as well as different positions of meshing. Nevertheless, a new method was adopted in this investigation by generating a model of the gears under consideration. The tooth form was predicted by using the enlarged image of the actual tooth. This was achieved by measuring the x,y coordinates after enlarging the image 50 times its original form (see Plate 3.1). The data of the tooth form was then fed to an in-house software package Unigraphics II (which is a second generation of CAD/CAM/CAE system from McDonnel Douglas, it offers advanced interactive graphics facilities with applications in many phases of the product development cycle).

Similarly, this generated gear was copied to form a second identical gear wheel and conjugated with the first predicted one at a specified angle of meshing (the point of contact being on the pitch circle). Then, by rotating the two gears at equal angular intervals, the area

of the trapped space was measured. By employing equations (3.6.1,2,3), the values of v_o, v_{o1}, v_{o2}, were calcualted and compared with those predicted from the analytical model if the two gears were rotated at the specified angle. The two results agree quantitatively (see Fig. 3.16).

3.6.4 Pressure Equations of the Trapping Fluid

In this section the general pressure equation for a viscous compressible fluid is developed. The first sub-section develops the equation for a general control volume.

3.6.4.1 General Compressible Pressure Equation

Consider a quantity of fluid having an absolute density ρ and volume v.

The mass M is given by:

$$M = \rho v \tag{3.6.4}$$

Differentiating the equation (3.6.4) with respect to a time t gives:

$$\frac{dM}{dt} = \rho \frac{dv}{dt} + v \frac{d\rho}{dt} \tag{3.6.5}$$

The isentropic bulk modulus β is defined:

$$\beta = \rho \frac{dp}{d\rho} \tag{3.6.6}$$

The mass flow rate into the control volume is related to the flow across the boundary by:

$$\frac{dM}{dt} = \rho(Q_{in} - Q_{out}) \tag{3.6.7}$$

where Q_{in} and Q_{out} are the flow in and out of the control volume.

Equating equations (3.5.2) to (3.5.4) and re-arranging gives:

$$Q = \frac{dv}{dt} + \frac{v}{\rho}\frac{d\rho}{dt} \qquad (3.6.8)$$

where $Q = Q_{in} - Q_{out}$

substituting equation (3.6.6) and (3.6.8) and re-arranging gives:

$$\frac{dp}{dt} = \frac{\beta}{v}\left(Q - \frac{dv}{dt} \right) \qquad (3.6.9)$$

The angular velocity ω is given by:

$$\omega = \frac{d\theta}{dt}$$

where θ is the angular position.

By using the above relationship, pressure equation with respect to angular position is obtained:

$$\frac{dp}{d\theta} = \frac{\beta}{\omega v}\left(Q - \omega \frac{dv}{d\theta} \right) \qquad (3.6.10)$$

By employing equation (3.6.10) to the pressure in the inter-tooth space of a metering gear pump, the variable Q, has two components. They are the flow of liquid from the enclosed volume through the end gaps at the inlet and exit from the pump. They can detrmine by the following equation:

$$Q_1 = \frac{b_1 h^3 \Delta p}{12 \mu l}$$

where b_1 is the slot width; h is the slot clearance, Δp is the pressure drop; μ is the viscosity of the liquid, and l is the slot length.

As applicable to this case, assuming $b_1 = 2.5m$ (wehere m is the engagement modulus) and $l = Km$, the flowrate of liquid to the inlet Q_1 is,

$$Q_1 = \frac{2.5\ h^3}{12\mu K}(p - p_{in}) \qquad (3.6.11)$$

similarly

$$Q_2 = \frac{2.5\ h^3}{12\mu K}(p - p_{out}) \qquad (3.6.12)$$

where h is the end plate clearance, P_T is the pressure in the enclosed volume (trapped space), p_{in} is the inlet pressure p_{out} is the delivery pressure, K is the equivalent length coefficient of the end plate clearance.

If the gears are located symmetrically relative to the side plates (Fig. 3.17), then by applying the condition of stream continuity, Q, will be:

$$Q_{out} = 2Q_1 + 2Q_2 \qquad (3.6.13)$$

By substituting equations (3.6.11) and 3.6.12) into equation (3.5.13) and re-arranging gives

$$Q_{out} = \frac{5h^3}{12\mu K}(2p - p_{in} - p_{out}) \qquad (3.6.14)$$

Because there is no flow into the control volume (trapped space),

$\therefore Q = -Q_{out}$

substituting equation (3.6.14) into equation (3.6.10) gives a general equation for the trapped space pressures as:

$$\frac{dp}{d\theta} = \frac{\beta}{\omega v}\left[\left(\frac{-5h^3}{12\mu K}(2p - p_{in} - p_{out})\right) - \omega\frac{dv}{d\theta}\right] \qquad (3.6.15)$$

3.6.4.2 Pressure of Trapped Oil at Single Point Contact

When the backlash is very small, the semi-trapped volumes are given as v_1, v_2 as it is explained in section (3.6.2.1), and its variation is

given by equation (3.6.1) and (3.6.2) respectively. By differentiating these equations with respect to θ gives:

$$\frac{dv_1}{d\theta} = 0.5bp_n^2\left(\frac{z}{\pi}\right)\left(\theta - \frac{0.5\pi}{z}\right) \quad \theta_{s_1} \leq \theta \leq \theta_{f_1} \qquad (3.6.16)$$

and,

$$\frac{dv_2}{d\theta} = 0.5bp_n^2\left(\frac{z}{\pi}\right)\left(\theta + \frac{0.5\pi}{z}\right) \quad \theta_{s_2} \leq \theta \leq \theta_{f_2} \qquad (3.6.17)$$

Substituting equation (3.6.16) and (3.6.17) into equation (3.6.15) gives:

$$\frac{dp_1}{d\theta} = \frac{\beta}{\omega v}\left(\frac{-5h^3}{12\mu K}(2p_1 - p_{in} - p_{out}) - 0.5bp_n^2\omega\left(\frac{z}{\pi}\right)\left(\theta - \frac{0.5\pi}{z}\right)\right) \qquad (3.6.18)$$

and, similarly,

$$\frac{dp_2}{d\theta} = \frac{\beta}{\omega v}\left(\frac{-5h^3}{12\mu K}(2p_1 - p_{in} - p_{out}) - 0.5bp_n^2\omega\left(\frac{z}{\pi}\right)\left(\theta + \frac{0.5\pi}{z}\right)\right) \qquad (3.6.18)$$

Solving equation (3.6.18) and (3.6.19), the pressure at the trapped space can be predicted analytically at different angular positions.

To solve these equations it is necessary to simplify the equations, in terms of constant for the independent variables, and, by assuming that:

$$C_1 = \frac{\beta}{\omega v} \; ; \; C_2 = 0.5\,\omega b p_n^2 \; ; \; C_3 = \frac{z}{\pi} \; ; \; C_4 = \frac{5h^3}{12\mu K}$$

and $C_5 = p_{in} + p_{out}$; equation 3.6.18 will be:

$$\therefore \quad \frac{dp_1}{d\theta} = C_1\left[-C_4\left(2p_1 - C_5\right) - C_2C_3\left(\theta - \frac{0.5}{z}\right)\right]$$

after simplification the equation becomes:

$$\frac{dp_1}{d\theta} = A\theta - Bp_1 + C \qquad (3.6.20)$$

Integrating equation (3.6.20) will give p_1 as:

$$p_1 = A\left(\frac{(B\theta-1)}{B^2}\right) + \frac{C}{B} + C_I e^{-B\theta} \qquad (3.6.21)$$

where:

$A = -C_1 C_2 C_3$

$B = 2\ C_1 C_4$

$C = 0.5C_1 C_2 + C_1 C_4 C_5$

C_I = Integral constant

similarly, p_2 will be

$$p_2 = A\left(\frac{(B\theta - 1)}{B^2}\right) + \frac{C}{B} + C_I\ e^{-B\theta} \qquad (3.6.22)$$

where A, B, C_I are similar as for p_1, but C for p_2 is

$$C = C_1 C_4 C_5 - 0.5C_1 C_2$$

3.6.4.3 Presure of Trapped Oil at Two Points of Contact

In the case where the trapepd spaces considered as one space ($\nu=\nu_1+\nu_2$), when the backlash size is large, the angular range of trapping is narrow and the amount of volume compressed is small.

The variation of trapped space is expressed in the following equation:

$$\nu = \nu_o + 0.5bp_n^2 \left(\frac{Z}{\pi}\right)\left(\theta - \frac{\pi}{Z}\right)^2 \quad (\theta_s \leq \theta \leq \theta_f)$$

$$\frac{d\nu}{d\theta} = bp_n^2 \left(\frac{Z}{\pi}\right)\left(\theta - \frac{\pi}{Z}\right) \qquad (3.6.23)$$

Substituting equation (3.6.23) into the general equation (3.6.15) and re-arranging gives:

$$\frac{dp}{d\theta} = \frac{\beta}{\omega v}\left(-\omega b p_n^2\left(\frac{Z}{\pi}\right)\left(\theta - \frac{\pi}{Z}\right) - \frac{5h^3}{12\mu K}(2p - p_{in} - p_{out})\right)$$

by assuming; $C_1 = \frac{\beta}{\omega v}$, $C_2 = \omega b p_n^2$, $C_3 = \frac{Z}{\pi}$, $C_4 \frac{5h^3}{12\mu K}$

and $C_5 = p_{in} + p_{out}$

$$\therefore \quad \frac{dp}{d\theta} = C_1 C_2 - C_1 C_2 C_3 \theta - 2C_1 C_4 p + C_1 C_4 C_5 \qquad (3.6.24)$$

After simplification equation (3.6.24) will become as:

$$\frac{dp}{d\theta} = A\theta - Bp + C \qquad (3.6.25)$$

$$A = -C_1 C_2 C_3 , \; B = 2C_1 C_4 \text{ and } C = C_1 C_2 + C_1 C_4 C_5$$

and, after integration equation (3.6.25) will give the pressure at the trapped space as:

$$p = \frac{A(B\theta - 1)}{B^2} + \frac{C}{B} + C_I e^{-B\theta} \qquad (3.6.26)$$

3.6.5 Results and Discussions

It is vital to verify the new expressions, describing the pressure in the trapped space as they are based upon rigorous mathematical derivations and assumptions. The theoretical pressure waveform calculated for the case of two points of contact (when the backlash size is large) is presented in figs. (3.18 - 3.22). These results show the variation of the trapped pressure with the angular position at different rotational speeds and delivery pressures, and that the peak pressure occurs at the angle of the maximum trapped volume. However,

one interesting point is that the pressure generated at the suction side has a negative value of pressure. The advantage of this is to increase the suction capability by having a pressure difference which will increase the filling efficiency of the teeth. On the other hand, this negative pressure will create cavitation and some disolved air will be released, thus the time for recovery will be small and will create a void in the tooth space. These voids will be compressed during the pumping action and it will collapse at the delivery side (i.e. when the oil vapour will condensate due to the high pressure at the delivery side). This phenomenon is seen in gear boxes (3.20), and it can damage the oil or the working component.

When the backlash size is small, an extremely high pressure will occur in the trapped spaces, and will reach several hundred MPa. Table (3.1) shows the results published by Stupa (3.21) compared with the predicted values calculated by the derived expression. Good agreement between the two results are experienced.

TABLE 3.1 - Experimental Results Compared with the Predicted Values of the Trapped Pressure

Type of Pump	backlash mm	ΔP (MN) Experiment Res.	ΔP (MN) Predicted Res.	% error
21 Nsh	0.068	176.3	182.8	3.6%
21 Nsh - 1,2K3	0.020	186.5	192.2	3.05%
11 Nsh - 1,8A3	gapless	477.0	501.5	5.03%

However, as the backlash size becomes greater, the pressure rise in the trapped space becomes lower. Fig. (3.23) shows the theoretical predictions compared with the corresponding experimental results published by Yanada [3.19]. The two results agree quantitatively.

Therefore, when designing gear pumps it is necessary to take into account the fact that the large backlash is necessary. Moreover, the contact length and the normal pitch must be kept to a minimum in order to avoid a high peak pressure (which may lead to the jamming and breakdown of the pump and/or the bearings), as well as to avoid a negative suction pressure (which may lead to cavitation and erosion).

3.7 Conclusions

Some useful conclusions may be drawn from the analysis introduced in this Chapter.

The theoretical equations describing the ideal discharge flowrate of involute profile external gear pumps with spur gears have been clarified and become well established.

The leakage inside the gear pump has carefully been studied. Due to the absence of the complete measurements of the tip power losses, an analytical expression for the efficiency losses, η_L, resulting from tip leakage and drag losses has been presented in a way which is useful for the calculation of the optimum design of gear pumps, as a function of the gear operating conditions and gear tip clearances.

This part of the work, which also represents a full investigation of the effect of the trapped oil on the pressure generated in the inter-tooth space, has been employed for the first time for the derivation of an expression to calculate the pressure in terms of gear geometry and operating conditions and it gives good results compared with published work.

Other aspects of gear pump theory given in the literature such as presure distribution around the gear rotor, suction capability, pressure and flowrate pulsation, have been examined in order to provide a complete package for gear pump design and performance.

REFERENCES

[3.1] BROWN, D., 'Roloid pump gears, Mech. World. V80,p260, 1926, David Brown & Sons Ltd.

[3.2] MENSHIKOV, N.H., 'On the calculation of gear pumps'. Soviet Kotloturbostroenie, 1938.

[3.3] HADEKEL, 'Displacement pumps and motors'. Pitman and Son, 1951.

[3.4] PUAL, A.K., McKHERJEE, B.C. BHATTACHARYYA, A., 'Analysis of gear pump'. I.E.(I)Journal, ME.Vol.52, May 1972.

[3.5] MELDHAL, A., 'Theory of gear pumps, Brown Boveri Review, 1939, Vol.26,No.11/12, 259-261.

[3.6] ICHIKAWA, T., 'Characteristics of internal gear pumps'. Bull. JSME, 1959, Vol.2, No.5, 35-39.

[3.7] YUDIN, E.M., 'Gear pumps. Principal parameters and their calculation'. Translation from Russian by E. Harres. Ed. Joseph Luces Ltd. (National Lending Library for S.C. and Tech. Yorkshire).

[3.8] ERNST, W., 'Oil hydraulic power and its industrial applications'. McGraw-Hill Book Co., New York, 4th Ed.,1960.

[3.9] ABDALLAH, Y.A.G., READ, A.G., and TURNBULL, D.E., 'Conditions for minimum tooth tip losses in external gear pumps'. Paper D1, 6th International Fluid Power Symposium, BHRA, 1981.

[3.10] WILLEKENS, F.A.M., 'Fluid-borne noise in hydraulic systems'. Proc. First European Fluid Power Conf., 1973, Paper No.28, N.E.L. Glasgow.

[3.11] KELLER, G.R., 'Hydraulic system analysis'. Published by Editors of Hydraulic & Pneumatic Magazine, December, 1974.

[3.12] HOOK, C.J. and KOC, E., 'End plate balance in gear pumps. Proc., Inst.Mech.E. Vol.198B, No.2, pp55-60.

[3.13] HIBI, A., IBUKI, T., and YOKOTE, H., 'Suction performance of axial piston pump', (1st report). Bulletin of JSME. Vol.20,No.139, Jan.1977.

[3.14] ZALKA, A., and LATRANYI, J., 'Suction capability and cavitation of gear pumps'. 2nd Fluid Power Symposium, Paper H3. Guildford, England, 4-7 Jan. 1971.

[3.15] STREETER, V.L., 'Handbook of fluid dynamics'. McGraw-Hill Book Company, 1961.

[3.16] BOWS, D.E., EDGE, K.A., and McCANDLISH, D., 'Factors effecting the choice of standard method for the determination of pump pressure ripple'. I.Mech.E. Conf. Quiet Oil Hydraulics, London, Oct.1980.

[3.17] STUPA, V.I., 'Analytical determination of the pressure in the inter-tooth space of a metering gear pump'. Translated from Khimicheski Volokan, No.2, pp53-55, March-April, 1984.

[3.18] ICHIKAWA, T., 'Gear Pump (in Japanee) Nikkan Kogyo, Shimbunsha), 1962.

[3.19] YANADA, H., and ALCHIKAWA, T., 'Study of the trapping of fluid in a gear pump'. Proc.Inst.of Mech.E., Vol.201, No.A1, pp39-45.

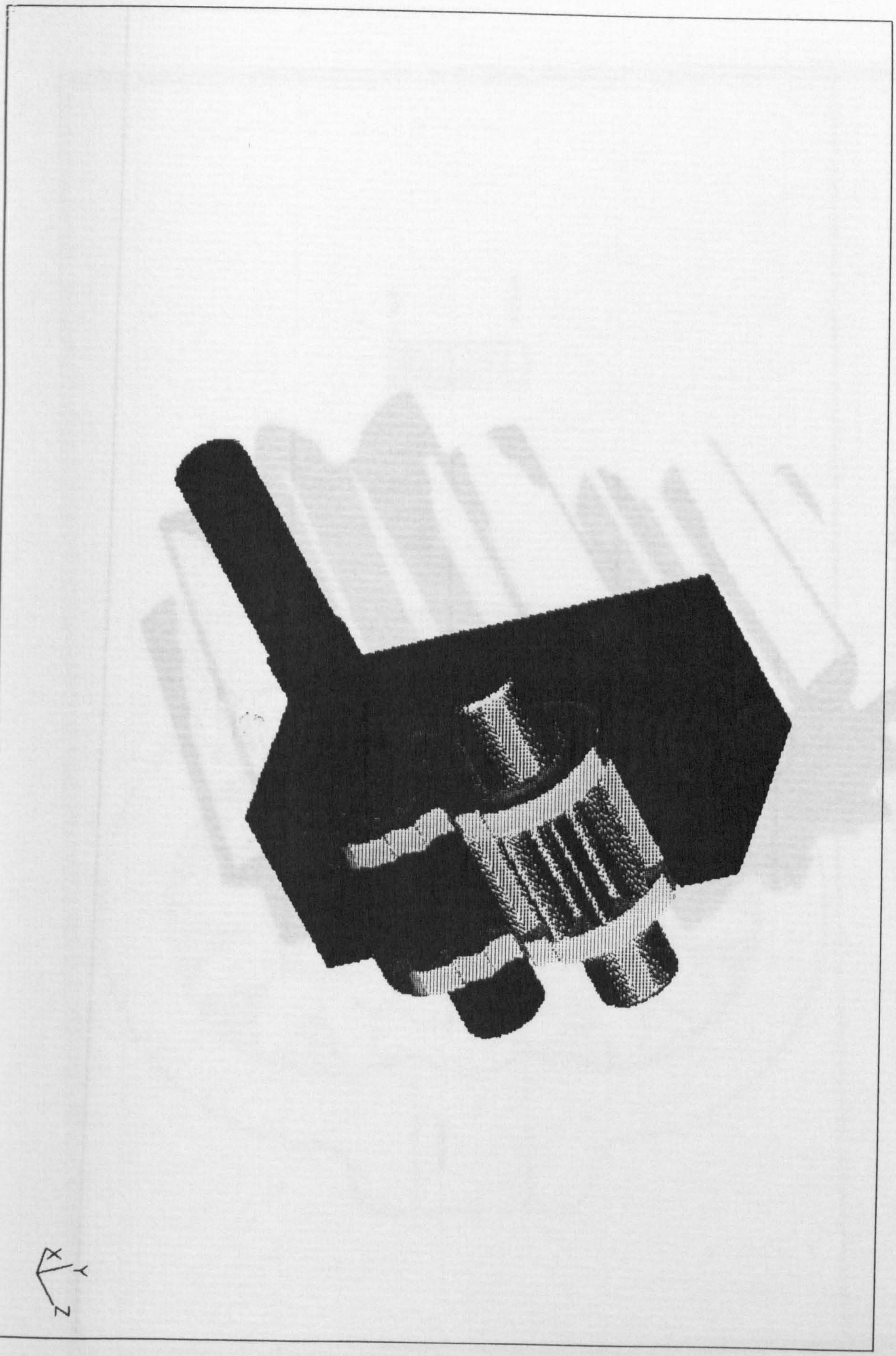

FIG.3.1 A


B

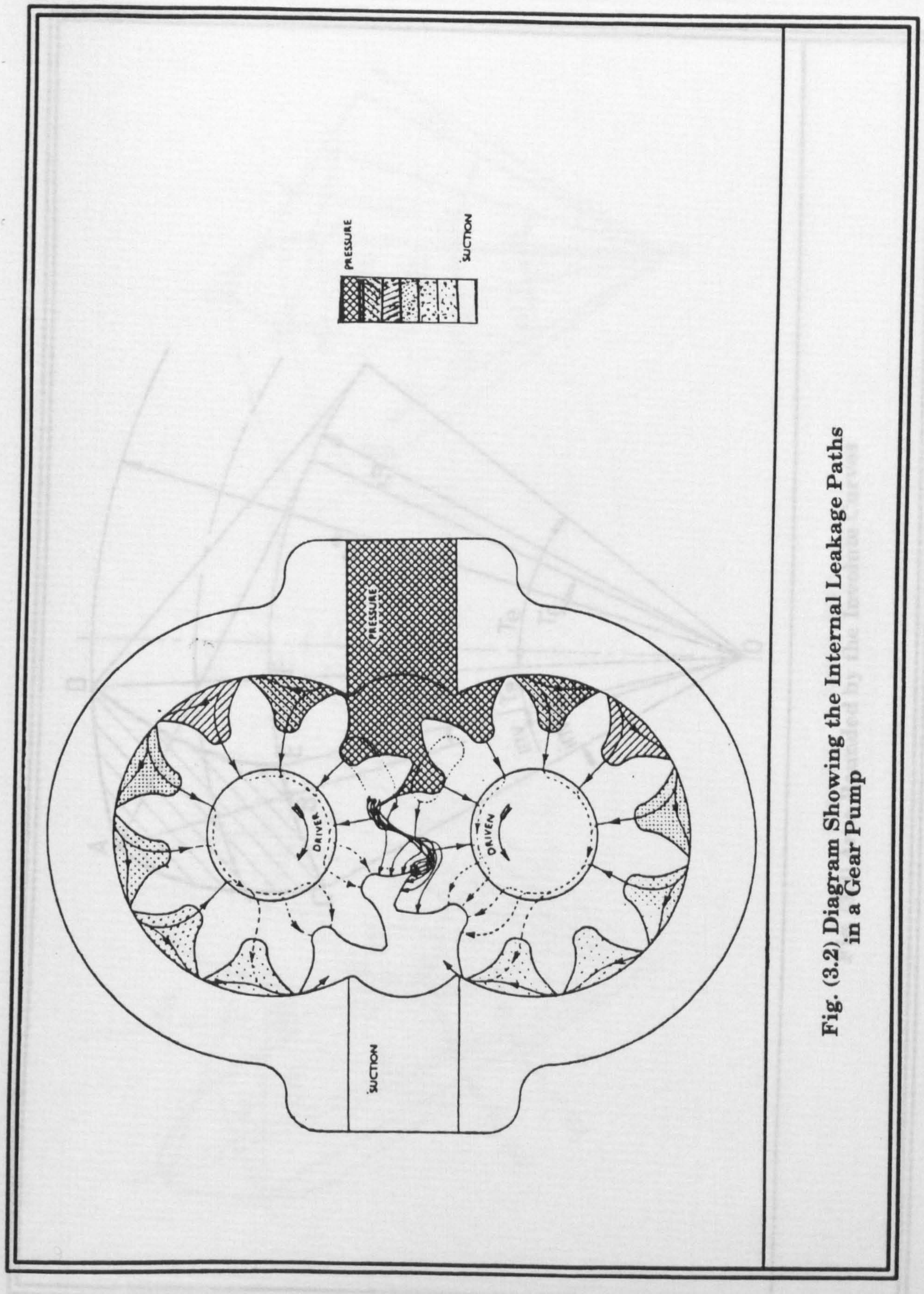

Fig. (3.2) Diagram Showing the Internal Leakage Paths in a Gear Pump

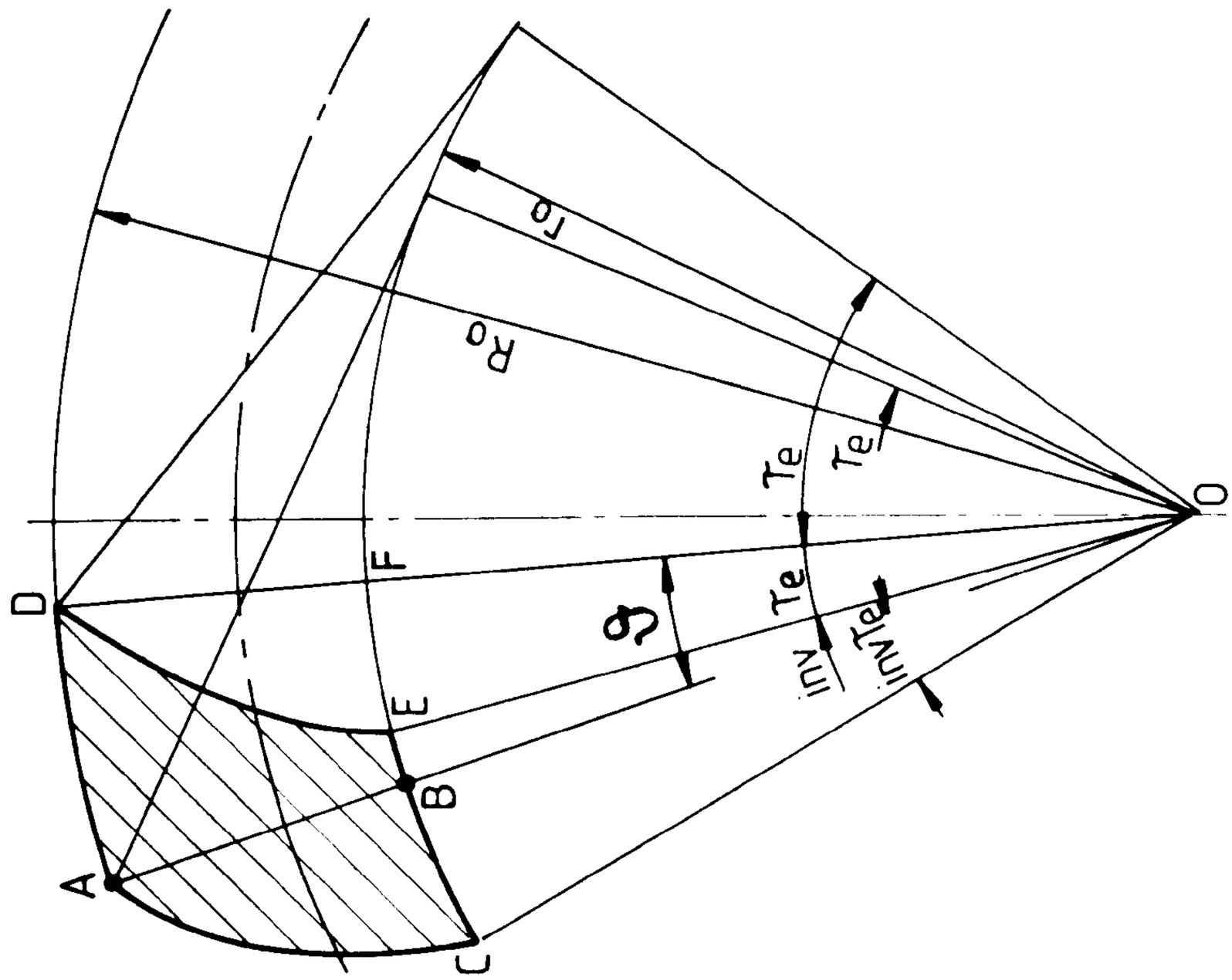

Fig. (3.3) Area Bounded by the Involute Curves

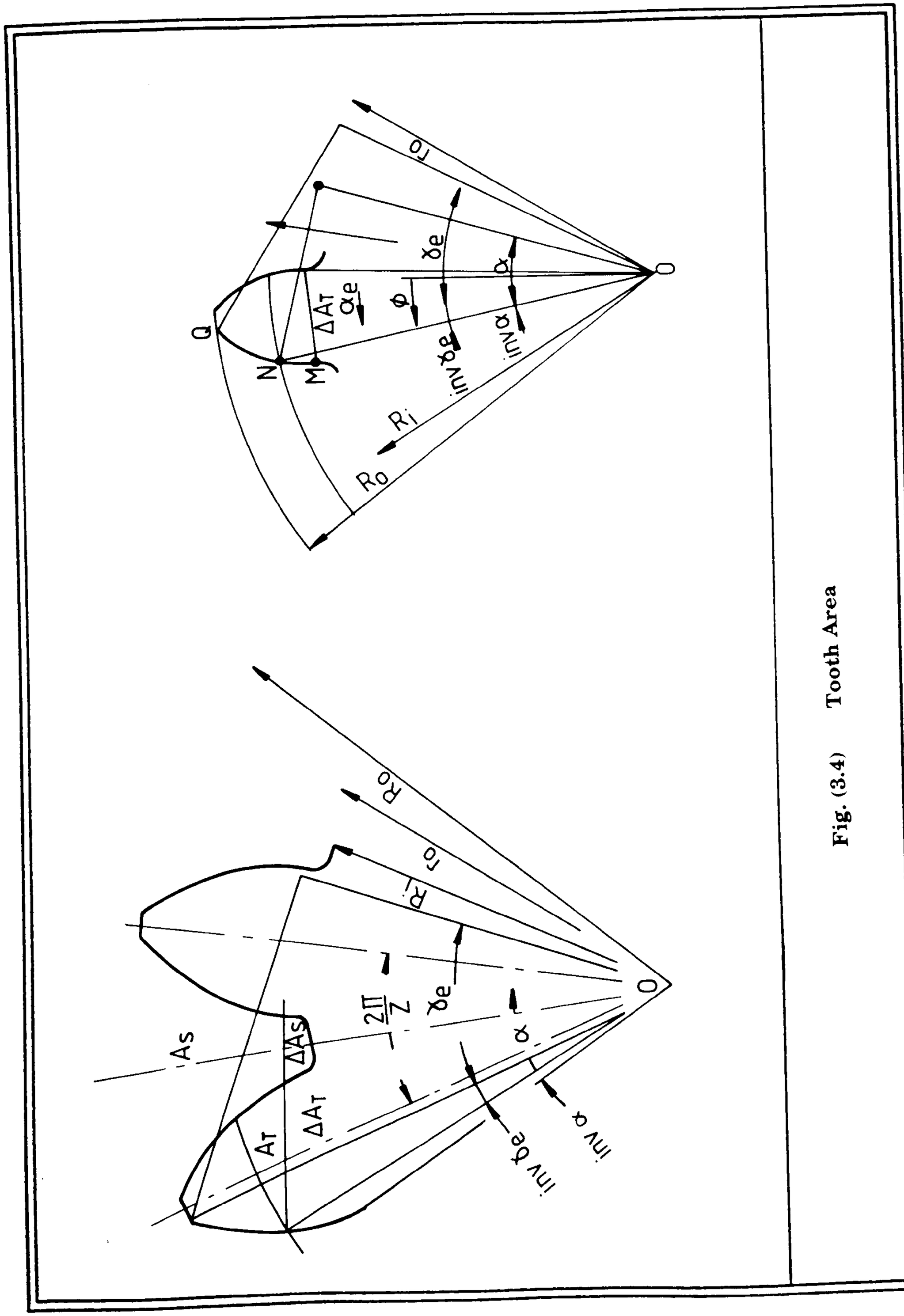

Fig. (3.4) Tooth Action Area

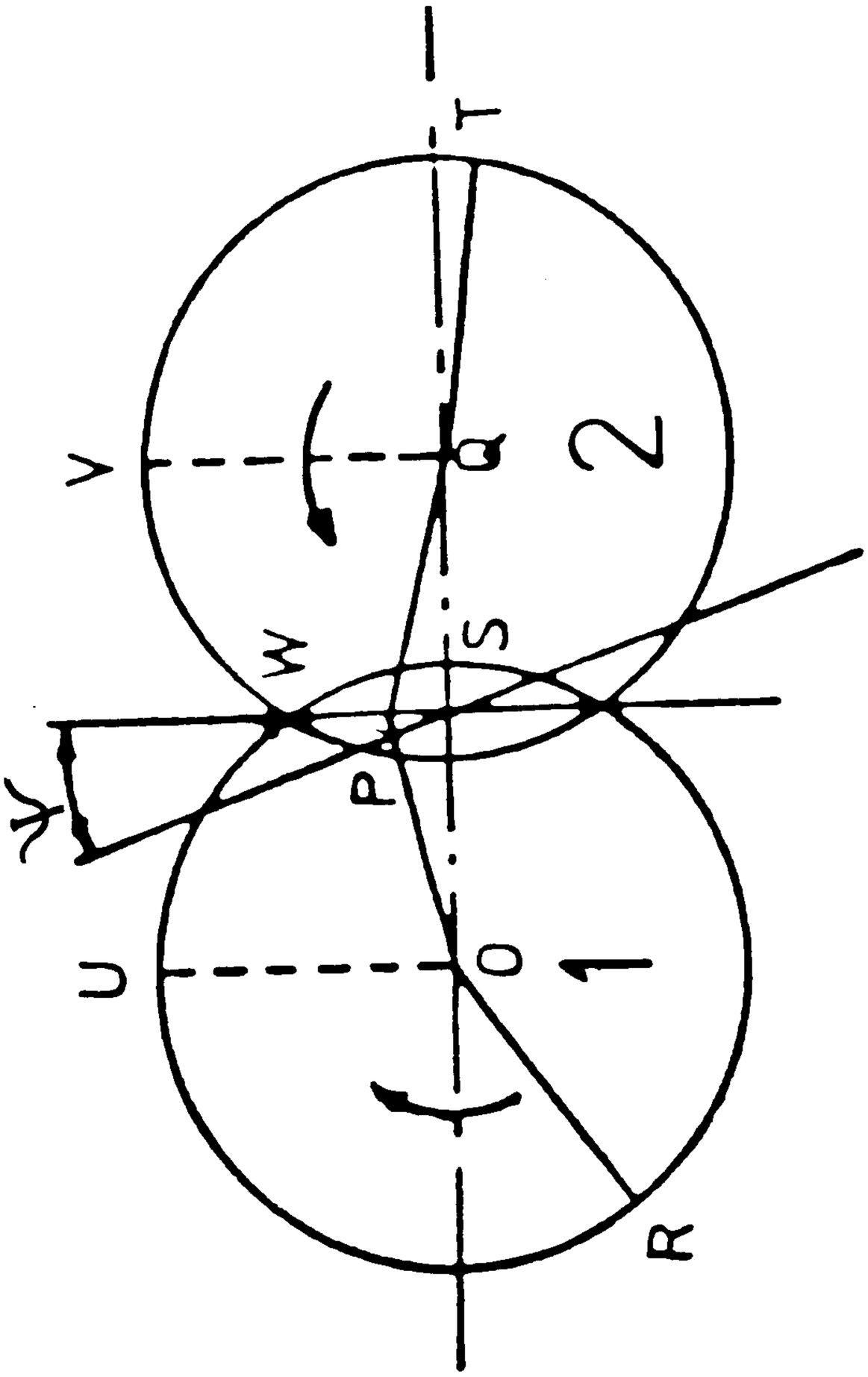

Fig. (3.5) Gear Pump Mesh Flow rate

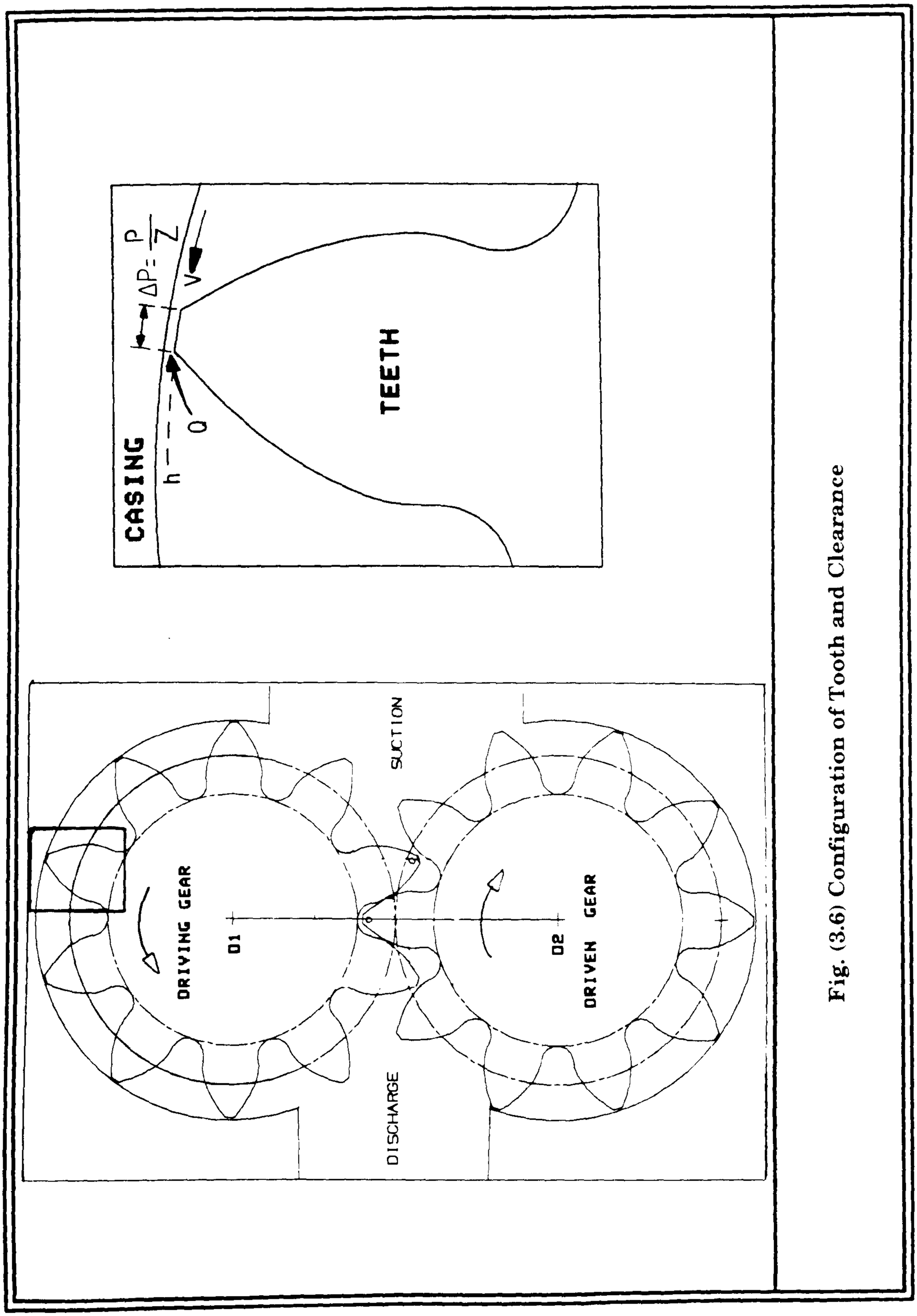

Fig. (3.6) Configuration of Tooth and Clearance

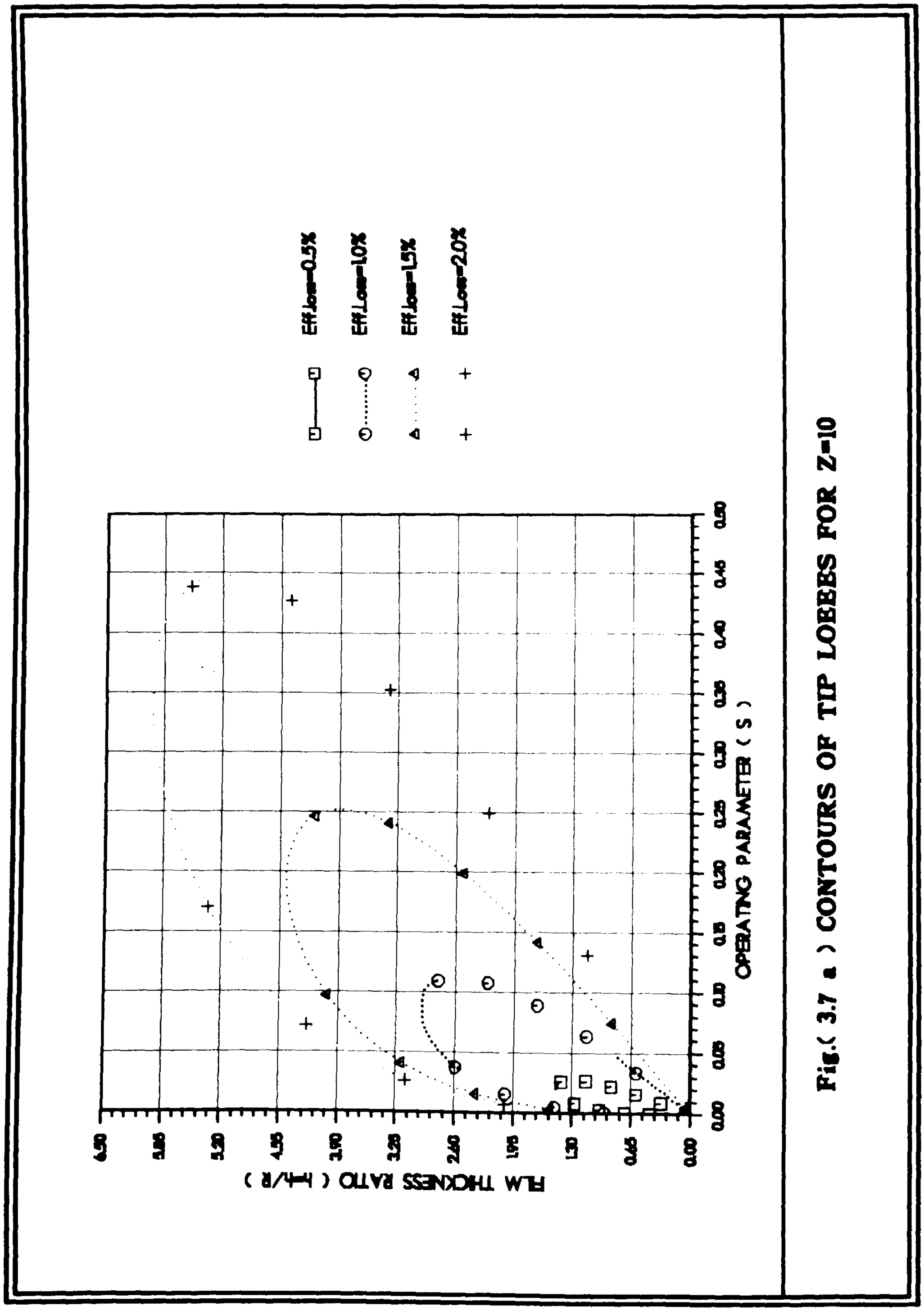

Fig.(3.7 a) CONTOURS OF TIP LOBES FOR Z=10

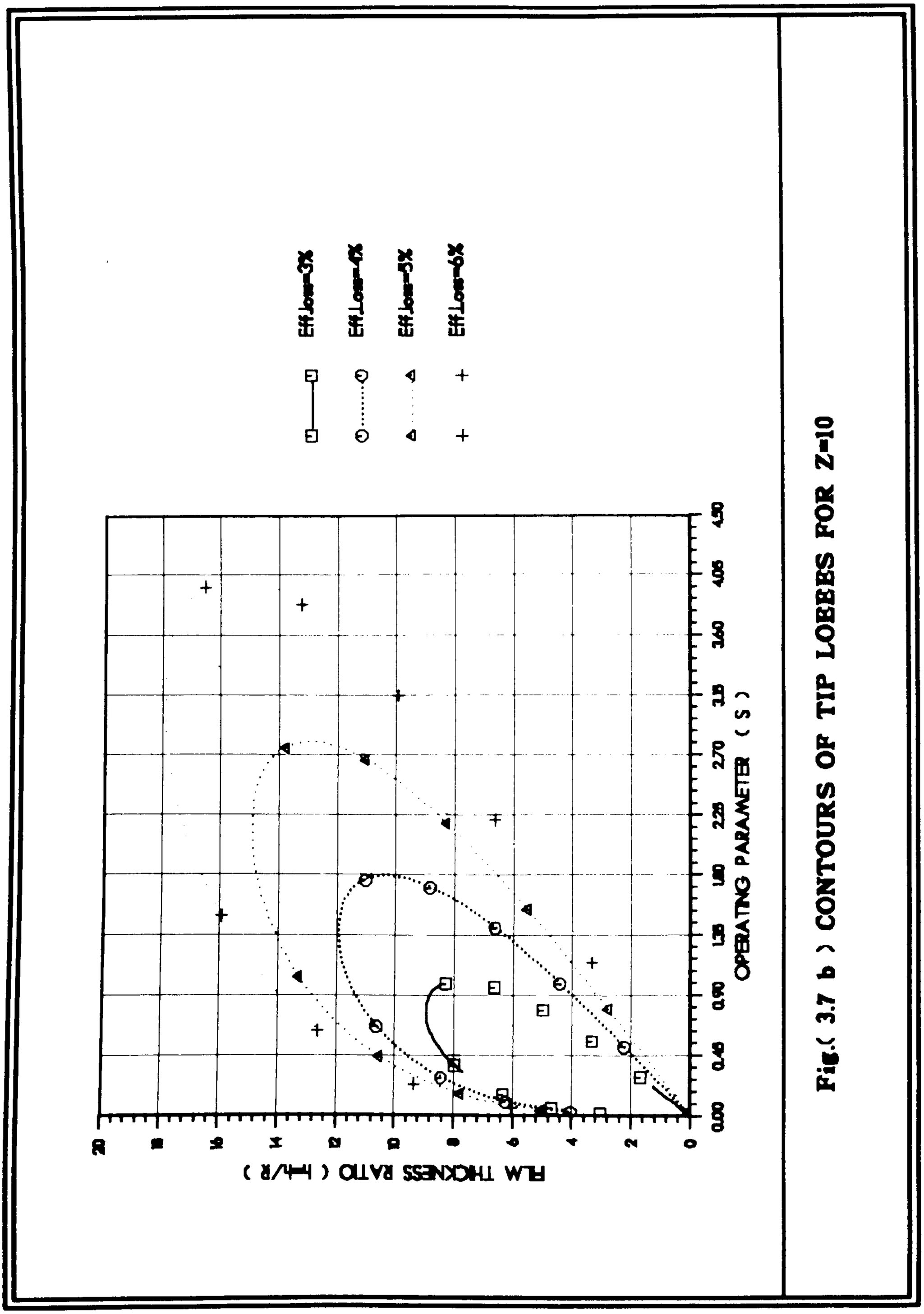

Fig.(3.7 b) CONTOURS OF TIP LOBES FOR Z=10

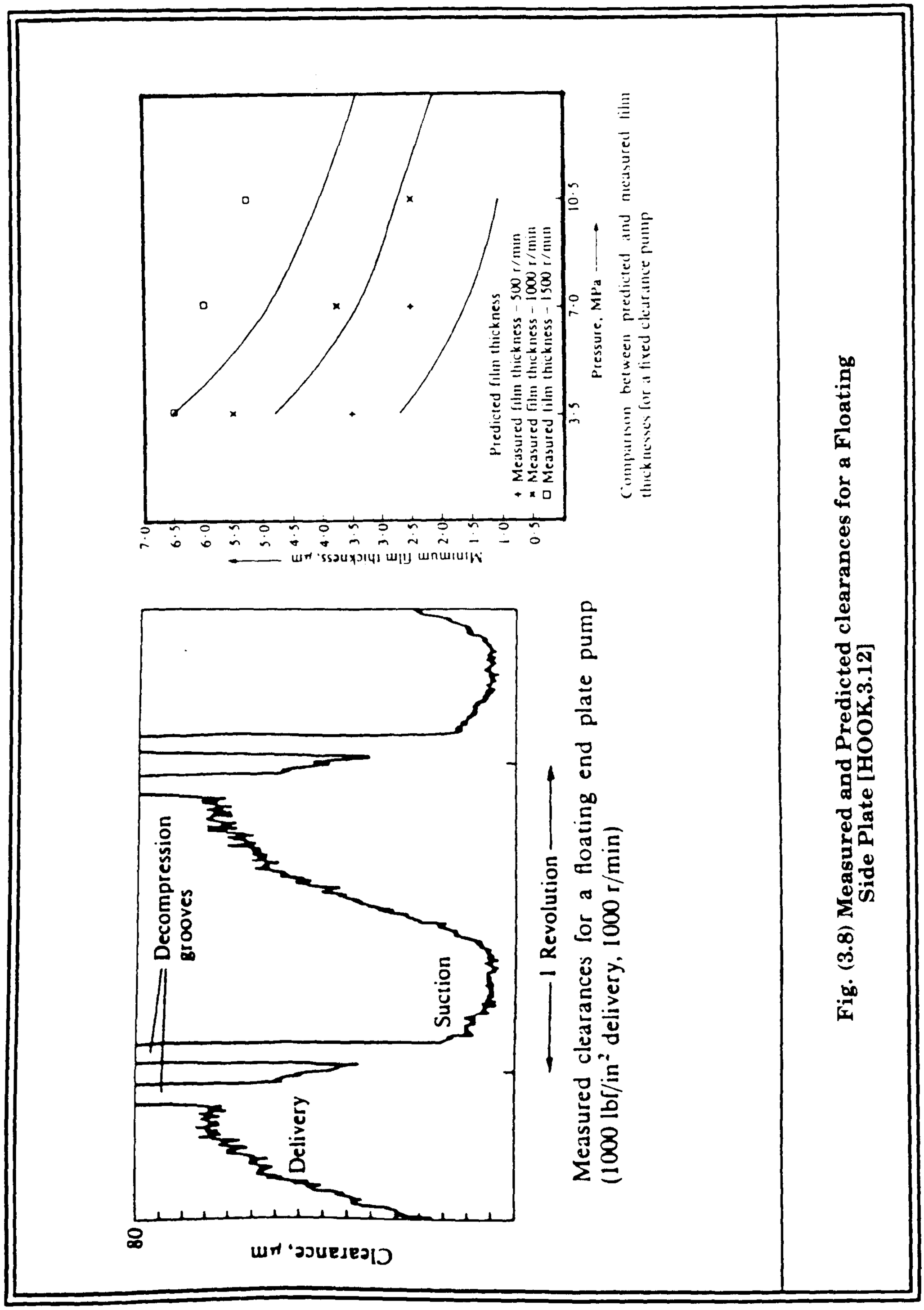

Comparison between predicted and measured thicknesses for a fixed clearance pump

Fig. (3.8) Measured and Predicted clearances for a Floating Side Plate [HOOK,3.12]

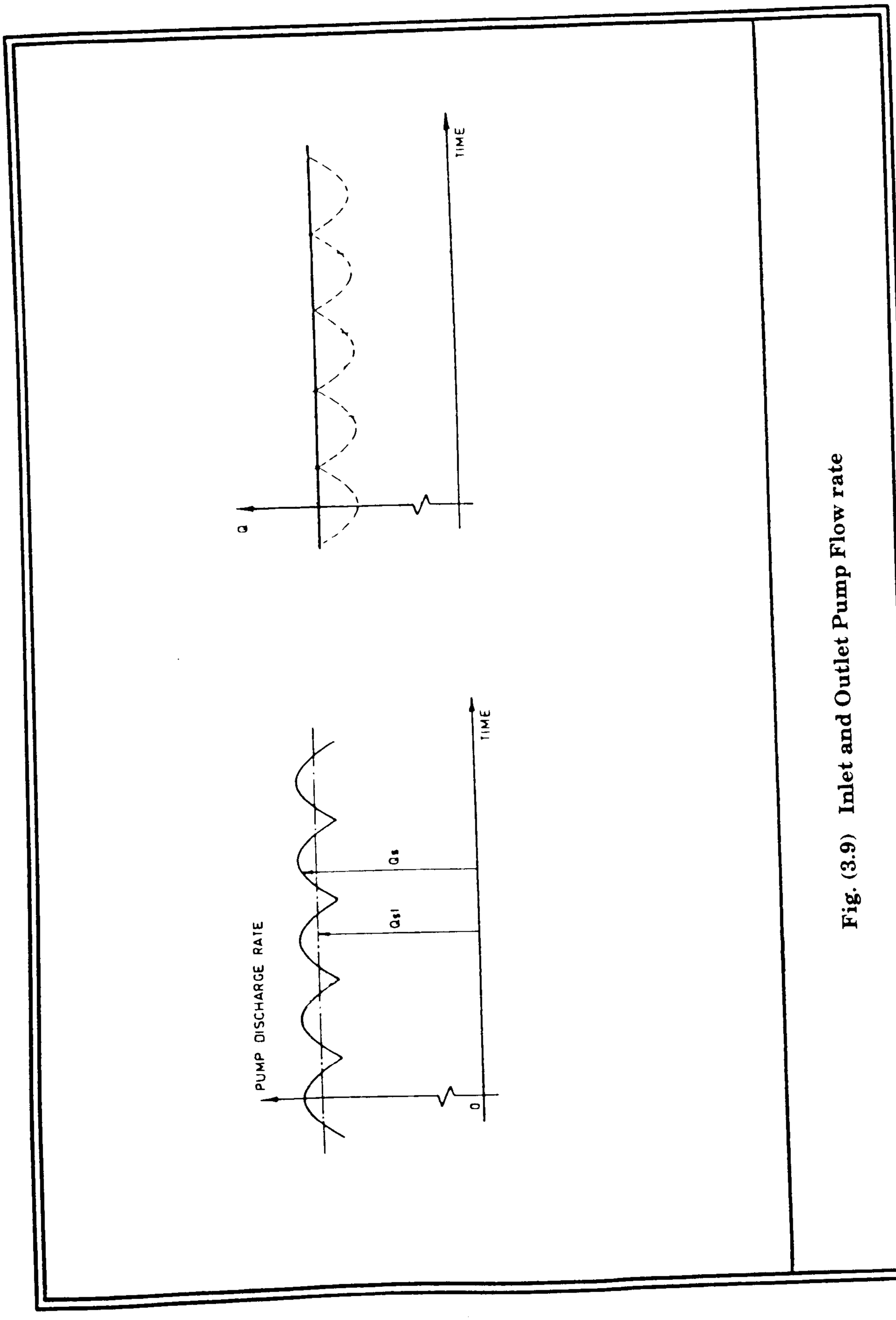

Fig. (3.9) Inlet and Outlet Pump Flow rate

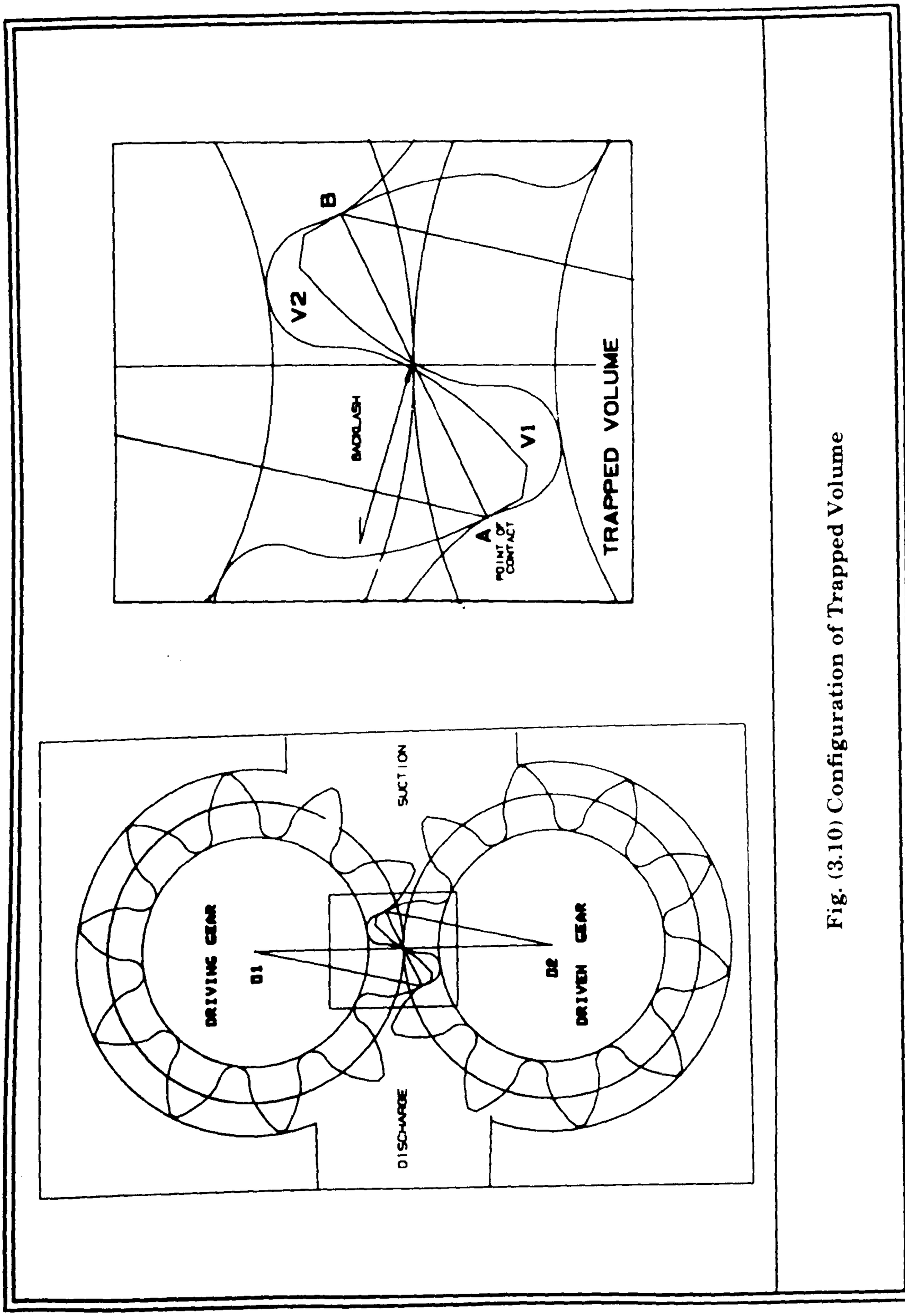

Fig. (3.10) Configuration of Trapped Volume

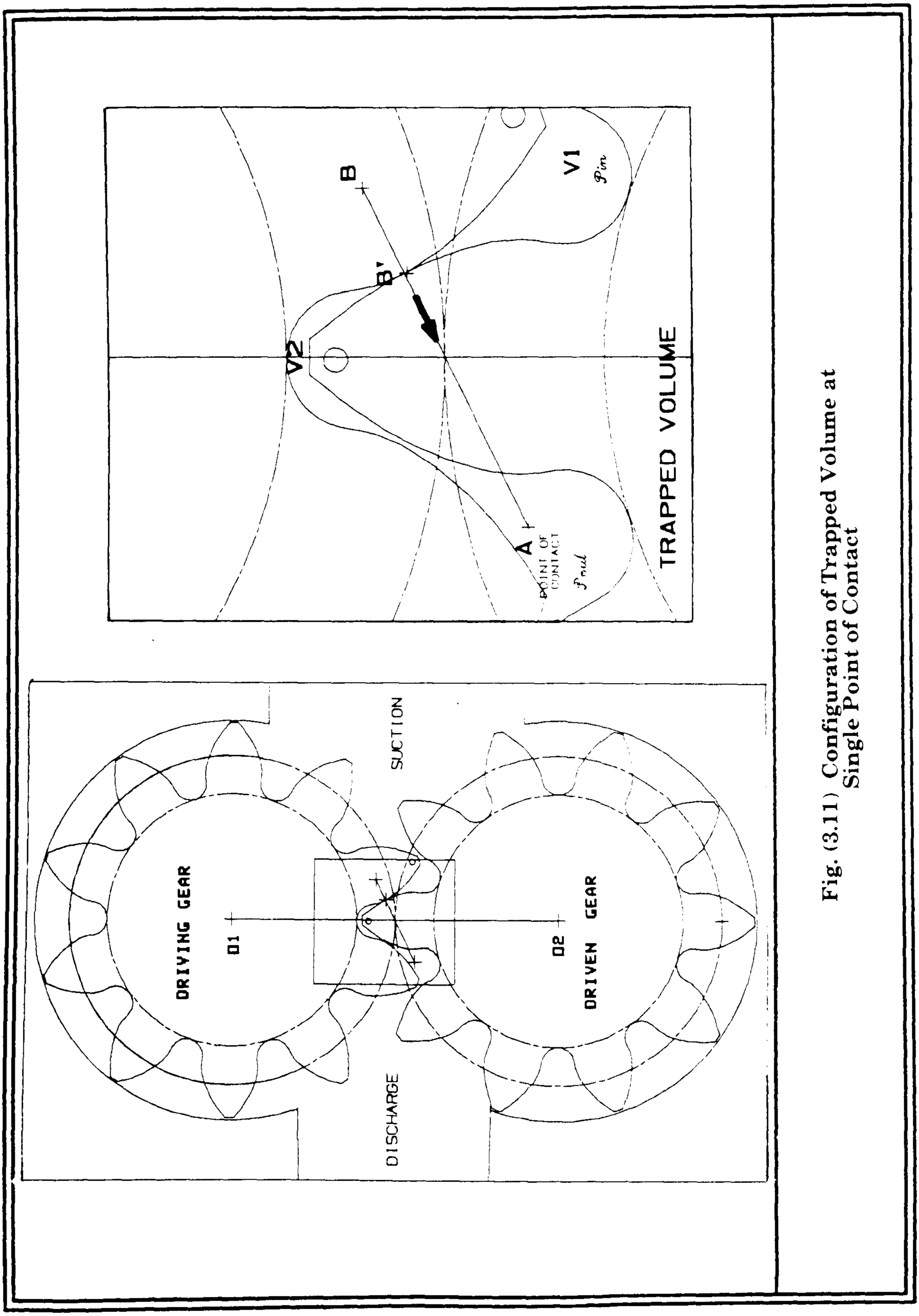

Fig. (3.11) Configuration of Trapped Volume at Single Point of Contact

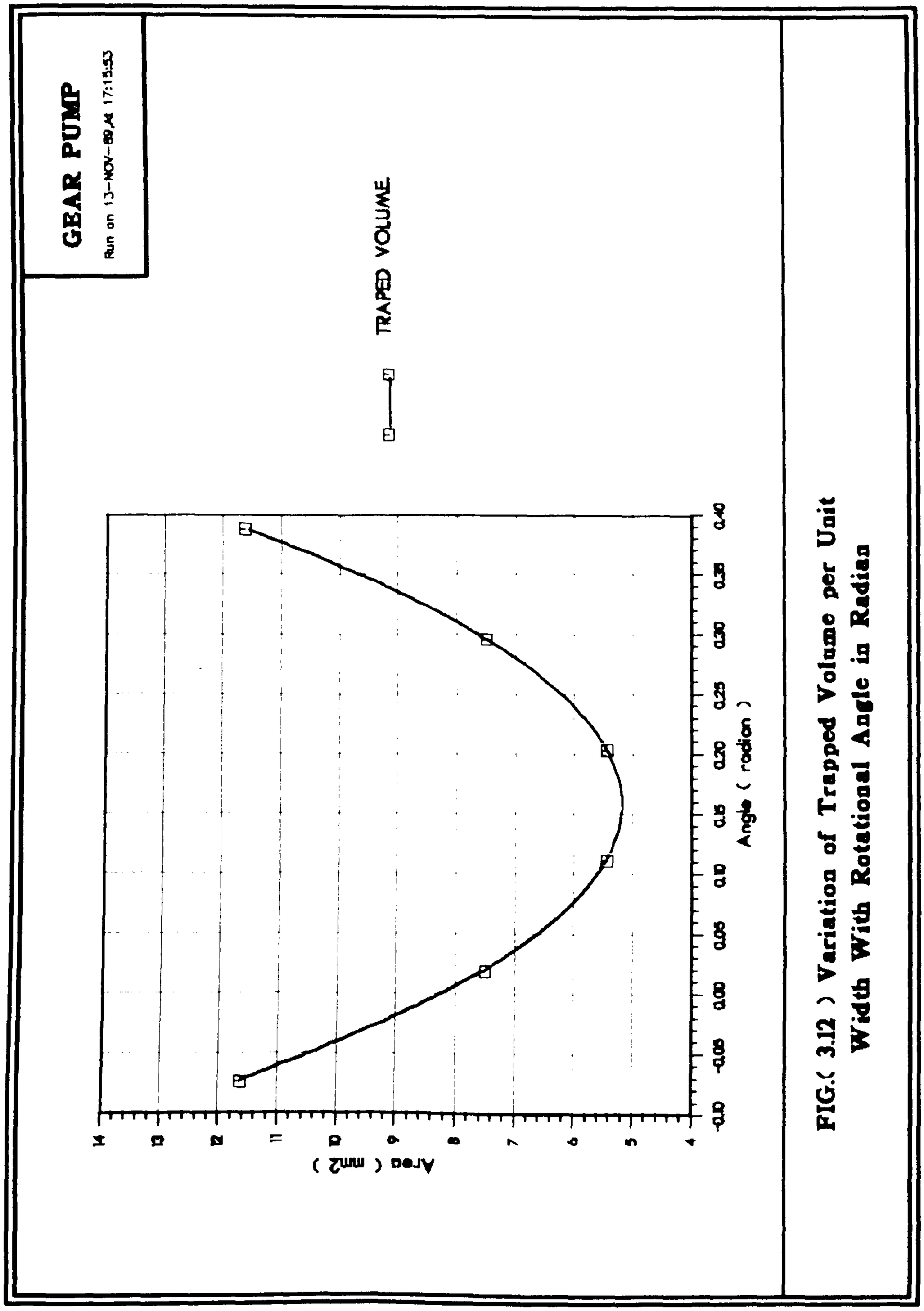

FIG.(3.12) Variation of Trapped Volume per Unit Width With Rotational Angle in Radian

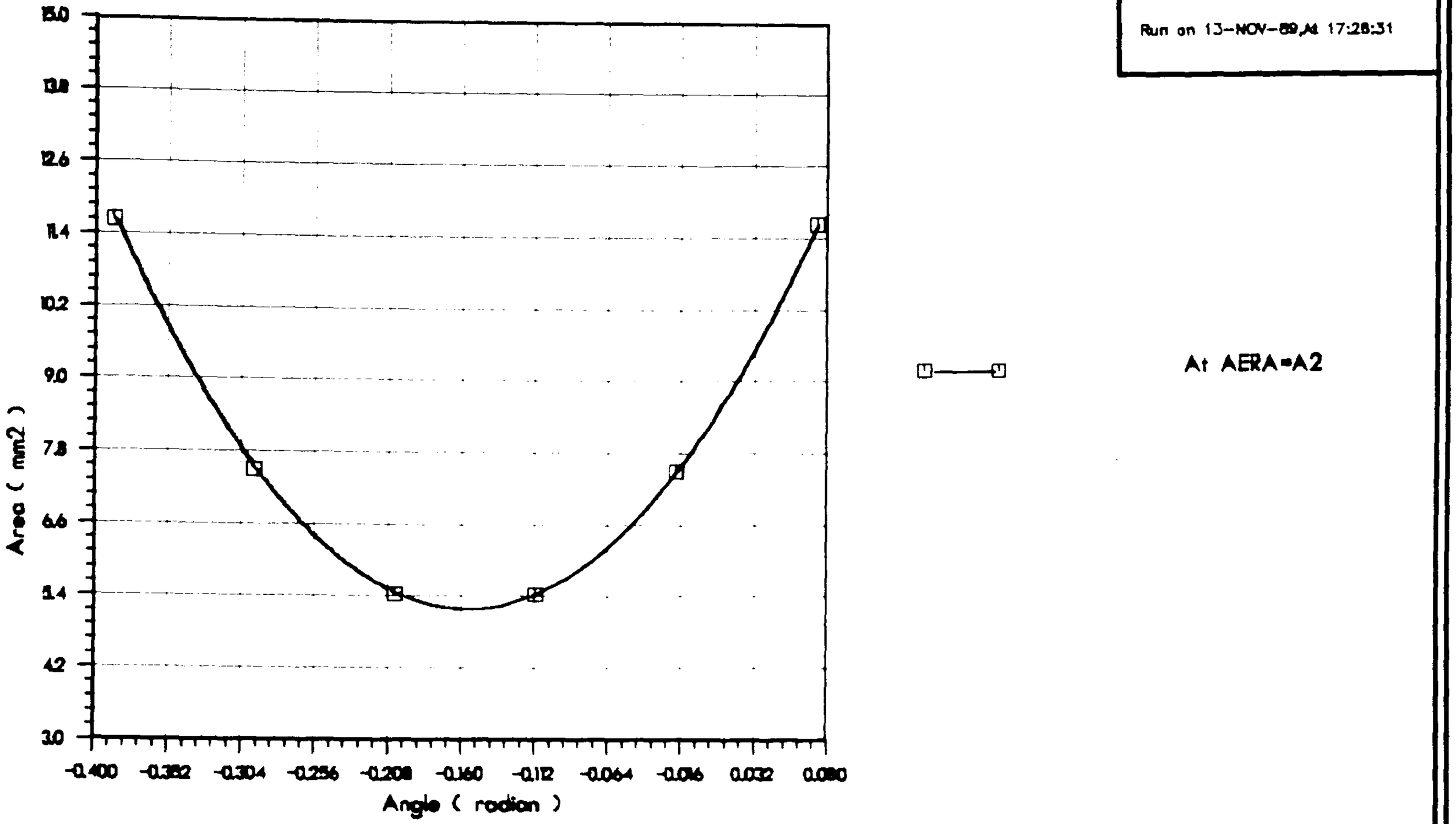

Fig.(3.13) Variation of trapped Area per uint width with rotational angle

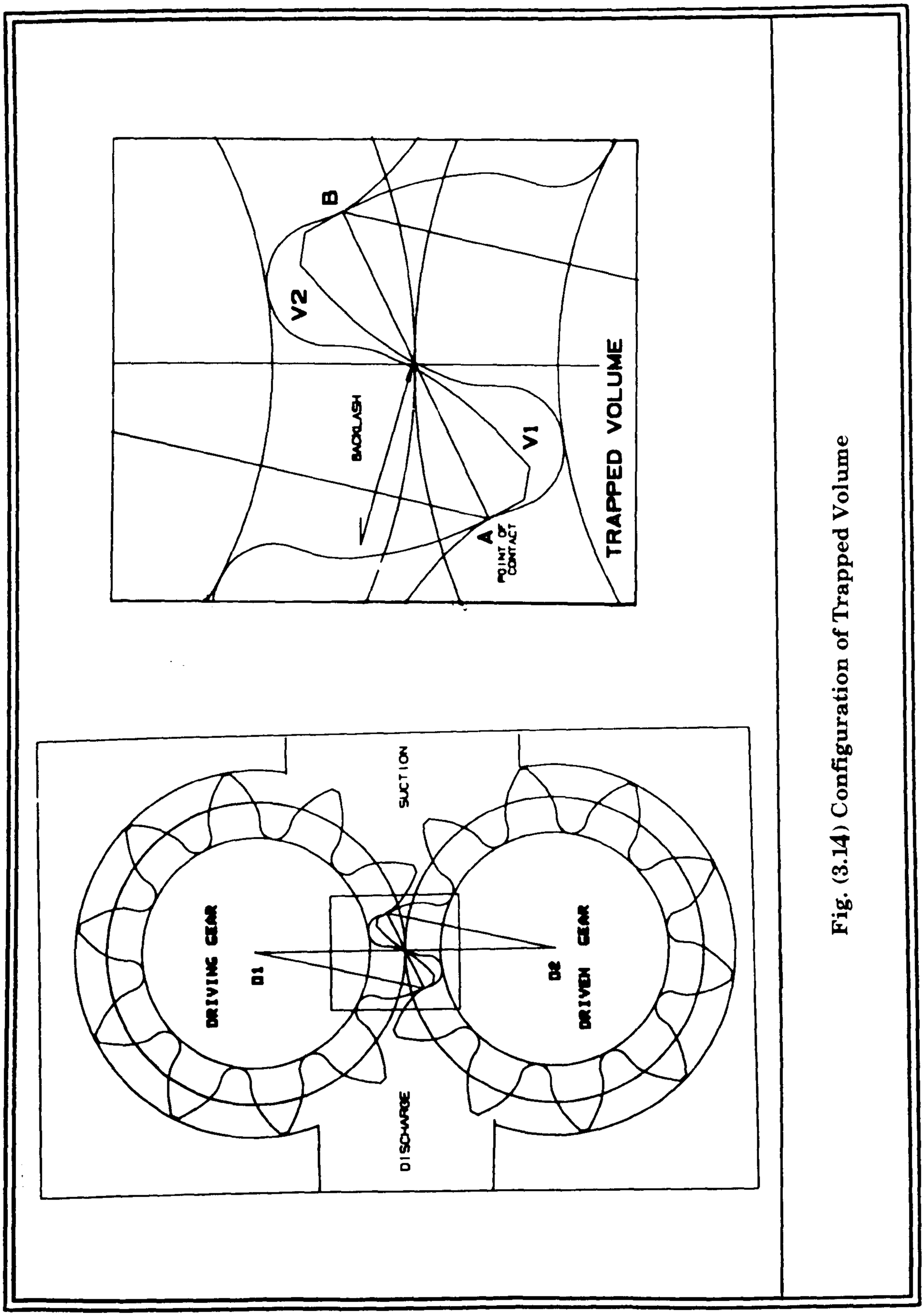

Fig. (3.14) Configuration of Trapped Volume

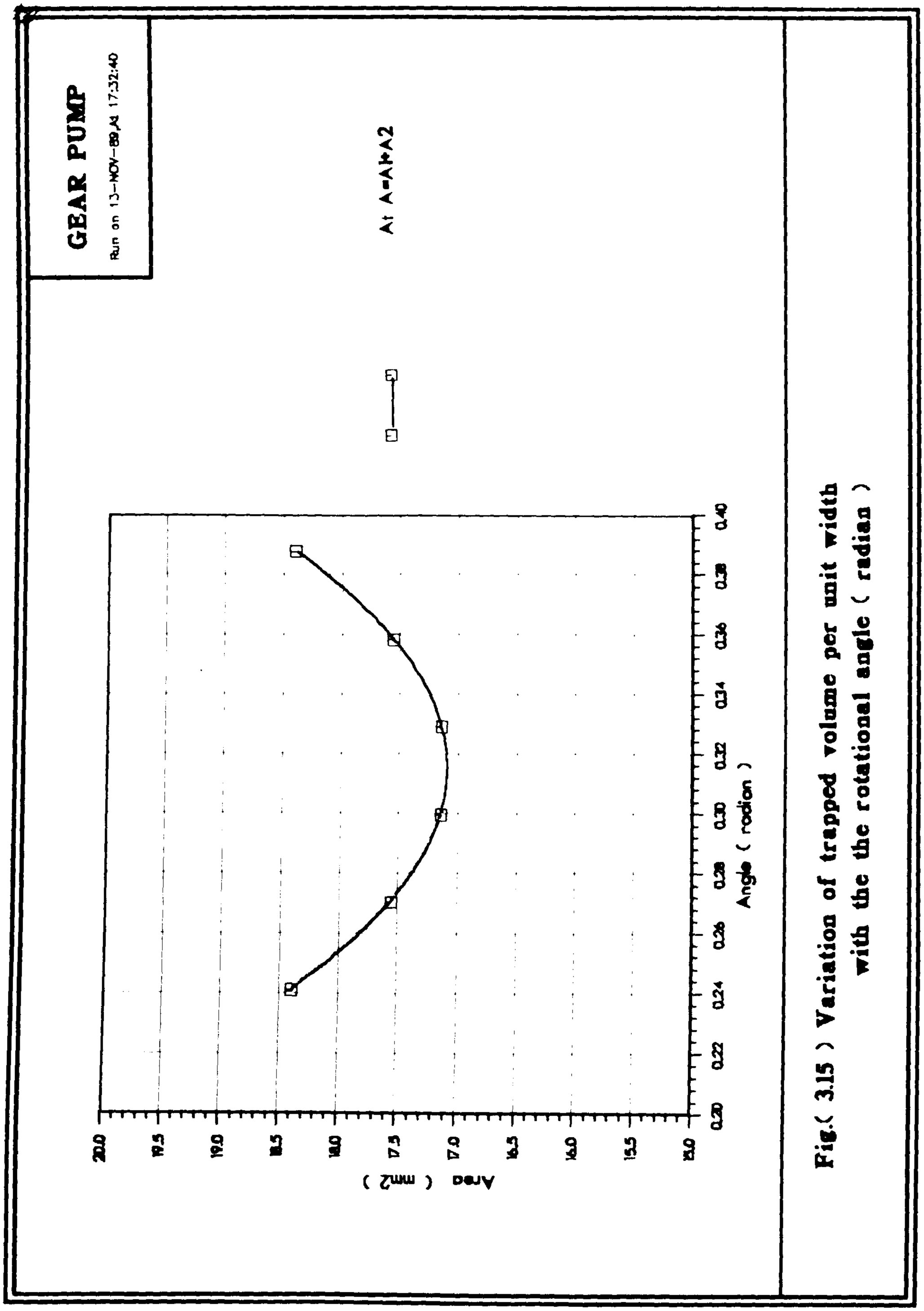

Fig.(3.15) Variation of trapped volume per unit width with the rotational angle (radian)

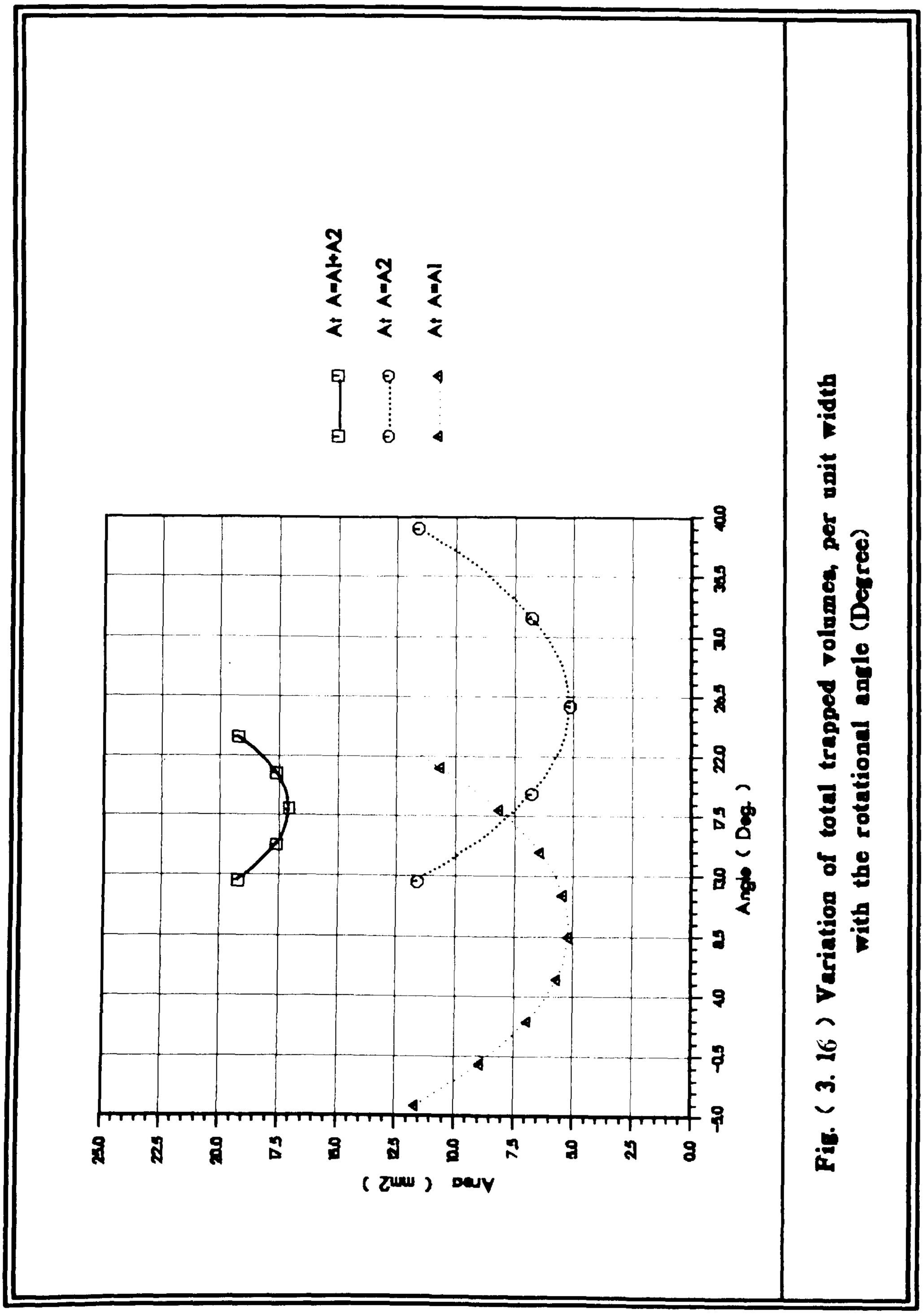

Fig. (3. 16) Variation of total trapped volume, per unit width with the rotational angle (Degree)

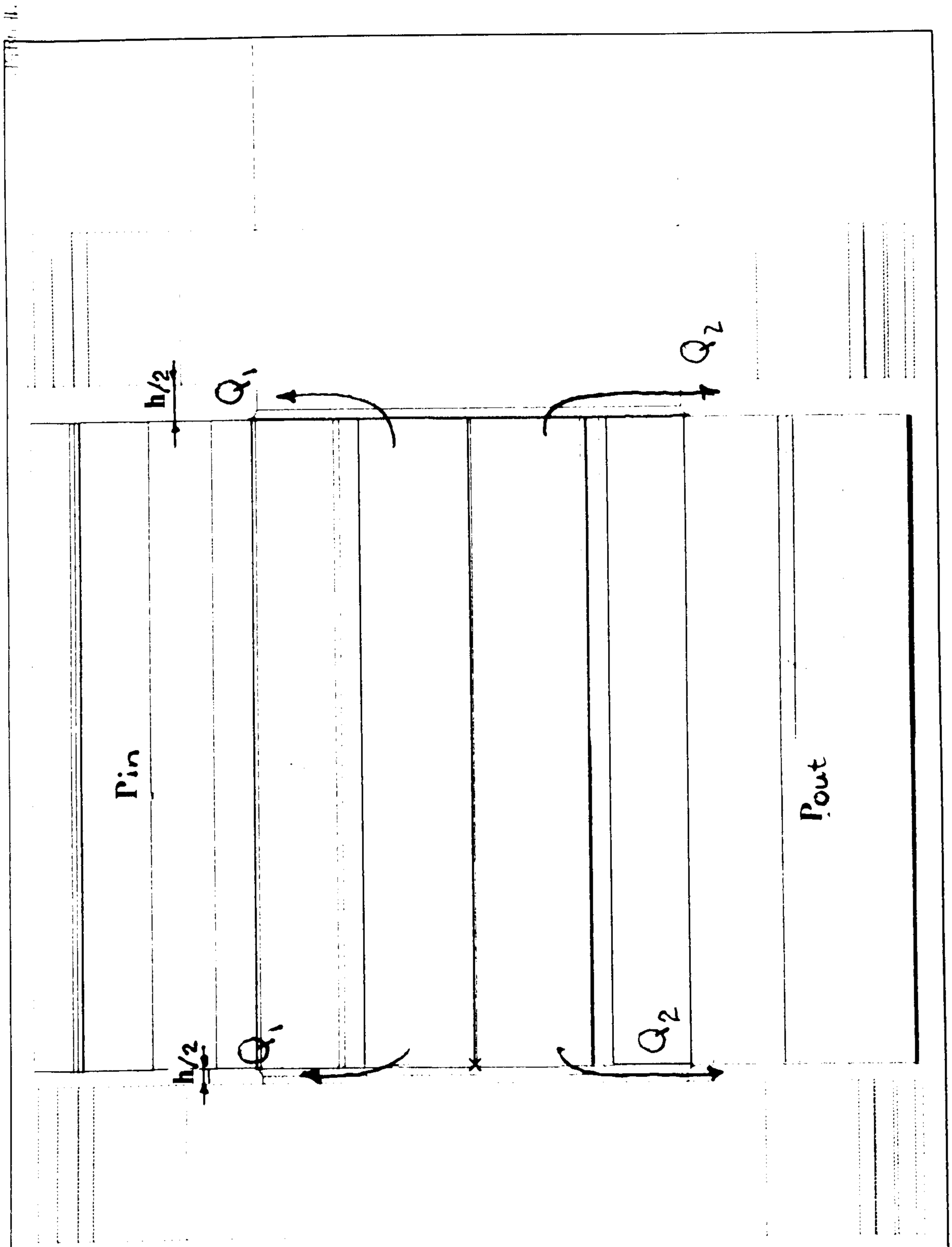

Fig 3.17 GBAR PUMP MESH

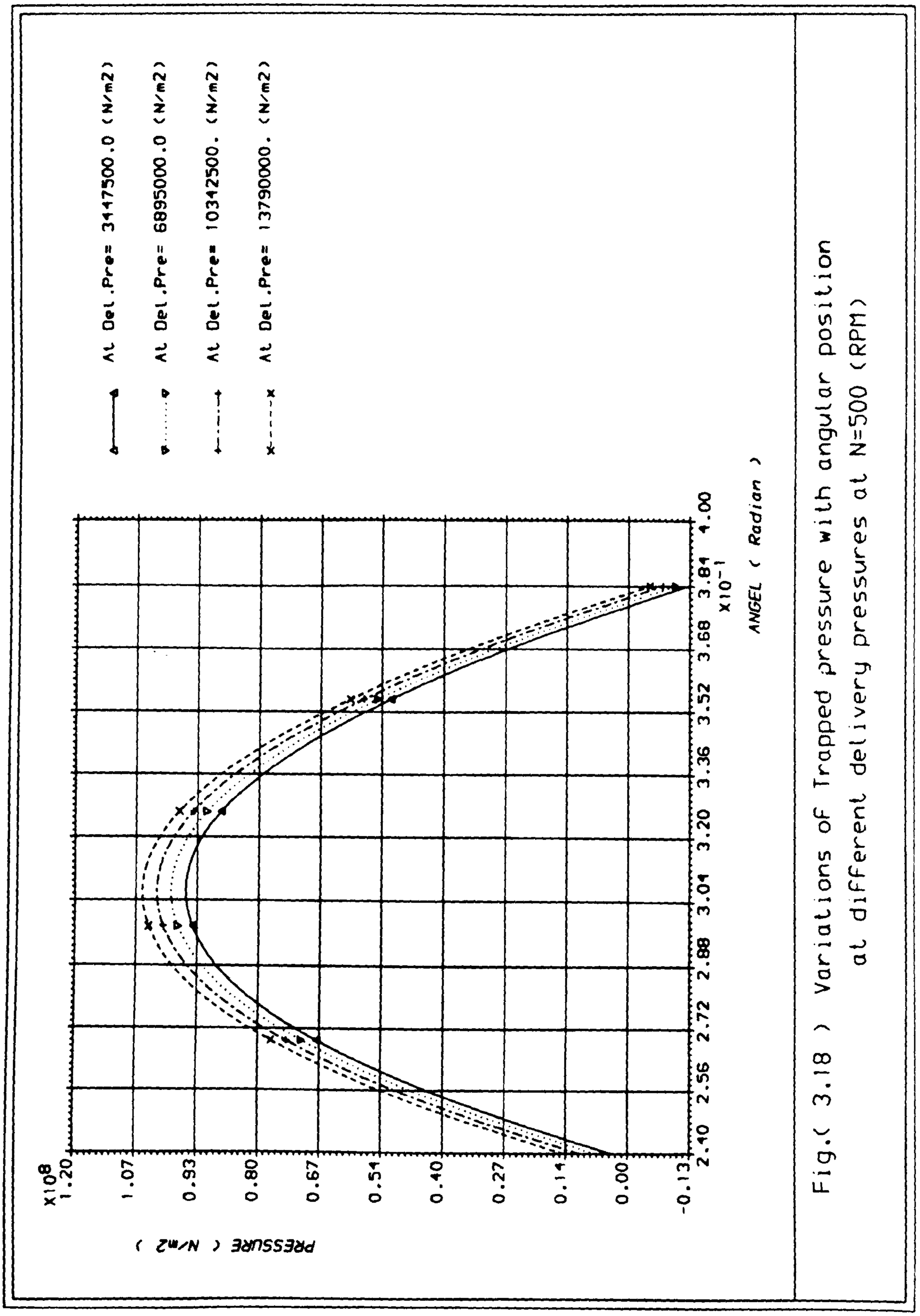

Fig.(3.18) Variations of Trapped pressure with angular position at different delivery pressures at N=500 (RPM)

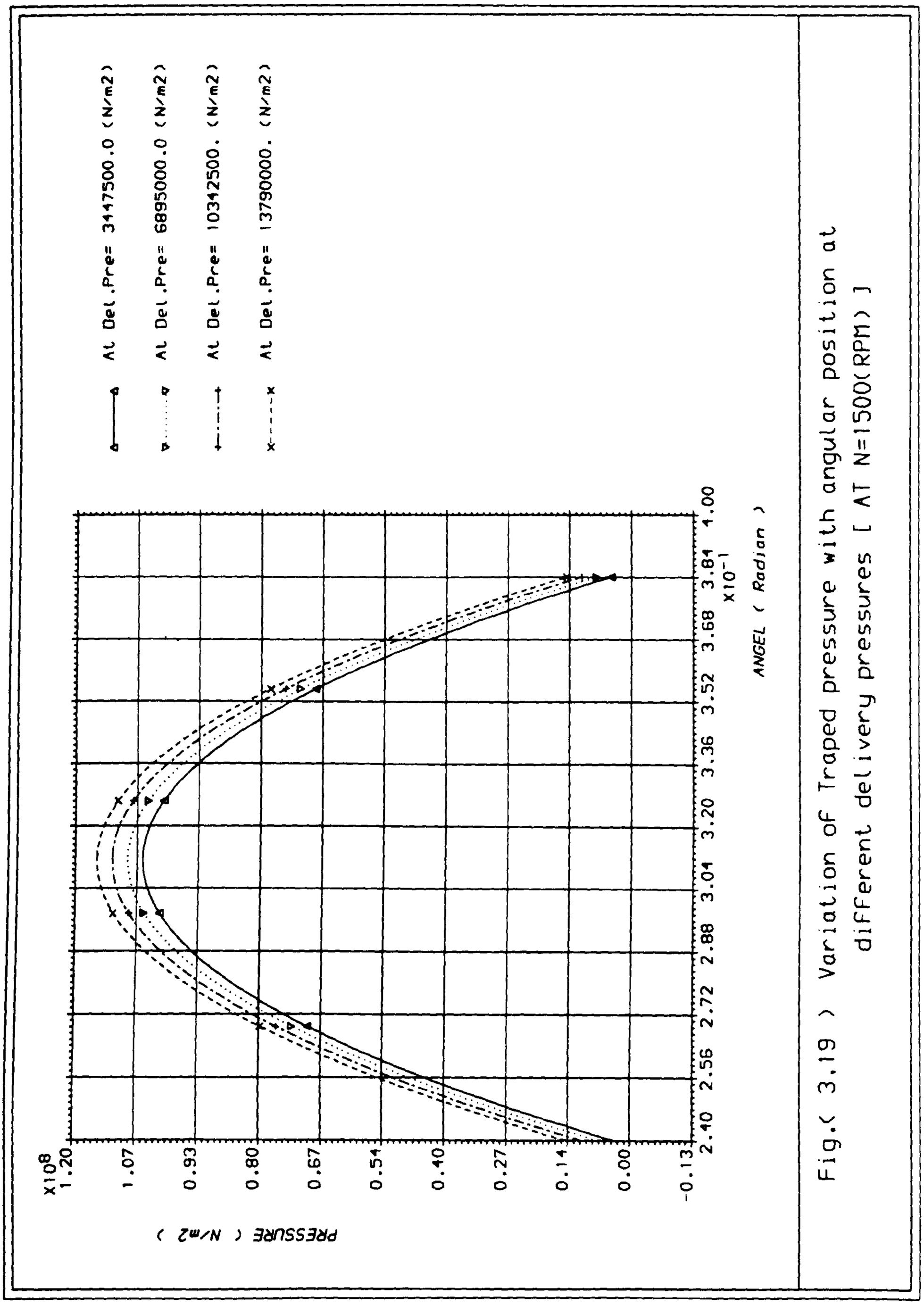

Fig.(3.19) Variation of Traped pressure with angular position at different delivery pressures [AT N=1500(RPM)]

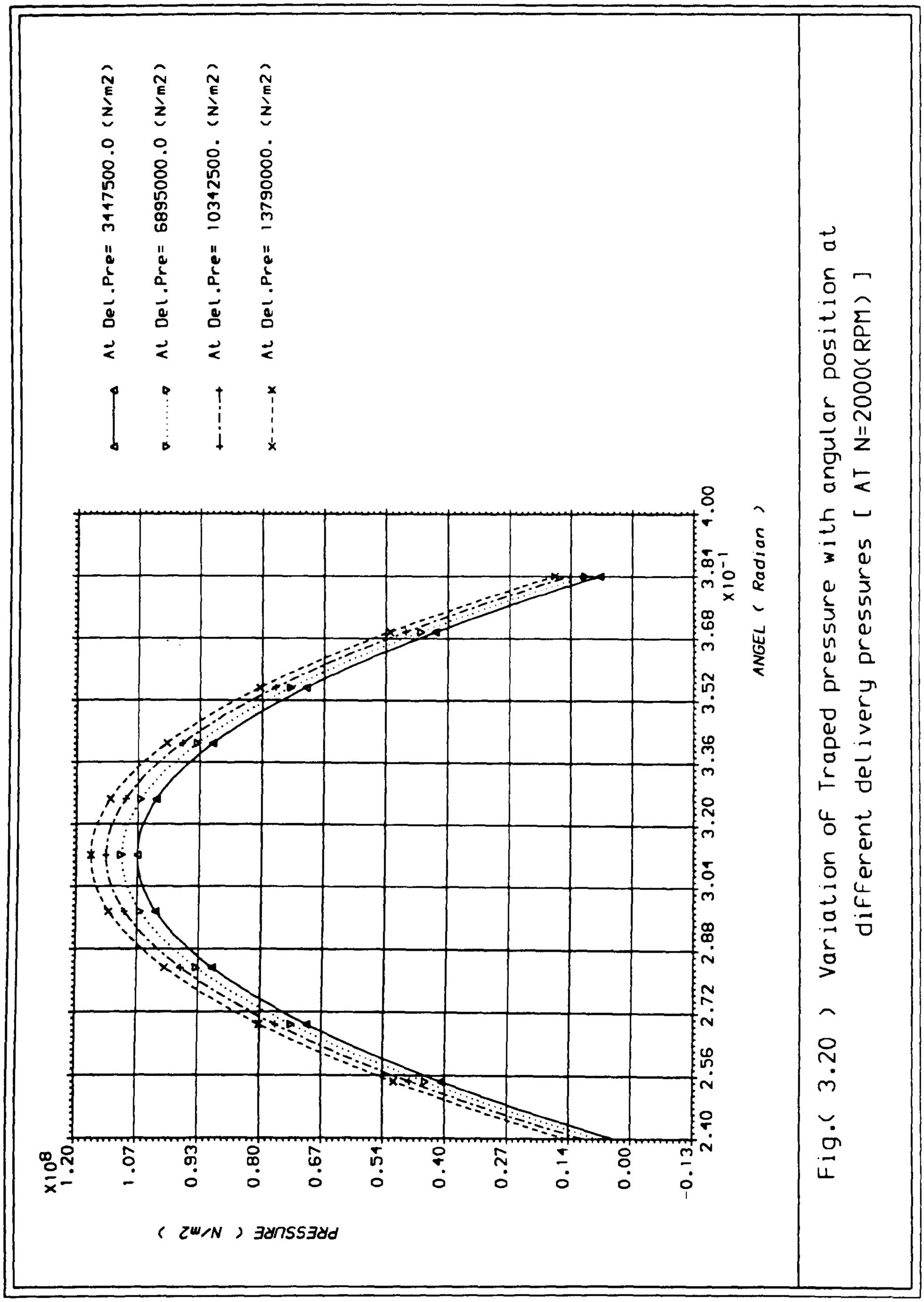

Fig.(3.20) Variation of Traped pressure with angular position at different delivery pressures [AT N=2000(RPM)]

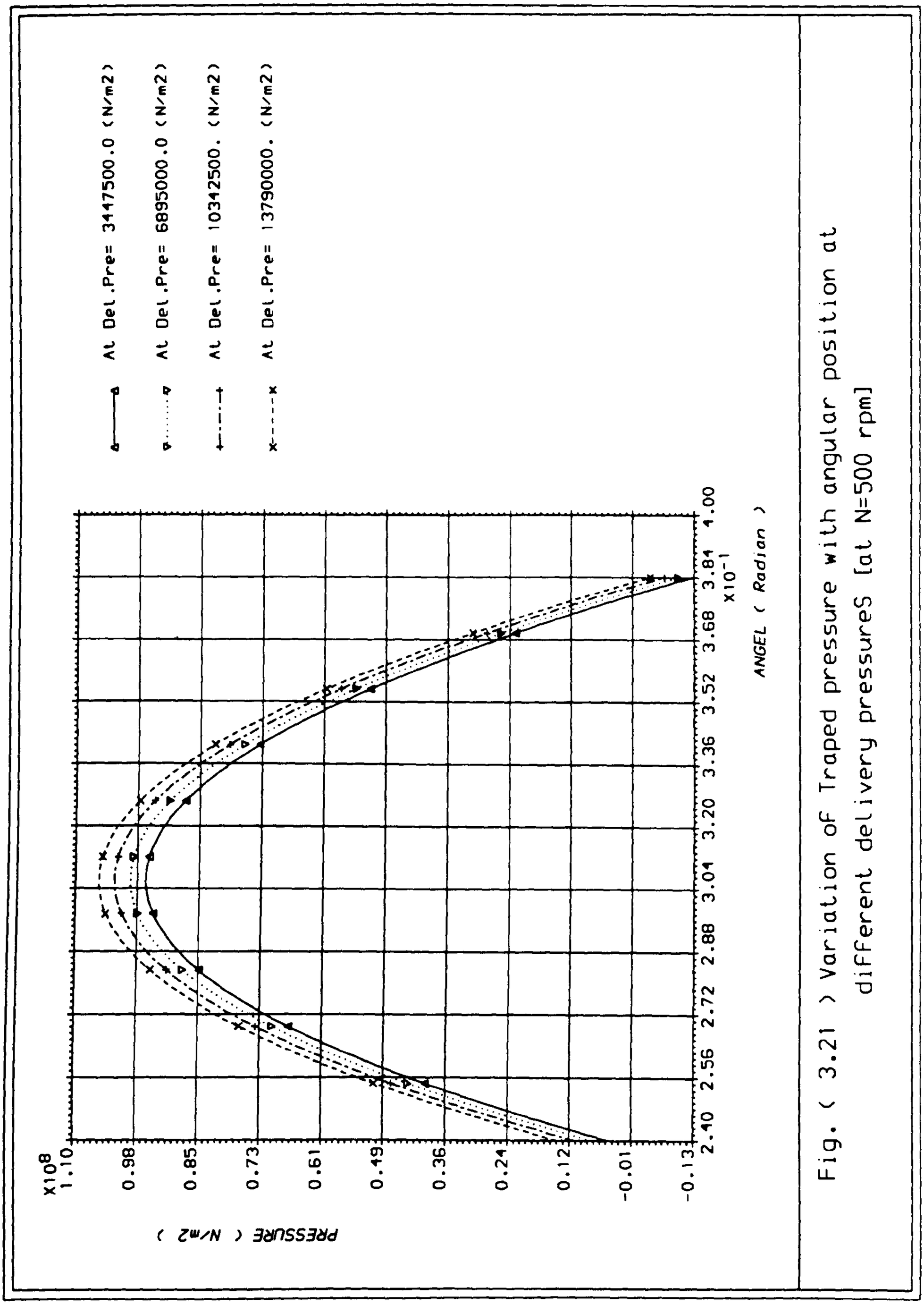

Fig. (3.21) Variation of Traped pressure with angular position at different delivery pressureS [at N=500 rpm]

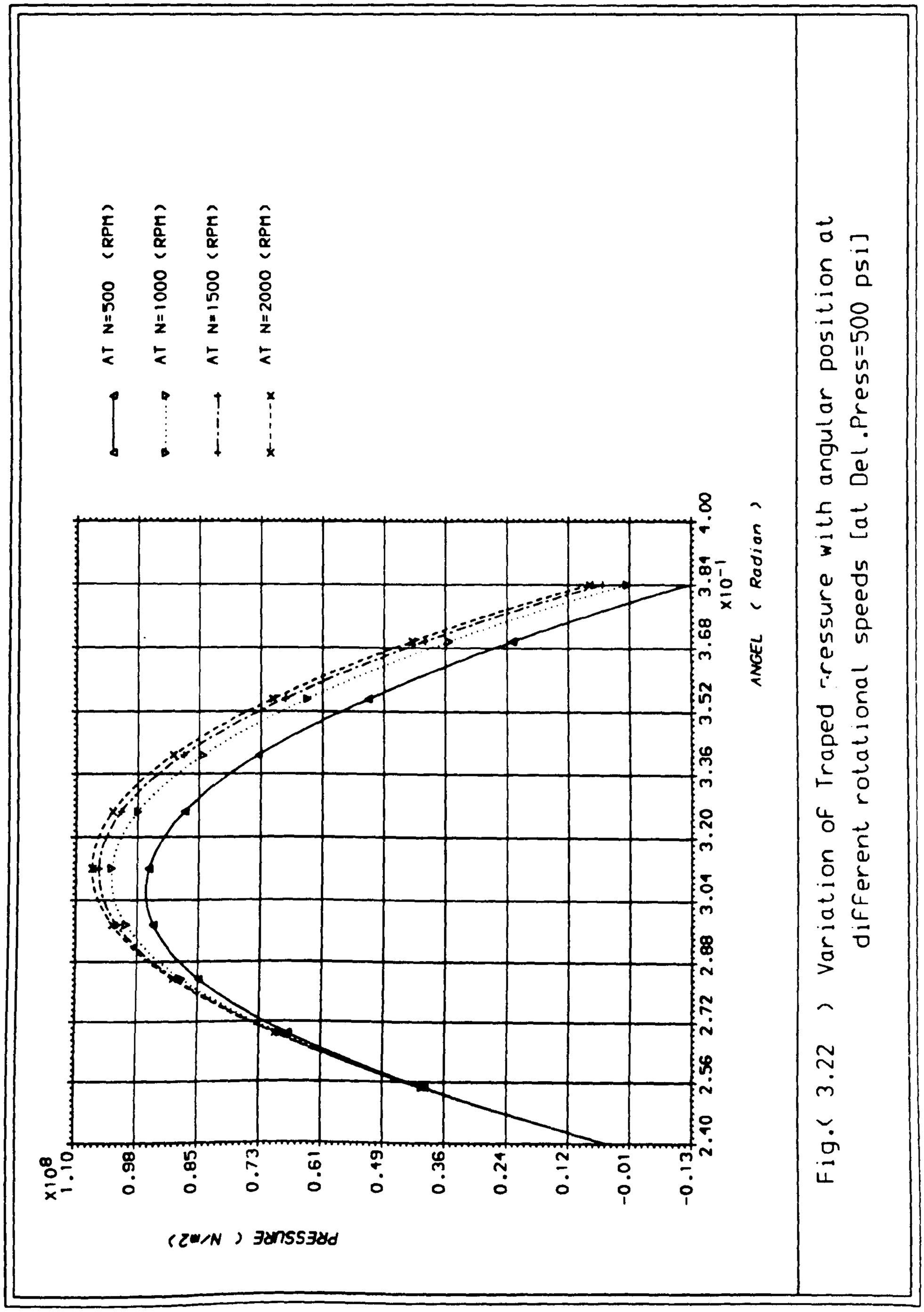

Fig.(3.22) Variation of Traped pressure with angular position at different rotational speeds [at Del.Press=500 psi]

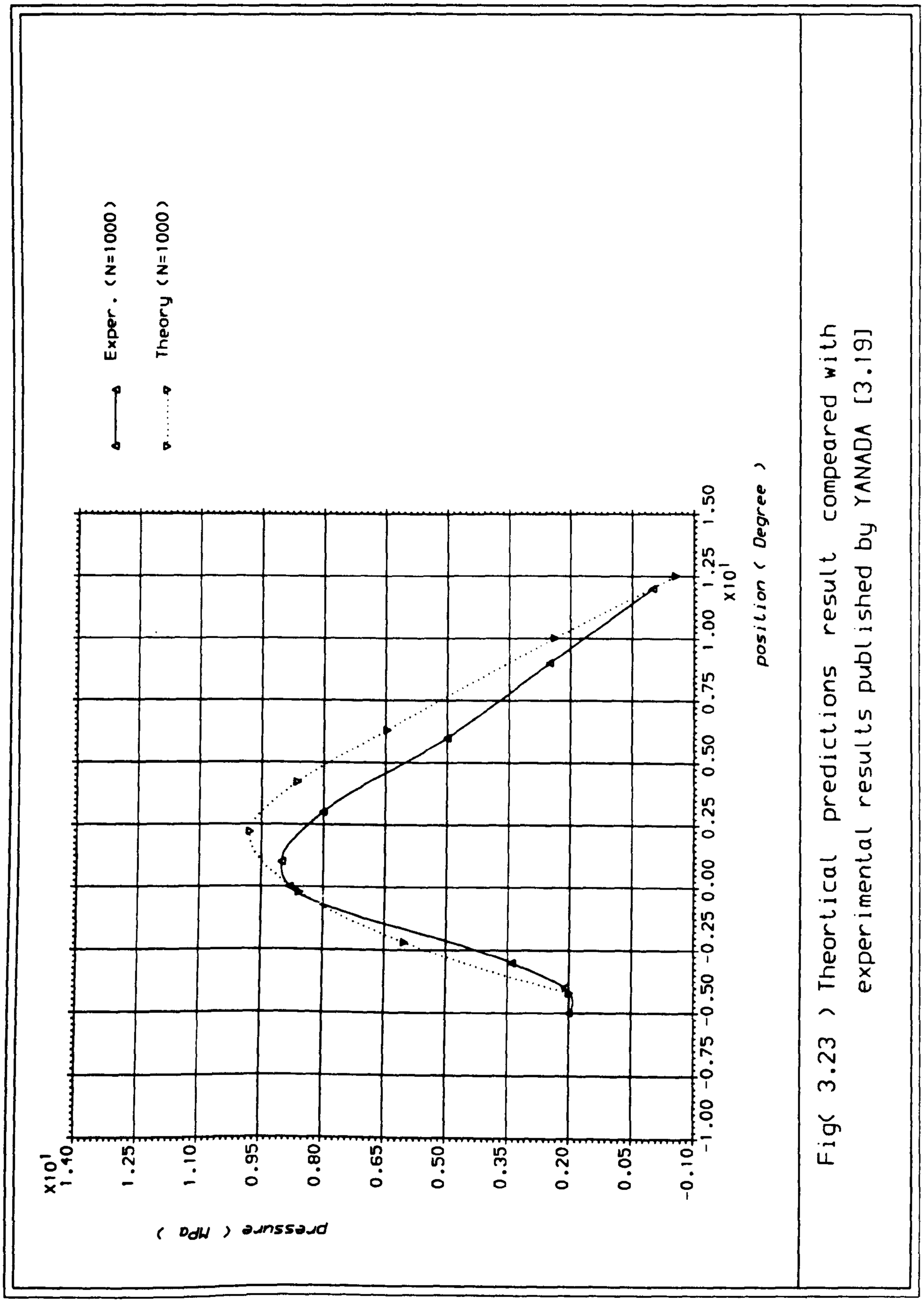

Fig(3.23) Theortical predictions result compeared with experimental results published by YANADA [3.19]

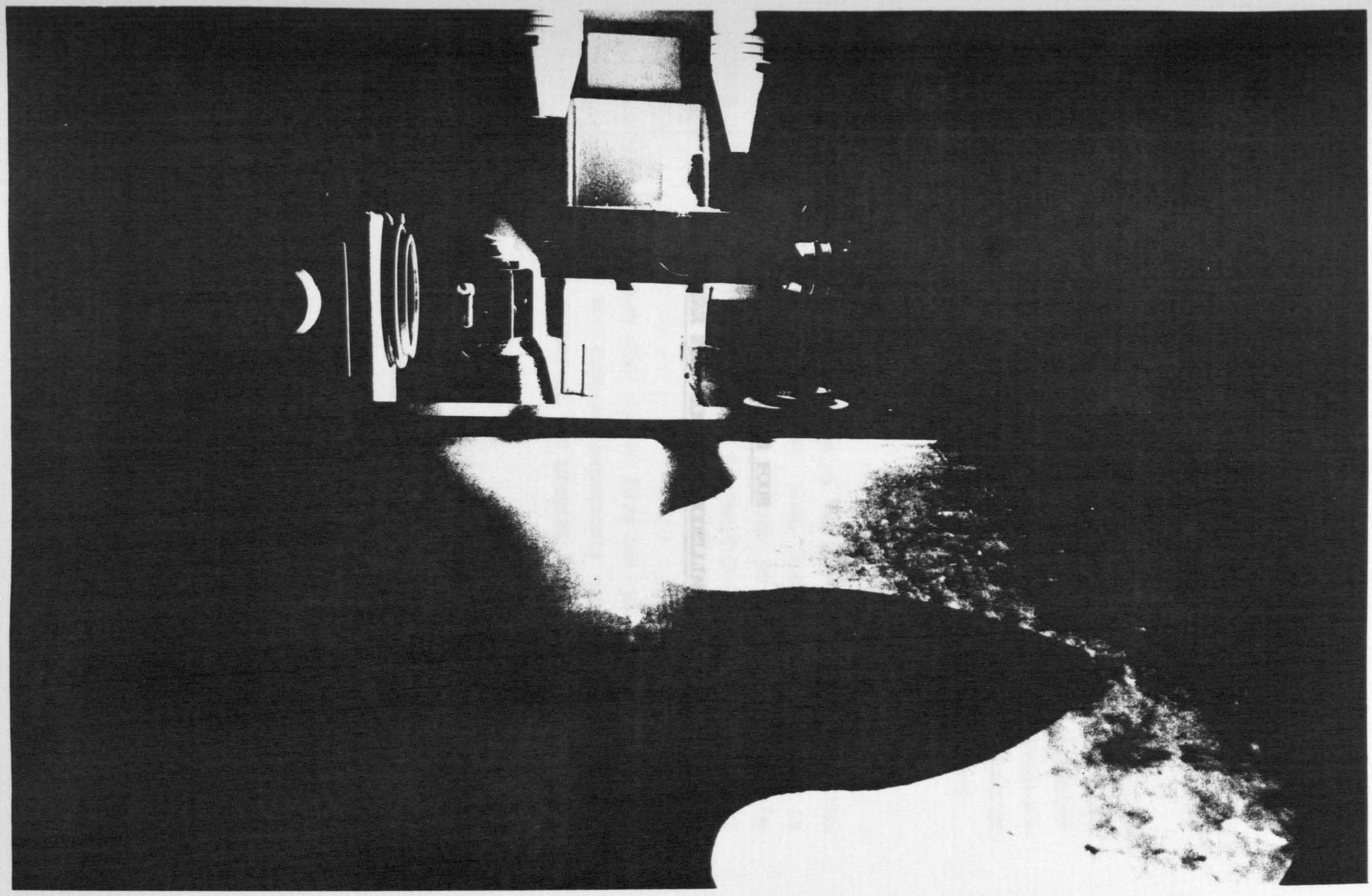

PLATE 3.1. TEETH PROFILE TEST.

CHAPTER FOUR

GEAR PUMP COMPUTER MODELLING

4.1 Introduction

Due to the increasing cost of materials, as well as the weight effects of the high pressure hydraulic systems, it is now becoming increasingly important to design gear pumps with a minimum weight/power ratio.

Computer programs based on the theory presented in the previous Chapter, as well as on the gear manufacturers' formulae and tables were developed. A review of the programs' theory and their structure is presented in this Chapter. A simplified flow diagram of the program appears in fig. (4.1), whilst a full listing is given in Appendix B.

4.2 Suite of Programs

In this section, the global structure of the suite of programs for the design and modelling of the gear pump under consideration is presented. The aim of which is to provide an appreciation of the program interconnections in relation to their processes, and the input and output requirements.

In order not to distract the reader from the primary goal of this section, the details are covered separately in the sections that follow. The general structure of the program interaction is presented pictorially in fig. (4.1).

Four programs constitute the main suite for designing and modelling the gear pump. They are divided into two groups; Design and Performance Simulations - these are provided by the programs "GPD" (Gear Pump Design) and "GPP" (Gear Pump Performance), respectively. The later program contains a group of minor programs which deals with the performance of a gear pump, such as leakages, flowrates, the pressure distribution around the gear rotor, as well as the trapped volume and pressure in the tooth space. Data transfer between the programs are via datafiles generated by the "GPD" or other programs which are accessible down the execution tree.

At the top of the flow diagram the program "GPD" can choose the optimum design parameters for the required duty and generates the parameters in the data file to the format required by the program "GPP". The data handled by this program is mainly pump geometry, the operating conditions and the hydraulic oil specification. This data is required for the program "GPP" to run.

Further along the structure is the main program "GPP". This simulates the performance of the designed gear pump. This is provided by three programs, namely: Mesh Flow Program (MFLOW), Pressure Distribution around the Gear Rotor (PDAGR), and trapped volume and pressure in the tooth space (PVTRAP). The theory of each program is presented in the next sections.

At the end of each run, the program delivers the predictions into a data file which at a later stage can be plotted using the program UPLOT. The output is displayed graphically in 2D coloured plots using either GINO or UNIRAS subroutines.

4.3 Gear Pump Design Parameters

In this section the method for obtaining the optimum design parameters of a gear pump for a specific service is outlined. The first of these programs is the "GPD" (Gear Pump Design).

4.3.1 GPD Program Theory

It is based upon the theory given in gear design literature [4.1, 4.2, 4.3]. Using this program the gear parameters can be selected to satisfy specific service conditions, which are the on-line data required for the program to run.

4.3.2 Basic Design Parameters of the Pump (m, b, z)

The pump parameters are to be selected to satisfy the required working conditions such as the delivery, Q, (L/min) and the speed, N, (rpm). From this data the program can calculate the other parameters in the following sequence:

(i) by assuming the volumetric efficiency of the pump, the theoretical delivery of the pump can be calculated.

To estimate the module, m,

$$m = C_m \sqrt{Qact} \tag{4.1}$$

where C_m = constant. Its recommended value is 0.4, Yudin [4.4], and it can be calculated depending on the maximum allowable velocity of the fluid, which is a function of fluid viscosity.

The theoretical delivery is given by:

$$Q_T = 2\pi b N m^2 \ (Z + \mathrm{Sin}^2 \psi) \times 10^6 \ [l/min]$$

The peripheral speed at the tooth tip is:

$$V_a = \frac{\pi D_e N}{60 \times 1000} \ [m/s]$$

where D_e is the outside diameter = $m(Z + 2)$

$$\therefore \quad N = \frac{60 \times 1000 \times V_a}{\pi m \ (Z + 2)}$$

Therefore, the actual delivery Q_A can be obtained from:

$$Q_A = 0.12 \ bm \ V_a \ \eta_v \left(\frac{Z + \mathrm{Sin}^2 \psi}{Z + 2} \right) \times 10^6 \ [l/min]$$

The velocity V_a depends upon the viscosity of the working fluid.

The specifications given by A.D. Brown are well known, Zalka [4.4]. They include the allowed maximum peripheral velocity as a function of fluid viscosity (Table 4.1) therefore:

$$Q_A = C_m m^2$$

Table 4.1 (Title)

Viscosity, ν, cst	11.8	45.1	76	150	306	508	755
Peripheral Velocity m/s	5	4	3.7	3	2.2	1.6	1.26

which can be employed for estimating the value of the module m.

The estimated value of m should be checked with the (OST-1597) standards and the nearest value to those given in the standards is to be selected.

After the module value being selected, the width of the gear b [mm] can be estimated:

$$b = \frac{Q_{act}}{c_b m^2} \qquad (4.2)$$

where: c_b = width constant. It is (6-9) times the module recommended, [4.4], is 1.7.

Then, the number of teeth (z) can be calculated as:

$$z = \frac{1}{C_z} (Q_{act} - \mathrm{Sin}^2 \Upsilon) \qquad (4.3)$$

where $C_z = 2\pi b n m^2 \eta_v \times 10^{-6}$

Υ = pressure angle

The nearest rounded figure to z will be selected as the number of teeth. According to the requisite delivery of the pump, the width b can be recalculated.

4.3.3 Gear Geometry

The parameters of gear geometry can be determined (after the module and its number of teeth have been chosen) by using the involute function form. These parameters include pitch circle diameter, diameter of the base circle, base pitch, root circle diameter, tooth thickness, etc., (see the computer output in Table 4.2). After

calculating such geometry parameters the tooth and the space areas are calculated, as well as the theoretical delivery, the contact ratio, and the flow pulsation.

4.4 Gear Pump Performance (GPP)

A computer program has been developed to simulate "GPP", the performance of the gear pump under test. The program consists of three main programs and four subroutines. The structures of all these programs are presented below.

4.4.1 Gear Pump Mesh Flowrate

The pump's mesh flowrate can be calculated using the previously discussed theory (Chapter 3). This can be achieved via the main program which contains a number of programs for calculating gear leakages (e.g. gear tip leakages, side plate leakages and the trapped volume relief groove leakages) which are computed individually via their corresponding subroutines. Then the main program adds these components and computes the net outlet flowrate of the pump.

The computation is performed by using the output data of the design program as an input and by rotating the gear ½ second of a degree, and evaluating all the needed variables that depend on the angle of rotation (e.g. like the starting point of contact). The predictions from this main program are shown in figs. (4.1) to fig. (4.5).

4.4.2 Pressure Distribution Around the Gear Rotor

The second computer program was developed to predict the pressure distribution around the gear pump, using the theory presented in Section 3.5.2. However, an assumption was made that the pressure drops for each gear tip are equal

$$(P_{out} - P_{in}) = \sum_{n=1}^{n=Z} \Delta P_n$$

Nevertheless this needs to be experimentally investigated in detail. The predictions from this program are shown in fig. (4.6).

4.4.3 Pressure Ripple in the Trapped Space

A third computer program was developed to predict:

(i) the variation of the trapped volume as a function of the gear parameters, and

(ii) after introducing the working hydraulic oil specification, the variation of the trapped pressure as a function of the rotational angle of the gear.

The output values predicted are stored in computer files to be used directly for analysis and/or plotting.

Extra parameters were also predicted fromthe model and are plotted in Figs (4.7 - 4.9) (e.g. the pump flow rate, variation of trapped volume and waveform trapped pressure).

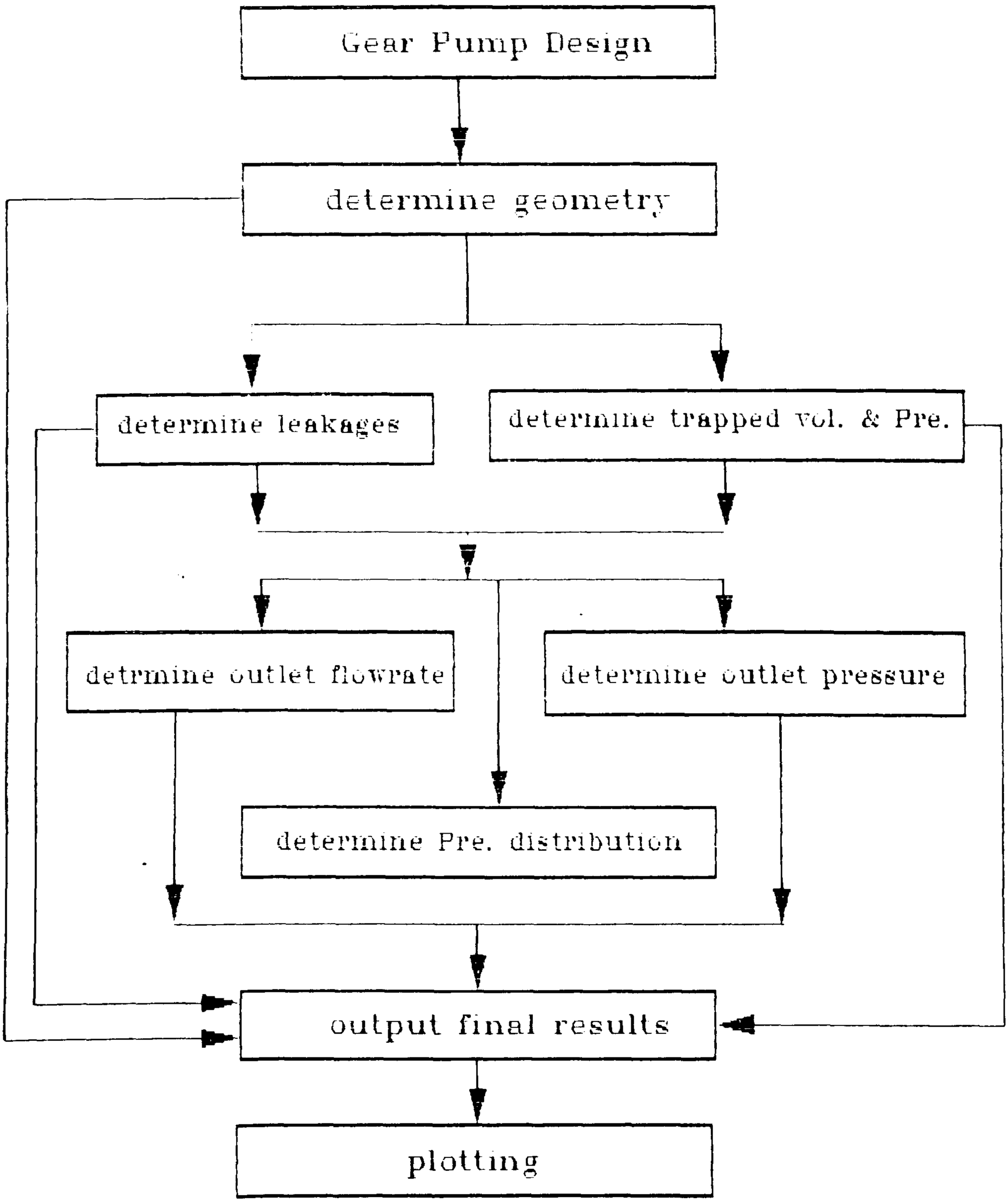

Fig.(4.1) Gear Pump Design and Performance Diagram.

TABLE (4.2)

*********** *INPUT DATA* **********

Enter your actual flow-rate .....[Lit/min] =120

Please enter your speed .....[RPM] =3000

Enter the volumetric efficiency..... =0.85

********** *OUTPUT DESIGN RESULT* **********

The culculated module is.....=4.381781

The value of the selected module is.....=4.5 mm

The recommended width is.....=36.00000 mm

The number of teeth is.....=10TEETH

****

Pith circle diameter.....[mm]= 45.00000

Diameter of base circle.....[mm]= 39.72849

Base pitch.....[mm]= 12.48610

Addendum circle diameter.....[mm]= 54.00000

Root circle diameter.....[mm]= 34.20000

Tooth thickness on pitch circle.....[mm]= 7.031428

Angle of arc. of Tooth on P.C.of Ingag..[rad]= 0.3125080

Angle of the crest of the involute.....[rad]= 0.7440780

****

Tooth area to base circle.....[mm sq]= 40.59537

Total tooth area (to root circle).....[mm sq]= 60.96222

Aera of tooth space (to base circle)...[mm sq]= 64.50549

Total area of tooth spaces.....[mm sq]= 143.4820

****

Contact ratio.....= 15 43983

Theortical approximat delivery .....[mm3]= 1.40567E+08

Discharge pulsation.....= 0.1749748

****

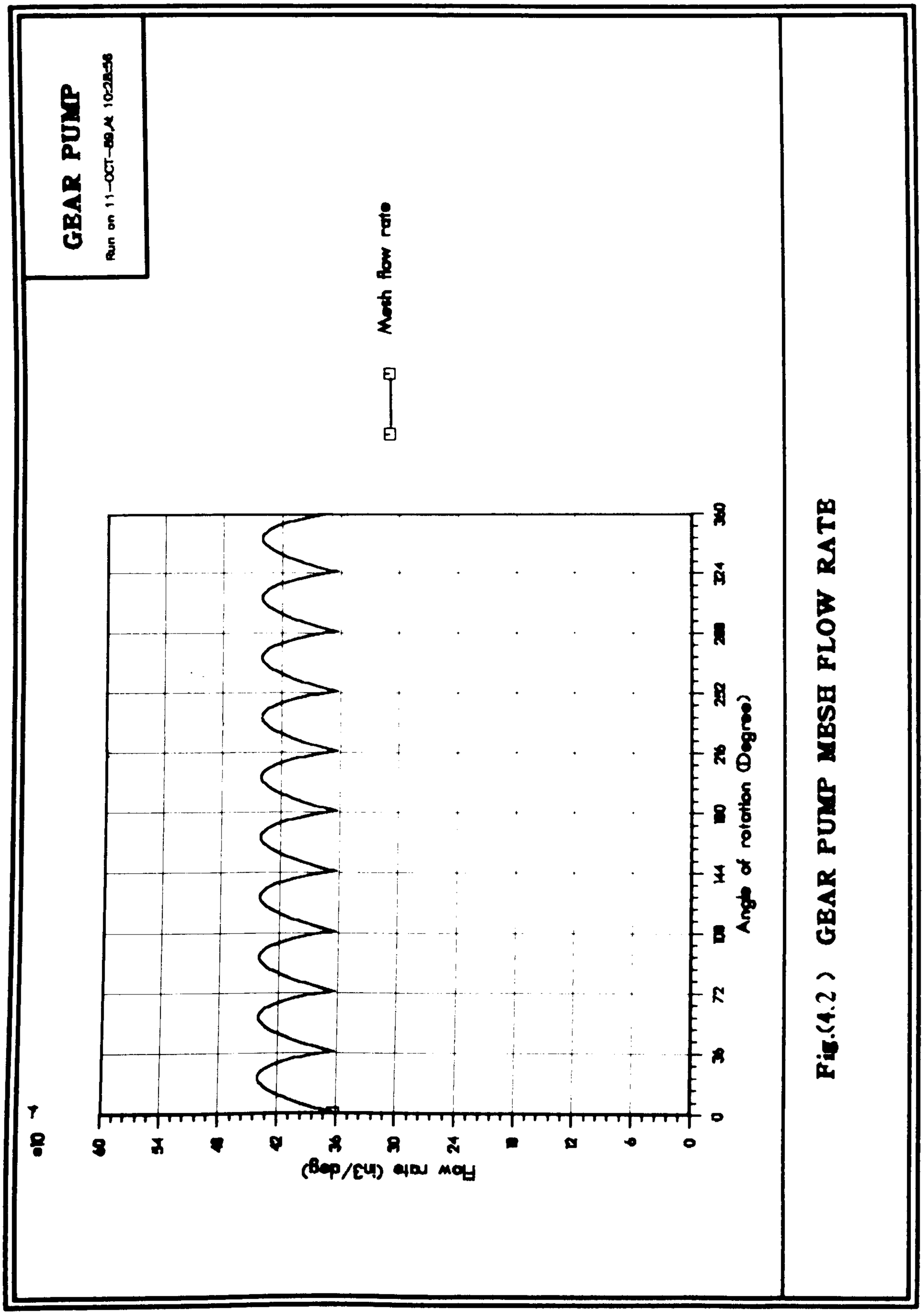

Fig.(4.2) GBAR PUMP MESH FLOW RATE

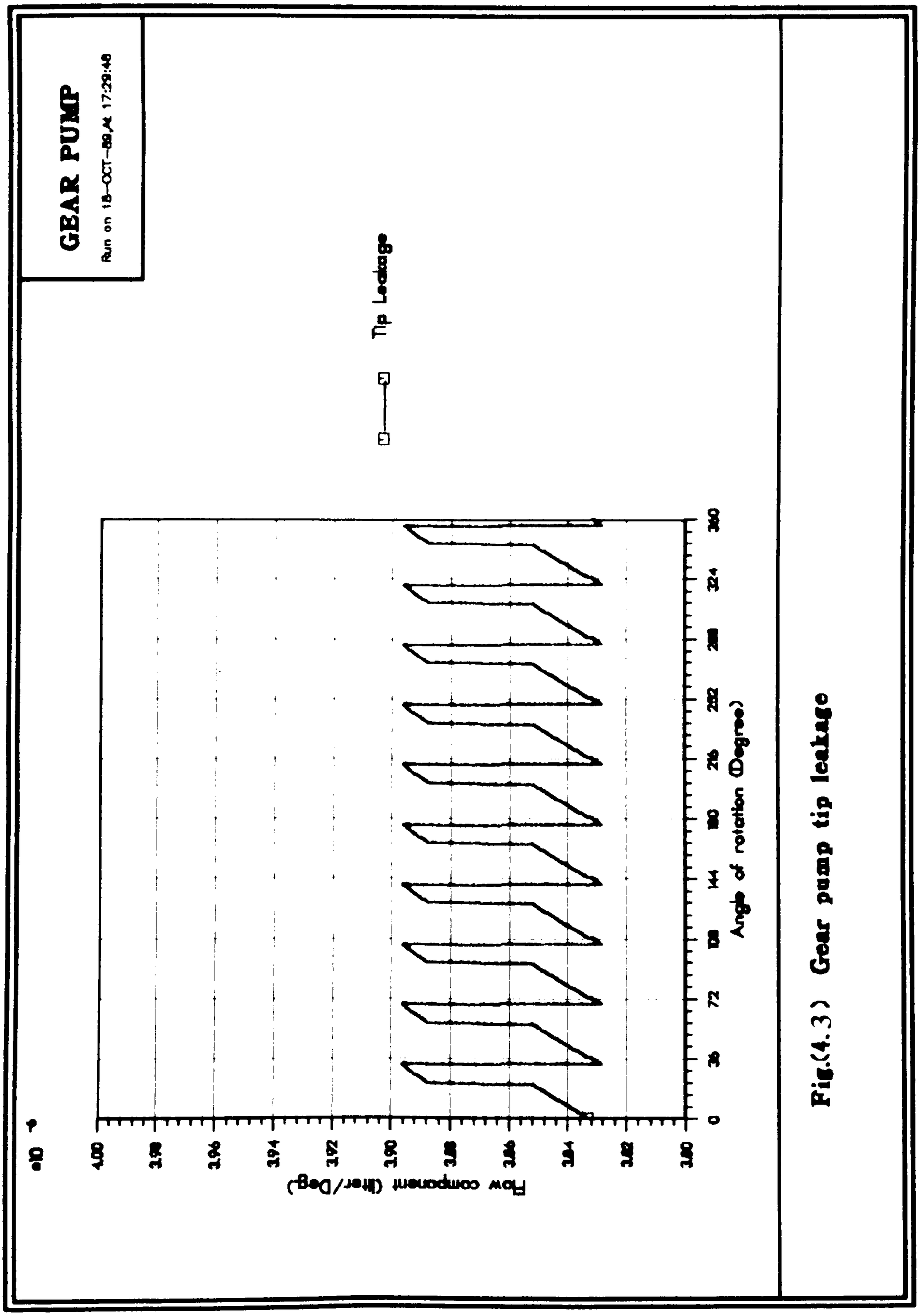

Fig.(4.3) Gear pump tip leakage

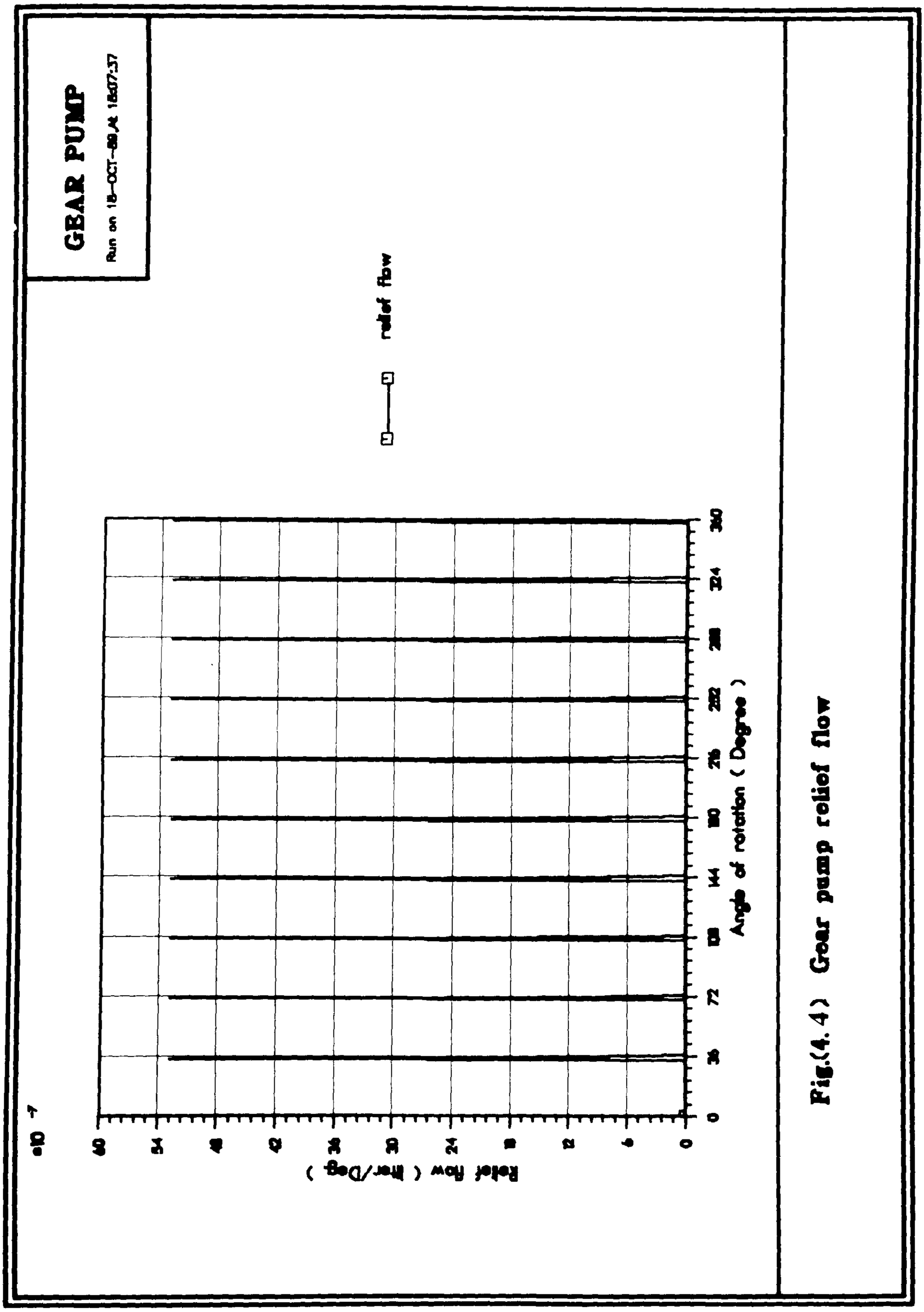

Fig.(4.4) Gear pump relief flow

ME945P

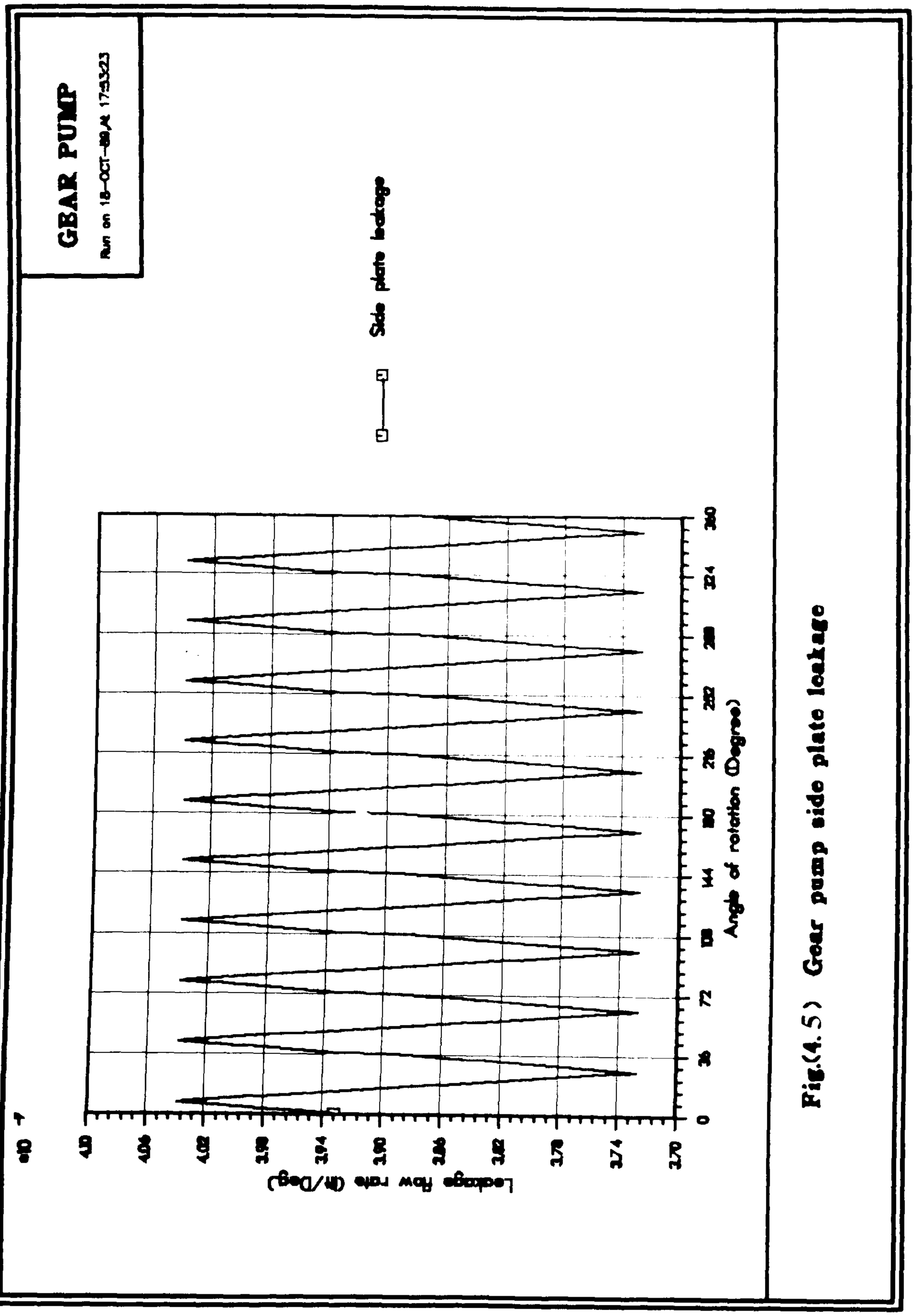

Fig.(4.5) Gear pump side plate leakage

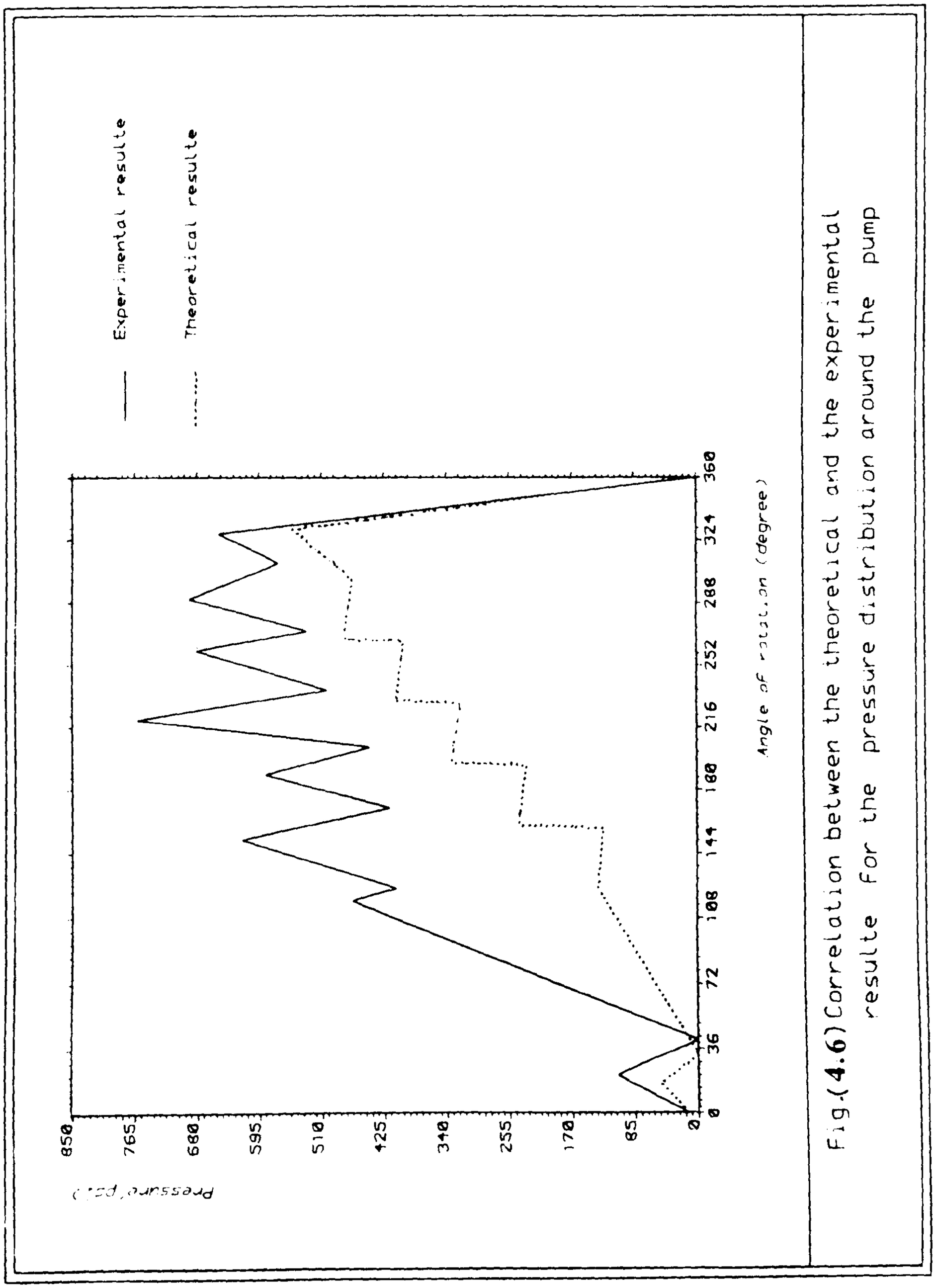

Fig.(4.6) Correlation between the theoretical and the experimental results For the pressure distribution around the pump

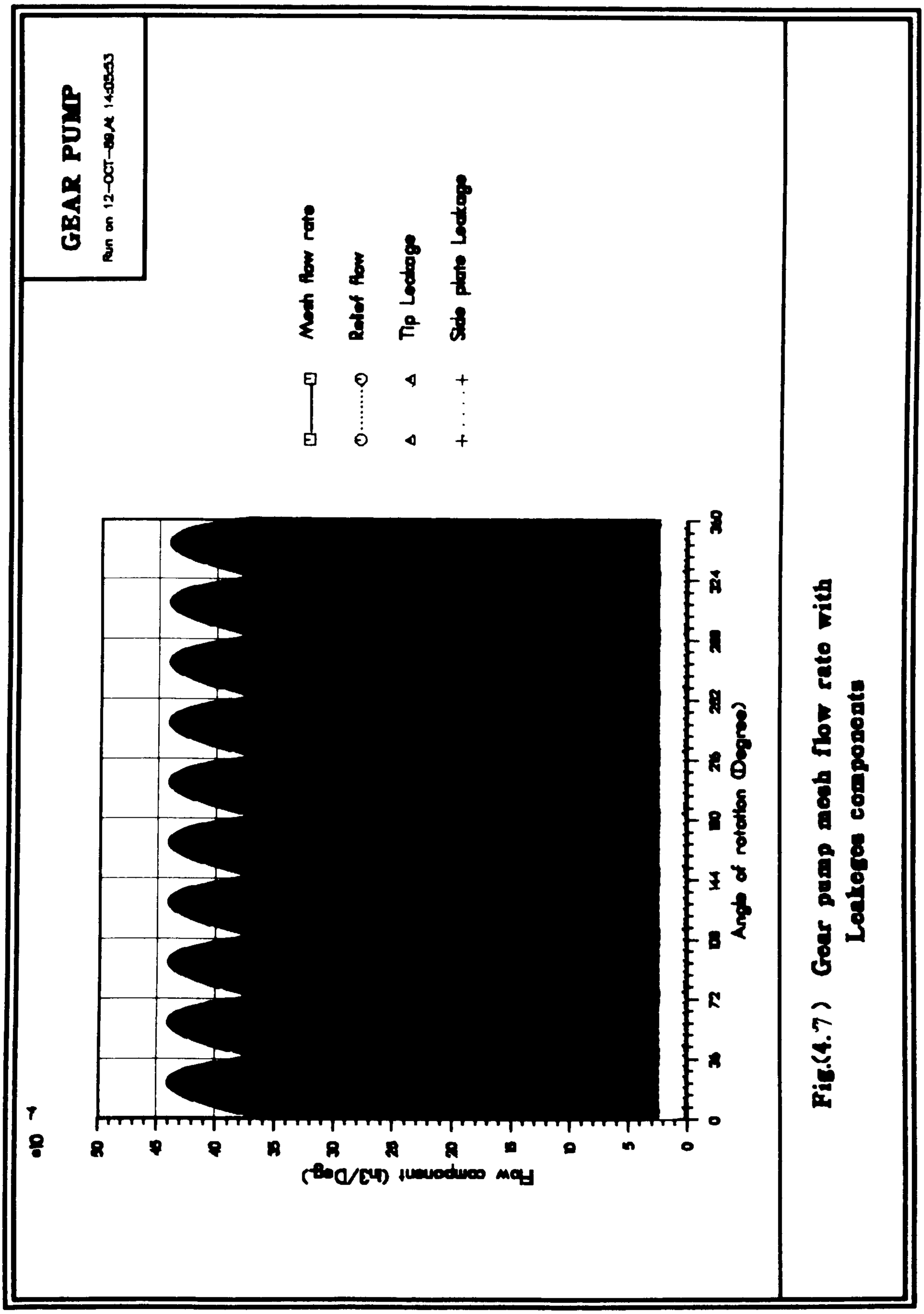

Fig.(4.7) Gear pump mesh flow rate with Leakage components

ME945P

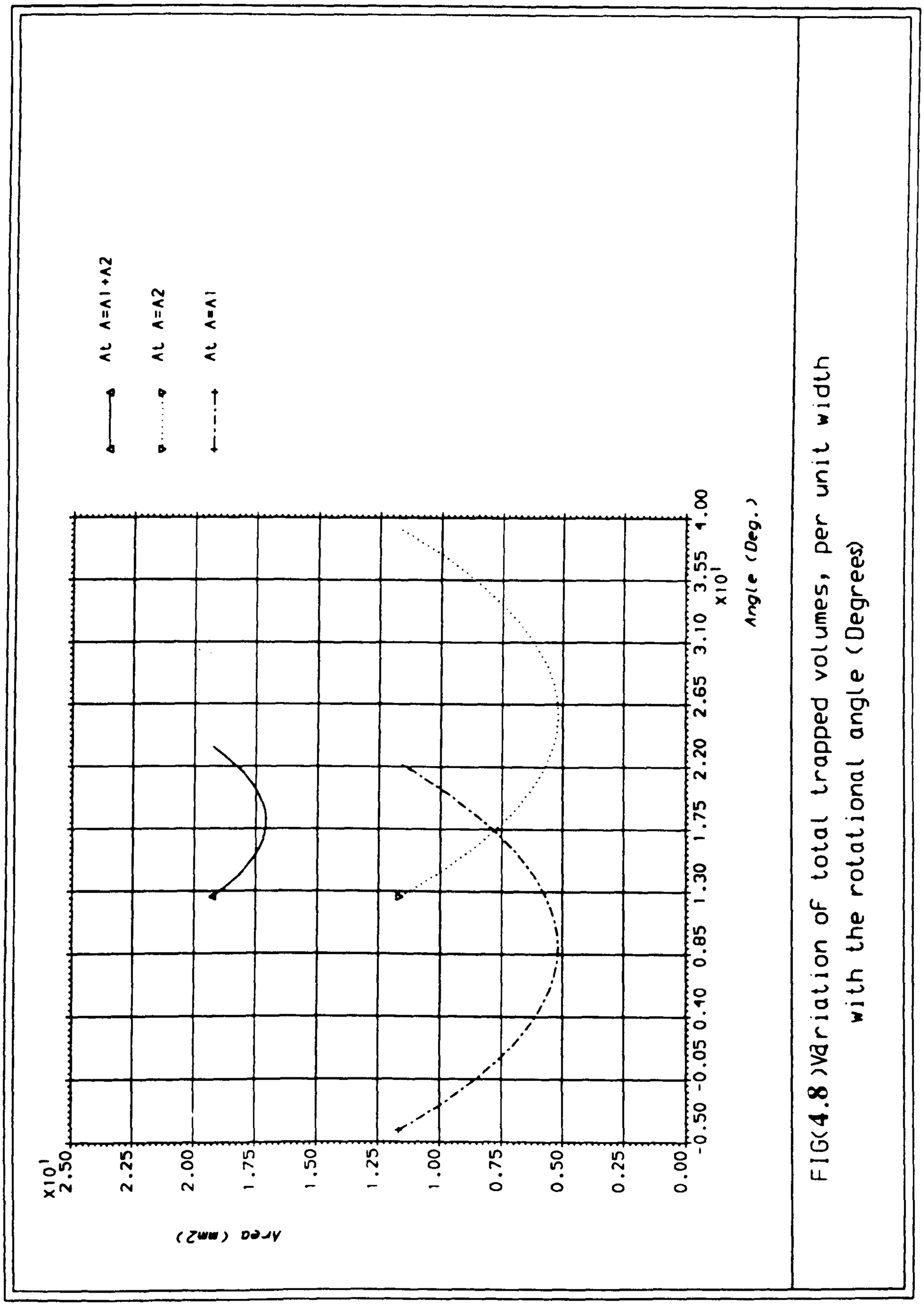

FIG(4.8)Variation of total trapped volumes, per unit width with the rotational angle (Degrees)

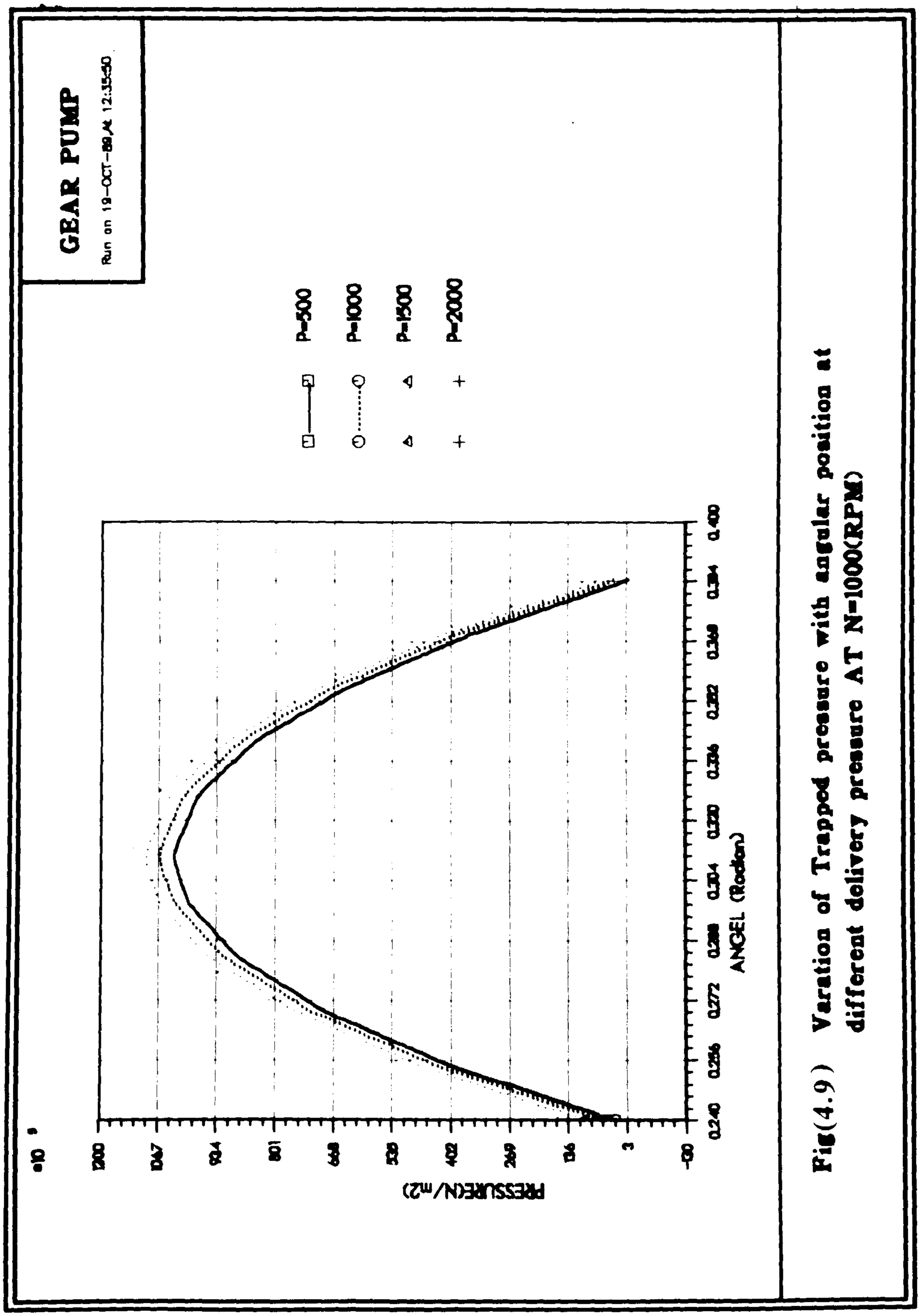

Fig(4.9) Variation of Trapped pressure with angular position at different delivery pressure AT N=1000(RPM)

MEJ45P

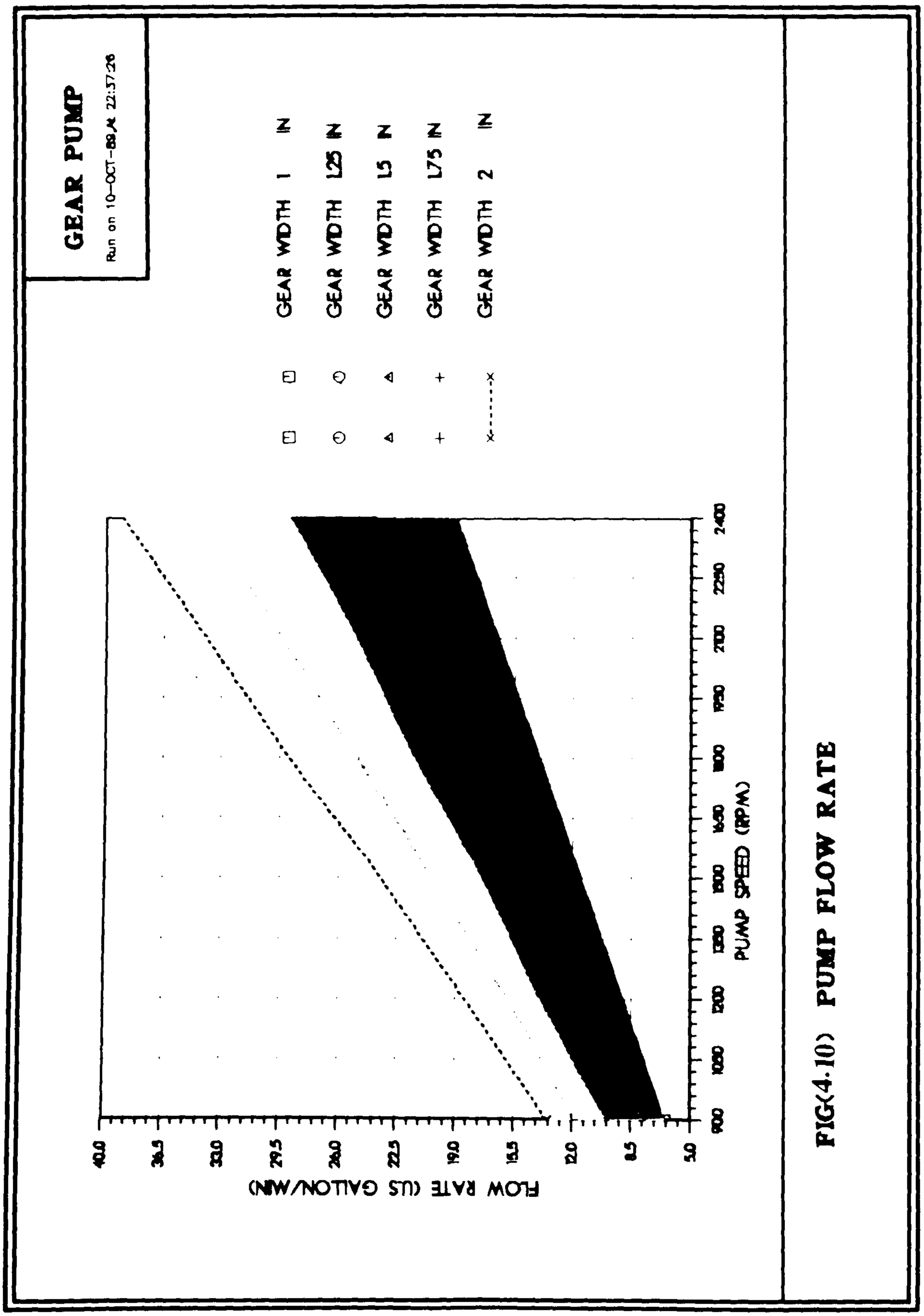

FIG(4.10) PUMP FLOW RATE

CHAPTER FIVE

THE EXPERIMENTAL PROGRAMME

5.1 Objectives

An experimental programme was adopted to verify the predictions of the theoretical investigation and, more generally, to provide results which could be used to lead to a better understanding of pump operation. In this chapter the experimental techniques being used in the current work are described together with the possibilities and limitations of these methods and other relevant approaches which are not employed in this study.

As described in the previous chapter, the pressure ripple can be used to predict the behaviour of the hydraulic components. The measurement of this ripple (pressure fluctuations) in a hydraulic system must be regarded as an essential part of all test methods and the reliability of the end result is very much a function of the quality of data acquired.

However, in most systems, the fluid borne noise characteristics of the component are unknown, and generally cannot be accurately predicted from their design details. Moreover, these characteristics of the components will vary with several factors such as pressure, temperature, fluid property, speed and component wear.

Developing a theoretical model may not be accurate enough to predict the effects of such parameters as leakage, pressure pulses (due to trapped space), timing effects, relief groove and cavitation inception. Therefore, it is important to establish methods for measuring and evaluating the fluid borne noise of the gear pump under normal marginal suction conditions, with a pressure ripple in the trapped space at cavitation inception and with erosion in the side plate (due to previous cavitation in the pump).

As concluded in Chapter 2, it was required to build a rig to perform these tests. Suitable instrumentation capable of measuring the test parameters with an acceptable band of error was employed as described later in this chapter.

5.2 Pump Performance

The tested pump used in the current system was a P31 TM, with a width of 38.1mm (1.5 in.), and a floating end plate with an external gear manufactured by Commercial Hydraulic Company, Bedford.

The specifications of the gears are shown in Table 5.1. The pump under investigation was tested according to standard test procedures, the purpose of which are to establish a uniform acceptable demonstration of the pump's capability to perform both mechanically and hydraulically in relation to the manufacturers' specifications. The important factors affecting the test results are the inlet conditions, outlet pressure, speed, liquid temperature, capacity and power. Recording and controlling all these parameters during the test are very important.

Nevertheless, the method of measurement must be accurate. The level of measurement accuracy is dependent on two parameters, (i) the kind of instrument used and (ii) the installation of the instrument. A discussion of the instrumentation used follows in the next sections.

A piezo-electric pressure transducer was used to measure the pressure ripple. A pressure transducer appropriate for this task must be able to work at very high pressure (up to 5000 psi), to cope with high temperature (120°C), to be reliable and to be insensitive to temperature variations and mechanical vibration. In addition, it must have good linearity and resolution, with low hysteresis, and have very good repeatability. Most important of all, the transducer must have a high frequency response (well above maximum audible frequency) and be sufficiently small to be able to locate it at any point in the system where the pressure must be measured. Transducers can be either of the piezo-electric or the piezo-resistive type. Ordinary foil strain-gauge pressure transducer does not normally have a high enough frequency response to give valid data for noise evaluation. A piezo-electric pressure transducer has been used.

Piezo-electric pressure transducers are an appropriate choice for this type of work. The material most commonly used as the basis of these

transducers is quartz which has excellent piezo-electric properties and operates because a number of tiny discs of quartz, jointed between a diaphram and the transducer body, become electrically charged in proportion to the force applied to the diaphram. Quartz has most of the properties desired for a transducer. Fig. (5.1) shows a typical transducer arrangement. These devices have, nevertheless two disadvantages which must be taken into consideration, (i) their high cost and, (ii) they are relatively fragile. These transducers, are sited at the pump inlet and outlet and are complemented by pressure gauges for DC measurements.

The experiments should be carried out at different speeds and a variable speed drive is needed. The measurement and control of the speed is very important and a reflective-opto-switch is used for measurement. This device consists of an infra-red emitter, L.E.D. and a photo-transistor sensor housed in a moulded package. The photo-transistor responds to radiation from the diode when a reflective object is placed within the field of view. In the present investigation the lay steel shaft was considered as the reflective object due to its shiny surface. In order to have the radiation in a signal mode, the shaft was striped in black around its periphery. The moulded case of the device incorporates a dust cover and an infra-red filter to prevent the ingress of dust and to reduce the effect of stray light. A schematic drawing of the device is shown in (Fig. 5.2).

In order to achieve consistent results, the oil temperature has to be kept constant during the test runs. Any rise in the temperature will effect the viscosity of the working oil as well as that of the dissolved air. Overheated oil may also damage the sealing due to the high power input by the drive motor to the system: the natural convective heat transfer through the pipe and tank surfaces will not be enough to dissipate all the heat generated to keep the system at a specific temperature. For this purpose a separate closed cooling system was used. Thermocouples were used to monitor the temperature of the oil and several mechanical parts of the system.

Measuring the flowrate is important when running a pump under normal or cavitation performance tests. The selected device should be able to cope with the required range of the flowrates, pressure and temperature.

It is also important that the device should not itself cavitate. In considering all the above requirements, a turbine meter has been chosen. It has (i) a high repeatability, (ii) high frequency output with linear calibration over a wide flow range, and (iii) good response to transients and fluctuating flows. All these parameters are to be considered in the present investigation and the test rig must be designed to accommodate the variable conditions of those parameters.

5.3 Pressure Distribution around the Gear Pump

In order to be able to examine the pump performance experimentally, it must be made possible to measure the static and the dynamic pressure (i.e., fluctuating pressure), at a specific point of the system. Moreover, the transient pressure inside the casing of the pump (around the rotor) must be monitored during the running of the pump. This was achieved using a high frequency response pressure transducer as described in the previous section, Heron [5.1].

The distribution of pressure around a gear pump rotor was investigated using a miniature peizo-electric pressure transducer, positioned between the gear pump teeth, see plate (5.1b). In this application the transducer was placed with its surface 20 thou. under the metal surface at the gear fillet. The transducer leads were passed through a hole along the main and the extension shaft to a slip ring assembly, see plate (5.1a). The signal acquired from the slip ring was then transmitted to the signal processing equipment.

5.4 Cavitation Test

It is very difficult to detect cavitation in a pump due to lack of a warning and is usually detected by its consequencial loss in performance. (It is generally acknowledged to be present when the pump head or efficiency falls off by approximately 3 per cent, or by the existence of typial cavitation erosion but visual inspection of parts is required for this latter criteria to be fulfilled).

Early interpretations of these criteria assumed no cavitation to be present in the machine if its performance was unaffected. There is, however, a non-intrusive technique of monitoring the existence of cavitation, via measuring the air borne noise emitted by the cavitating part, [5.2, 5.3, 5.4]. Maroney [5.5], concluded that ultra sound measurement can detect incipient cavitation, that is before any damage is likely to occur, or before the pump and consequently the system performance is lowered.

Furthermore, Maroney [5.5] found that the pump-generated airborne noise decreases with the decrease in the mean inlet pressure and that below a certain pressure the airborne noise increases again as a result of cavitation effects. He concluded that when 'micro-cavitation' occurs in the inlet line, the pump airborne noise is minimum. This is apparently due to the attenuation provided by microscopic air bubbles, even though no noticeable pump performance degardation occurs, Maroney. According to this conclusion the fluid borne noise technique was adotped for this investigation to indicate the cavitation inception in the pump. This was achieved by fitting two piezo-electric transducers at the inlet and outlet lines of the pump and monitoring the pressure ripple under normal and marginal suction conditions using a standard arrangment technique.

The Hydraulic Intitute's standards for centrifugal, rotary and reciprocating pumps, define three arrangements, Fig. (5.3), to control NPSH, and therefore cavitation when within the test pump. The first method involves changing the ambient pressure in the main loop tank which can be used to achieve very low NPSH values without creating cavitation along the pipe before the pump (which may occur if the NPSH is changed at the pump inlet). In order to control the ambient pressure in the main tank, either below or above atmospheric pressure, a vacuum pump or pressurised air line must be used respectively. Thus, the system will be capable of fulfilling another requirement, by changing the amount of dissolved gases in the oil.

5.5 Erosion

5.5.1 Introduction

In hydraulic machinery, one of the major design considerations is related to cavitation in flow passages, which can cause several deleterious effects including noise, vibration and erosion. The design engineer needs to know the effect of changes in flow velocity, pressure delivery, pump speed and size of the cavitation source on performance and pump durability.

In order to determine the extent of cavitation damage, several of the following criteria were considered in this project:

(a) The rate at which material was lost by measuring weight loss (this was not considered practical in this case).

(b) Number and size of pits formed.

(c) Volume eroded.

(d) Mean depth of penetration, Knapp [5.6].

These criteria are valid for most standard laboratory test methods which include vibratory devices, acoustic field generators, rotating disc devices and venturi flow apparatus. However, some of them are not valid (practical) for the real case of cavitation erosion (side plate erosion).

The ability to make appropriate measurements of both material loss and material redistribution assists in providing quantitative data related to cavitation damage. Denoting cavitation damage as either (or both) material loss (obtained by a measure of the change in weight), and material redistribution (without an appreciable change in weight). Beside the limitations of the weight loss methods to identify material redistribution there are other factors that are to be satisfied for the collection of accurate weight loss data. For instance, a very high resolution balance is needed to detect a small change in a fairly

large mass of the test piece. The matter is even more complicated because there is a loss in weight due to normal wear.

In the present study, the profile geometry techniques was selected to determine the cavitation damage characteristics as it had been shown to be a useful tool in wear studies, Thomas [5.7]. It can also be extended easily to cavitation erosion studies by obtaining the surface profiles of tested area before and after cavitation. A three-dimensional topography of the surface can be generated and analysed.

5.5.2 Three-Dimensional Surface Topography

Engineering surfaces are actually three-dimensional and the majority of the techniques include the profilometry, to measure only a two-dimensional profile. However, to obtain a three-dimensional representation of the surface, it is necessary to map a surface area rather than a line scan. Although the signal trace method is adequate for most applications, it falls short when studying the topographical changes after cavitation.

One means of overcoming this is to map a surface by making a number of closely spaced profile traces, to produce a three-dimensional surface description. This can be achieved by either using an adequate mini or micro computer for the large data handling required [5.8] to [5.9], together with a normal stylus method based on a standard Talysurf 4 instrument system incorporating a motorised traversing relocation stage. In this arrangement, one traverse table is indexed perpendicular to the stylus arm, while a second table travels parallel to the arm, thus enabling parallel profile traces, across the area of interest, the system shown in Plate (5.2).

The alignment accuracy of the traversing table sideways was ± 1 μm over a length in excess of 100 mm. An optical encoder coupled to the reduction gearbox, was used to accurately position the traversing table. A minimum traversing intervals of 3.06 μm by 2.051 μm could be achieved 'along' and 'perpendicular' to the stylus arm respectively. Movements of the traversing table could also be used for presetting

the required sample interval, number of traces and traverse position limits.

Outputs from the stylus head were fed directly to a North Star Horizon computer through an 8 bit ADC input channel, and recorded on floppy discs as x,y,z, data in binary form. The binary information, was converted to decimal form and then processed by a UNIRAS package, to provide both coloured and black and white 3D surface representation. The volume eroded, and the weight of the material lost could then be determined. Typical plots of a cavitation erosion surface are shown in Figs. (5.4) and (5.5).

REFERENCES

[5.1] HERON, R A — "Noise from fluid power system". Lecture notes for M.Sc. student, Noise and Vibration, SME, Cranfield, Inst. of Tech.

[5.2] DEEPROSE, W M; KING, N W, and McNULTY, P J — "Cavitation noise and erosion". Conference on cavitation (Edinburgh) I.Mech.E. 1974, pp373-381.

[5.3] PEARSALL, I S and McNULTY, P J — "Comparisons of cavitation noise with erosion, ASME Cavitation Forum (June 1968) pp6-7.

[5.4] HERON, R A and HANSFORD, I — "Airborne noise due to structure borne vibration transmitted through pump mountings and along circuits". I.Mech.E. Conference - Quiet Oil Hydraulics - Where Are We? London, Nov. 1977.

[5.5] MARONEY, G E — "The efffect of air/liquid volume ratios on pump noise emission". Paper No.76-55 Fluid Power Research Conference, Oklhoma State University, Oct. 1976.

[5.6] KNAPP, R T, DAILY, J W and HAMMITT, F G — "Cavitation". McGraw-Hill, New York

[5.7] THOMAS, T R — "Rough Surface' 1982. Longman, London.

[5.8] EDMOND, M J; JONES, A M; O'CALLAGHAN, P and PROBERT, S D — "A three-dimensional relocation profilmeter stage, wear, 1977 V49, pp329-340

[5.9] SAYLES, R S and THOMAS, T R — "Mapping a small area of surface". Journ.Phys.E,V9, pp855-861, 1976.

Table 5.1 Test Pump Parameter Values

TYPE OF PUMP : Extrnal Spur Gear Pump

SUPPLIER : Commercial Hydraulics Bedford Ltd.

PUMP ASSEMBLY CODE: 612-9610-99

SER. NO. : E017 1761

PARAMETER	SYMBOL	VALUE
Diameter Ratio of Gears		1:1
Number of Teeth/Gear	Z	10
Modul	m	4.5 mm
Face Width	b	38.1 mm
Pressure Angle		28
Center Distance	C	44.45 mm
Gear Form		Involute
Theoretical Delivery per Revolution		3.228 x 10
Pulsation Factor of Theoretical Delivery		17.5 %
Suction Port Diameter		38.1 mm
Delivery Port Diameter		25.4 mm
Max. Delivery Pressure		2500 psi

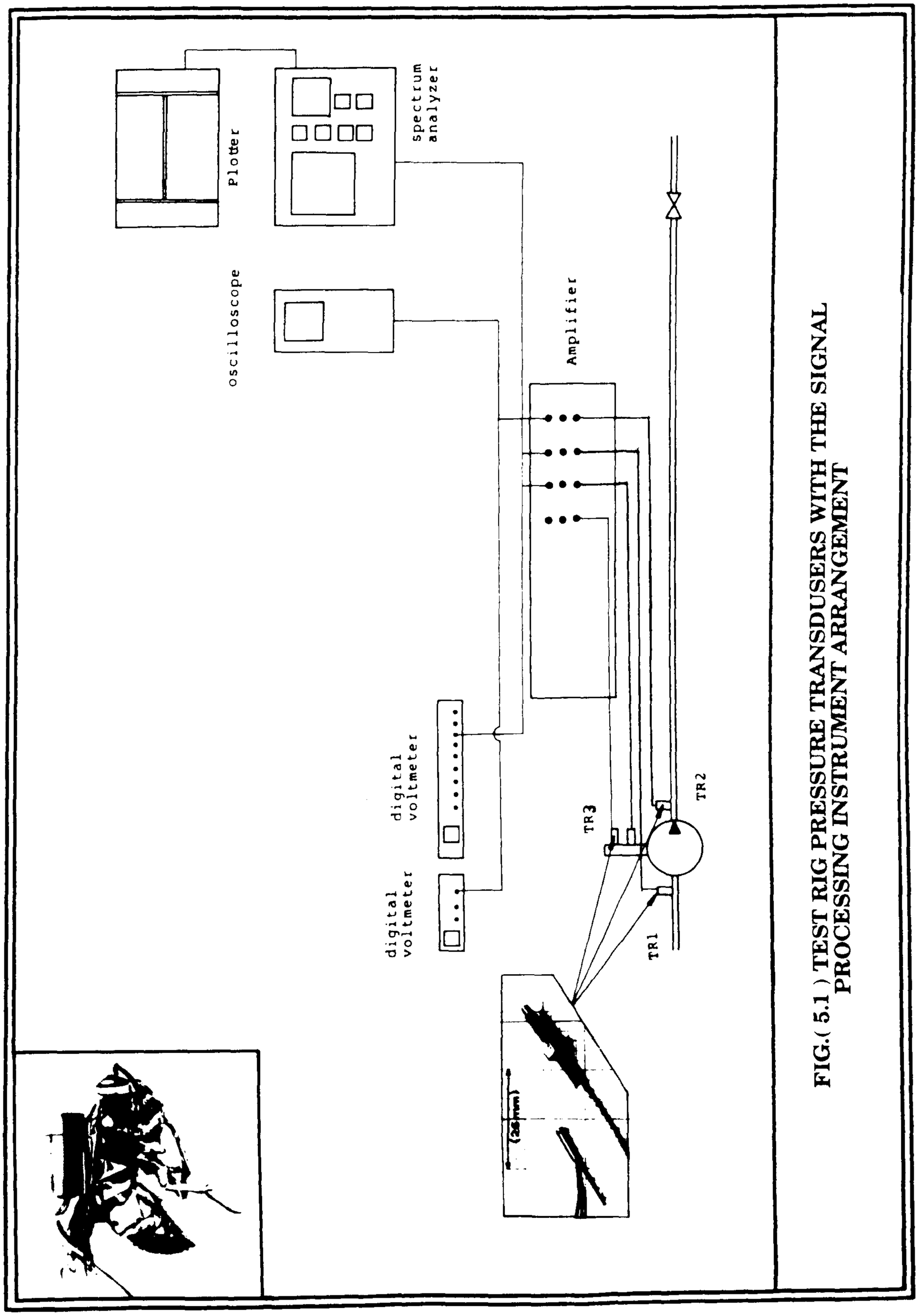

FIG.(5.1) TEST RIG PROCESSING PRESSURE TRANSDUSERS WITH THE SIGNAL PROCESSING INSTRUMENT ARRANGEMENT

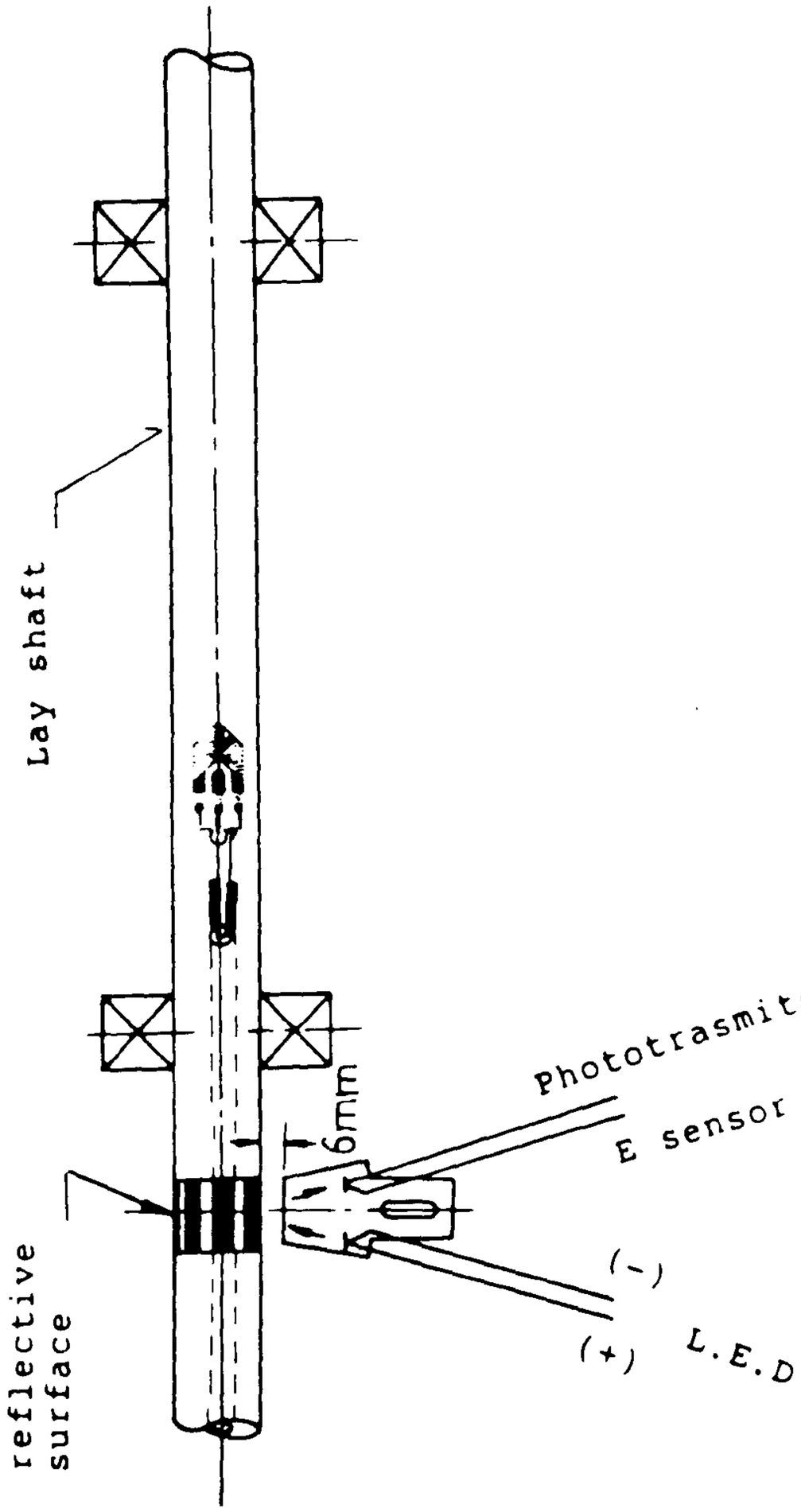

FIG.(5.2) SPEED AND TORQUE MEASUREMENTS ARRANGEMENTS

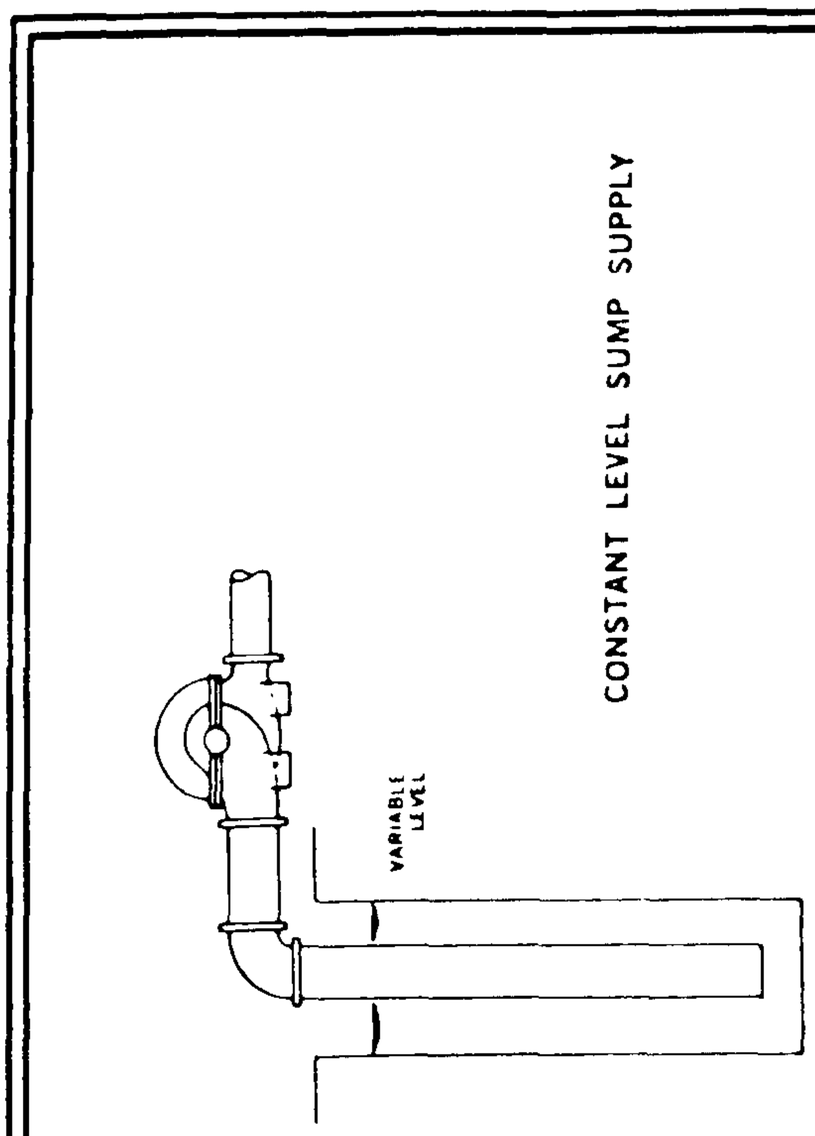

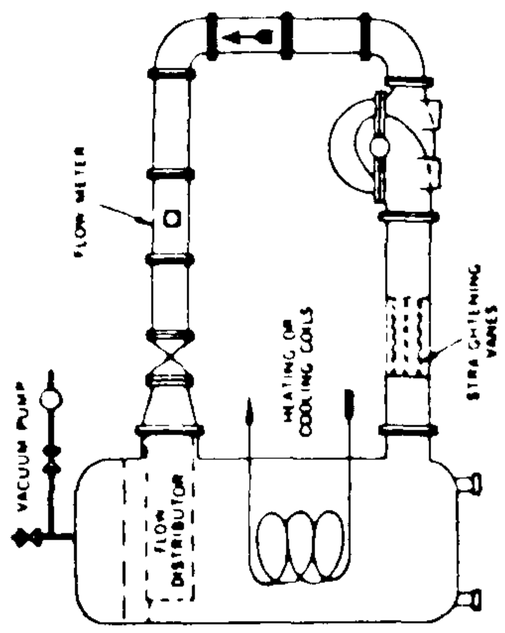

CLOSED LOOP SET-UP HORIZONTAL PUMP

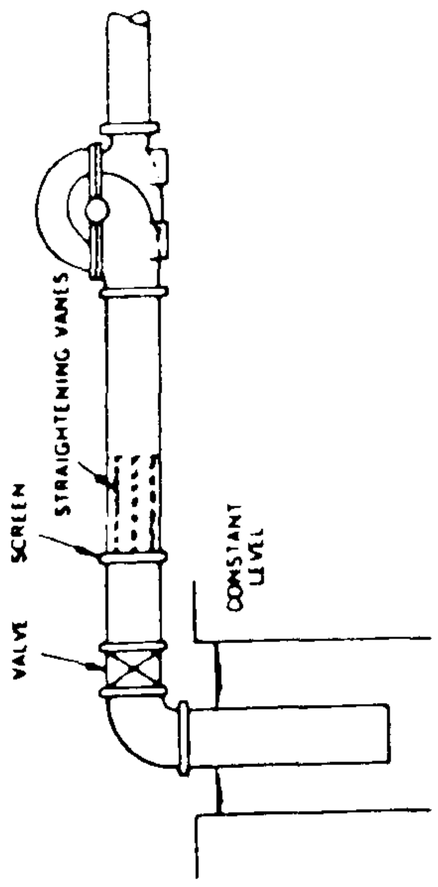

DEEP SUMP SUPPLY

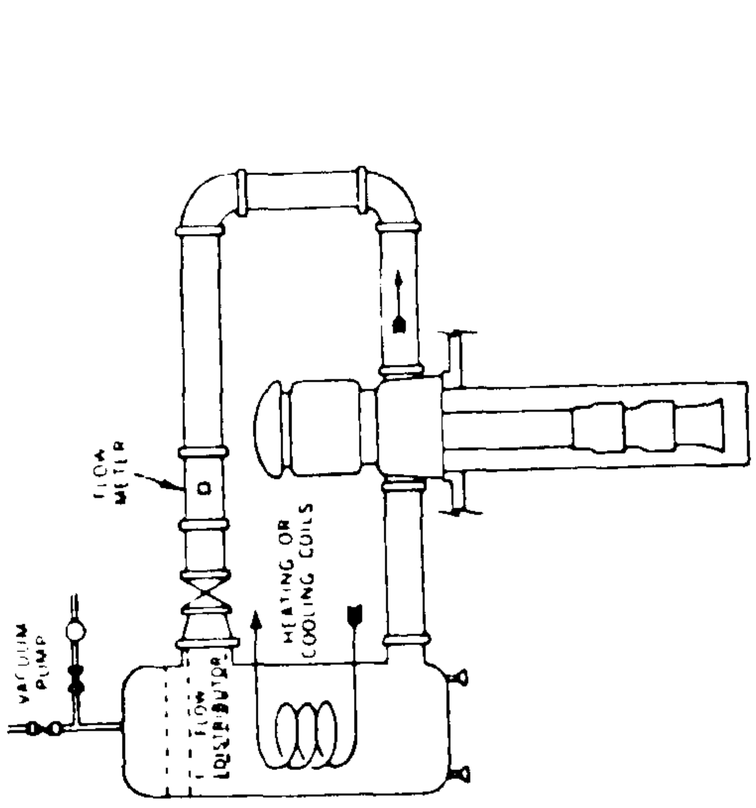

CLOSED LOOP SET-UP VERTICAL PUMP

FIG.(5.3) CAVITATION TESTS ARRANGEMENTS

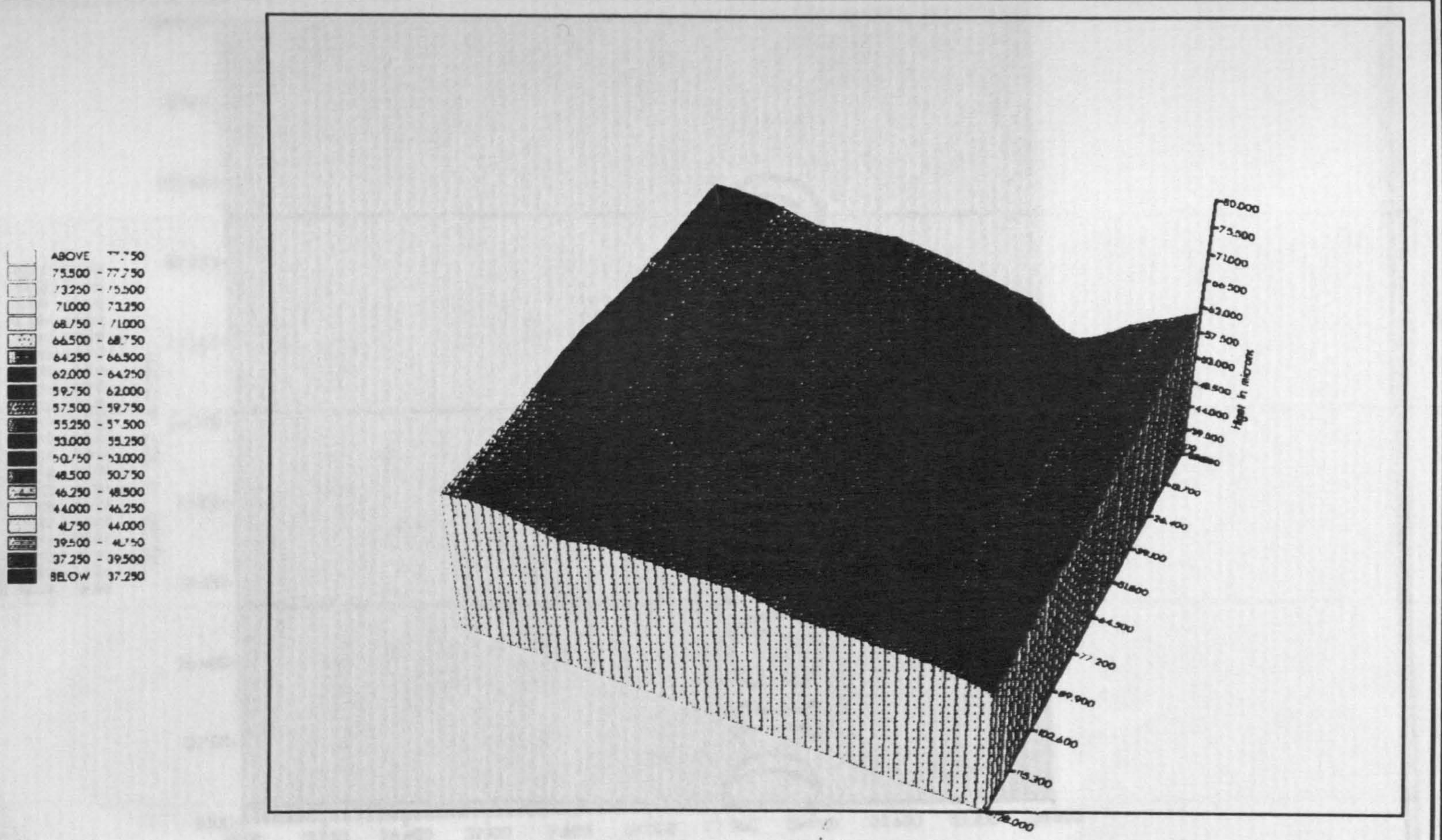

FIG(5.4) CAVITATION EROSION(1/4 HOUR UNDER CAVITATION)
(at Pout=500 psi) APPLIED MCH. GROUP (SME)

SIDE PLATE

Run on 24-MAR-88 At 16:12:54

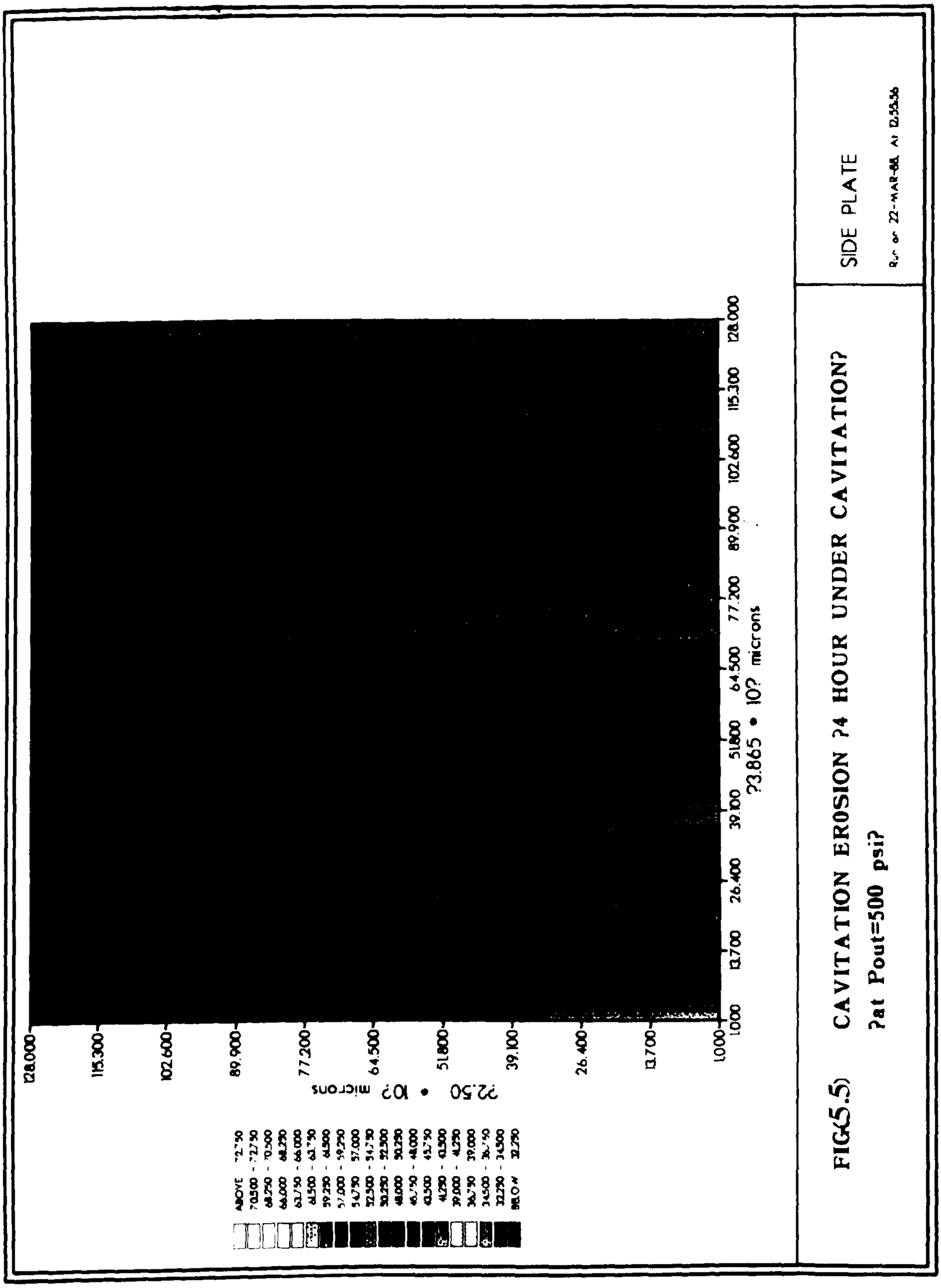

FIG(5.5) CAVITATION EROSION ?4 HOUR UNDER CAVITATION?

?at Pout=500 psi?

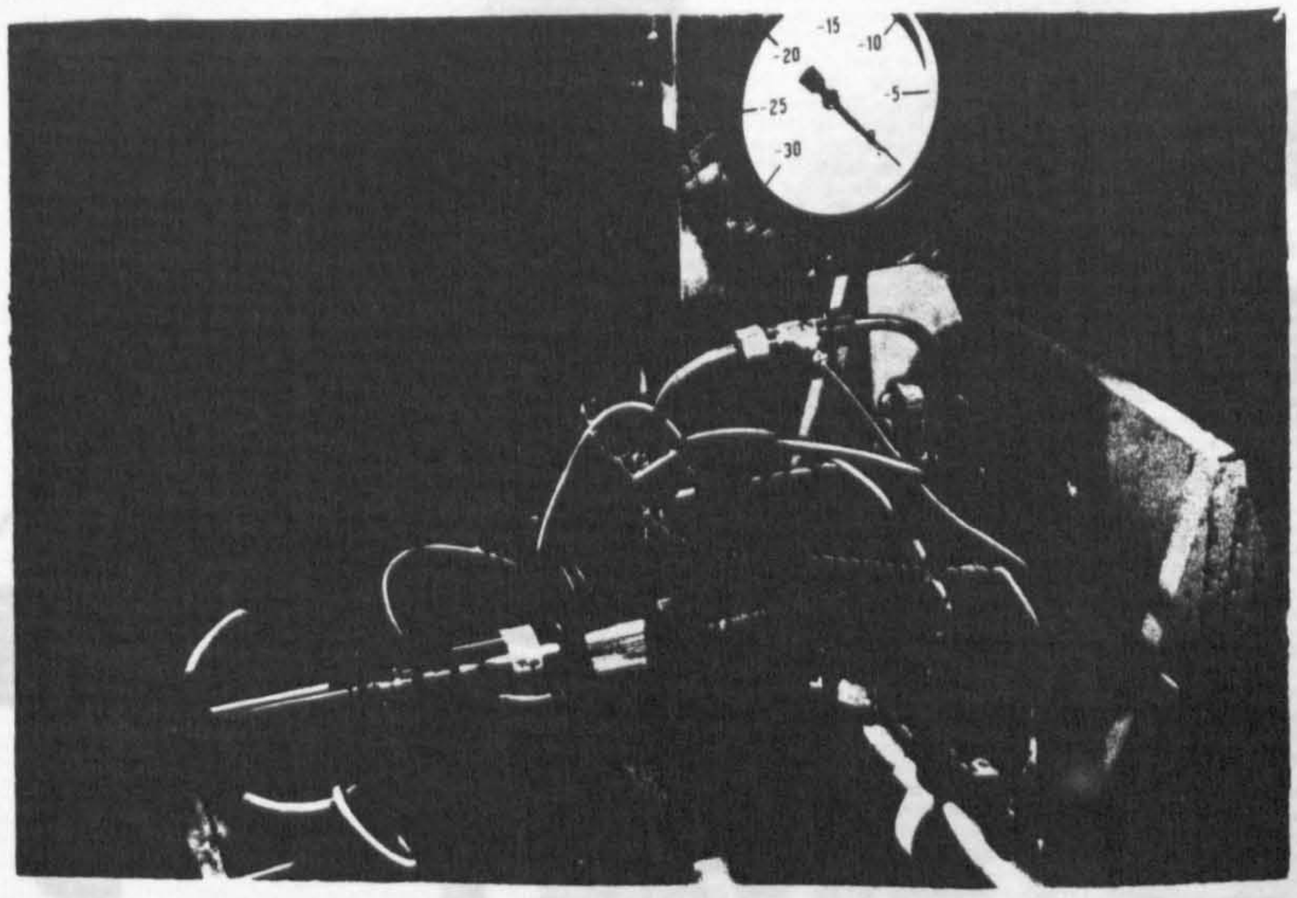

(a) GEAR PUMP

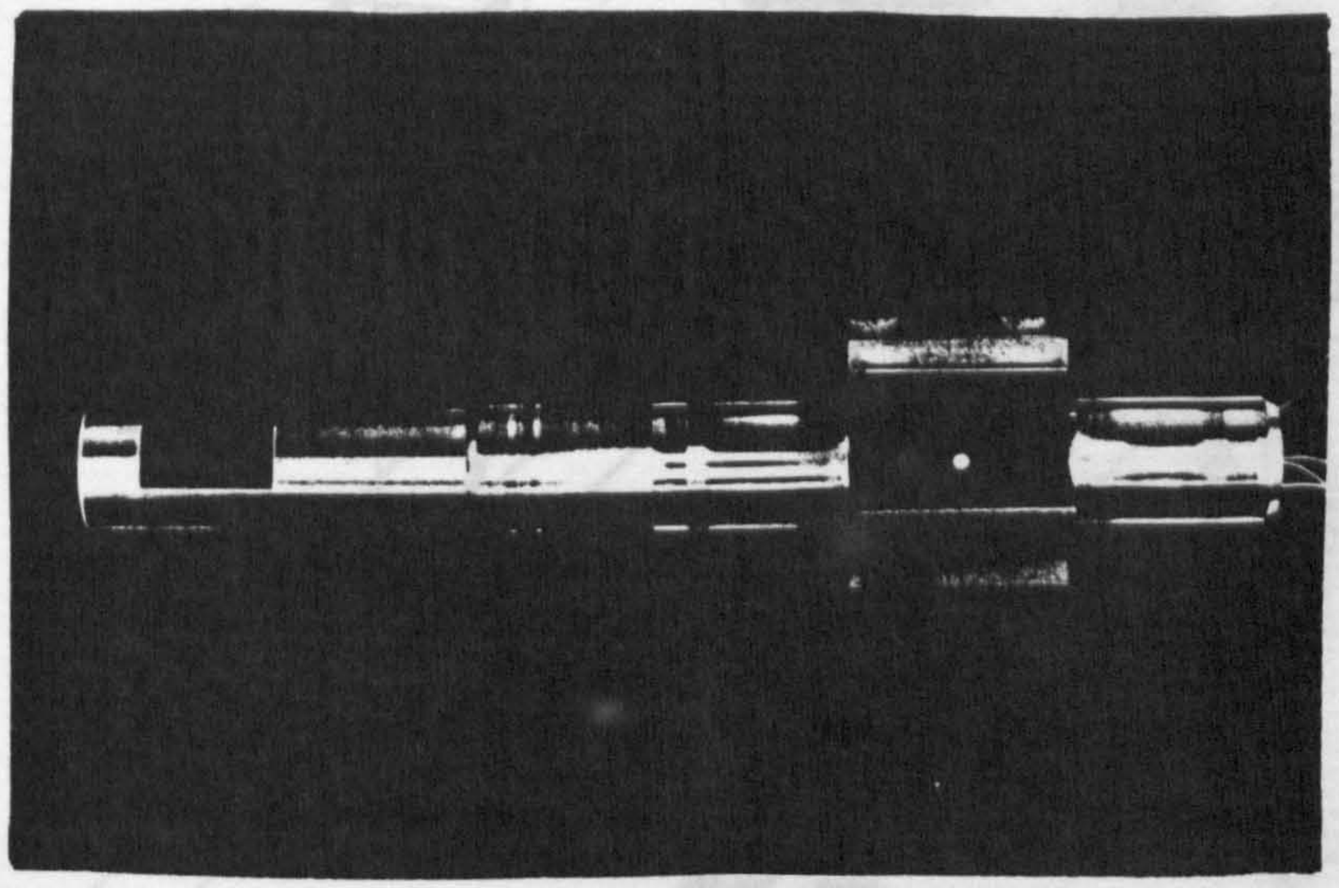

(b) GEAR ROTOR

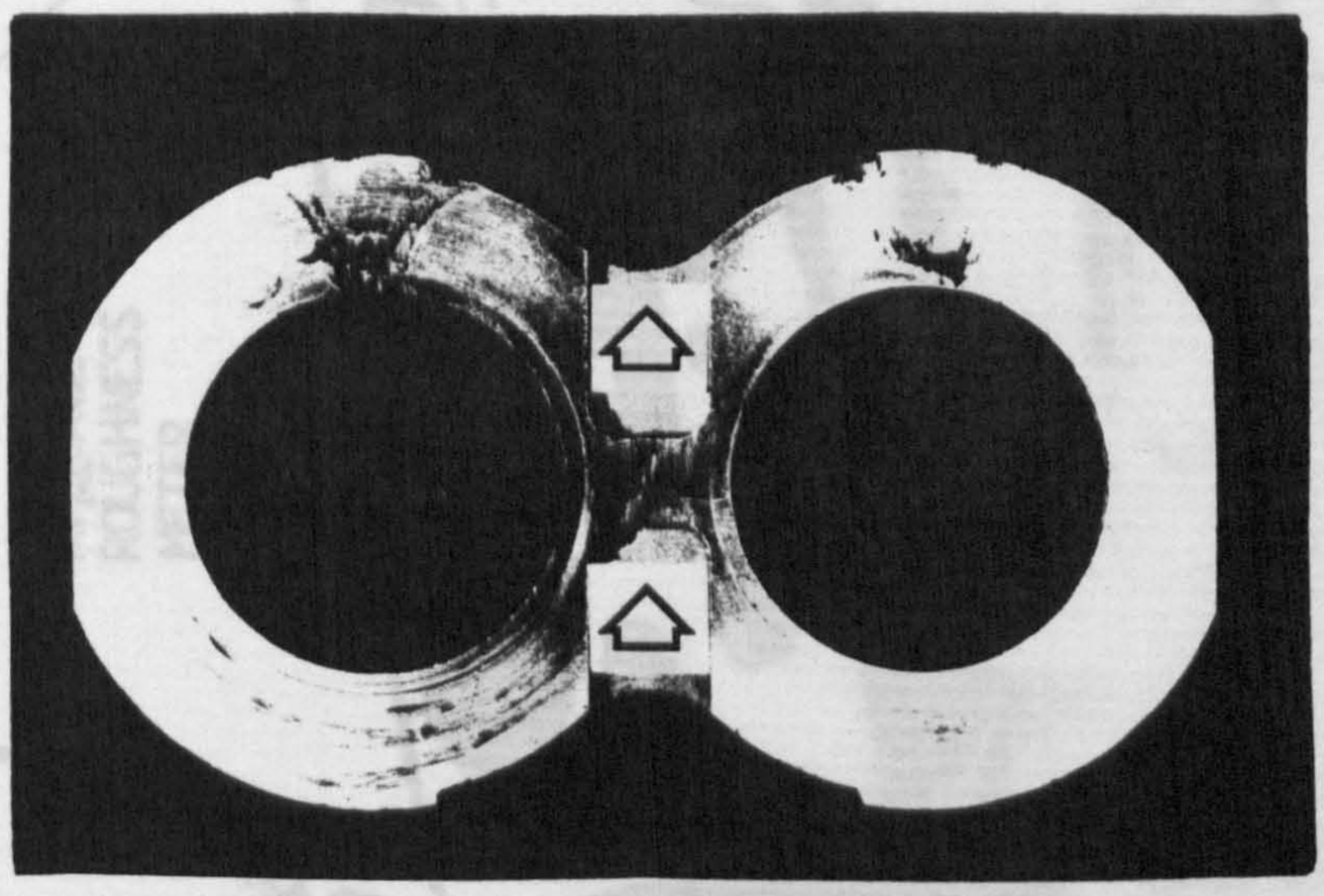

(c) SIDE PLATE

PLATE 5.1

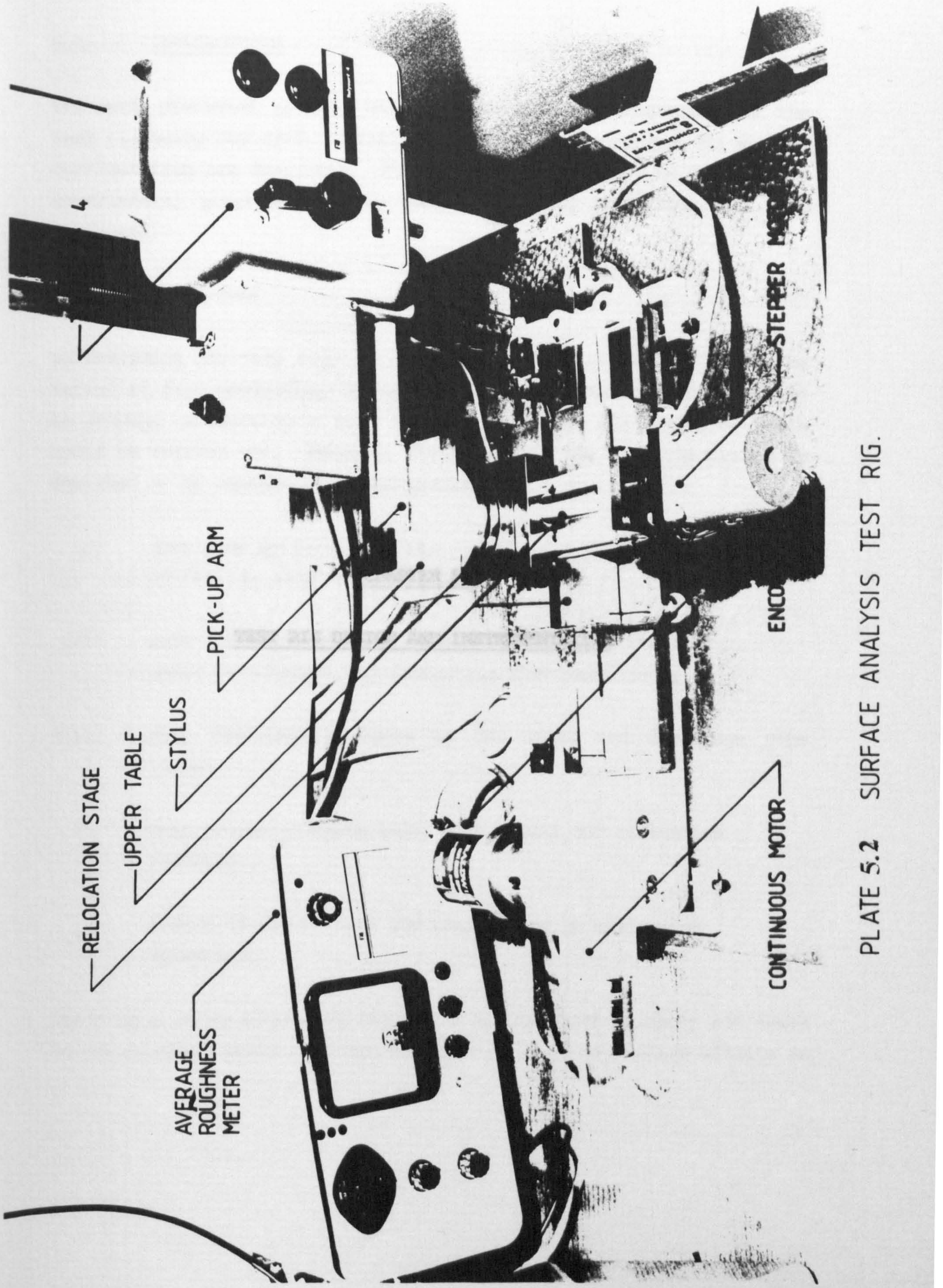

PLATE 5.2 SURFACE ANALYSIS TEST RIG.

CHAPTER SIX

TEST RIG DESIGN AND INSTRUMENTATION

6.1 INTRODUCTION

The work presented in this chapter describes the components of the test rig being employed. Details of its specification and its general configuration are described. The instrumentation used to support the experimental programme and to monitor the rig operation, are also presented.

6.1.1 Objectives

In designing any test rig, it is necessary to outline the aims to be satisfied from conducting the investigation. It would be impractical to attempt to develop a test facility in which all types of tests would be carried out. However, for this work the test rig has to be designed to be capable of investigating:

(i) gear pump performance under normal (non-cavitating) and cavitation conditions;

(ii) pump transient pressure distribution around the rotor under both normal and cavitating flow conditions;

(iii) pump transient pressure in the inlet and discharge pipe lines;

(iv) pump pressure ripple under both normal and cavitation condition;

(v) effect of air-contact and temperature on cavitation inception.

There is a major difference between a rig designed to carry out tests on rotordynamic pumps and that designed to study cavitation effects in

hydraulic power system incorporating a positive displacement pump. The features can be identified as:

(i) positive displacement pumps can withstand a very high pressure, thus attention should be given to the sealing and pipe materials, wall thickness and the type of connection;

(ii) positive displacement pump operates by a forcing fixed volume of liquid from the inlet into the discharge zone of the pump. This means that it cannot operate with zero flowrate, for that a relief valve sited in the high pressure point of the rig, to protect the system component from damage, is necessary; and

(iii) due to critical clearances a fluid conditioning unit (e.g., a filter) for dirt removal is needed.

The design and analysis of hydraulic systems and circuits are systemmatic in that they consider several activities in sequence in order to develop and prove the operation of the considered machine. Typically the recommended steps to be followed are to:

(1) defining the output objective;

(2) establish work cycles using time, pressure, and horse power plots;

(3) design the circuit;

(4) size and select components;

(5) assemble the circuit or system;

(6) monitor performance of the machine; and

(7) check the machine for safe operation and compliance with occupational safety as well as health administration standards.

6.1.2 Rig and Pump Specifications

The general layout of the test rig and its associated equipment is shown in Fig. (6.1).

The pump used in the system is the external P31™ gear pump (see Fig. (6.2) for its cross-section.

The test rig, was designed so that it can accommodate several test conditions (e.g., speed, pressure delivery, temperature, air content and suction pressure).

The suction and delivery pipes were sized to keep the flow velocity in the suction line within their acceptance limits (2-4.6 m/s for the delivery line and 0.6-0.2 m/s for the suctin line). The maximum allowable flowrate was 0.1818 dm^3/sec (24 gal/min) at the maximum speed of 2500 rpm. The system maximum pressure was 17.1368 MPa (2500 psi) and a maximum oil temperature of 100°C was imposed to protect the system seals and components from deterioration.

6.2 Hydraulic Components Selection

The selection and arrangement of components to build the test rig was a complex and time consuming task. For many applications, there are standard approaches and it is usually more favourable to adopt a conservative attitude and yet the choice of components should be both reliable and economic. Following these criteria the following items were manufactured.

6.2.1 Hydraulic Oil Reservoir

From early dates hydraulic systems have found applications in many varied fields of engineering. In each of these fields, specific hydraulics systems have evolved and the reservoir has suffered many modifications depending on the type of application.

More recently, there has been a trend towards the use of hydraulics in air space vehicles, and pumps have been developed to increase their power-to-weight ratio. This has led to higher shaft speeds and pressures, closer tolerances and better material to ensure an improved reliability and longer lives.

However, pump manufacturers claimed, Eley [6.1], that "a high percentage of pump failures which occur during the first 500 hours can be directly traced to the reservoir". This statement has great significance for hydraulic system designers who should clearly pay considerable attention to reservoir design.

An appropriately sized industrial reservoir in which several features are apparent is shown in Fig. (6.3). The overall dimension should enclose all the oil needed and sufficient volume for expansion due to the high thermal expansion of oil compared with the systems components (the thermal expansion coefficients for steel and oil are 1.6×10^{-5} (m/m.K) and 2.4×10^{-4} (m/m.K) respectively). This makes the wall thermal expansion negligible compared with oil thermal expansion.

In addition a sufficient surface area is needed to allow air bubbles and foam to escape from the fluid. the depth must be sufficient to ensure that, during peak pump demands, the oil level will not drop below the suction line. The reservoir should be sized so that when the fluid is contacting the walls and bottom of the tank adequate exposure for cooling of the fluid is permitted. However, in hot countries (e.g., Iraq) most of the earth moving machines are provided with heat exchangers.

Baffles are provided to separate the systems suction and return oil, promote circulation toward the bottom and side walls, and drop out foreign material such as dirt, sludge, as well as metallic particles. The return line is usually cut at a 45° angle to assist the redirection of the fluid. The drain is usually located at the lowest point of the reservoir, and a clean-out plate is provided for inspection and cleaning purposes. Sight gauges are often included to monitor the fluid level. The suction and return lines are sealed where they enter the reservoir to prevent dirt from entering the system. A filtered breather system is included to admit clean make-air to maintain atmospheric pressure as fluid is pumped out of the reservoir. The strainer prevents recirculation of particulate material back through the system.

Location of the return line below the surface of the fluid reduces the tendency for the oil to mist or form air bubbles as it enters the tank. However, in some cases, the return line is purposely located above the surface level to reduce the back pressure or syphoning on the system which might impede flow in a gravity return system. The capacity of a tank has traditionally been linked to the size of the pump. 'Rule of thumb' give guidelines which have in fact turned into standard recommendations. The National Fluid Power Association standard [6.2], for non-integral industrial fluid power hydraulic reservoir recommends that: the tank capacity (l) to be a minimum of three times the pump maximum operating capacity (l/min). In the test facilities used in the current investigation, two tanks were used: a main system tank and de-aeration/pressurisation tank, connected to each other via a 1 in. diameter pipe, see Fig. (6.3). Both tanks are identical with a capacity twice that of the pump.

The tanks are made of steel with thick walls in order to sustain both vacuum and pressure.

6.2.2 Pipe Sizing

The sizing of parts and pipe work is usually based on the recommended fluid velocities, whereas the wall thickness is based on the working pressure.

Normally, the piping in industrial hydraulic systems needs only to be sufficiently strong with nominal margins. Only occasionally is weight to power ratio or space critical. Weight to power ratio is the paramount factor in tubing in aircraft and space vehicle hydraulic systems.

Where steel pipe is used, the strength recommendations of the American Petroleum Institute are often adopted using the following criteria; that the tubing shall be capable of withstanding an internal hydrostatic pressure calculated from the following formula:

$$p = \frac{KtF_{tu}}{D-1.4t} \tag{6.1}$$

where

$$K = 0.6 + 0.4\,\frac{F_{ty}}{F_{tu}}$$

t = tubing wall thickness

D = tubing OD

F_{ty} = yield tensile stress

F_{tu} = ultimate tensile stress

For a thick-walled cylindrical member ($t>0.1r_1$), the formula must be mofidied to account for the radial variation in stress. The hoop tension at the inner wall, Keller, [6.3], is

$$S_1 = p\,\frac{r_2^2+r_1^2}{r_2^2-r_1^2} \tag{6.2}$$

The meridional stress is:

$$S_2 = p\,\frac{r_1^2}{r_2^2-r_1^2} \tag{6.3}$$

The stress in the radial direction acting at the inner wall is:

$$S_3 = p\,\frac{r_2^2}{r_2^2-r_1^2} \tag{6.4}$$

For thick walled tubes the displacement in the radial direction at the inner bore due to pressure is:

$$\Delta r_1 = p\,\frac{r_1}{E}\left[\frac{r_2^2+r_1^2}{r_2^2-r_1^2} + \nu\right] \tag{6.5}$$

where E = modulus of elasticity

ν = Poisson's ratio

r_1 = inner radius

r_2 = outer radius

Where weight is critical, the system designer must look carefully to the effect on the tubing thickness when raising both the ultimate tensile stress and the ratio of the yield stress to the ultimate.

A steel suction pipe of 5.5 ft. long, 1.25 in. bore diameter, 1/8 in. thickness and a steel straight pipe of 7 ft. length, 1 in. bore diameter 1/8 in. thickness have been connected to the main loop tank via steel flanges provided with the vacuum seal, and the pump outlet and provided with a regulator valve at the end to control the pressure in the delivery line, respectively. A positive displacement pump cannot work against a closed valve, a relief valve with a setting pressure of 2500 psi was installed across the regulator valve relieving the oil to the delivery line before the oil cooler.

6.2.3 Heat Exchanger

Heat exchangers are used in a hydraulic system to maintain the operating temperature of the fluid within specific limits. Normal operating temperatures range between 40°C and 70°C. High temperatures promote thinning, oxidation, and breakdown of the hydraulic oil; deterioration of seals, packings, and hydraulic hoses; and cause manfunction or inefficiency in components because the required clearances between parts (e.g., valves and pump parts) cannot be maintained.

The maximum amount of heat energy that can be generated internally by the hydraulic system is equal to:

$$\text{Energy loss} = (\text{pump input hp} - \text{Actuator output hp}) * \text{time}$$

$$\text{Temperature increase} = \frac{\text{Rate of heat generation}}{\text{Oil specific heat x oil mass flowrate}}$$

Because no actuator was employed in the system under consideration, all the pump input power was converted to heat. The temperature of

oil was controlled by using a closed loop cooling system. The cooling system used an oil-water counter flow heat exchanger connected to the main high pressure oil (hydraulic system) line. A cooling tower is used to cool the hot water via air radiators equipped with 3 KW circulating fans to control the temperature of the system. A centrifugal water pump was used to circulate water through the system. All the components of this system are shown in Plate. (6.1).

6.2.4 Relief Valves

All hydraulic systems with fixed displacement pumps use a relief valve to limit system pressure, and to protect the system parts from any unwanted forces.

Two relief valve with a pressure setting of 2500 psi and 300 psi were installed; the first across the regulator valve (load valve) to protect the pump, and the second at the inlet of the heat exchanger to protect it and relieve the oil back to the reservoir via a 1 in. bore diameter pipe provided with an eye-glass tube for flow detection.

6.2.5 Filtration

Contamination in hydraulic systems is very difficult to avoid, for example, the contamination from the initial system insulation, from the wearing of parts and from external sources during maintenance. Therefore, components must be designed and handled in order to minimize the retention of contamination as well as for the installation and the chemical incompatibilities. However, preventing contamination is easier and simpler than cleaning out dirt.

Contamination removal is dealt with by the filter. These are mechanical screens which can remove particles from the fluid stream by forcing the fluid to pass through a multiplicity of holes or paths which are so small they they block the passage of particles. Filters used in hydraulic systems are either of the depth type or of surface type.

A depth type filter has an appreciable thickness in the direction of the path and does not have controlled openings. The usual method for

analysing depth filters assumes that the filter medium consists of a series of surface-type filters. The change in the total contamination dW in the hydraulic system having initial contamination Wo, and a volume V of fluid, circulating at rate Q through a filter having a total efficiency E, if various mechanisms in the system add contamination at a weight rate A, at time t, dW can be deduced from:

$$dW = Adt - W\ Q/V\ E\ dt$$

or:

$$\frac{dW}{dt} + \frac{Q}{V} EW = A \tag{6.6}$$

If the initial contamination is considered and the removal assumed to approximate an exponential decay. The general solution to the amount of a contaminant present at any time, as determined by Tao, [6.4] is:

$$W = W_o\ e^{-\int \frac{QE}{V} dt} + Ae^{-\int \frac{QE}{V} dt} \int e^{\int \frac{QE}{V} dt}\ dt \tag{6.7}$$

The first term on the right side indicates that the initial contamination is removed at a rate dependent on the flow and the system volume. It is also removed at a rate which is dependent on the total efficiency E. On the other hand, the Efficiency, E, changes with time and loading, as the contaminant is picked up in the filter, the number of openings decreases and the average size of the openings grows smaller. Therefore, in terms of contamination removal ability, the efficiency of a filter improves with use, but the price paid for this efficiency increase is in having greater pressure drop. This means that the filters, after some time will have higher pressure losses. For this reason, they are usually placed in the return line to the reservoir rather than in suction lines which might cause the pump to cavitate as they become loaded.

The cleanliness of hydraulic fluid is described by the number and size of foreign particles it contains, and the standards accepted by the ISO and BSI is ISO/TC131/SC-6 at 1974, Sullivan [6.5]. The code range number that is assigned to particular hydraulic fluid to describe its

contamination level reflects the number of particles per unit volume greater than five micrometers and 15 micrometers in size per millilitre of fluid [6.3,6.5].

During cavitation tests the contamination becomes worse due to particles generated by cavitation erosion. Also contamination control plays a more significant part when running a cavitation test, because the presence of the foreign particles leads to significant reduction in the oil tensile strength and accelerates cavitation inception.

For these reasons a hydraulic filter is needed in the hyudraulic system.

The system under consideration is provided with a high pressure cleanable element depth type oil filter with 5 micron mesh to ensure, as far as possible, that clean oil is running through the system. The filter is located in the return line, in order to collect any contamination due to an eroded side plate, as well as to attenuate any pressure peaks in the following manner. In the test faiclity employed, the filter was fitted after the oil cooler thereby acting as a significant peak pressure attenuator because of its small cooling pipes. The general arrangement is shown in Fig. (6.4).

6.3 HYDRAULIC FLUIDS

6.3.1 Introduction

The fluid is the lifeblood of hydraulics and ties the system together. It is pumped from the reservoir through the control valves to cylinders and motors, expending power, before it returns at low pressure, back to the reservoir where it settles before starting the cycle again. In 1795 when Joseph Bramah utilised Pascal's discovery, and developed the first hydraulic press, water was used as the fluid and continued to be used as the only type of medium for a number of years, Hatton [6.6]. Until 1910, when mineral oils were found to be more suitable fluids, giving good protection against wear of the pump components, rust and corrosion, which were one of the major disadvantages of water.

At that time, however, mineral oil still provided difficulties as it was found to soften and destroy the natural rubber seals and packings. It was not until the mid-1930s with the development of oil resistant nitrite rubbers that it was possible to make reliable hydraulic systems to complete effectively with electrical and mechanical drives.

The hydraulic fluid needs a considerable number of specific characteristics. These include good anti-wear properties, compatibility with component materials, physical and chemical stability, resistant to shear, absence of toxicity, high bulk modulus, low foaming and air entrainment, low specific gravity, fire resistance, good heat transfer, low vapour pressure, low coefficient of thermal expansion, and low cost. The increasing need for fine filtration to protect critical components against wear requires the fluid to have good filterability.

No single fluid will meet all these requirements and therefore there are many different hydraulic fluids on the market, many tailored to meet the requirements of a specific application.

The two most difficult conditions for a fluid to accommodate are the presence of dirt and heat. Large particles of dirt, up to 40 microns, wear the system severely, whereas silt in 5-10 microns range promotes wear by lapping. Heat deteriorates the fluid by oxidation. Heat thins out the fluid causing inefficiency in the transmission of power, wear because of insufficient oil cushion between close fitting parts, and leakages.

6.3.2 Transmission of Pressure

6.3.2.1 Compressibility and Bulk Modulus

The compressibility of a hydraulic fluid governs the energy absorbed by, and the time required for, generation of pressure by the pump, and the energy released on decompression. It also governs the performance of hydraulic systems due to its effect on the stiffness of power transmission. In both connections it is desirable that the compressibility of the oil should be as low as possible. This requirement is met by keeping the oil sufficiently free from entrained air or other gases.

The presence of free gases in the oil sharply reduces the stiffness of the actuator oil column and the viscosity of the oil resulting in an increase in the oil temperature of the system as explained below. Regarding the stiffness of the oil, air at atmospheric pressure is more than 10,000 times as compressible as a hydraulic oil, so even less than 0.1% of entrained air at atmospheric pressure will reduce the bulk modulus of the fluid by a factor of 10, if the pressure of the fluid is atmospheric. This reduction in the system oil bulk modulus affects the system response and stability.

The bulk modulus of a liquid-gas mixture is given by:

$$\frac{1}{\beta_m} = \frac{1}{\beta_l} + \frac{V_a P_a}{V_m P_m^2} \qquad (6.7)$$

where

m = mixture

l = liquid

As the viscosity of the air is much less than that of oil, the presence of air reduces sharply the lubricating film effectiveness; this leads to a direct contact between metal surfaces of the system components, especially in the regions with small clearances. In addition, when air bubbles pass from a low pressure to a high pressure region they will be compressed isothermally rather than a diabatically, Hayward, [6.7], and a heat rejection, from the air to the oil, takes place. These two effects constitute a large and early risk to the system components. The relationship between compressibility and 'Bulk Modulus', which is a more precise method of expressing compressibility, is as follows:

$$\text{Compressibility} = \frac{1}{\text{Bulk Modulus}}$$

Fluid bulk modulus can be determined either by measuring changes in fluid volume as a function of pressure at isothermal conditions, (this value is relevant where pressure and volume changes are slow). and is often referred to as 'static'. Alternatively the bulk modulus may be determined through measurements of the speed of sound in the fluid under isentropic condition, Peeler [6.8], which is the relevant

parameter when pressure changes are very rapid. This value is often referred to as the 'dynamic' value.

The values of bulk modulus may be reported as secant or tangents as follows. The secant bulk modulus is the average or mean of the change in pressure divided by the total change in volume per unit of initial volume,

$$\beta_s = \left[\frac{\Delta p}{\Delta V / V_o} \right]_{T.E.} \qquad (6.8)$$

The tangent bulk modulus is the inverse of the compressibility at specific point,

$$\beta_t = -V_o \left[\frac{\partial p}{\partial V} \right]_{T,E} \qquad (6.9)$$

where : T = subscript indicating isothermal

E = subscript indicating isentropic

The higher the value of the bulk modulus the 'stiffer' the system and hence quicker response.

The working fluid used in the tests undertaken was a Shell-Tellus 37 hydraulic oil (its specification is shown in Appendix B). All the experiments were conducted under the oil temperature of 40° ± 2°C. The density and viscosity of the oil at 40°C are 870 Kg/m^3 and 0.0322 Pa.s respectively.

The relationship between the Bulk Modulus β and the pressure p, for Shell Tellus oils (see Fig. 6.4) given by:

$$\beta = \beta_o + mp - np^2$$

where β_o = bulk modulus at atmospheric pressure and a given temperature

p = pressure at which β need to be calculated

m,n = constants depending on the grades of the oil.

6.3.2.2 Gases in Hydraulic Oil

Air can be dissolved or entrained in hydraulic fluids, and it is possible for air to change from one of these forms to another depending on the conditions to which the fluid is subjected. Entrained gases are present in the oil when it sweeps air out off a free pocket due to drag forces between the two surfaces and carries it along the stream.

Entrained gases also occur as a result of dissolved air that has come out of the solution as bubbles when the oil passes through passage with a high local velocity or low pressure. As the oil evolution process is quicker than the solution process [6.9], these gases keep circulating inside the systems.

The dissolved gases per unit volume of oil is in proportion to the pressure, (Henry's law). According to this law, the liquid can dissolve an amount of gas directly proportional to the partial pressure of the gas. It has been established that the small quantities of gases, dissolved in water, do not effect the water capability to dissolve another gas independently (acting as though other gases were not present) [6.10]. In the case of air, the stability of Oxygen and Nitrogen is governed by their separate solubility coefficients, with Oxygen dissolving rather more readily in almost all liquids than Nitrogen. If this effect is ignored, the solubility of air in the oil can be taken as the solubility of oxygen in oil which is proportional to the absolute pressure.

Mixture of air and oil exists in nature in three different states, saturated, supersaturated and undersaturated. The equilibrium state is the saturated state, when the oil cannot dissolve more air even when its surface is in contact with free air. During the circulation of oil in the system, it changes from one state to another depending on the pressure and temperature at the considered position. However, when the oil is compressed after the pump, it will change from the saturated to the undersaturated state and tends to disolve more air. On the other hand, when the oil is subjected to a pressure drop, it

will become supersaturated and its solubility will drop, and air will tend to come out off the solution and become entrained air.

The forces acting on the gas bubble are the buoyancy and viscous drag forces. The buoyancy force is:

$$F_b = \frac{4}{3} \rho_l U_g^2 \, C_d \pi r^2$$

where r = gas-bubble radius

ρ_g = mass density of oil

g = gravitational acceleration

C_d = drag coefficient

U_g = gas bubble ship velocity

at equilibrium $F_b = F_d$, therefore

$$U_g = \sqrt{\frac{8}{3} \frac{rg(\rho_l - \rho_g)}{C_d \rho_l}}$$

Gas removal can be performed by increasing the bubble slip velocity, either by increasing the site of the gas bubble or Reynolds number. This can be achieved by heating up the oil, or by increasing the gravitational pull by performing swirling and centrifuging of the oil. Practically entrained gas removal can be utilised by pasing the oil through a screen of a very small mesh.

None of the above techniques can be used for dissolved gases. The only way is by applying a vacuum pump to the reservoir, (the benefit of Henry's law). In the current test facility, however, the entrained air was removed by increasing the oil temperature, and by letting the return oil impinging on a metal surface to release the bubbles.

For the dissolved gas control, a vacuum pump was used and in addition liberated free gas from the system was removed.

6.3.3 Net Positive Suction Head Control

In any cavitation test, the rig should have an accurate control over a wide range of the NPSH (i.e., Net Positive Suction Head) at the pump inlet.

The Hydraulic Institute Standards for centrifugal, rotary and reciprocating pumps outlines three methods which can be used to control NPSH. The preferred one is by changing the ambient pressure in the main loop tank. This method can reach a very low NPSH without creating cavitation along the pipe, before the pump, which may occur if a valve is used to change the NPSH at the pump inlet. A vacuum pump was employed to change the ambient pressure in the main tank loop below the atmospheric pressure.

The vacuum pump used in the rig could achieve 28 inches of Mercury Vacuum (0.5 lb/in^2 absolute pressure). In order to reduce the rest of the atmospheric pressure and the head of the oil in the tanks, a diaphram valve was installed at the inlet line of the pump. This method was selected because it created the least tendancy for pump cavitation. From the pressure measurement, the net positive suction head (NPSH) can be evaluated by using the following expression:

$$NPSH = P_s + \frac{U^2}{2g} - P_v$$

where

P_s = absolute pressure at the pump inlet

U = pump inlet flow velocity

P_v = fluid vapour pressure at the prevailing fluid temperature

6.4 DRIVE SYSTEM

For experimental purposes the gear pump ran between 500 and 2400 rpm using a variable speed electric motor. The drive motor which has been

chosen and utilised consists of an S charge A.C. variable-speed commuter motor with a starter. The motor speed could be changed by a mechanical device which changes the commutator slip rings. The electric motor speed range was between 270 and 2500 rpm. Because the maximum speed required for the gear pump was more than those values, two pulleys of 790 mm and 315 mm PCs were fitted on the pump drive shaft and the motor driveshaft respectively. This increased the speed ratio to 1.6579.

The motor horsepower is 15-50 HP, with a frequency of 50 Hz using 3-phase 400 volts supply power. A banded 3-vee belt transmitted the power to the pump thorugh a low noise coupling drive shaft.

6.5 SYSTEM INSTRUMENTAION

Details of the instrumentation used in conjunction with the system are given in Table 6.1. The relative positions of all instruments are shown in Plate 6.2.

6.5.1 Description of Instrumentation

The instrument required to test the performance of a gear pump with or without cavitation as fluid borne noise analysis has been discussed in Chapter 5.

For the present studies, up to 4 piezoelectric pressure transducers were mounted on the pump inlet, the pump outlet, the gear rotor, and the side plate. Pressure transducers were used to pick up the signal as a sensing element. The transducer utilises a metal diaphram as a force collector and the combined non-linearity and hysteresis is 1% full-scale. In all utilised transducers, the compensated temperature is between 80-180°C.

The small size of the force collector allows the transducers to be used for high frequency measurements. Typical response ranges are 67% of the transducer natural frequency which amounts to 125 KHz for the transducers at the pump inlet and pump rotor and 375 KHz for the transducers at the pump outlet and the side plate. All transducer readings were absolute pressure.

Each transducer was connected to a charge amplifier, which consisted of four channels, the maximum response frequency was 32 KHz. The output of the charge amplifier is a voltage output amplified to the required level by the specified gain which can be readily displayed on an oscilloscope. A four-channel storage oscilloscope was used. During signal analysis, all the transducers were connected to a continuous frequency analyser with the fast Fourier transform (F.F.T) algorithm and data acquisition capabilities. The mean pressure level was measured by connecting the output from the amplifier to a digital voltmeter. This can be compared with the reading obtained from a high quality pressure gauge. A plotter was connected to the spectrum analyser to obtain a permanent record. Figure 6.6 indicates the signal processing system used. Plate (6.2) also shows the system measuring and signal processing instruments.

6.5.2 System Measurement

Fundamentally, measurement is the result of a quantitative comparison between a predefined standard (response) and an unknown magnitude. If the result is to be meaningful, two requirements must be met in the act of measurement:

(i) the standard (response) must be accurately known and internationally accepted, and

(ii) the apparatus and procedure employed for obtaining the comparison must be approved.

Therefore, the calibration of all instruments is essential and subsequently reduces the error in the measurements. Details of the instrumentation used in conjunction with the system are given in Table 6.2.

The variables monitored, and their methods of measurement, were as follows:

1. Pump speed: a reflective-opto-switch (to sense the speed of the pump) was mounted 4.6 mm from the lay shaft.

2. Mean pressure levels in the pump's delivery and suction lines: these variables were sensed and measured using high quality pressure gauges.

3. Fluctuating pressures: these were measured in the inlet and delivery lines by pressure transducers mounted through tapping points which were designed to accommodate either a pressure transducer or blanking plug. The transducers were then connected via an amplifier to, either a storage oscilloscope, or, a two channel Frequency Analyser to record the signal.

4. Pressure distribution around the rotor was measured by installing a small-sized entrant pressure transducer in the tooth flank. The transducer was connected via a slip ring to either a storage oscilloscope or a Frequency Analyser.

5. Temperature measurement: six thermocouples connected were used to define the operating temperature, three of these were used to control the system oil temperature and the other three to monitor the temperatures of the two bearings on the lay shaft and the temperature of the gear pump casing. All the thermocouples were connected to a multipoint switch and then to a digital temperature built-in cold junction readout.

6. Flow measurement: a high resolution, linear calibration turbine flowmeter was used. The flow level in the system was indicted by counting the number of pulses per second generated by this meter. The limitation of this turbine flowmeter is that it is not linear below 4.546 l/min (10GPM).

7. Shaft torque was measured by a strain gauge type of torque transducer connected via a slip-ring to a digital voltmeter.

8. Fluctuating pressure on the side plate due to cavitation bubble collapse was measured by a high frequency, small side, "Entran" pressure transducer mounted on the side plate at a specified position to sense the pressure at the eroded area.

All the system instrumentation was calibrated. The calibration methods and results are presented in Appendix C.

6.6 PUMP MODIFICATION FOR INSTRUMENTATION

6.6.1 Measurements from the Rotating Assembly

In this experimental work, the study of the distribution of pressure around a gear pump, and the shaft torque, under cavitating and normal conditions, were of primary interest. The problem encountered was how to get the signal from the pressure transducer and the strain gauge of the rotating gear assembly which required a slip-ring assembly. The pump for the current project was supplied with two shafts: (i) the drive shaft and (ii) an extension shaft in line with, and coupled to the drive shaft but projecting from the other side of the pump, see Figure (6.2). the connections to the rotating assembly were achieved using a hole through the extension shaft which carried the transducer and strain gauge leads to the slip ring unit, see Plate 6. The problem of oil leakage through the shaft was overcome by special high pressure seals.

6.6.2 Side Plate Measurements

The pump under test was a floating end plate type which needs to be fixed to carry a pressure transducer to sense the pressure fluctuation generated by cavitation bubble collapse. The side plate was fixed by two screws to the main casing after a special slot was milled to carry the Entran, EPL-125 Flatline Pressure transducer and a 2 mm hole drill over the 3 mm diameter pressure sensitive area of the transducer diaphram. The leads were carried through a hole in the casing which was sealed by epoxy seals. The position of the pressure transducer on the side plate is shown in Fig. 6.6).

6.7 CONCLUSIONS

A test rig was built which is capable of:-

- Testing a pump under normal and cavitation conditions

- Providing a range of pump test speeds
- Testing various inlet and outlet conditions of the pump
- Accurately measuring the following parameters:-

Delivery dynamic pressure
Suction dynamic pressure
Shaft speed
Dynamic pressure around the rotor
System temperature in many points
Pump oil flowrate
Oil inlet and outlet temperature
Shaft input torque

REFERENCES

[6.1] ELEY, J.M. 'Reservoir Design as Viewed by Pump Manufacturers'. S.A.E. Paper 70071, Sept. 1970.

[6.2] ANSI-B93-18-1973 'Non-integral Industrial Fluid Power Reservoirs'. National Fluid Power Association, Milwarkee, Wisconsin 53222.

[6.3] KELLER, G.R. 'Hydraulic System Analysis'. Published by the Editors of Hydraulic & Pneumatic Magazine, 3rd Ed., 1978.

[6.4] TAO, T.C. 'Media and Filtration Mechanics'. From Aerospace, Pawtucket, R.I. March 1966.

[6.5] SULLIVAN, J.A. 'Fluid Power, Theory and Applications'. Second Edition, 1982. Reston Publishing Comp., Reston, Virginia.

[6.6] HATTON, R.E. 'Introduction to Hydraulic Fluids'. Reinhold, 1962.

[6.7] HAYWARD, A.T.J. 'Aeration in Hydraulic Systems - It's Assessment and Control'. Proc. of Conference on Oil Hydraulic Power Transmission and Control, 24-30 November, 1961.

[6.8] PEELER, R.L. and GRAN, J. ASTM 'Bulletin' No. 235, 5 January 1959.

[6.9] SCHWIZER, P.H. and SZEBENELEY, V.G. 'Gas Evaluation in Liquid and Cavitation' Journal of Applied Physics, Vol. 21, Dec. 1950.

[6.10] TAYLOR, P. and HILLWARD, A. 'A Method of Predicting the Effect of the Dissolved Gas Content of Water on Cavitation Inception', Proc. of I.Mech.E., Vol. 198, No. 12, 1984.

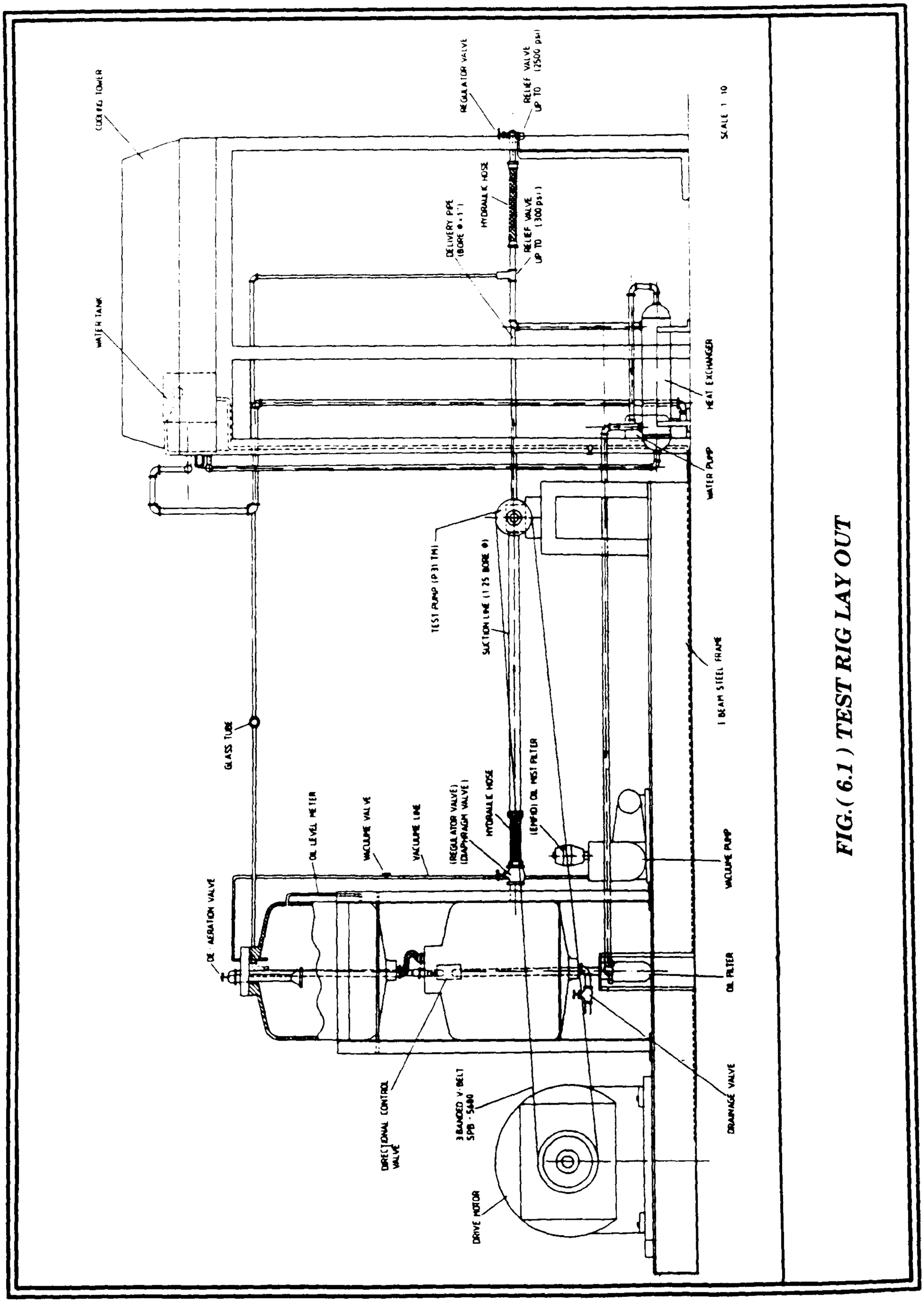

FIG.(6.1) TEST RIG LAY OUT

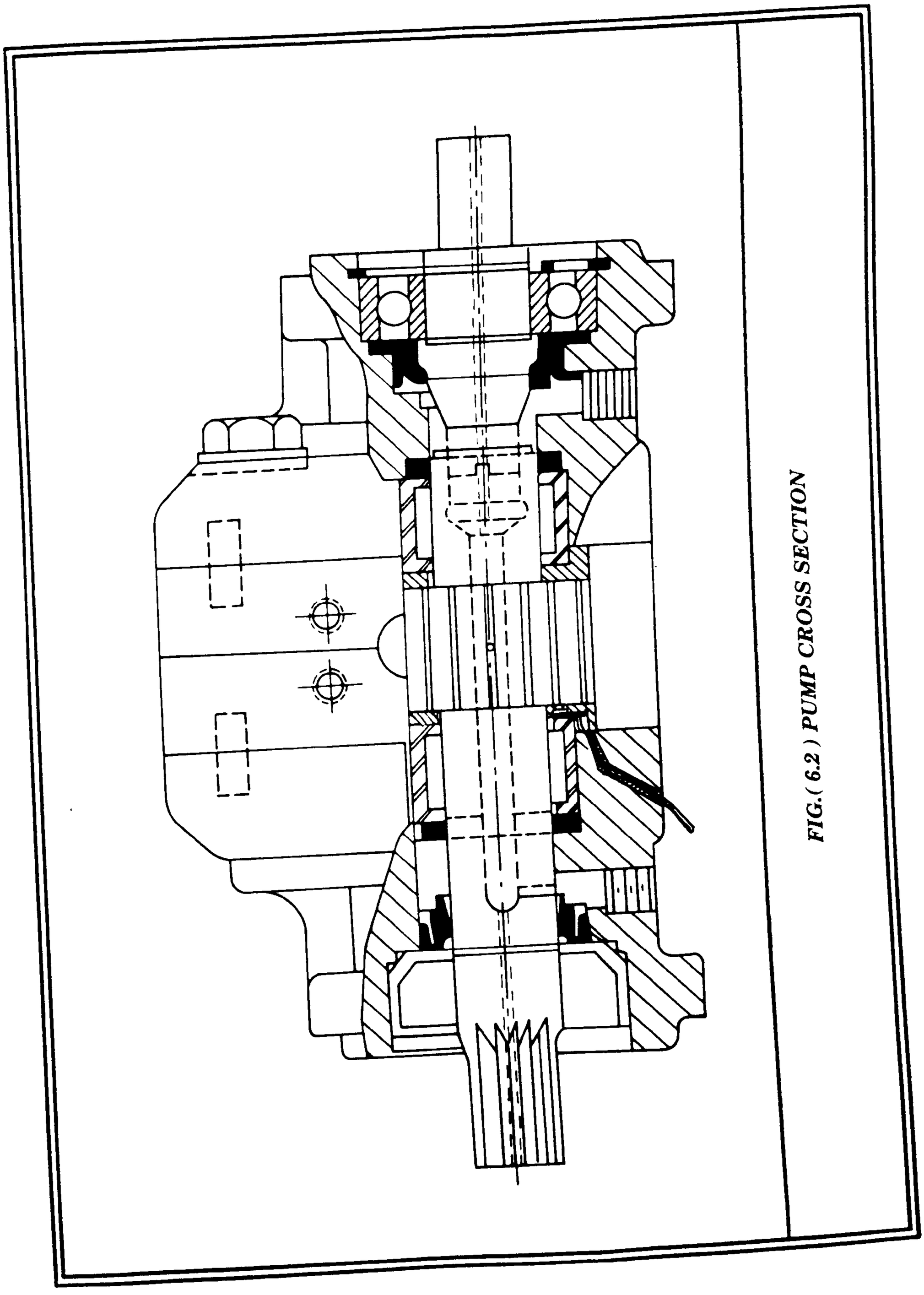

FIG.(6.2) PUMP CROSS SECTION

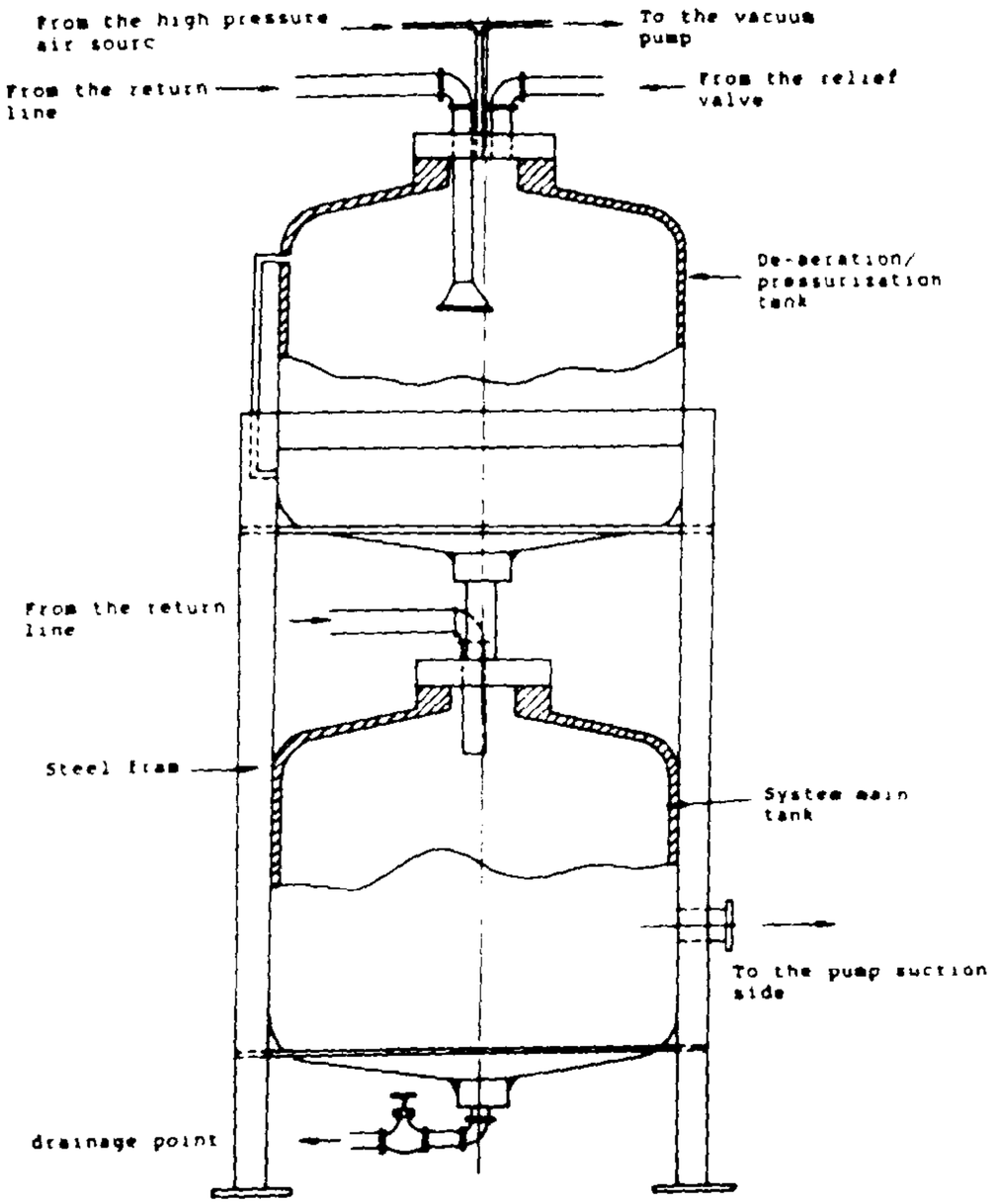

The main and the de-aeration/pressurization tank arrangement

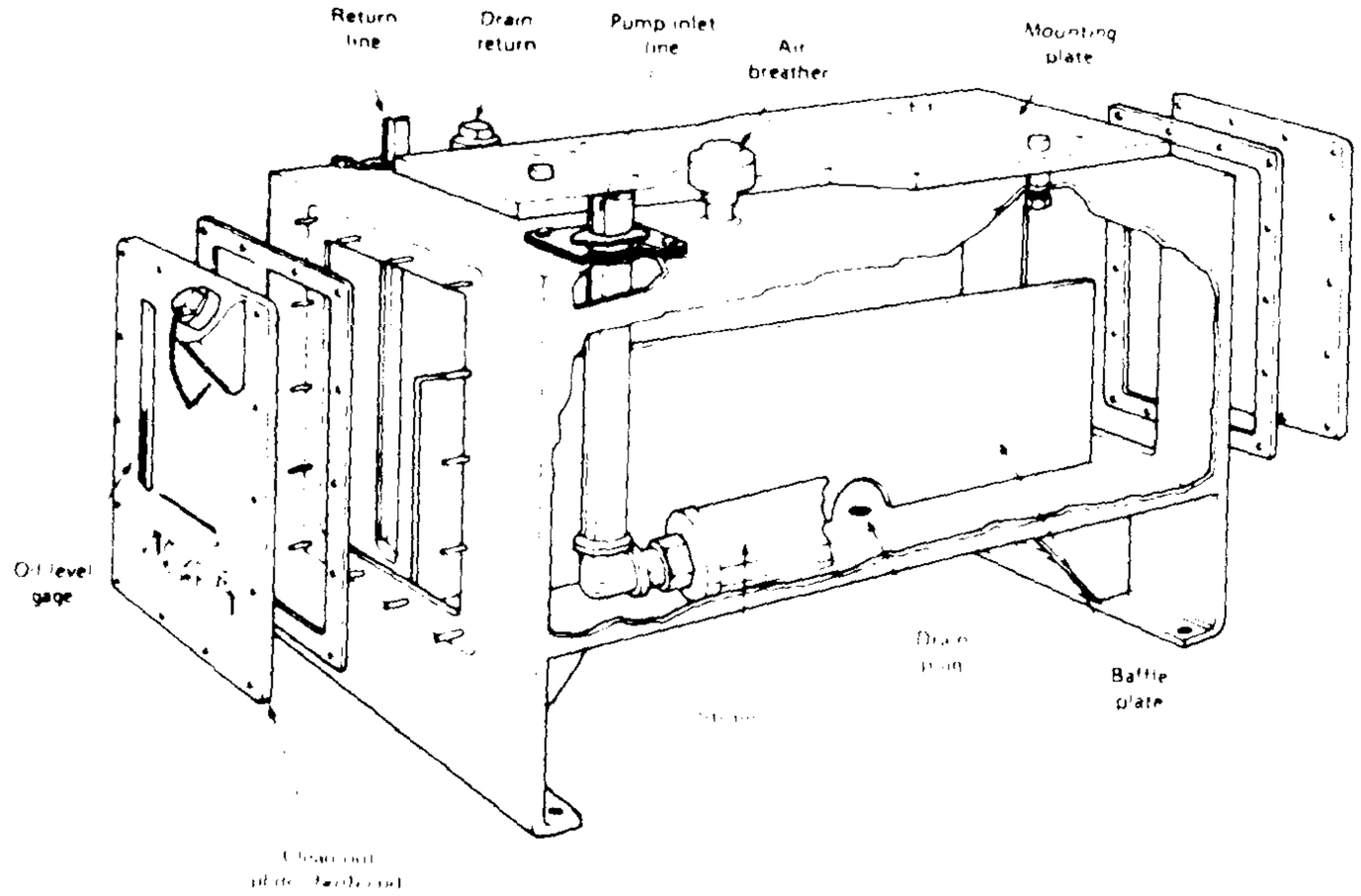

industrial hydraulic reservoir *(courtesy of Sperry Vickers).*

FIG.(6.3) HYDRAULIC OIL RESERVOIR

PARTS LIST

1. pump under test
2. drive motor
3. pressure transducer
4. temperature measurement point (thermocouple)
5. delivery pipe
6. pressure transducer
7. regulator valve
8. relief valve
9. hydraulic hose
10. oil cooler
11. high pressure oil filter
12. turbine flowmeter
13. pressure gauge
14. temperature measurement point (thermocouple)
15. directional control valve
16. regulator valve
17. relief valve
18. glass tube
19. exhaust muffler
20. vacuum pump
21. filter
22. relief valve
23. de-aeration isolating valve
24. vacuum isolating valve
25. pressure isolating valve
26. pressure gauge
27. oil level side glass
28. de-aeration/pressurization tank
29. main tank
30. drainage valve
31. regulator valve (diaphragm valve)
32. hydraulic hose
33. suction line
34. temperature measurement point (thermocouple)
35. pressure transducer

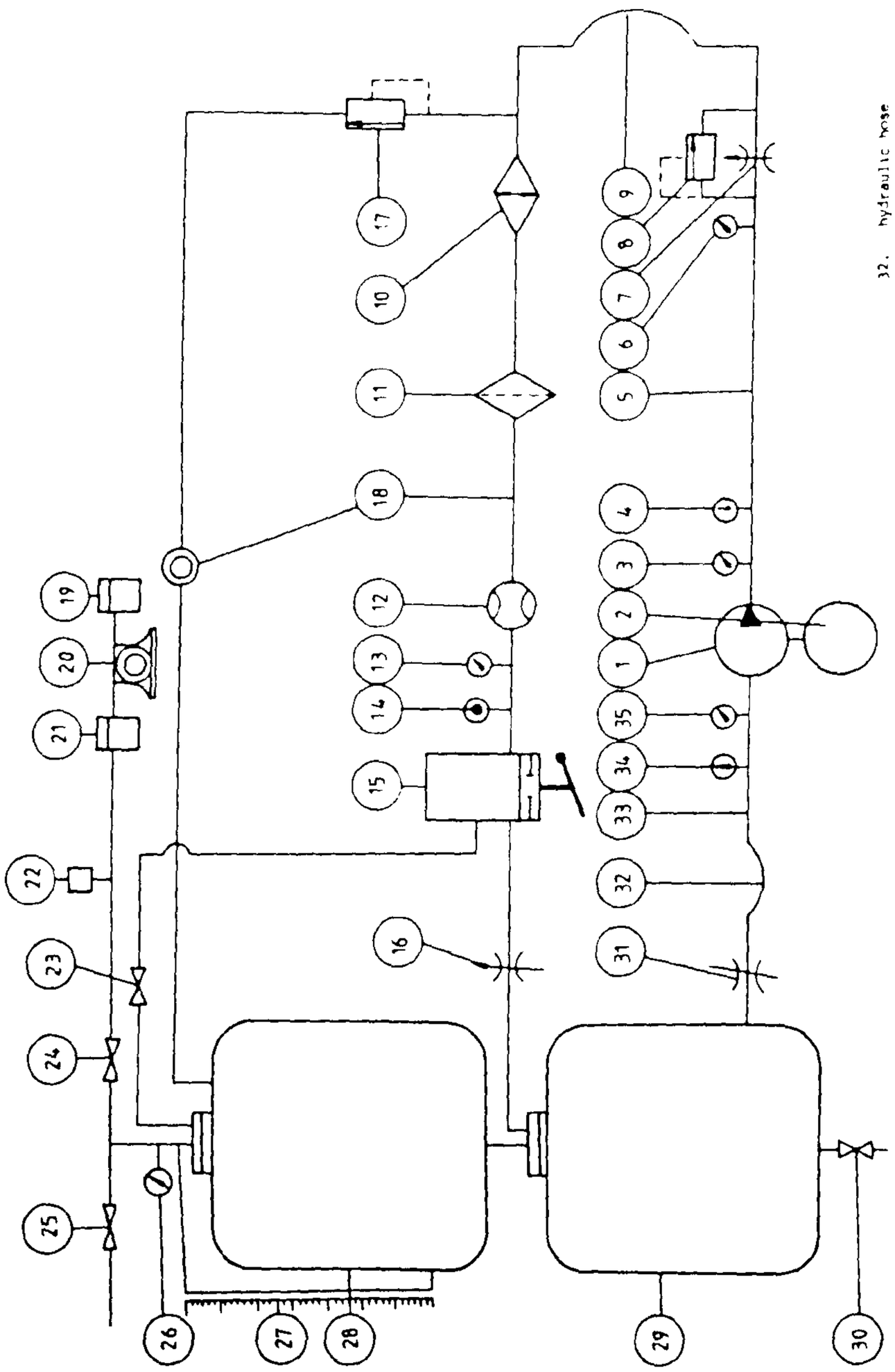

FIG.(6.4) SCHEMATIC DRAWING FOR THE TEST COMPONENT ARRAGEMENT

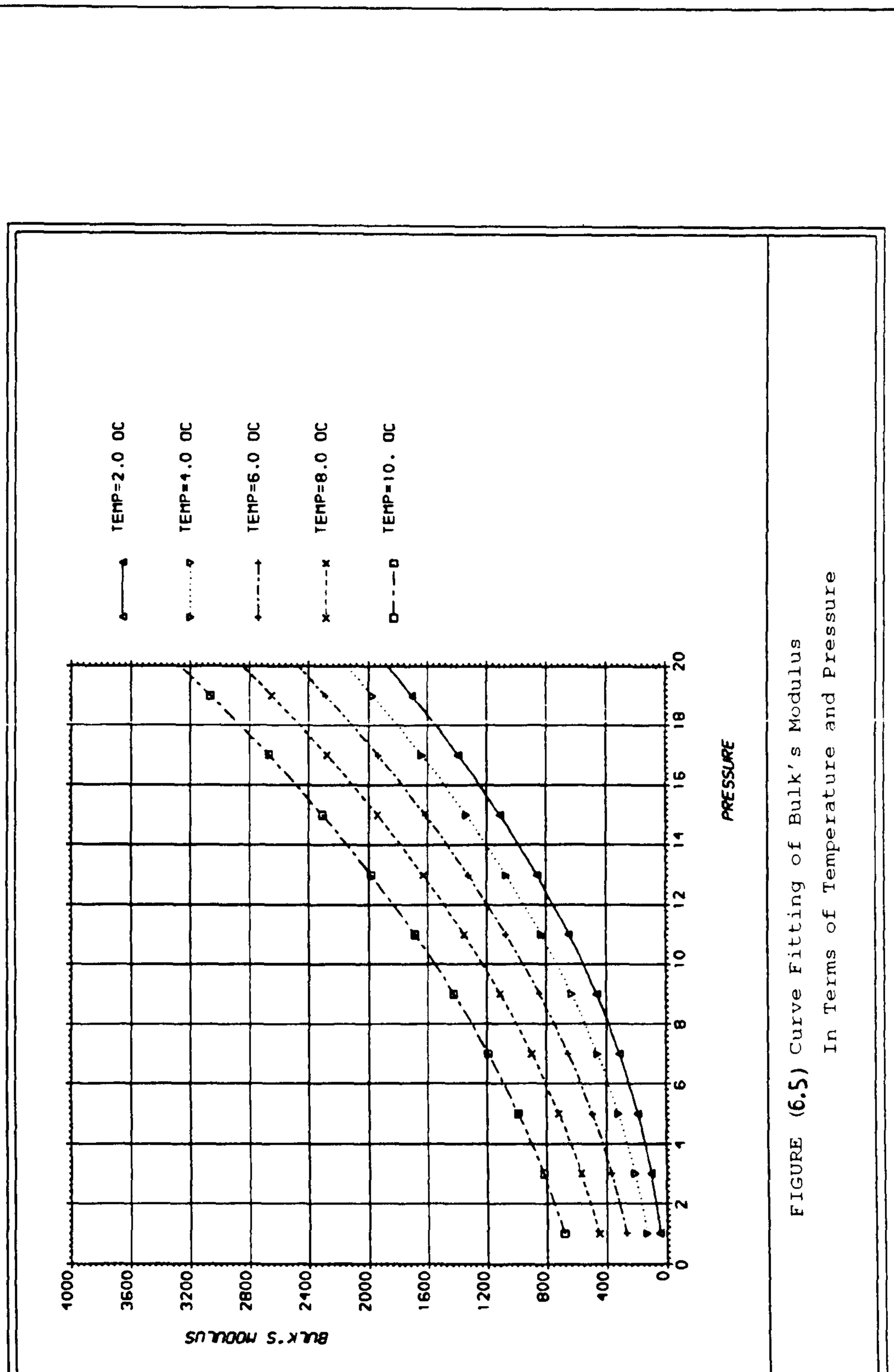

FIGURE (6.5) Curve Fitting of Bulk's Modulus
In Terms of Temperature and Pressure

Fig 6.6 Side Plate

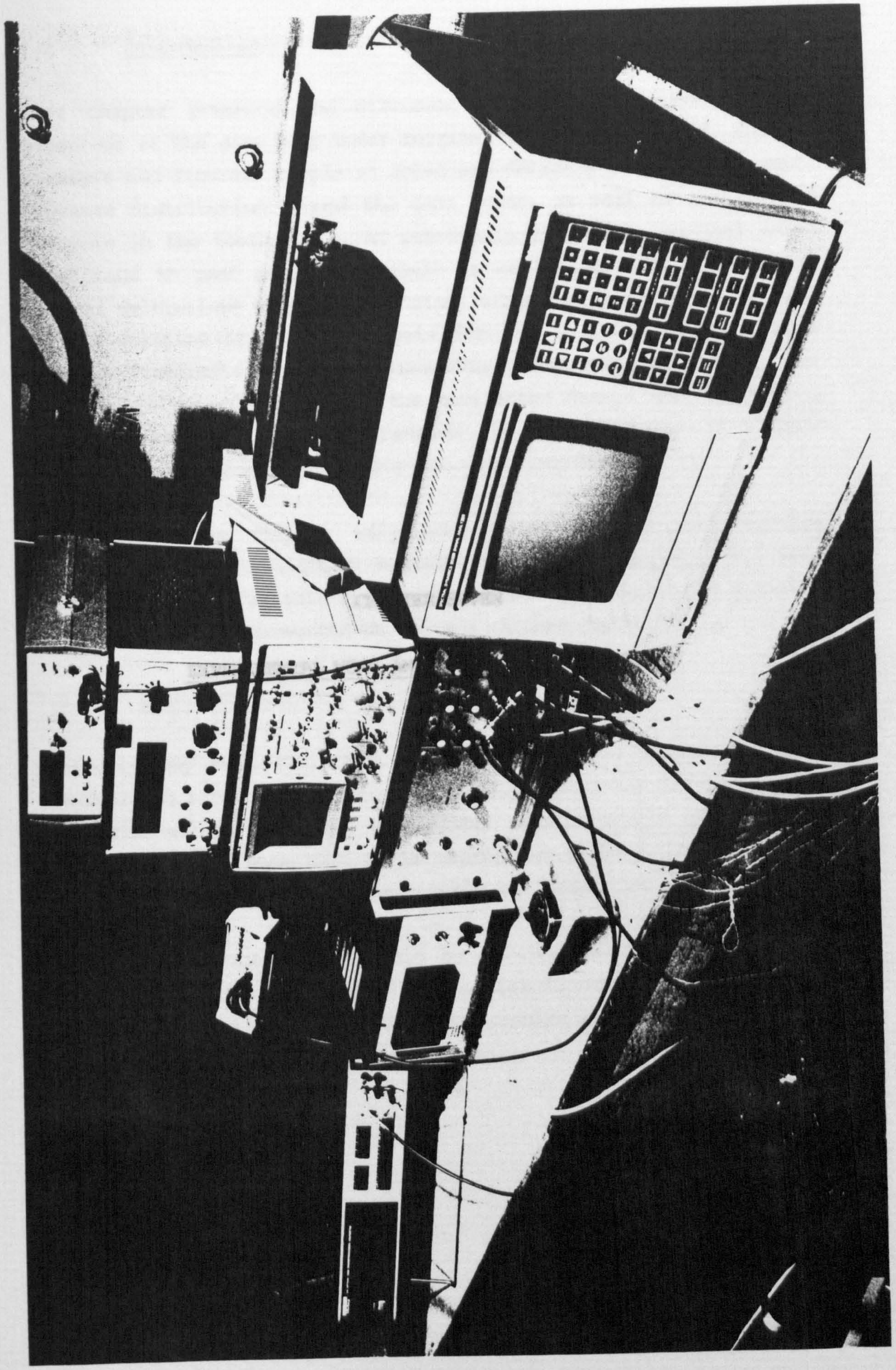

CHAPTER SEVEN

EXPERIMENTAL WORK AND DISCUSSION OF RESULTS

7.1 Introduction

This Chapter presents and discusses the results related to the behaviour of the gear pump under marginal suction conditions, such as pressure and flowrate ripple at inlet and delivery sides of the gear, pressure distribution around the gear rotor, as well as the trapped pressure in the tooth space. As previously discussed, marginal inlet conditions in gear pumps may result in cavitation, which can cause several deleterious effects like noise, vibration and erosion. In this work a detailed study and analysis for the cavitation in terms of pressure ripples, time and frequency domain has been carried out. The analysis is extended to study the cavitation damage characteristics using surface profilometry techniques, by obtaining the 3D surface profiles of the side plate before and after cavitation.

The tooth space filling efficiency under the marginal suction condition was investigated experimentally. The experiments were carried out under variable speed and pressure conditions. The plotting of the results are presented at the end of this Chapter.

7.2 System Preparation

Obviously any test rig, when used for the first time, should be commissioned according to design specifications. A set of tests should be carried out to deal with any problem related to the design of the rig, so as to be sure that it is capable of performing the required experiments satisfactorily. These tests are summarised as follows:-

1. A set of experiments should be carried out for the test pump under normal conditions, to check its flowrate, (see Fig. 7.1), and pressure, to correlate these results with the manufacturers specification.

2. A second set of experiments embarked upon the induced cavitation in the pump is to check the suction part of the rig to investigate whether it functions correctly or not. A check should also be made on the test pump parts to check its limitations in the system as well as the pump limitations.

3. The two sets of experiments mentioned above should be repeated to insure that the results are repeatable.

4. Different instrumentation should be checked during the operation of the system for measuring pressure, temperature, flowrate and speed.

When all the above tests had been checked satisfactorily, the main experimental work was carried out.

The first phase of the experimental work had been achieved by running the oil through the de-aeration tank to release the oil from the entrained gas bubbles and to reduce the amount of dissolved gas in the oil. The pump is run at a low speed usually between 500 - 700 rpm to let the oil stay as long as possible in the de-aeration tank which has a large area for the oil surface exposed to vacuum so as to ensure an accelated de-aeration process.

Before taking any measurement, the system is usually de-aerated at -15"Hg for 1-1½ hours which is enough to let all the instrumentation reach its stability point, so as to improve the repeatability of the results.

After the system oil is completely de-aerated, the first phase of experimental work had the objective of studying the effect of cavitation on the pump hydraulic performance, as well as its effect on the pressure distribution around the gear rotor. The trapped pressure in the tooth space, was also included.

7.3 Gear Pump Performance

The performance of the pump was investigated experimentally under normal conditions, to correlate such results with the manufacturers specification, as well as to be taken as a reference for correlating other conditions like cavitation.

In hydraulic systems the direct measurement of flow fluctuation is a difficult task. However, pressure fluctuation can be measured accurately and easily.

In these experimental tests the pressure fluctuation was measured by providing the system with two transducers, one being at the inlet (TR1), the second at the pump outlet (TR2), those transducers have high natural frequencies which are 125 KHz for TR1 and 375 KHz for TR2. From this point onwards, P1 refers to the readings of the transducer TR1 and P2 refers to the readings of the transducer TR2.

Within a hydraulic system, fluctuations in pressure and flowrate are related. The mean flowrate was measured using turbine flowmeter because the flowmeter measures the flowrate at different conditions from the pump outlet. The flowmeter reading should be corrected to find the actual pump flowrate. This can be carried out by the means of the following equation:-

$$Q_A = Q_F \left[1 - \left(\frac{P_P - P_F}{\beta_f} \right) + \alpha \, (T_P - T_F) \right]$$

where:

Q_A = actual pump flow rate
Q_F = flowmeter reading
P_P = pressure at the pump outlet
P_F = pressure at the flowmeter
T_F = temperature at the pump outlet
β_f = fluid bulk modulus
α = coefficient of thermal expansion

7.3.1 Gear Pump Performance Under Normal Conditions

This experimental work was started from the point when the pump suction line was under atmospheric pressure plus the hydraulic head of the oil in the tank about 3ft. of oil. After some alterations had been made to the system return pipe, in which the returning fluid enters the main system tank and the process of de-aeration is performed, the signal was improved considerably. The reason for the signal instability before the de-aeration can be the presence of the entrained and dissolved air in the system oil. It can be seen from figs. (7.2 - 7.5) that the suction pressure wave is fluctuating with 2-3 times more than the mean suction pressure. In the case of lower peak pressure the dissolved air is released in a very short time resulting in an interruption to the dissolved air to oil mixture construction, which sometimes leads to cavitation.

It is clear from the pressure ripples at the pump outlet, Figs. (7.6 - 7.8) that they are stable and repeatable. The amplitudes of these pressure ripples depend upon the system components characteristics which are a function of the test conditions. It can be represented by fluctuations above and below the mean pressure in the pipe. These ripples remain stable and repeatable with no appreciative change in amplitude and shape as the mean pressure at the suction pipe is reduced.

A set of results about pump performance shown in Figs. (7.9 to 7.14) represents the variation of pump flowrate with NPSH at various pump speeds. In each of the above figures, it is clear that there is no variation of flowrate as the NPSH is reduced, until the NPSH reaches a point when cavitation inception occurs in the system.

7.3.2 Gear Pump Performance under Cavitating Conditions

In this experiment the effect of cavitation on the pump hydraulic performance was studied. The procedure of this experimental work started by reducing the pump suction pressure step by step and at each step a complete set of measurements was taken. The cavitation stages were classified as three stages, the first of which was cavitation

inception, at which an obvious reduction in the flowrate and pressure accompanied a considerable change in the pressure signal coming out of the pump (see Fig. 7.15). The next stage to follow was the condition of discrete-cavitation which led to a further reduction in the flowrate and pump outlet pressure. The cavitation was observed in one or two pressure ripples and the rest of the signal was undisturbed. The last stage covered by the experimental work was the stage during which cavitation occured in the whole pressure ripple as a continuous-cavitation taking place with further large reductions in flowrate and pressure.

The noisiest stage was the stage of discrete-cavitation where there is a discrete noise and screaming coming out of the pump. As the pump starts to become effected by cavitation-inception the signal is effected by another random signal generated by cavitation bubble collapsing on the delivery side. The pressure ripples results at the cavitation and non-cavitating conditions for the three cavitation stages were presented in time and frequency domain.

7.3.3 Time Domain Analysis

The pressure ripples generated from the pump under different inlet conditions is shown in Figs. (7.16 to 7.21), which illustrate the variation of the pressure ripple at the inlet and outlet of the pump during the three stages of cavitation.

It is clear from those figures that as the pressure is reduced in the suction pipe, during the cavitation inception stage, the ripples become quiet, with its amplitude being reduced sharply and the ripples are also unstable and unrepeatable although the suction pipe is under very low mean pressure. This behaviour of the presure ripples is due to the presence of gases released from the oil as the suction pressure becomes very low. When the pump reaches the point of continuous-cavitation the flow has no ripples at all or it has ripples with too small amplitudes to be seen, which leads to the effect of cavitation not being easily detected at the suction side of the pump.

Considering the pressure ripples at the pump outlet, it can be seen from Figs. (7.21 - 7.24) that such ripples are repeatable with

amplitudes varying from case to case depending upon the system components characteristics which are a function of the test conditions.

As the pump starts to become affected by cavitation-inception the presure signal starts to become unsteady over the mean pressure. When the suction ripple mean pressure is further reduced the cavitation effect appears at first in one or two teeth only and does not necessarily occur in each cycle of rotation. The amplitude of the resulting pressure ripples will have a sharp peak of pressure due to the collapse of some existing bubbles at the delivery side and the value of these peaks pressure may reach 3MPa at the delivery side, as shown in Fig. (7.21).

This phenomenon is observed at the stage of discrete-cavitation which is, from the author's point of view, the most serious stage of cavitation that can cause maximum damage and erosion to the pump parts, as well as being associated with a high level of noise in the system.

Due to some drop in oil flow energy, the oil may not be able to fill one or two teeth spaces completely, which results in oil accumulation in the suction pipe, leading to an increase in the oil flow potential energy which makes the oil completely fill the next teeth and continue randomly, and it can provide a physical explanation to the stage of discrete-cavitation.

The last and final stage of cavitation is the stage of continuous-cavitation, which is characterised by continuous noise in the entire pressure ripples, associated with a further reduction in the pump flowrate.

The cavitation shown can be detected by shocks appearing in the ripple with less amplitude than that observed with the discrete-cavitation. It can be concluded that the cavitation can be recognised easily at the pump outlet pressure ripples which can give an early warning about cavitation occurrence.

7.3.4 Frequency Domain Analysis

The pressure signals were analysed in terms of their frequency components, as presented in Figs. (7.25 - 7.32).

The frequency-domain analysis for inlet and outlet pressure pulsation of the pump running at normal conditions without cavitation is shown in Fig. (7.25) which illustrates the frequency amplitude spectra for the pressure pulsation shown in Fig. (7.24). It is clear from this figure that pressure pulsation decreases monotonously after the second harmonic of the outlet pressure signal.

A linear-scale plotting for frequency-domain analysis of different pressure signals is presented in Figs. (7.26 - 7.32), the first three of which are for cases without cavitation and the others deal with signals at the different stages of cavitation (i.e. cavitation-inception, discrete-cavitation and continuous-cavitation). Each plot consists of the analysis of inlet and outlet pressure signals at the same running conditions to facilitate the comparison and discussion.

The inlet pressure signal in frequency domain at which the inlet condition is atmospheric is shown in Fig. (7.26b) and it can be noticed from this figure that there are up to 15 harmonics, the highest of which in amplitude is the second harmonic while the rest have approximately the same amplitude, which is a function of the pump suction side impedance. Considering the pump outlet signal it is clear from Fig. (7.26a) that the first harmonic is the highest in amplitude and the amplitude of the harmonic for pressure pulsation decreases monotonously up to the fifth harmonic. After that it can be deduced that the rest of the harmonics do not pose any serious problem to practical application because of their relatively low amplitude compared with the amplitude of the fundamental component.

During the first stage of cavitation, which is cavitation-inception, a new frequency component appears close to the vertical axis (see Figs. 7.30b and 7.31b). This component is lower than the first harmonic in both frequency and amplitude. As cavitation is developing in the

system this generated component can be seen clearly, until it disappears when the continuous-cavitation stage affects all the pressure ripples and at that stage the second harmonic becomes the highest in amplitude instead of the first harmonic. This is because of the change in pump impedance due to cavitation.

7.3.5 Spectrum Map

It is useful to check the repeatability of the frequency domain signals with operating time and this can be achieved by using the waterfull facility in the spectrum analyser. Such a facility can also be used for the comparison of a sample of signals when the system is under different cavitation conditions.

The variation of the spectrum map signals for inlet and outlet presure ripples at different inlet conditions is demonstrated in Figs. (7.33 - 7.36) and it can be understood from these figures how cavitation influences the frequencies of pressure signals for the entire map of operating times.

7.4 The Distribution of Pressure Around the Gear Pump Rotor

The second phase of experimental work is the measurement of pressure distribution around the gear rotor. In the present work such measurements of pressure in time domain was carried out by a miniature pressure transducer (TR3) situated at the gear fillet with the signal being taken out via a slip ring coupled to the pump extension shaft. The measured variation of the pressure with the gem revolution in a tooth space is shown in Fig. (7.37) which indicates that the pressure begins to build up just after the tooth cavity forms a closed volume with the pump casing. Then the pressure signal shows some peaks on the top of the mean output pressure, due to the reverse flow on the tooth tip as well as to the turbulent region of the passing tooth. After that, the pressure starts to decay towards the outlet pressure. The most interesting result is the waveform of the trapping oil in the trapped space which reaches a pressure of twice the working pressure inspite of the gear having an effective relief groove which is extended into the pump sideplate to prevent damage to the pressure tranducer. This signal was measured at a speed of 1200 rpm and a

delivery pressure of 500 psi. It can be mentioned that the pressure distribution around the gear pump (as shown in Fig. 7.37) is building up because of the side and tip leakages around the pump periphery. The low pressure on the graph, which is represented by the suction pressure, continues until the oil leakages can fill the tooth cavity. After that the pressure builds up in the gear space cavity.

As cavitation is developing in the pump, the tooth filling efficiency will be drastically reduced and the tooth cavity takes time to become filled, this is due to the lack of flow energy in the suction port to fill the tooth space, and it is shown in Fig. (7.37) that as the cavitation is more developed in the system the filling efficiency is reduced and the tooth cavity takes longer to be filled. This will cause a reduction in the pump flowrate which is associated with the cavitation. The filling efficiency as a function of the NPSH is presented in Fig. (7.39), that the filling efficiency breaks down at NPSH 9 ft. which agrees reasonably with the behaviour represented by the performance curve as shown in Fig. (7.40).

The pressure distribution around the gear rotor at different stages of cavitation is presented in Figs. (7.41 - 7.46), from which it can be concluded that the rateof pressure building up in the tooth mesh is a function of the gear load, and the gear eccentricity, and the teeth are not sharing the pressure load equally.

When the pump is run at 1500 rpm some pressure profiles show spikes in the pressure signal. The author believes that the cavitation taking place between the gear tip and the pump casing is due to the presence of a high shear stress at the slip passage since the direction of oil slippage is in the opposite direction to the gear motion, and it dies away immediately due to the presence of a high pressure point just after that (i.e. tooth cavity).

7.5 Cavitation Erosion

7.5.1 Introduction

One of the general pump problems caused by cavitation is the cavitation erosion which may seriously reduce the life of the pump and

will adversely affect its performance by causing more leakage, leading to a reduction in the volumeric efficiency.

In gear pumps, erosion occurs on the side plates, particularly around the delivery port. This erosion may create a new leakage channel which themselves will cause an increase in cavitation and the erosion can therefore be accelerated rapidly once initiated.

The mechanisms of cavitation erosion are still not fully understood, this may be because the phenomenon takes place in a very short time and at a very small space. Further complications arise because this phenomenon involves very high local temperatures and pressure.

However, there are two apparent mechanisms for the cavitation erosion, the first of which is due to the pressure shock wave analysed first by Lord Rayleigh, in his theory on infinite pressure predicted at the point of complete collapse which radiates shock waves. These shock waves can cause mechanical damage to a solid surface lying close to the collapse centre.

The second cavitation erosion mechanism is the micro-jet mechanism. After a cavity is initiated it collapes asymmetrically at its upper surface while moving toward the solid surface. As the collapse continues the cavity becomes toroidal until the fluid penetrates the centre of the cavity forming a micro-jet at the centre of the toroid. This micro-jet has a very high velocity which causes mechanical damage as it impinges on the solid surface (see Fig. 7.46).

The characteristics of cavitation erosion are dependent upon the intensity of cavity collapse and the properties of the material being eroded.

7.5.2 Experimental Set-up and Procedure

In the present study a gear pump side plate was tested under cavitation conditions. The pump was running at 900 rpm and the delivery pressure was 500 psi. The surface profiles characteristics of the tested side plate were obtained before and after the test using a standard 'Talysurf' instrumentation system.

The Talysurf consists of a pick-up arrangement which is driven across the surface of the test specimen and a sharply-pointed stylus tracing the profile of the surface irregularities. A three-dimensional topography of the surface can be generated and analysed.

The material of the sideplate used in the test was high-leaded tin bronze (promet 65K). The temperature of the hydraulic oil was maintained constant at 45°C during the test. The area expected to be eroded was well defined from the pressure signal in which the peak pressure signal generated by the collapse of cavitating bubble took place.

The results obtained were based on the experiments of only single tests because of the shortage of supply of sideplates as well as the long time required for fixing it in the pump which needed the company assembly and test.

7.5.3 Analysis of Results

The test started by obtaining the surface profile of the sideplate which is shown in 2-D and 3-D plots Figs. (7.47) and (7.48).

After the pump ran for 15 minutes under a continuous-cavitation stage the surface profile was checked and the results shown in Figs. (7.49) and (7.50) indicate that erosion damage has occurred. Such damage happens at the early stages of erosion and it starts due to the high pressure generated by the bubble collapse which leads to a multiplicity of impulsive blows due to high speed micro-jets and shock waves. These impulsive blows have pressure values higher than the yield stress of the material and hence generate some plastic deformation in the sideplate material.

The instantaneous pressure, near to the fluid boundary, in a spherical bubble in liquid is given by means of Rayleigh's theory as:-

$$P = \frac{2P_o}{3\rho}\left\{\left(\frac{R_o}{R}\right)^3 - 1\right\}$$

where P_o is the pressure at an infinite distance, ρ the density of the liquid, R_o the original radius of the bubble and R the radius of bubble at any instant.

If therefore a bubble collapses to a radius of one-tenth of its original radius, for example, i.e. $R_o/R = 10$, in the oil at the delivery side with 100 psi, the instantaneous pressure ρ will be 148000 psi (1020 MNm^{-2}). This pressure is sufficiently high to cause the local yielding of the side plate material (yield stress of high tensile steel is of the order of 600 MNm^{-2}) when the impulsive blows cause plastic deformation to the material, the material flows and craters are formed, as can be seen in Fig. (7.49). These craters have a diameter of 850μm and depth of 10μm.

The variation of cavitation erosion with time is shown in Figs. (7.51 to 7.54). Fig. (7.54) generally follows an 'S' shape, from which it seems that the cavitation erosion has started slow because expected fatigue failure of the surface material would take some time to occur. After that the rate of erosion has increased because of the surface distortion or after the craters have been formed which could channel the cavitation micro-jet to attach the surface. It could also be increased due to the surface roughness effect, which increases the stress concentration and the level of cavitation. After that the rate of erosion decreases due to the effect of trapped oil or possibly air in the eroded volume which can damp the pressure pitting on the side plate. The shape of such a curve, represented by Fig. (7.54) depends upon the properties of the material as well as the conditions of the test and the working fluid. The results of this test are comparable with the results presented by NEL for the erosion test on non-ferrous materials using vibratory cavitation tests (NEL Report No. 496).

The present study illustrates the use of surface analysis techniques to investigate cavitation damage, specially for the moving parts which sometimes have mechanical erosion due to contact.

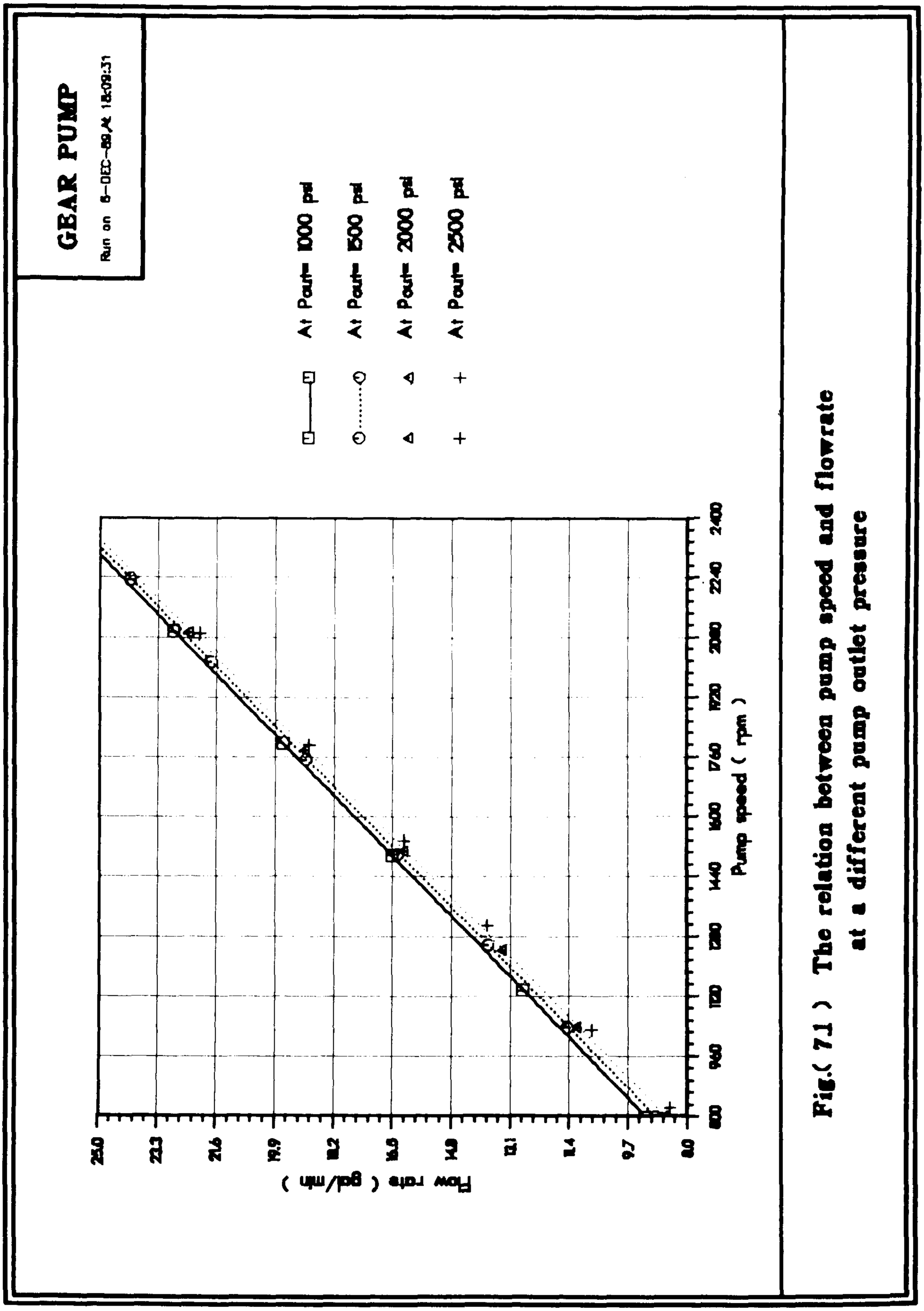

Fig.(7.1) The relation between pump speed and flowrate at a different pump outlet pressure

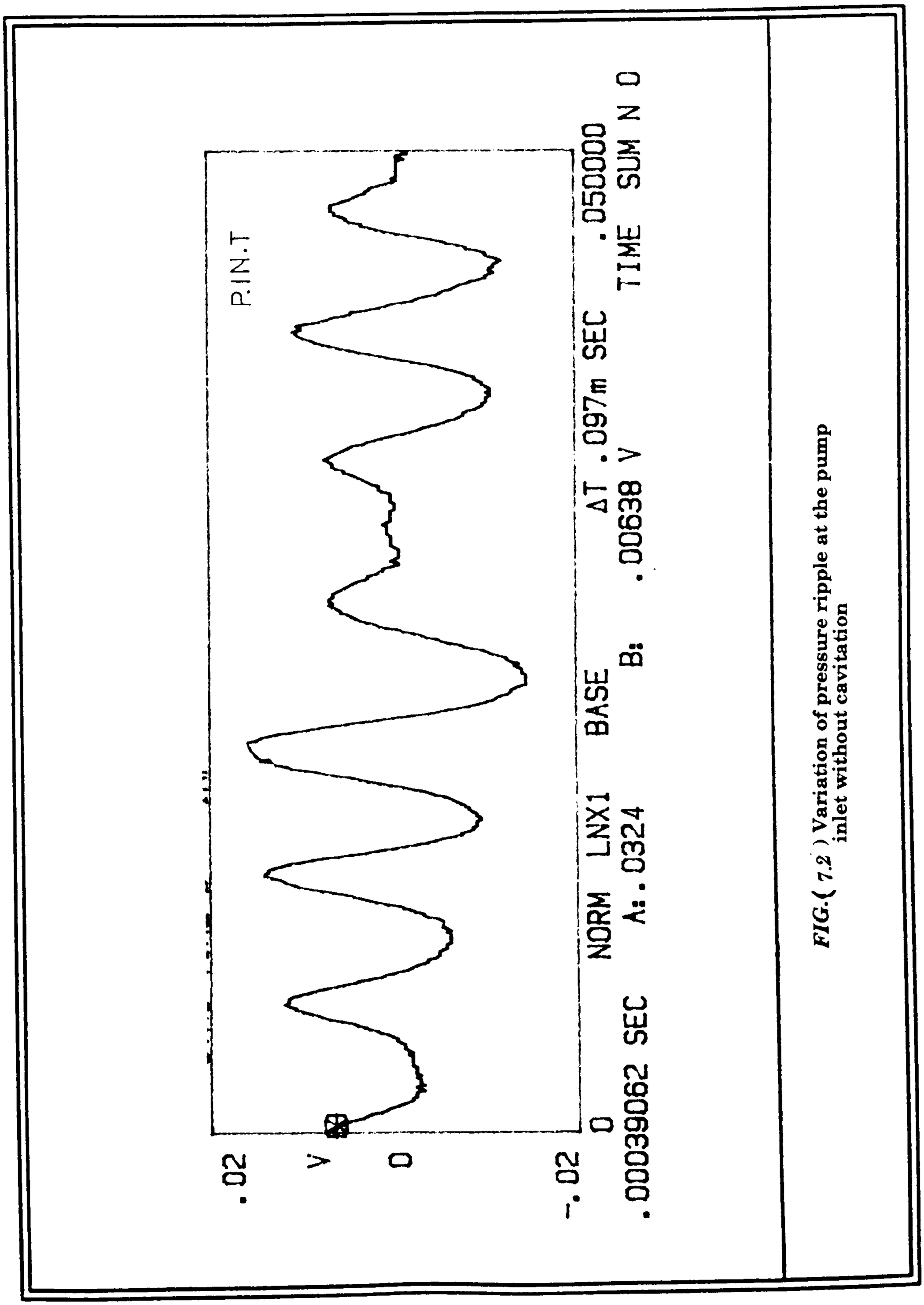

FIG.(7.2) **Variation of pressure ripple at the pump inlet without cavitation**

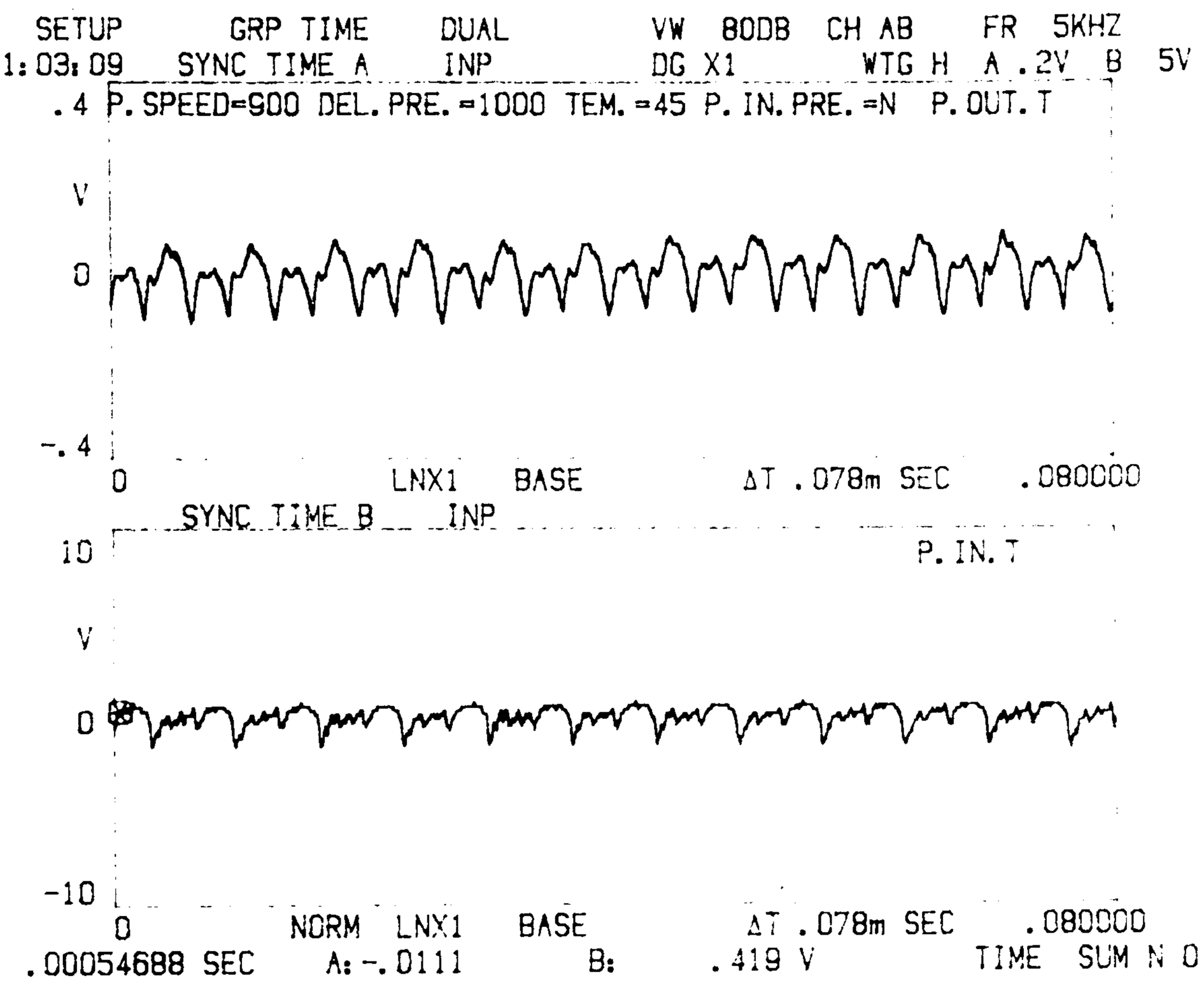

FIG.(7.3) **Variation of pressure ripple** ***at the pump inlet and outlet without cavitation***

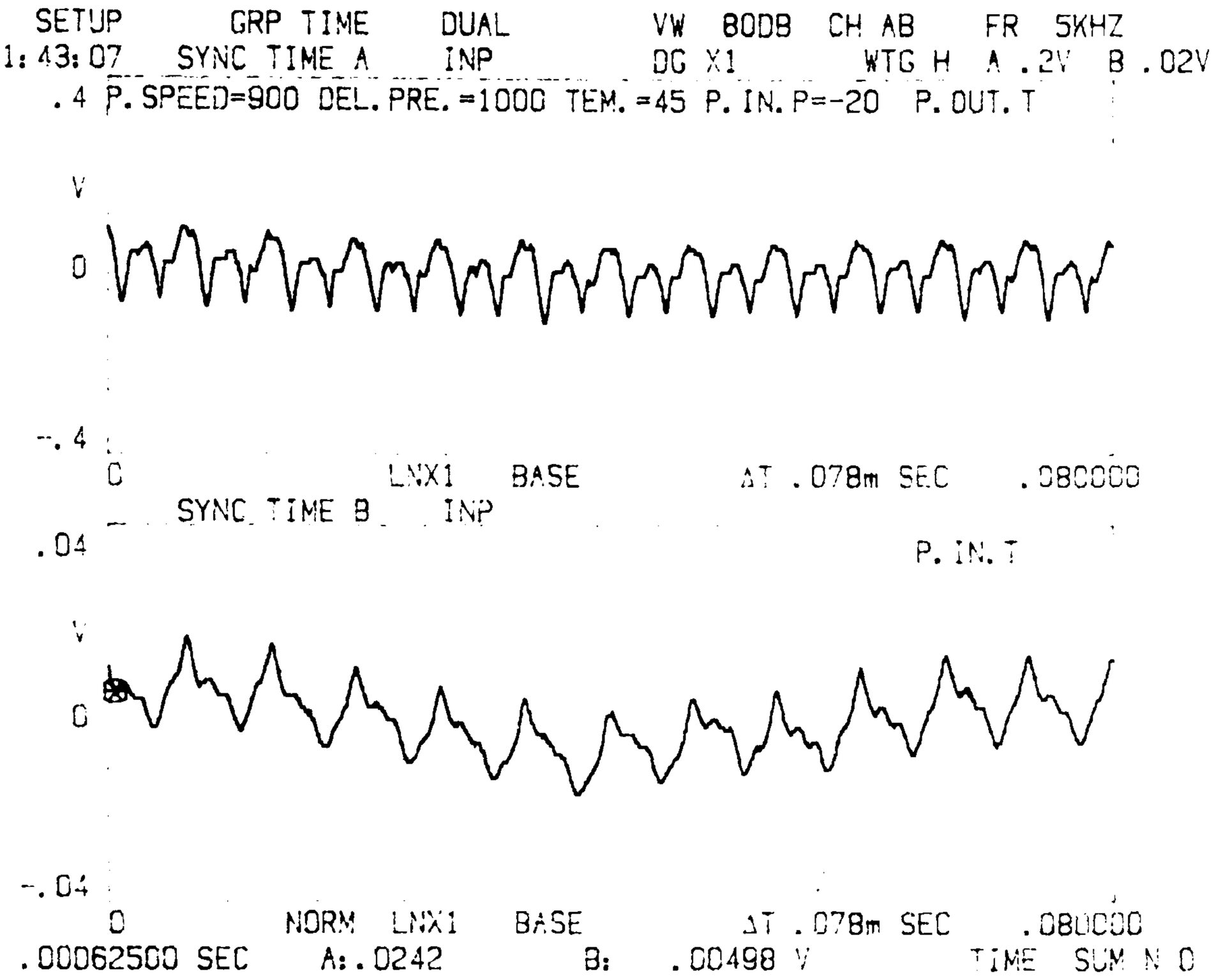

FIG.(7.4) Pressure-signal at the pump inlet and outlet without cavitation

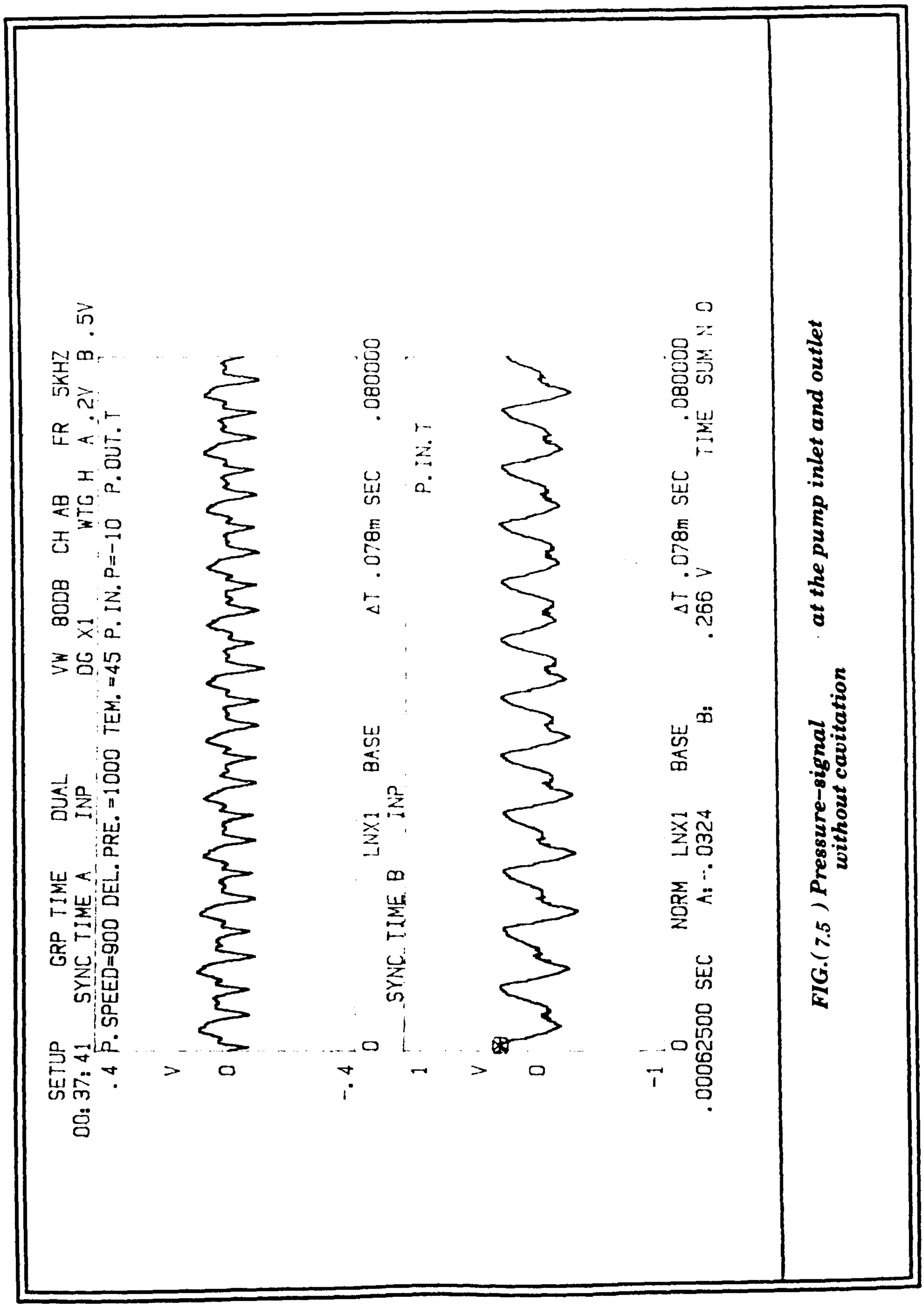

FIG.(7.5) Pressure–signal at the pump inlet and outlet without cavitation

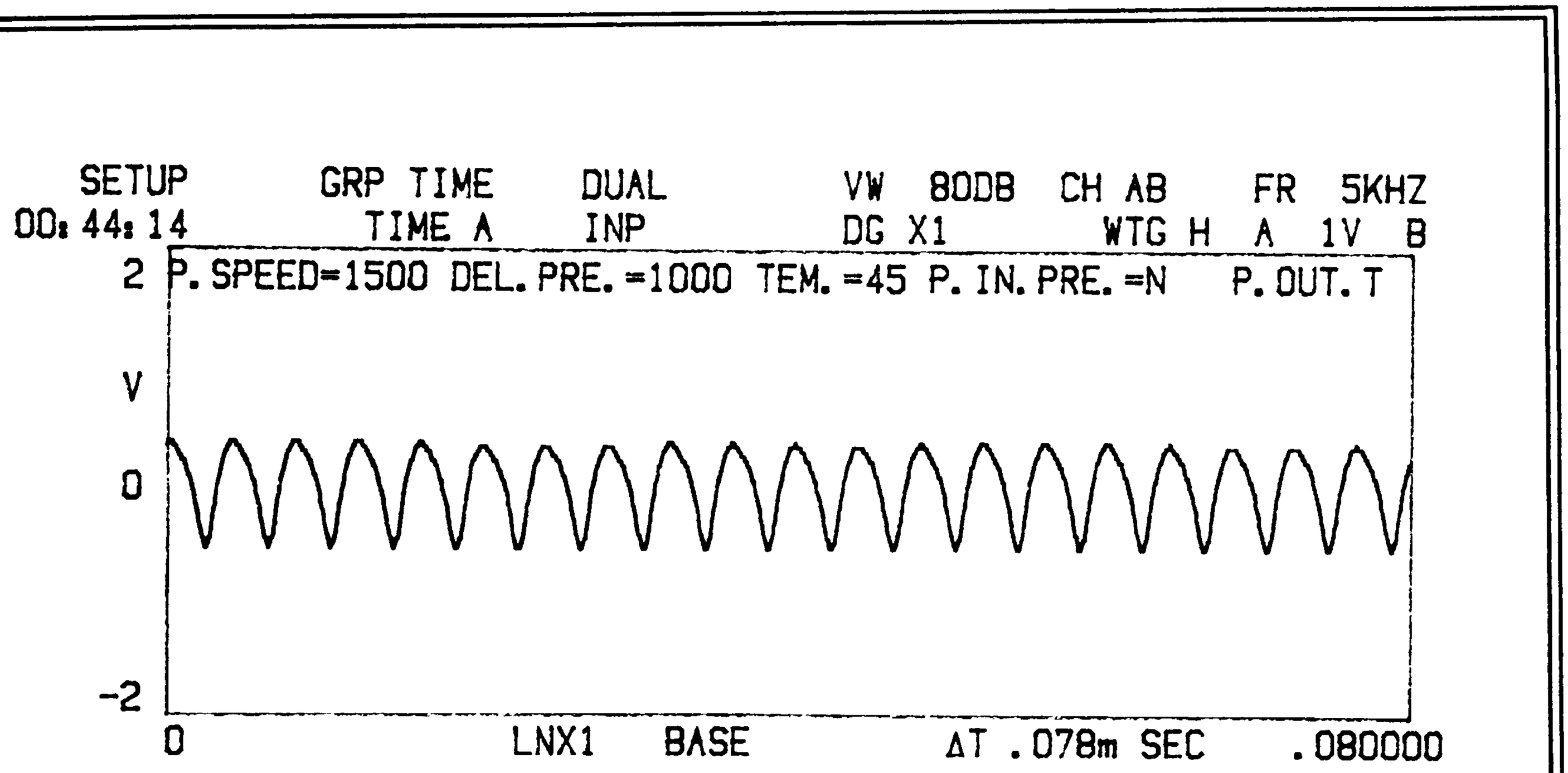

FIG.(*7.6*) Variation of pressure ripple at the pump outlet without cavitation

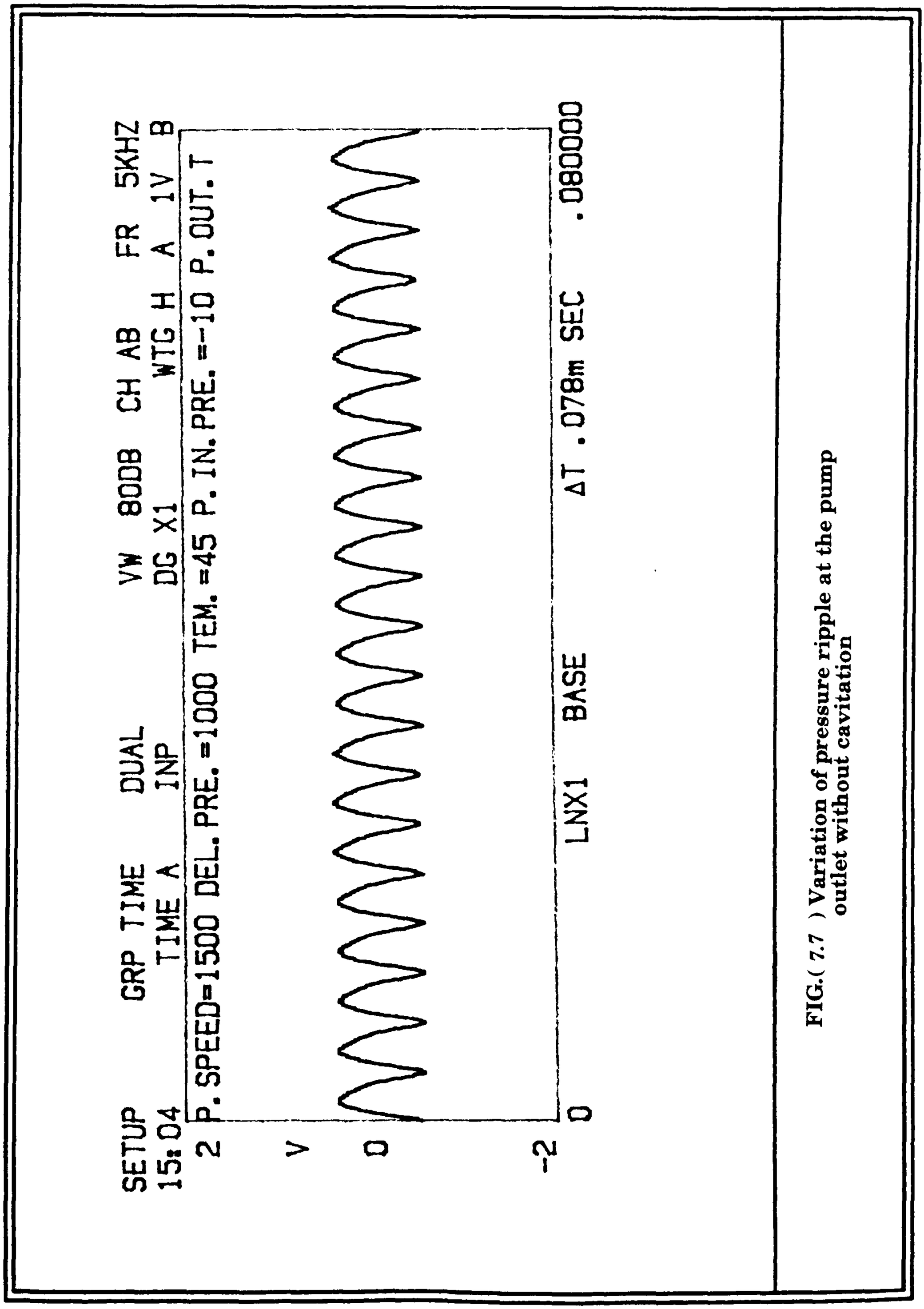

FIG.(7.7) Variation of pressure ripple at the pump outlet without cavitation

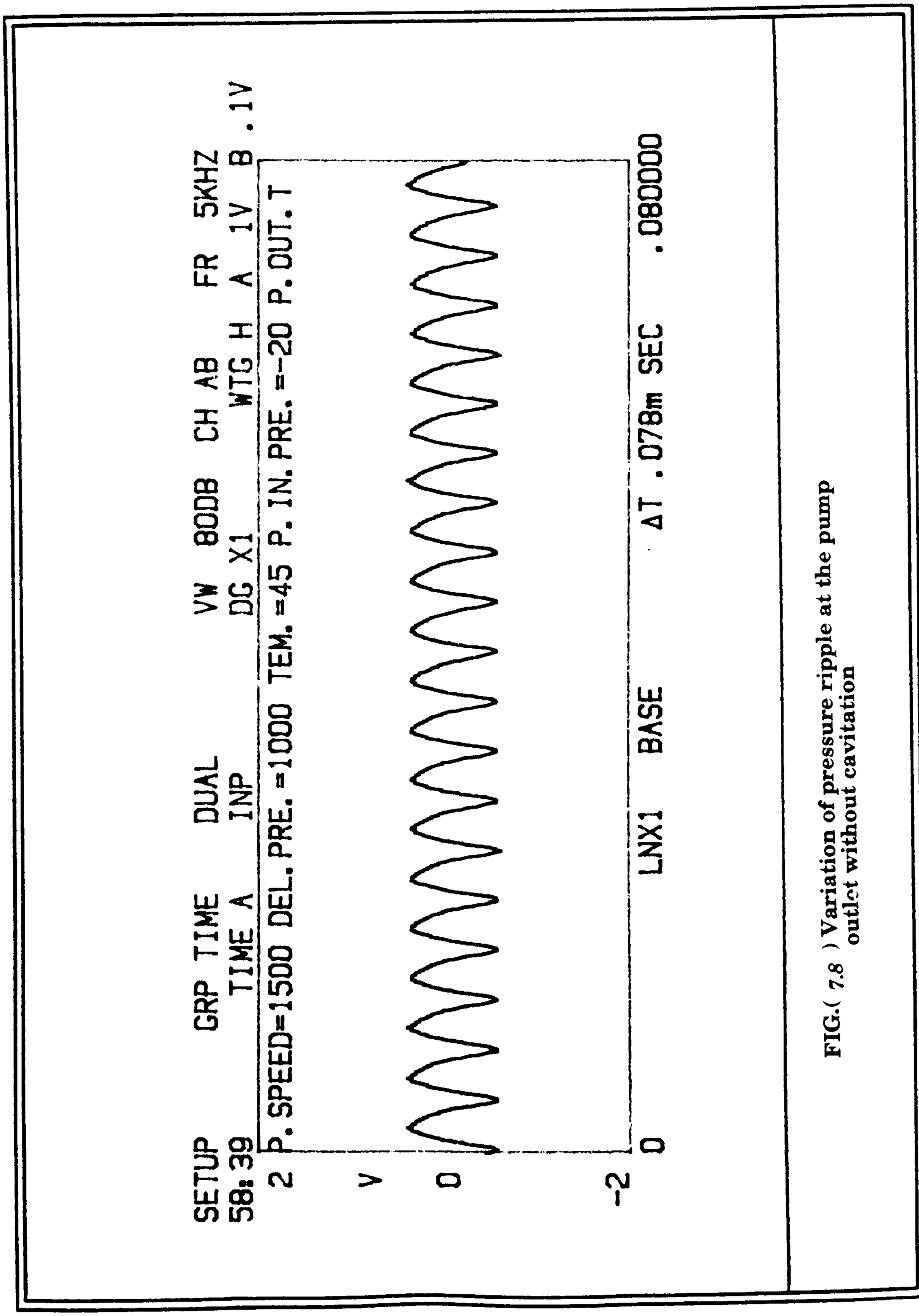

FIG.(7.8) Variation of pressure ripple at the pump outlet without cavitation

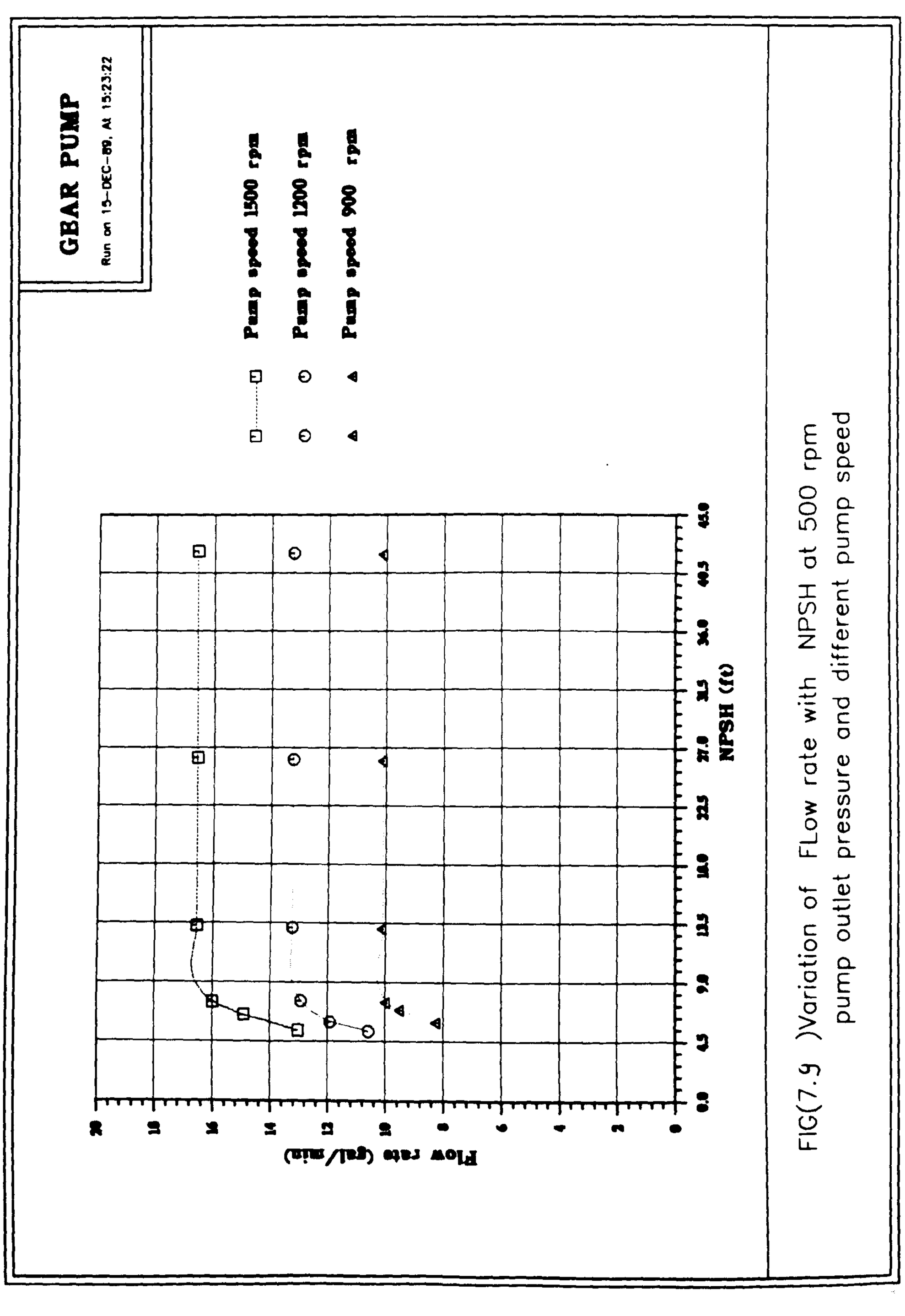

FIG(7.9)Variation of FLow rate with NPSH at 500 rpm pump outlet pressure and different pump speed

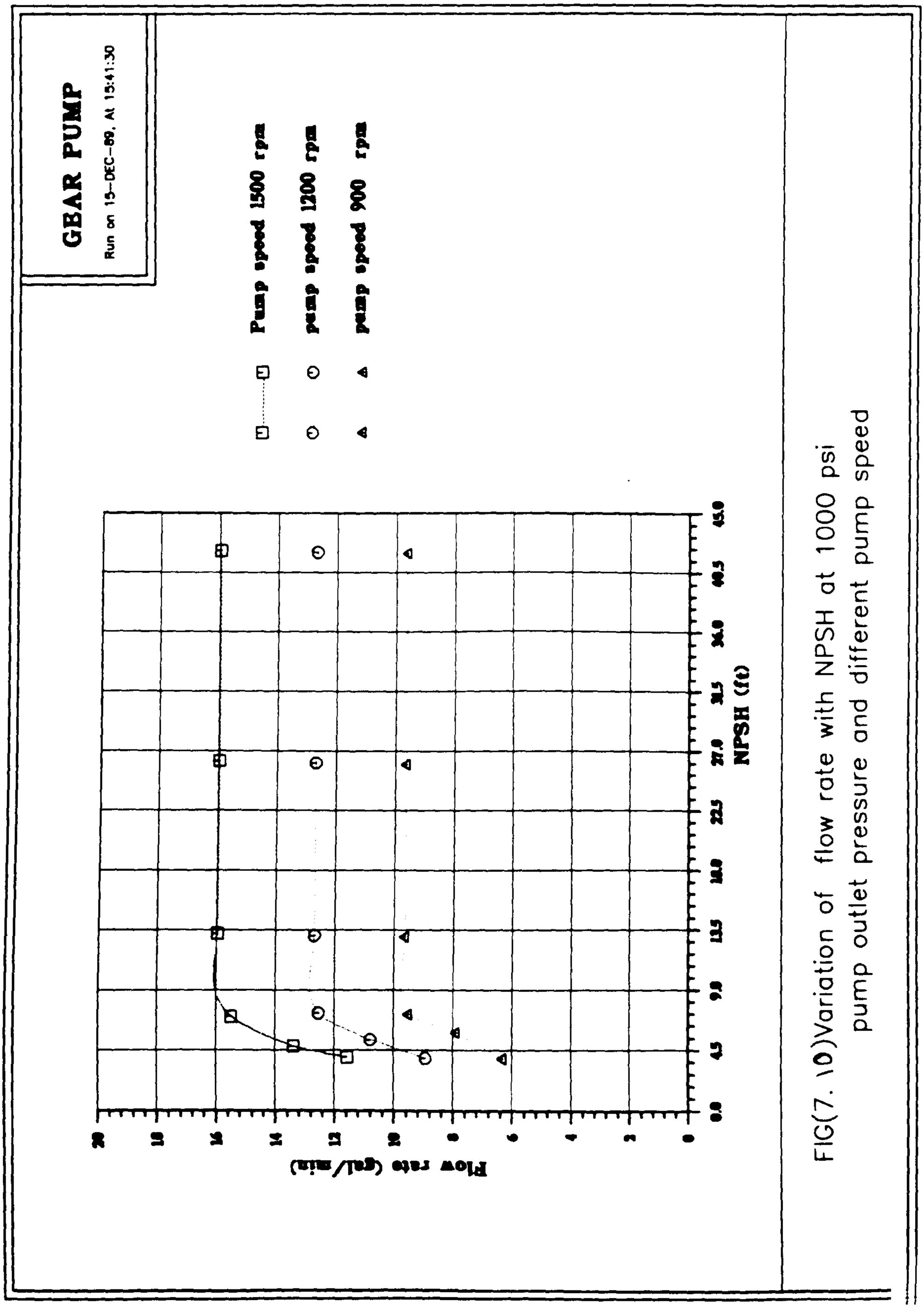

FIG(7. 10)Variation of flow rate with NPSH at 1000 psi pump outlet pressure and different pump speed

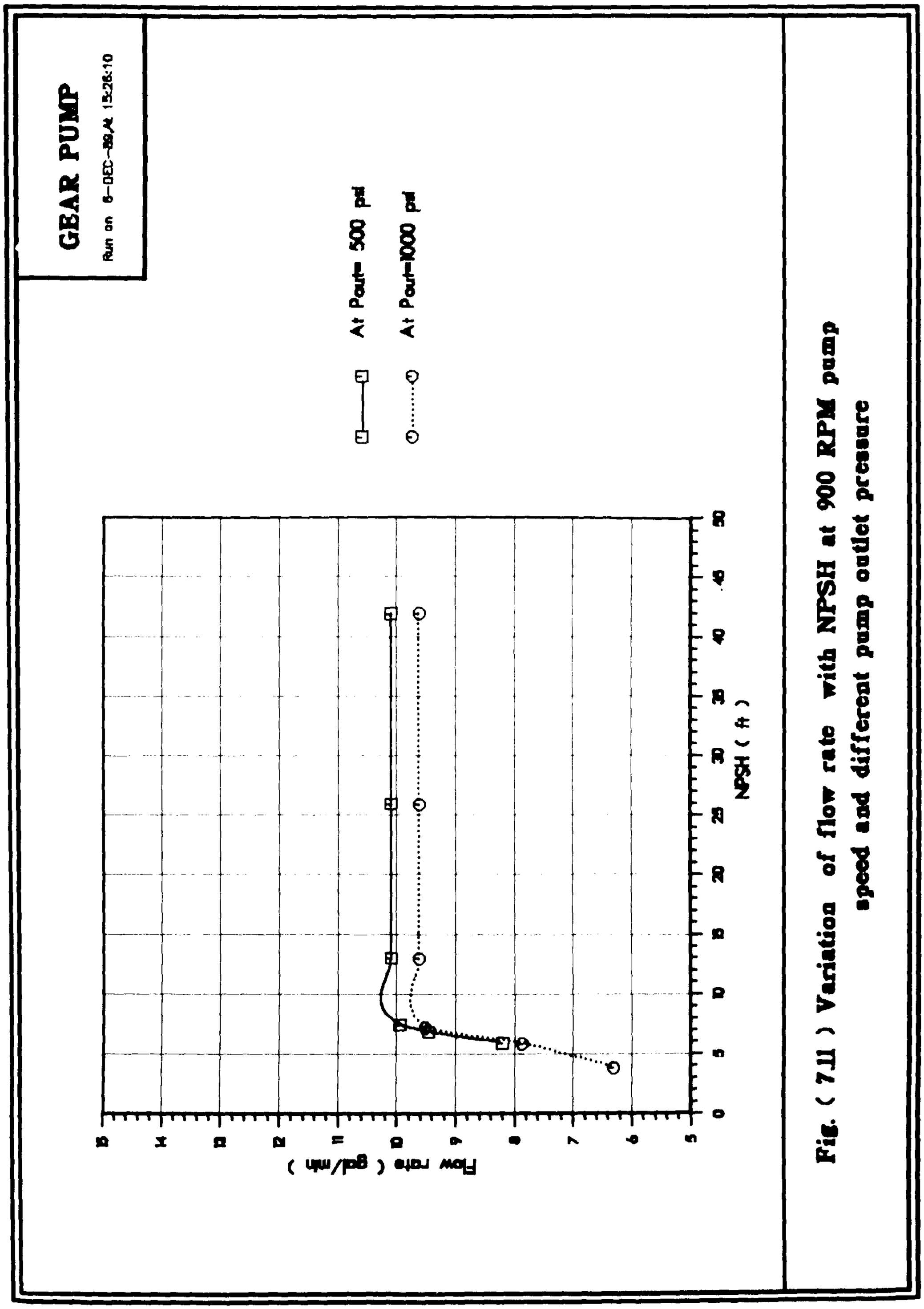

Fig. (7.11) Variation of flow rate with NPSH at 900 RPM pump speed and different pump outlet pressure

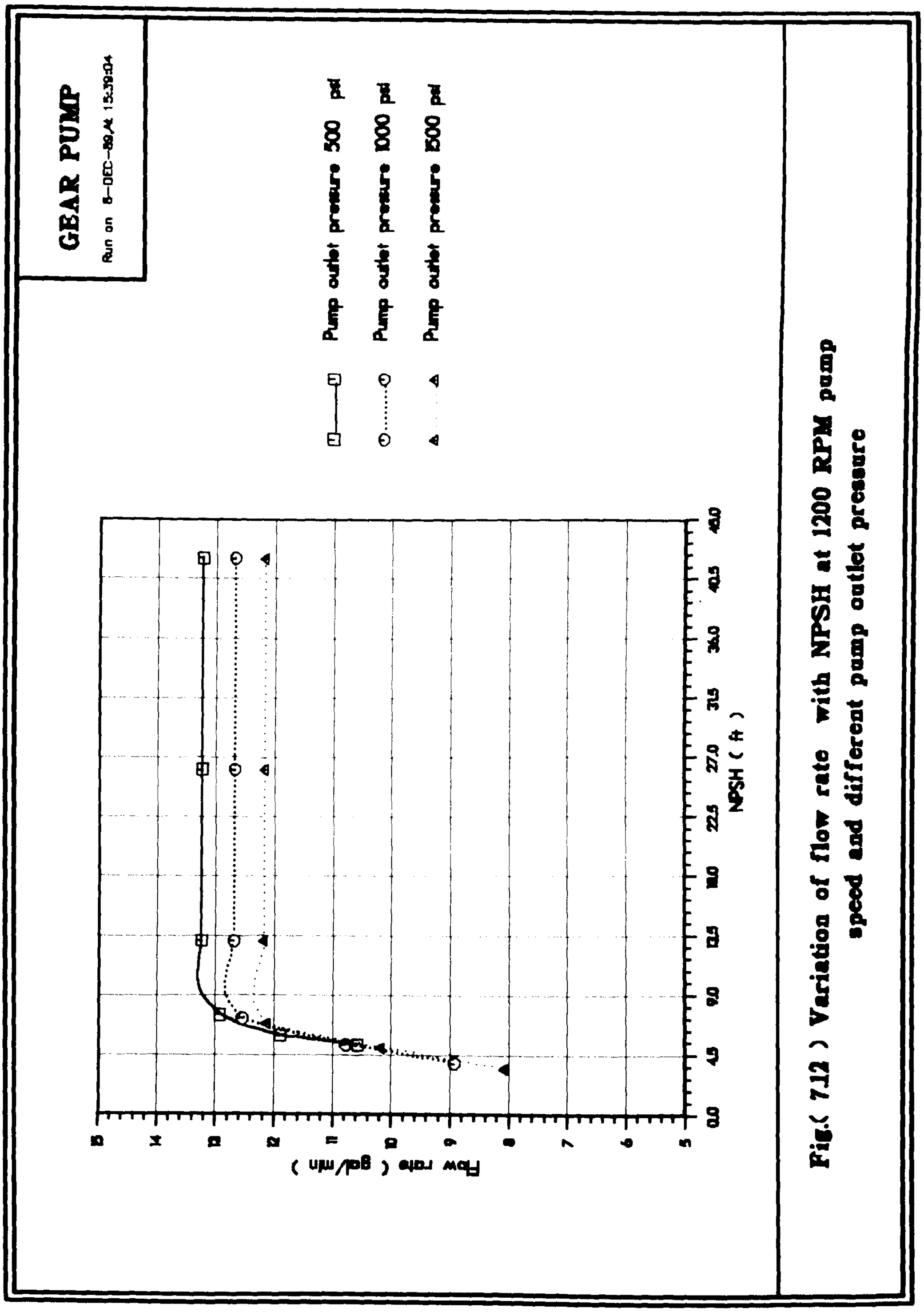

Fig.(7.12) Variation of flow rate with NPSH at 1200 RPM pump speed and different pump outlet pressure

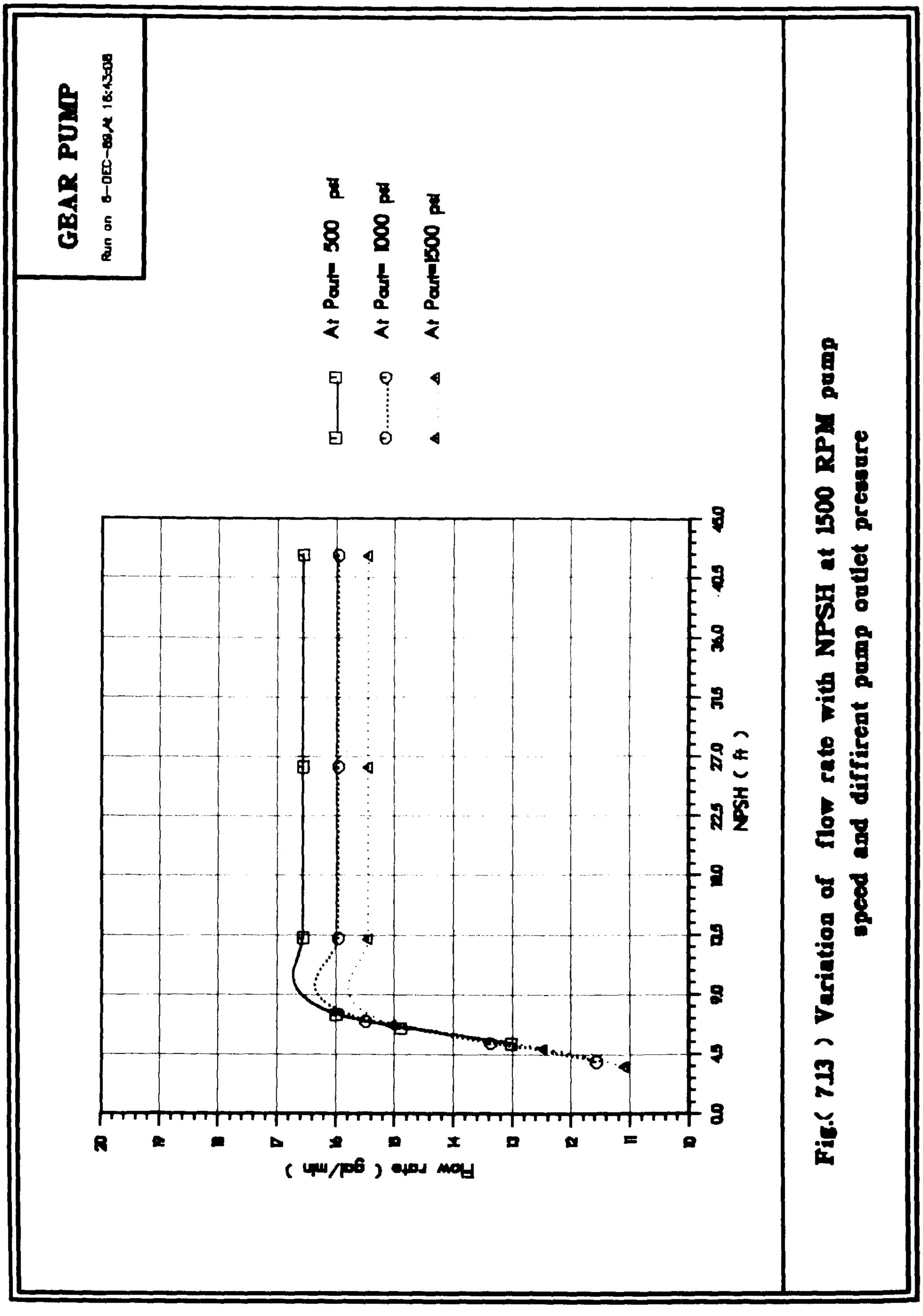

Fig.(7.13) Variation of flow rate with NPSH at 1500 RPM pump speed and different pump outlet pressure

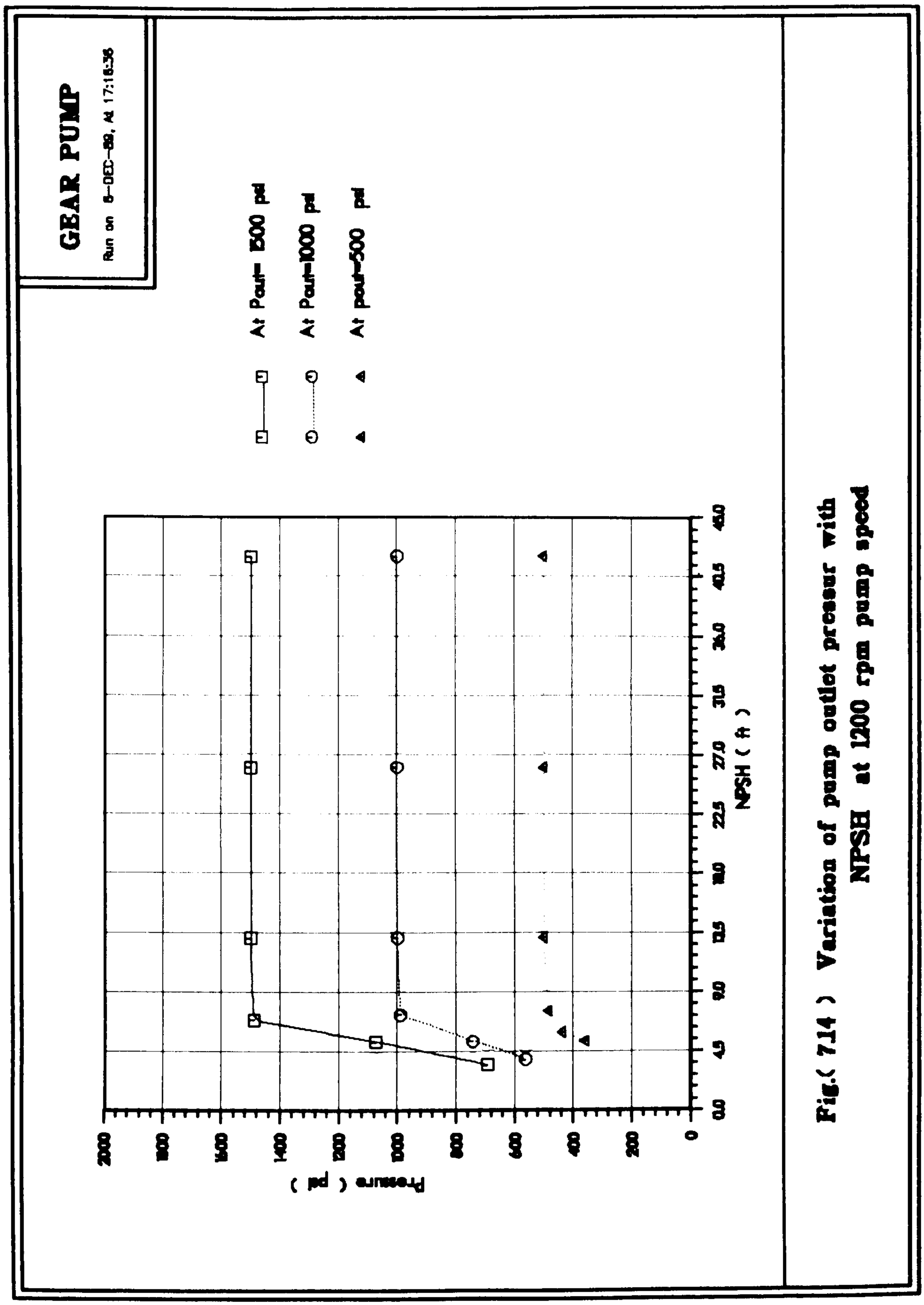

Fig.(7.14) Variation of pump outlet pressure with NPSH at 1200 rpm pump speed

MES45E

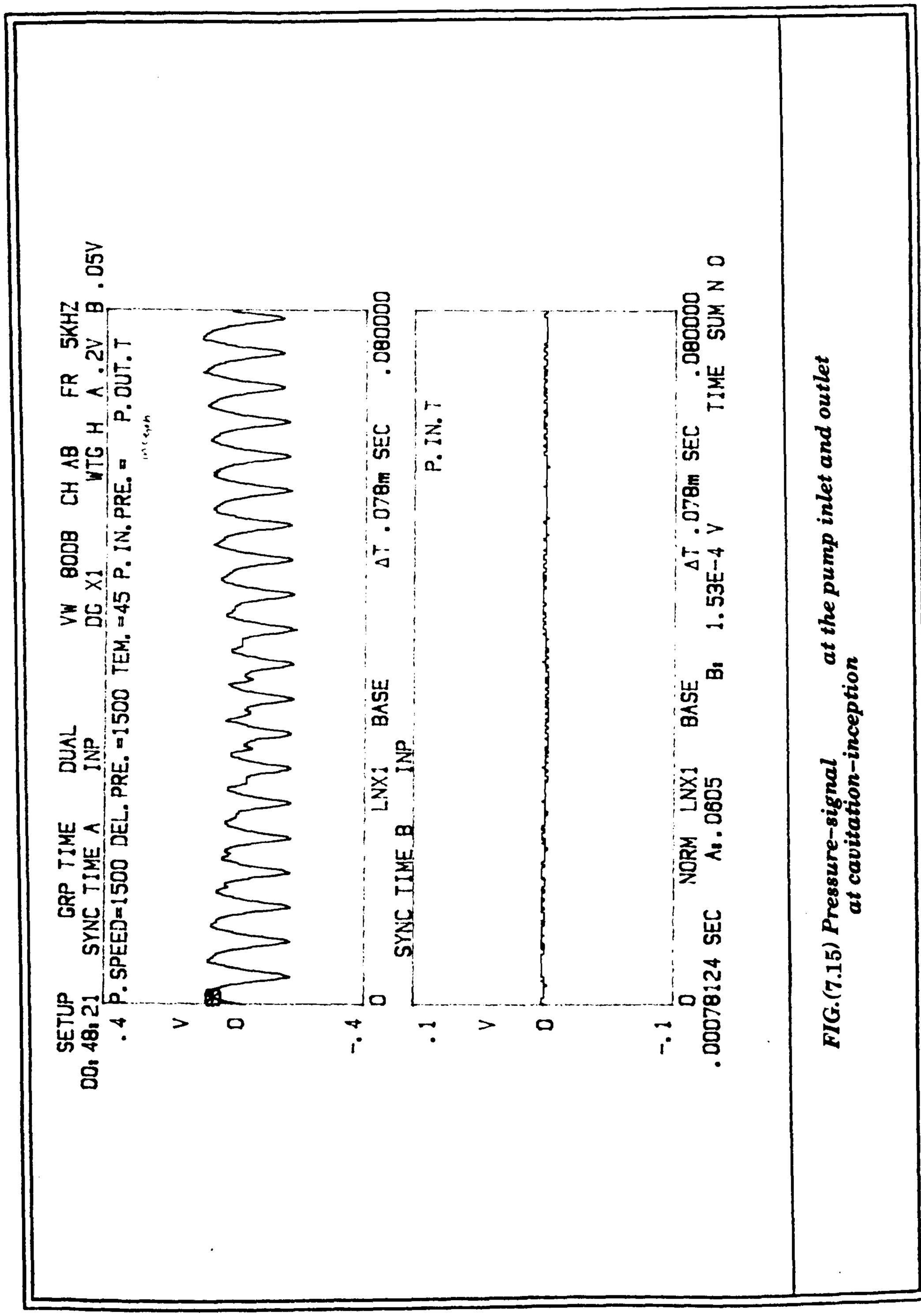

FIG.(7.15) Pressure-signal at the pump inlet and outlet at cavitation-inception

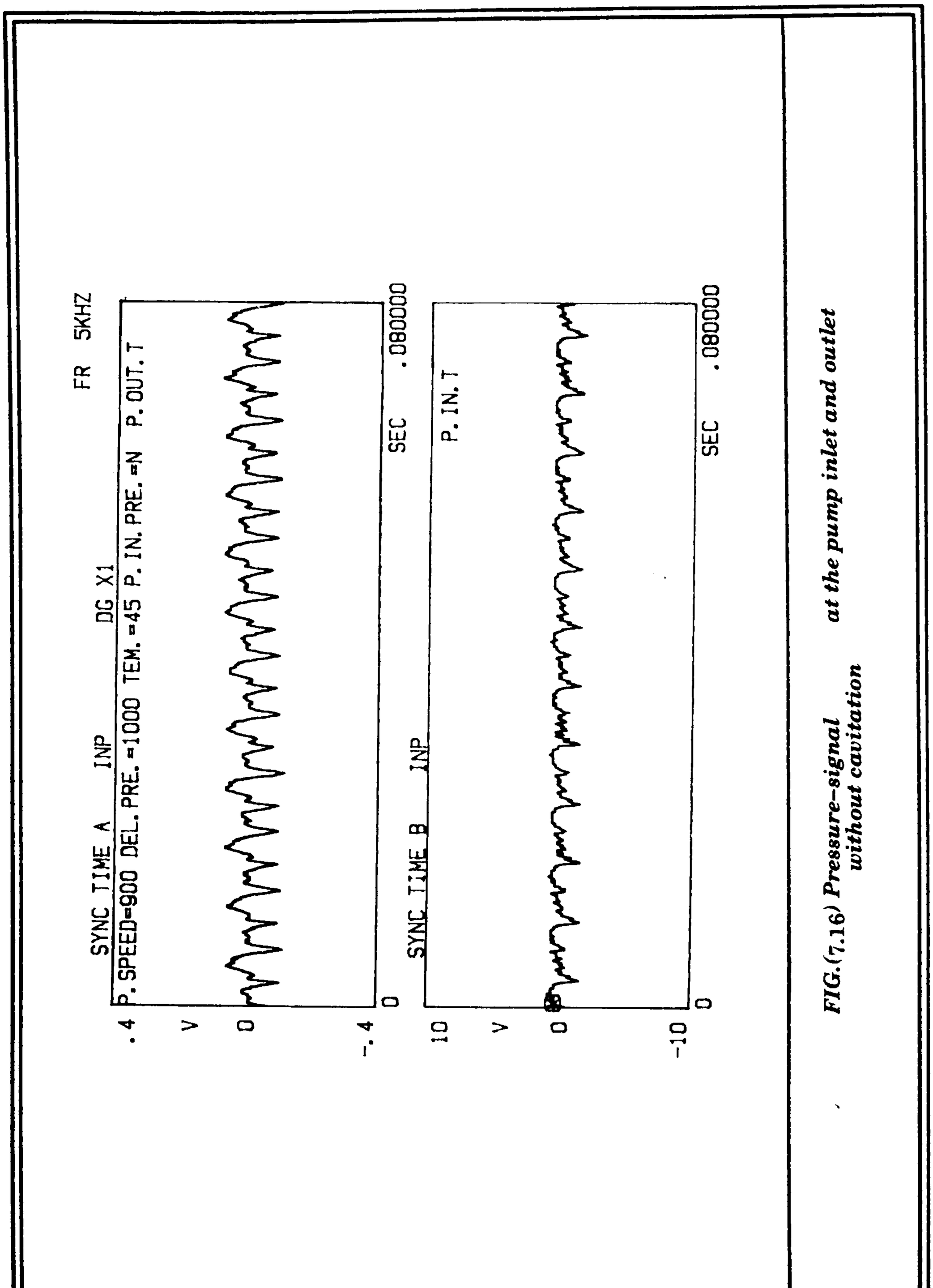

FIG.(7.16) Pressure–signal without cavitation at the pump inlet and outlet

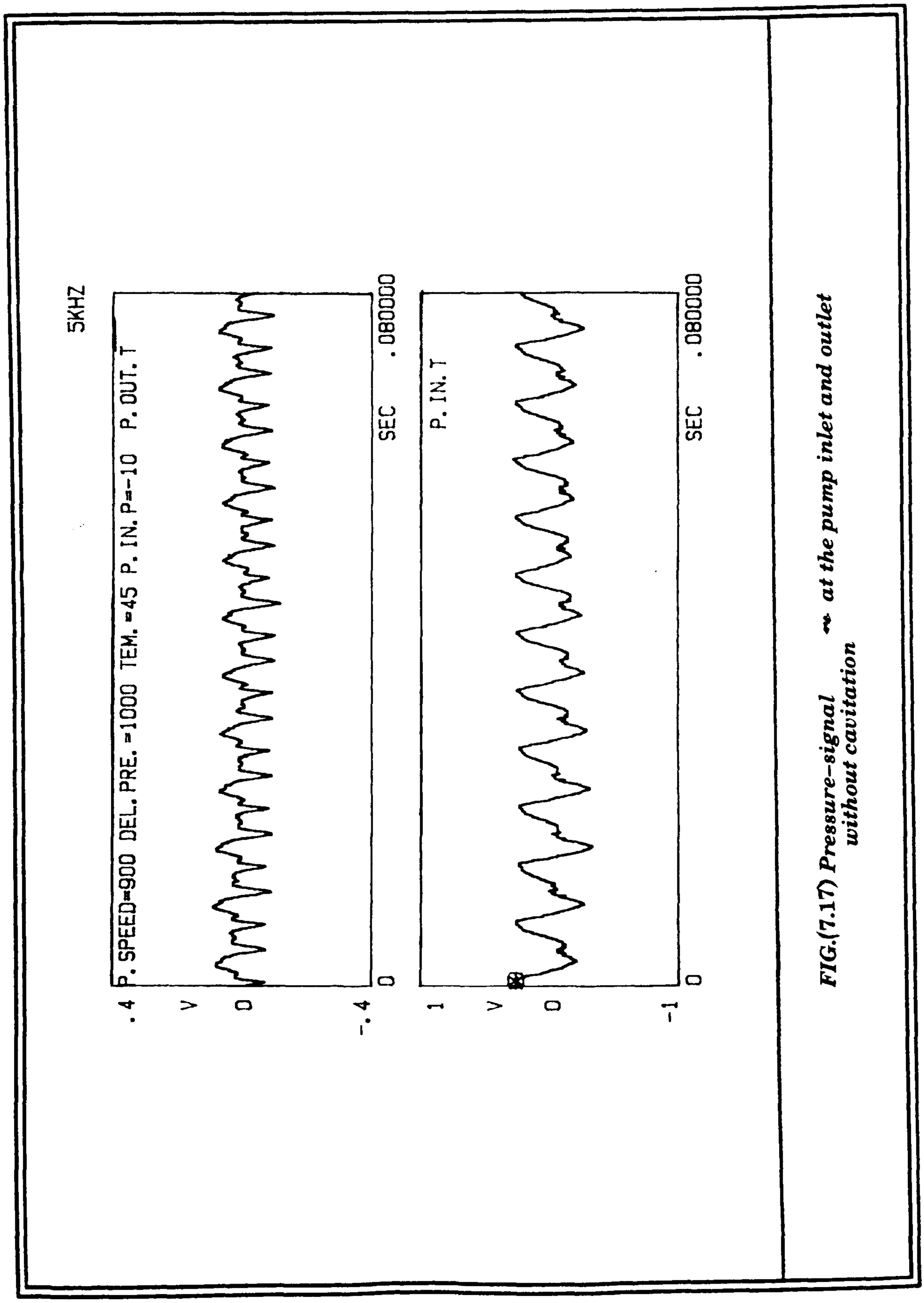

FIG.(7.17) Pressure–signal at the pump inlet and outlet without cavitation

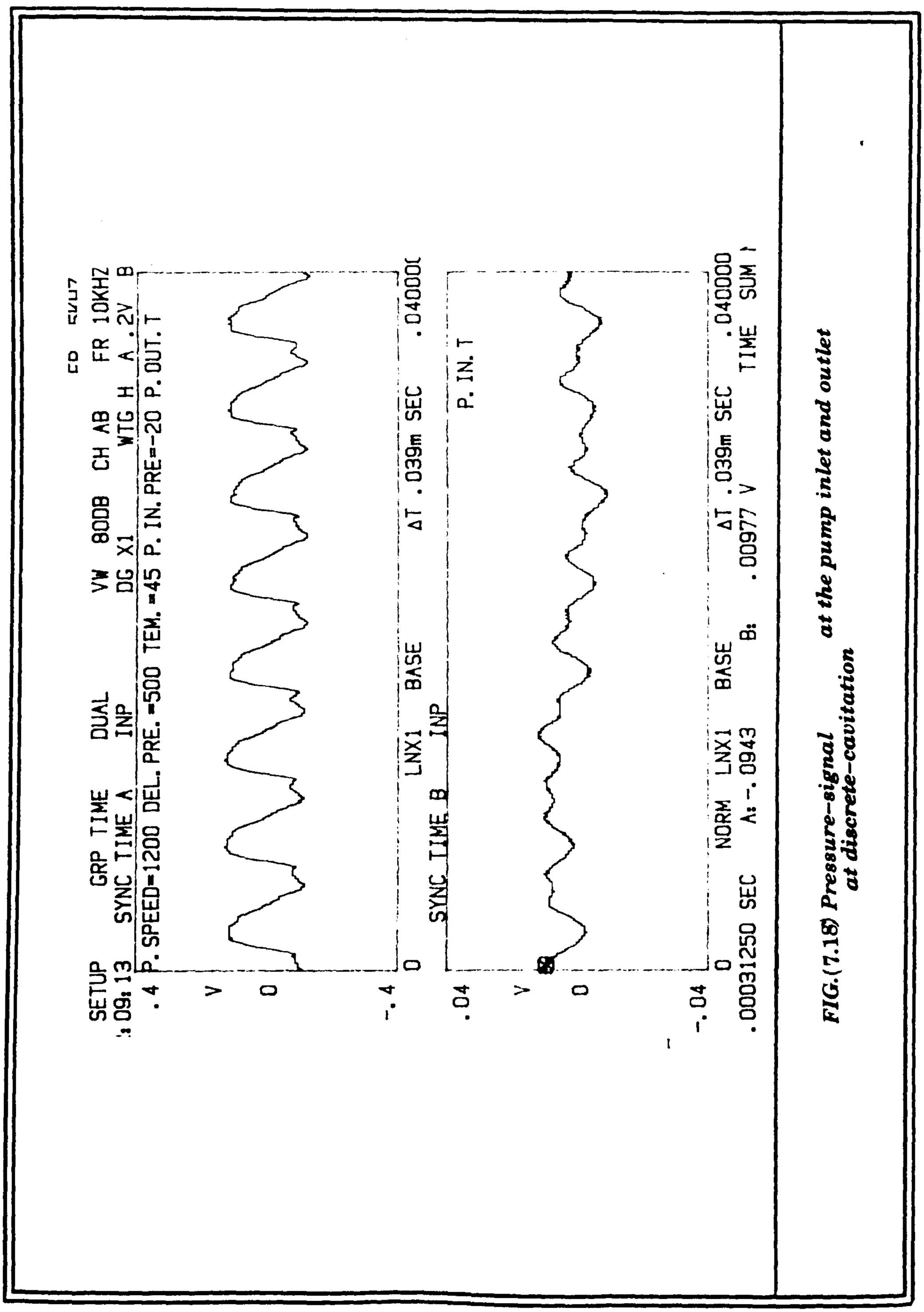

FIG.(7.18) Pressure-signal at the pump inlet and outlet at discrete-cavitation

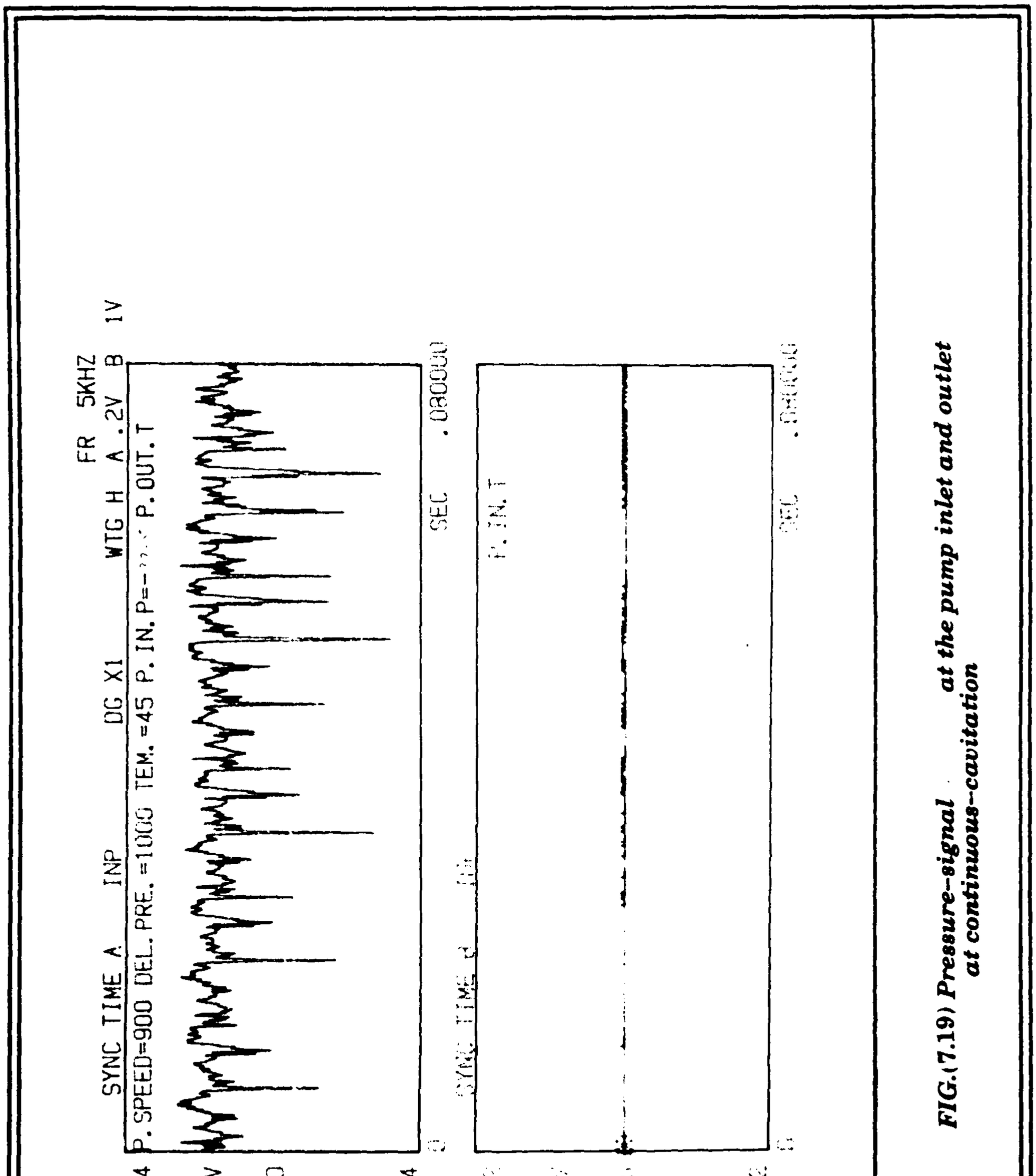

FIG.(7.19) Pressure-signal at the pump inlet and outlet at continuous--cavitation

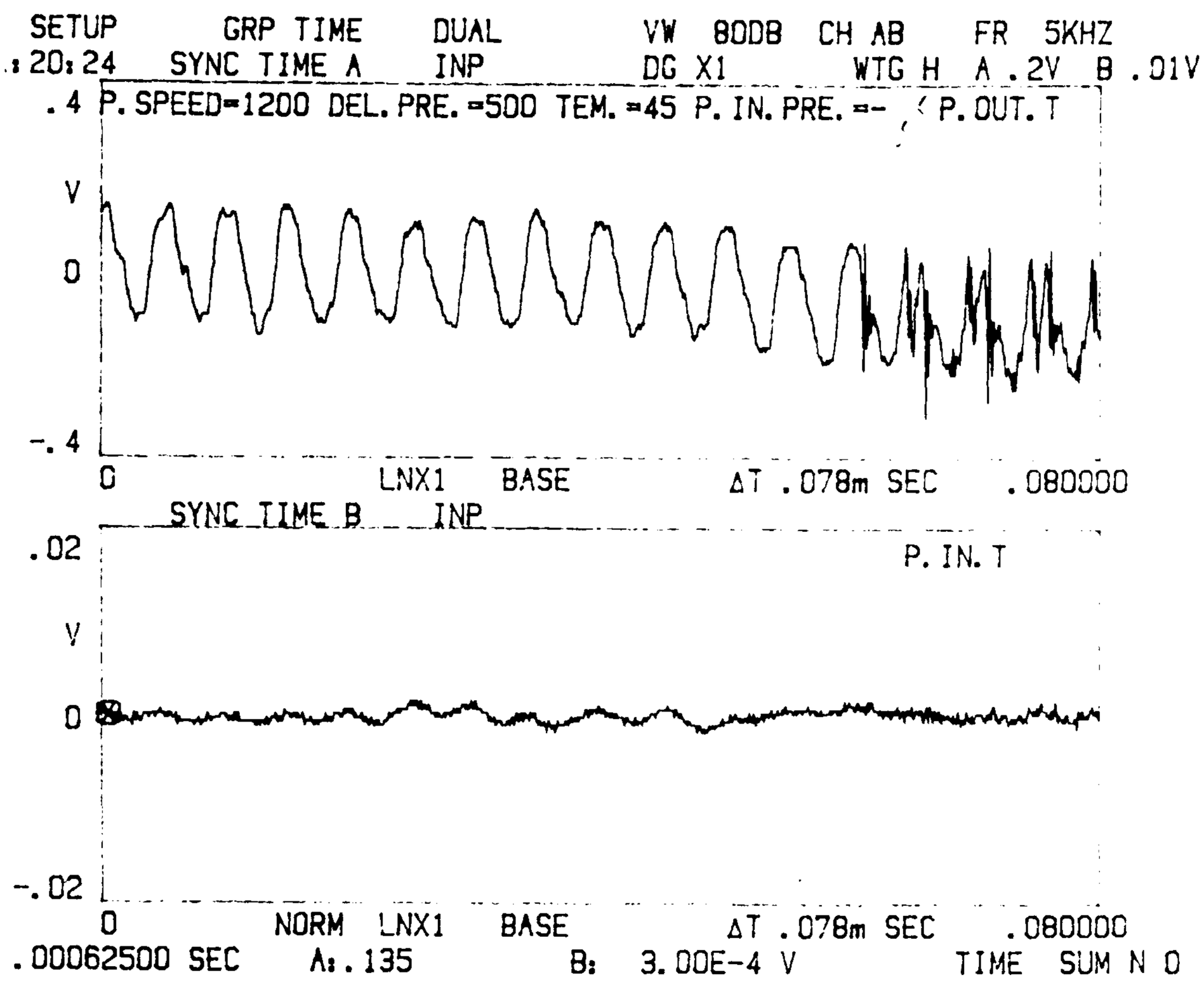

FIG.(7.20) Pressure-signal at the pump inlet and outlet at cavitation-inception

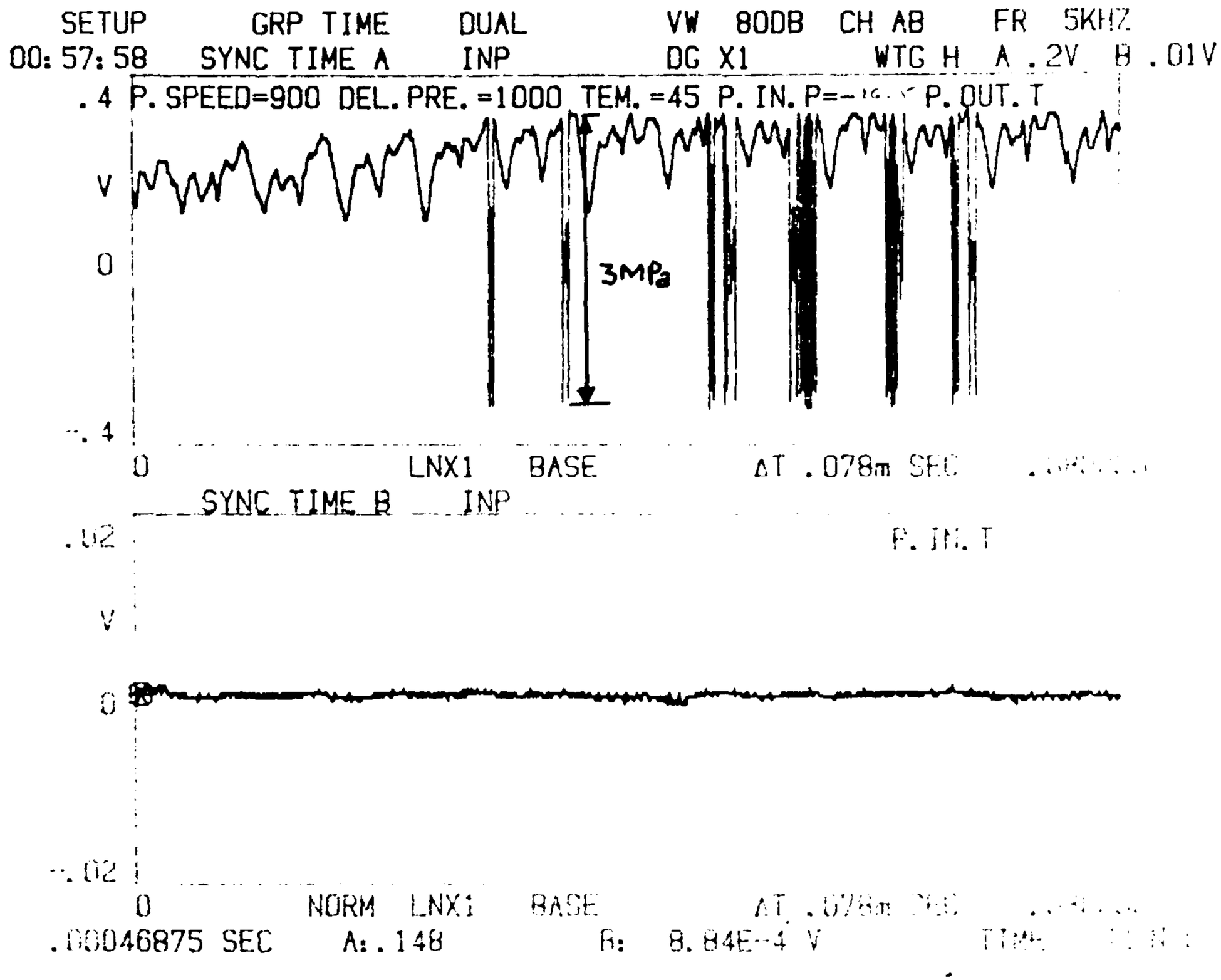

FIG.(7.21) Pressure-signal at the pump inlet and outlet at discrete-cavitation

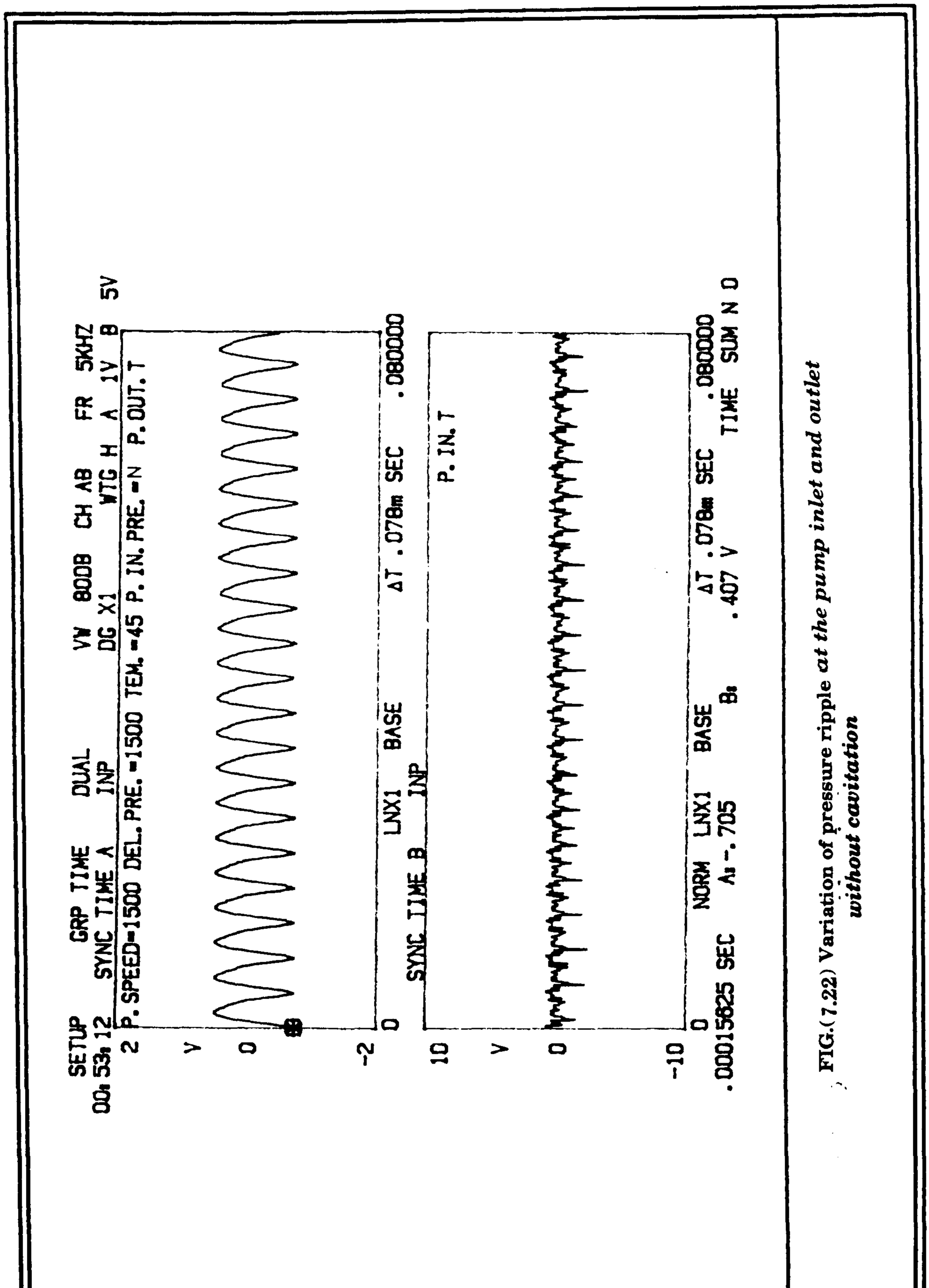

FIG.(7.22) Variation of pressure ripple *at the pump inlet and outlet without cavitation*

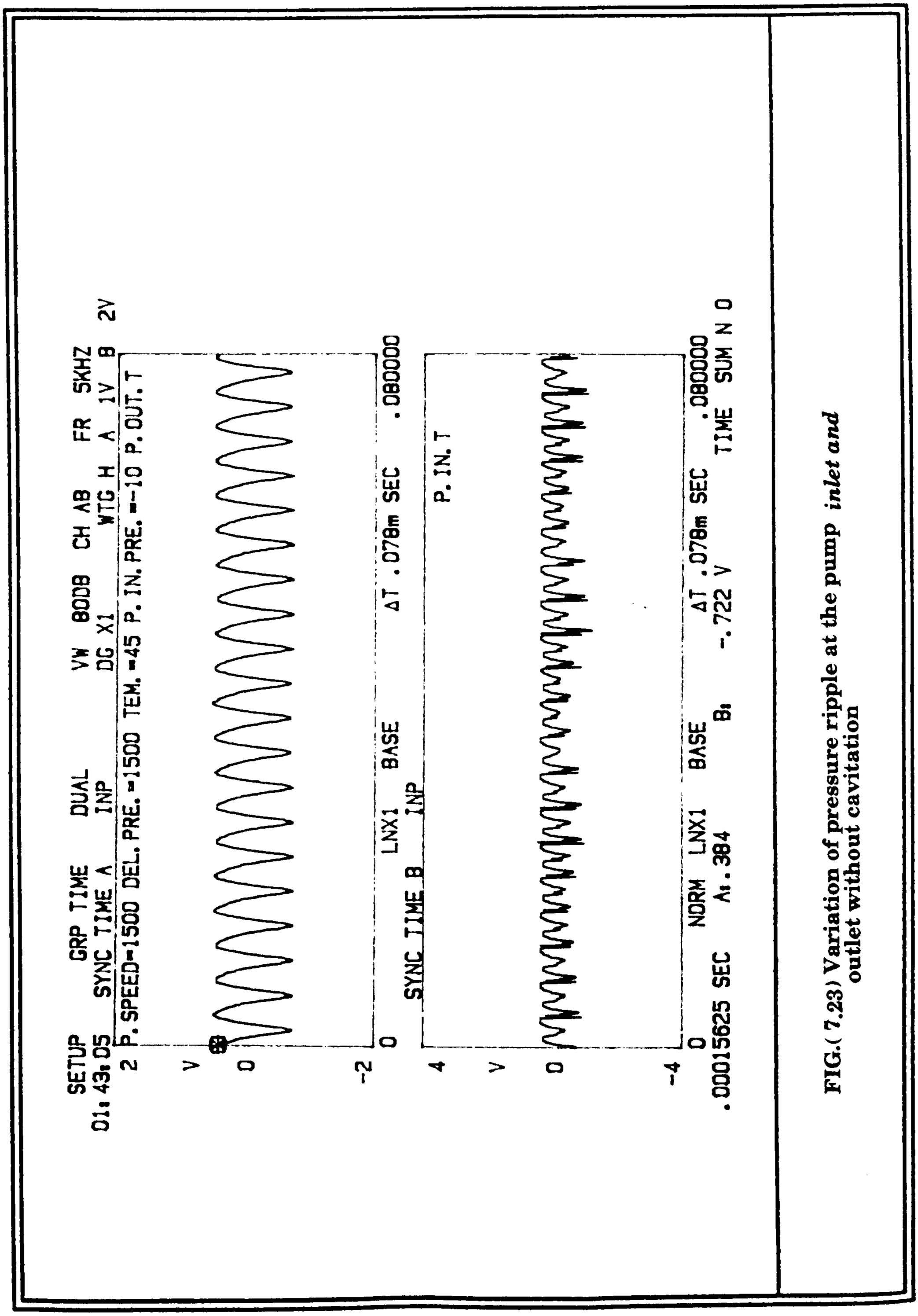

FIG.(7.23) Variation of pressure ripple at the pump *inlet and* outlet without cavitation

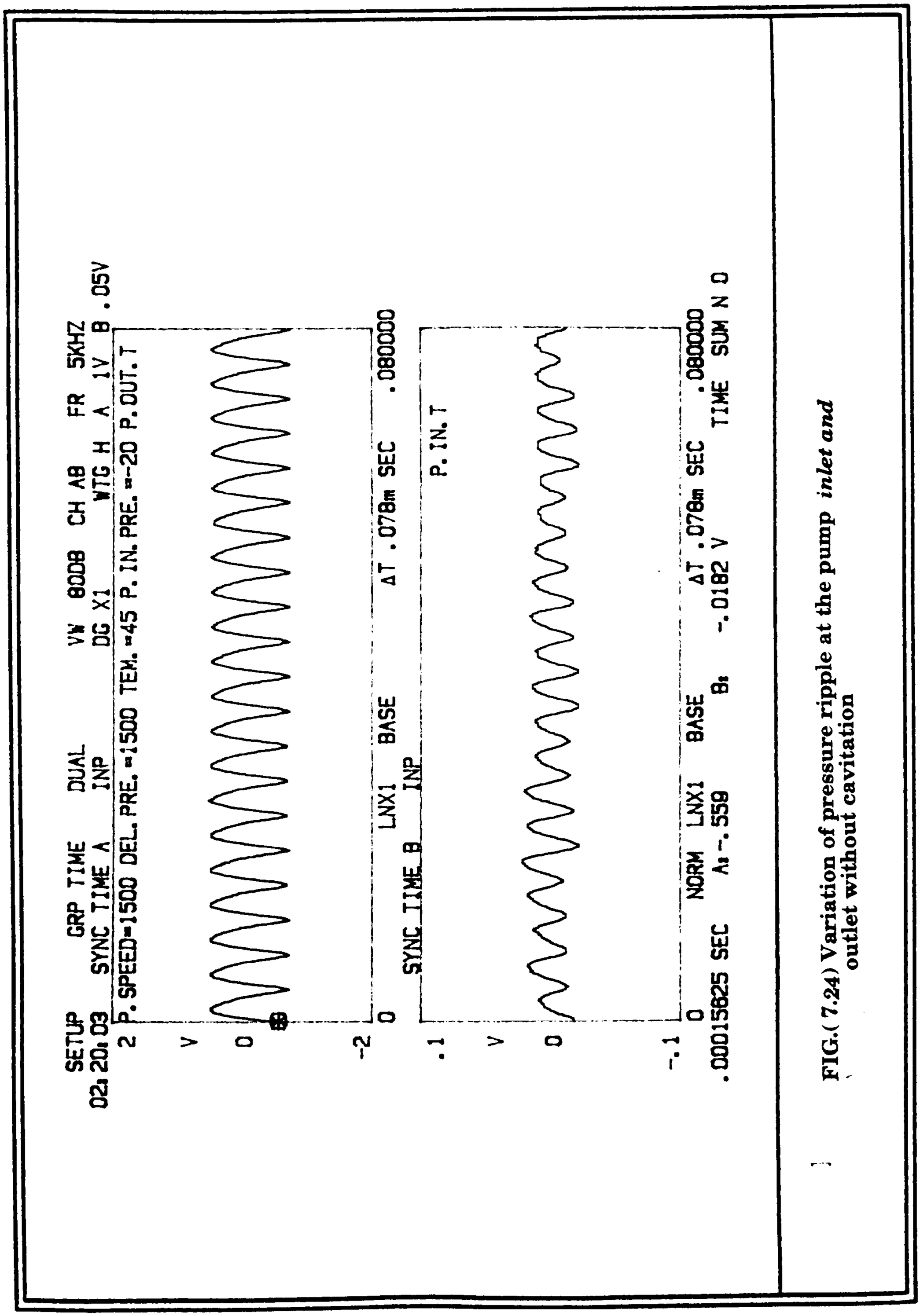

FIG.(7.24) Variation of pressure ripple at the pump *inlet and* outlet without cavitation

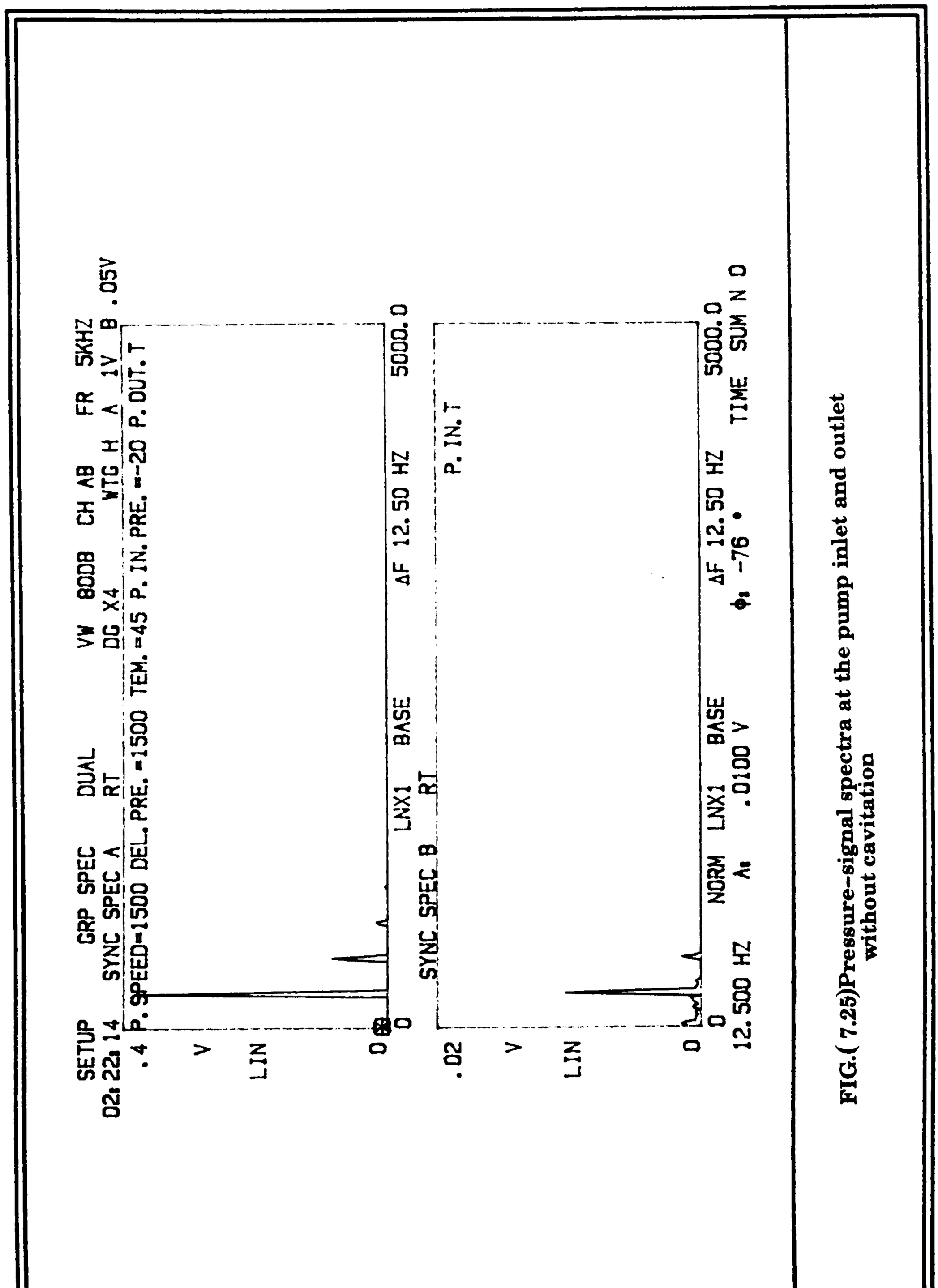

FIG.(7.25)Pressure-signal spectra at the pump inlet and outlet without cavitation

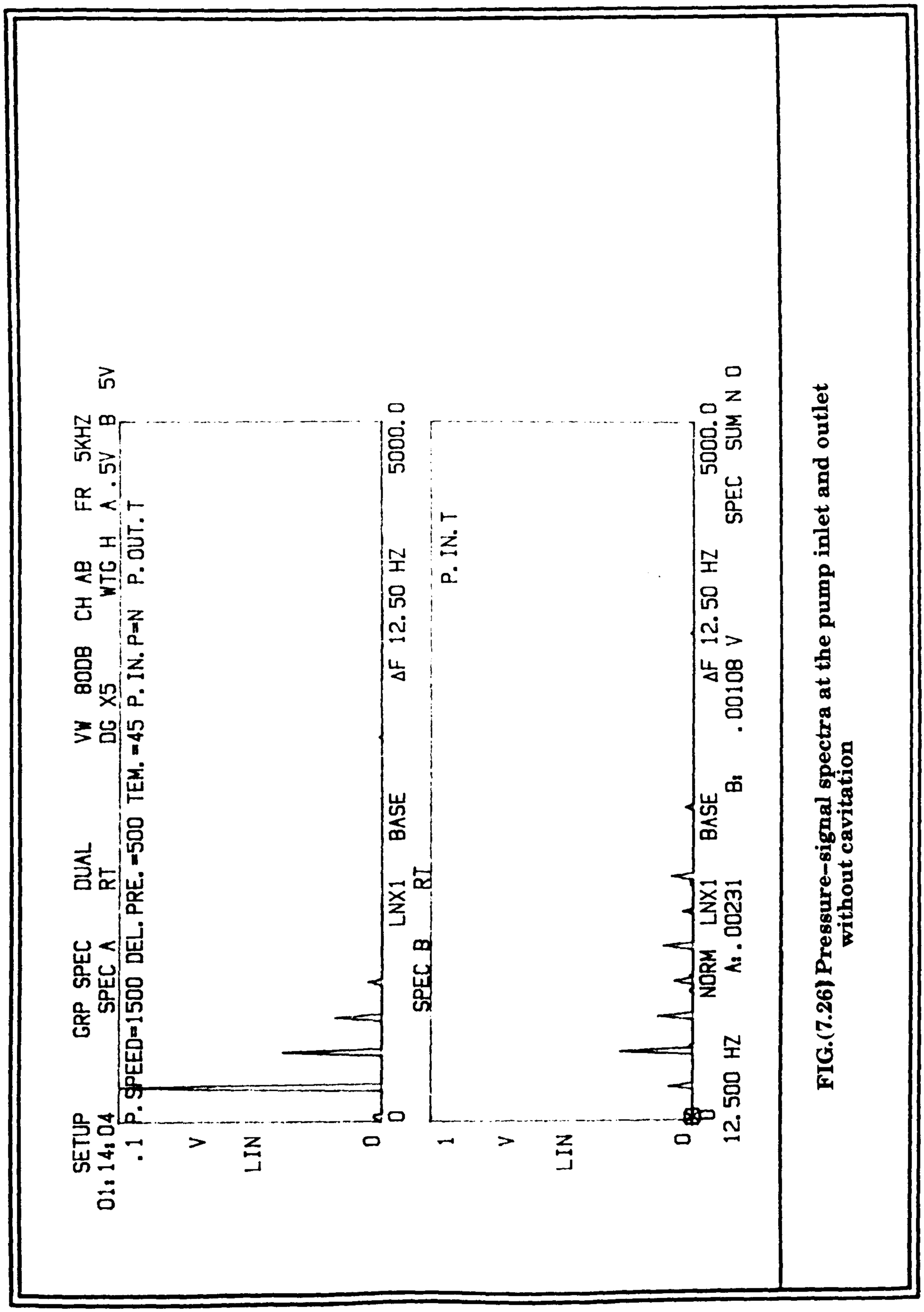

FIG.(7.26) Pressure-signal spectra at the pump inlet and outlet without cavitation

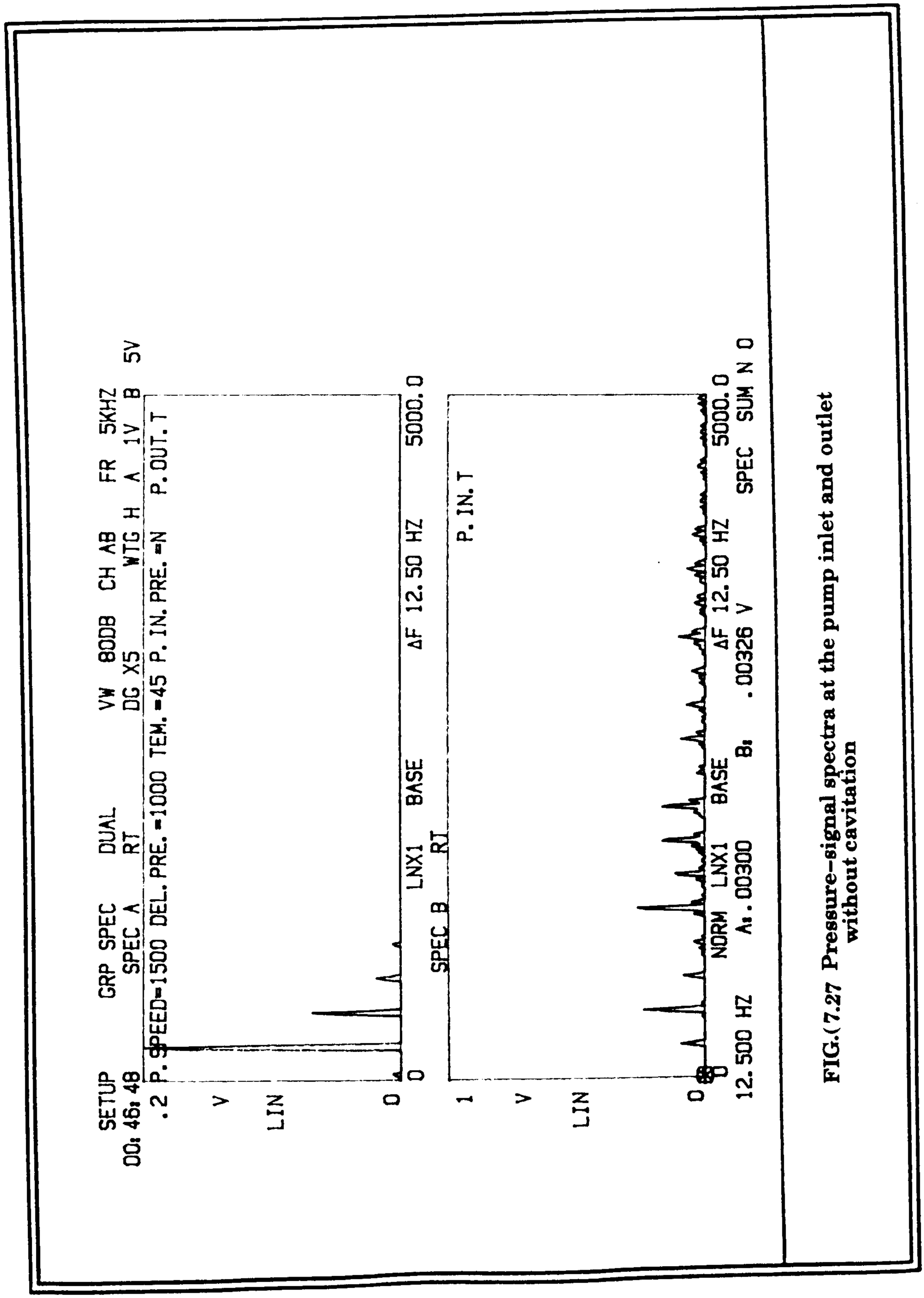

FIG.(7.27 Pressure–signal spectra at the pump inlet and outlet without cavitation

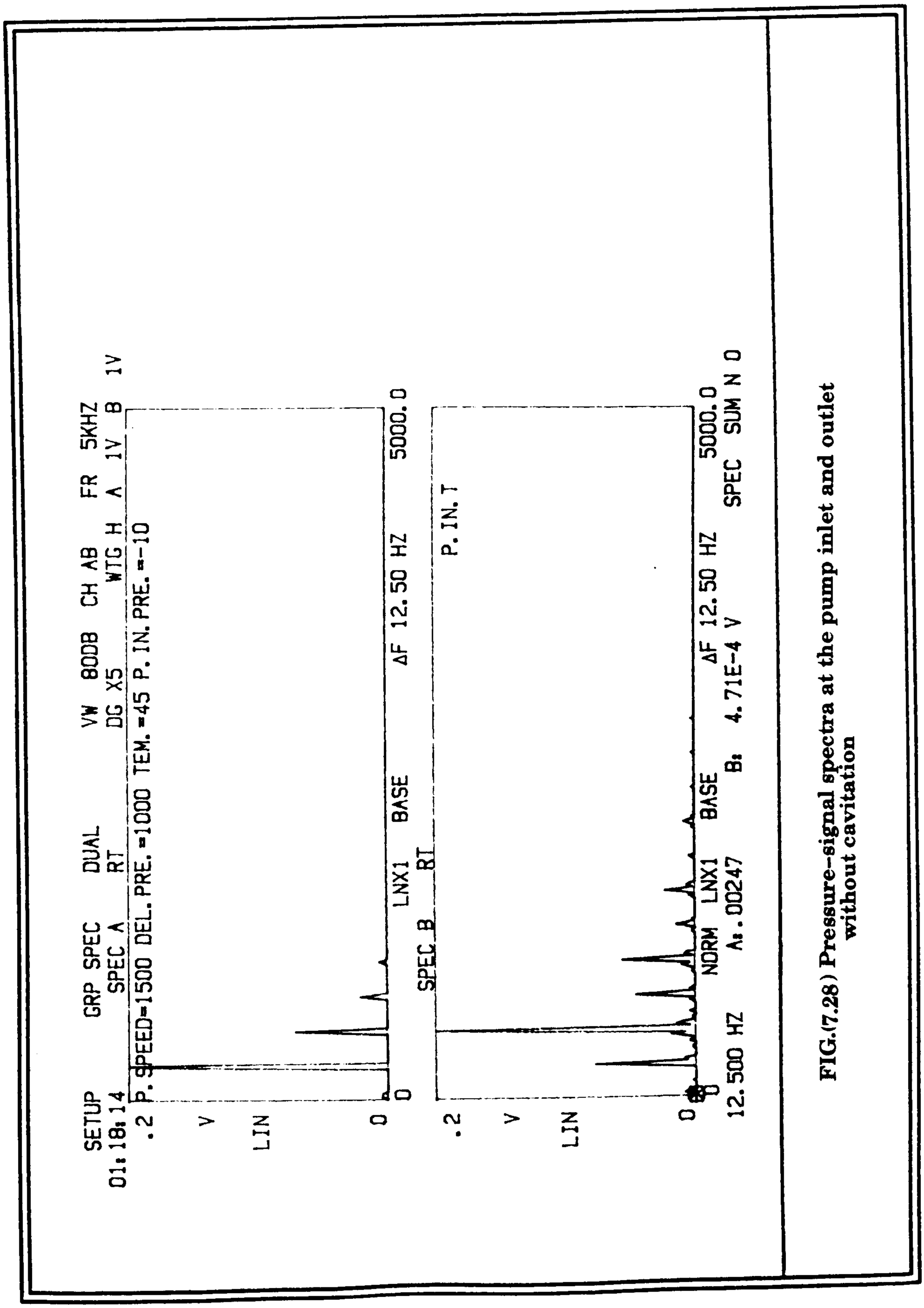

FIG.(7.28) Pressure-signal spectra at the pump inlet and outlet without cavitation

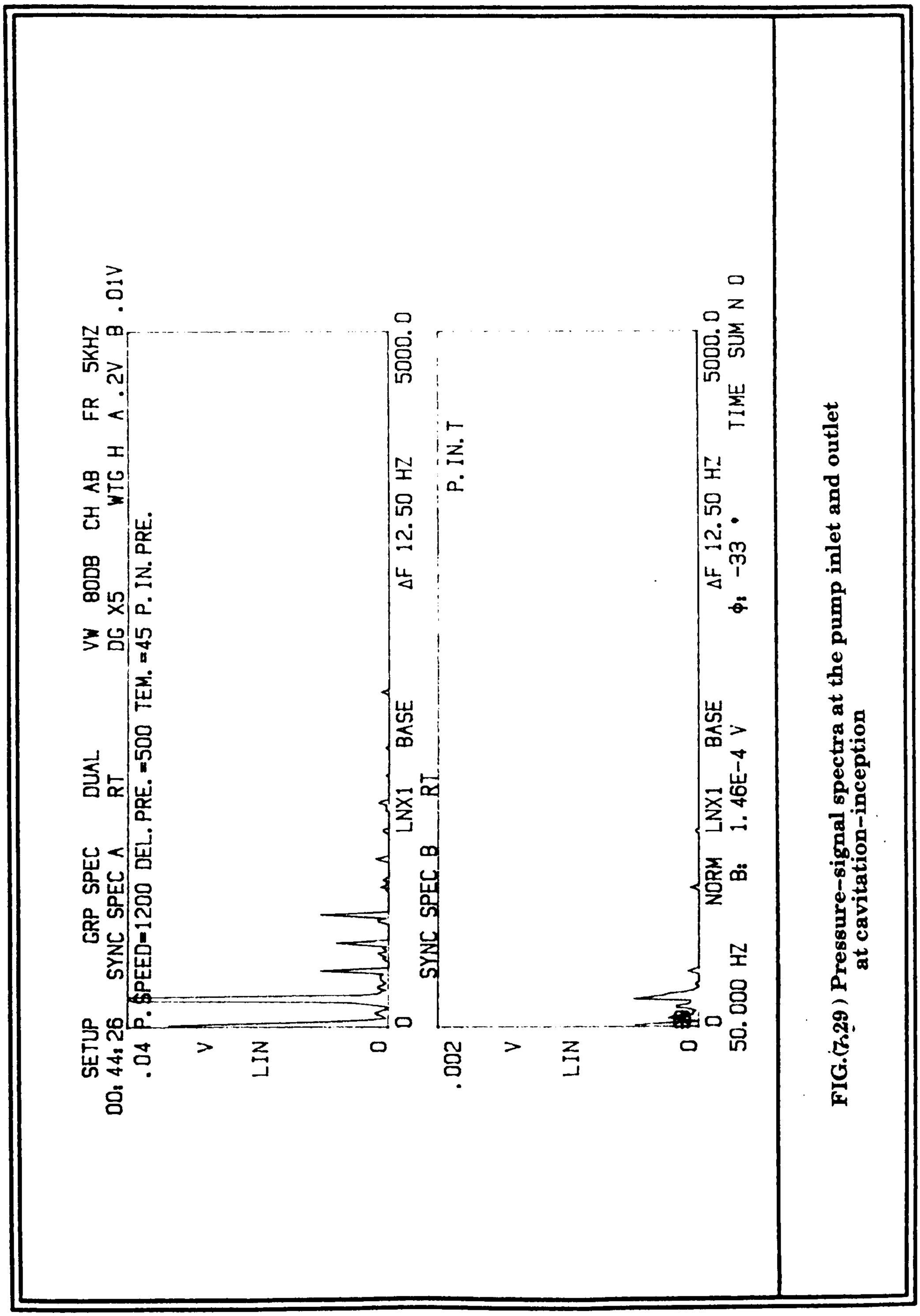

FIG.(7.29) Pressure-signal spectra at the pump inlet and outlet at cavitation-inception

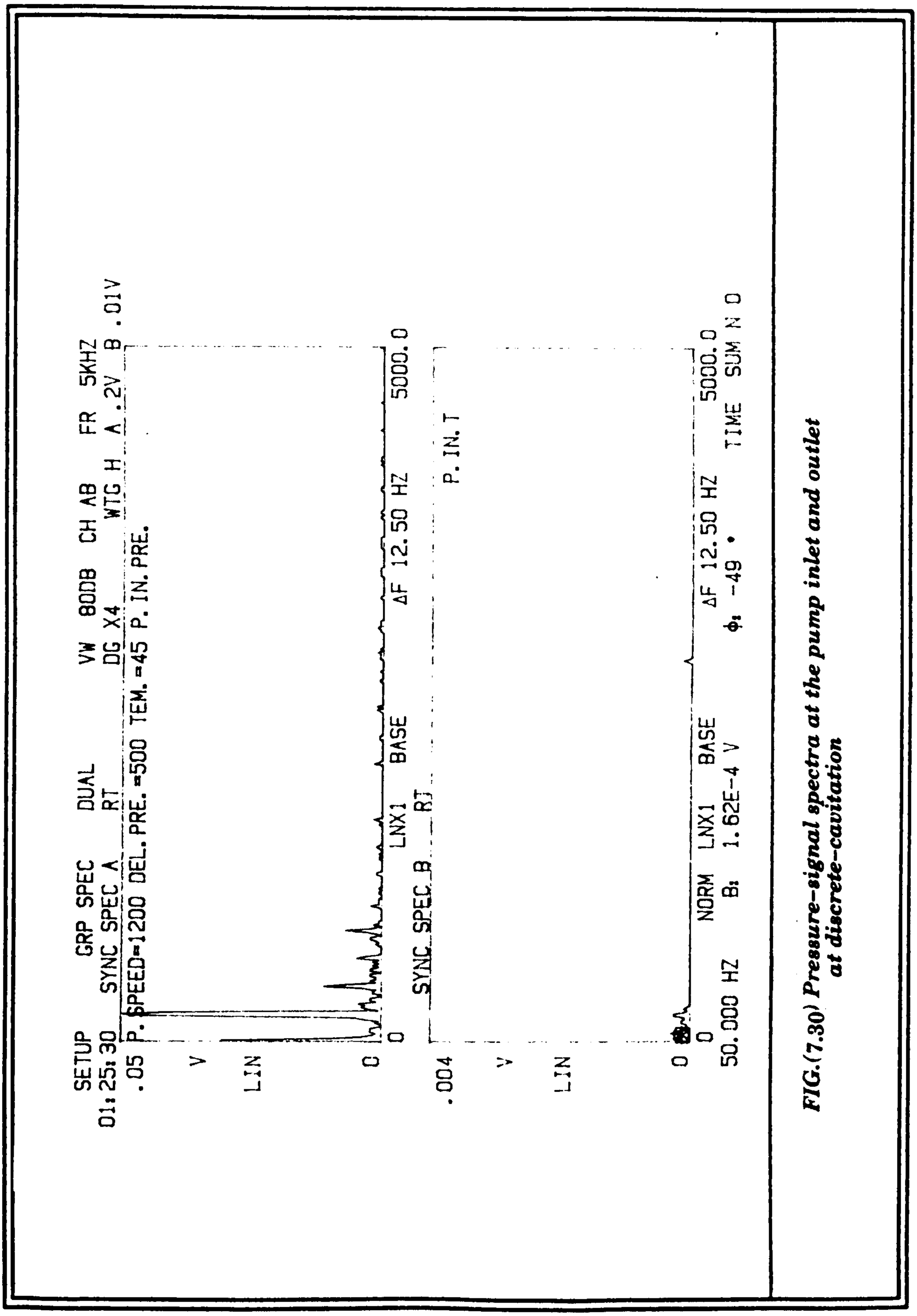

FIG.(7.30) Pressure-signal spectra at the pump inlet and outlet at discrete-cavitation

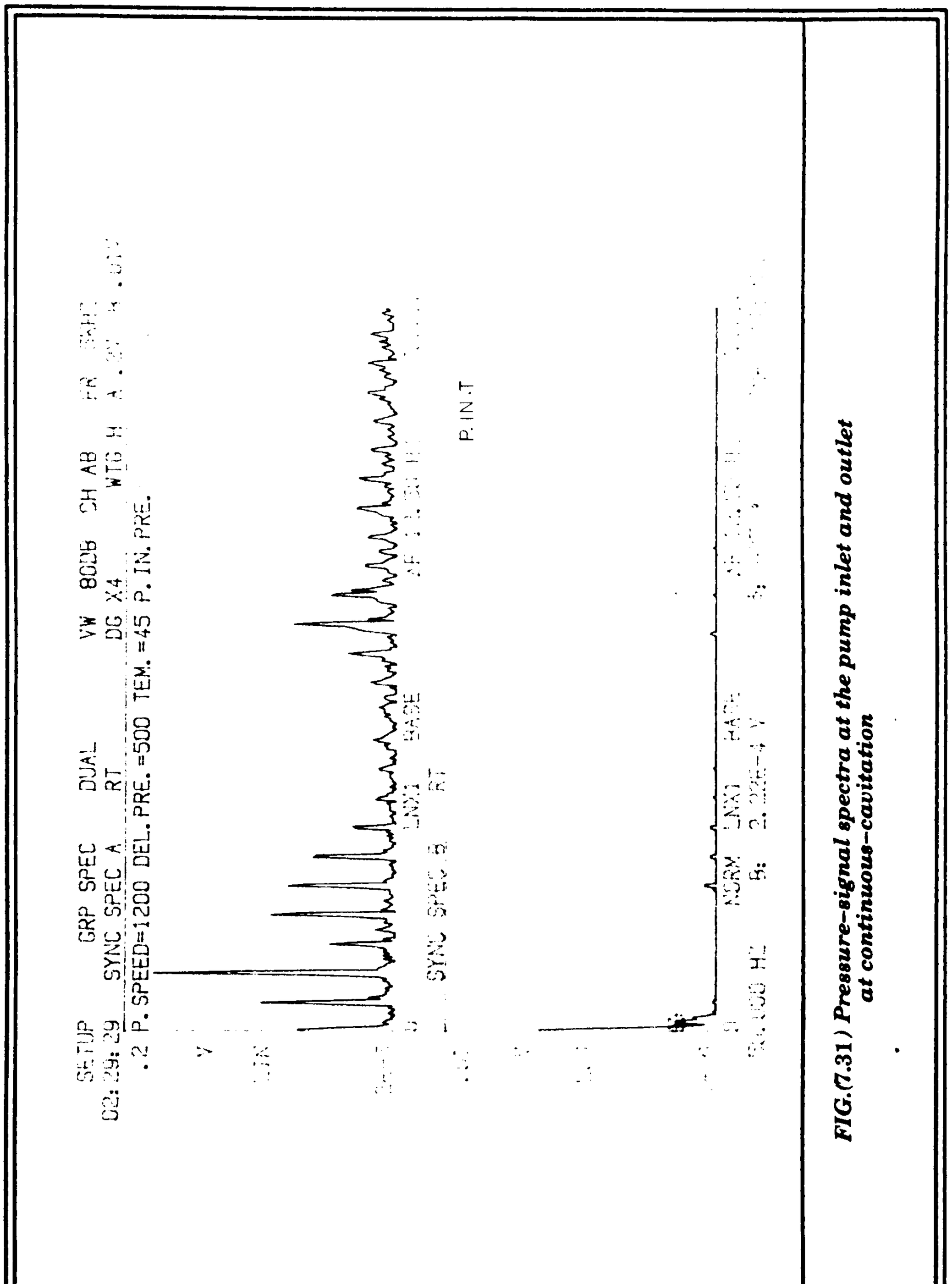

FIG.(7.31) Pressure-signal spectra at the pump inlet and outlet at continuous-cavitation

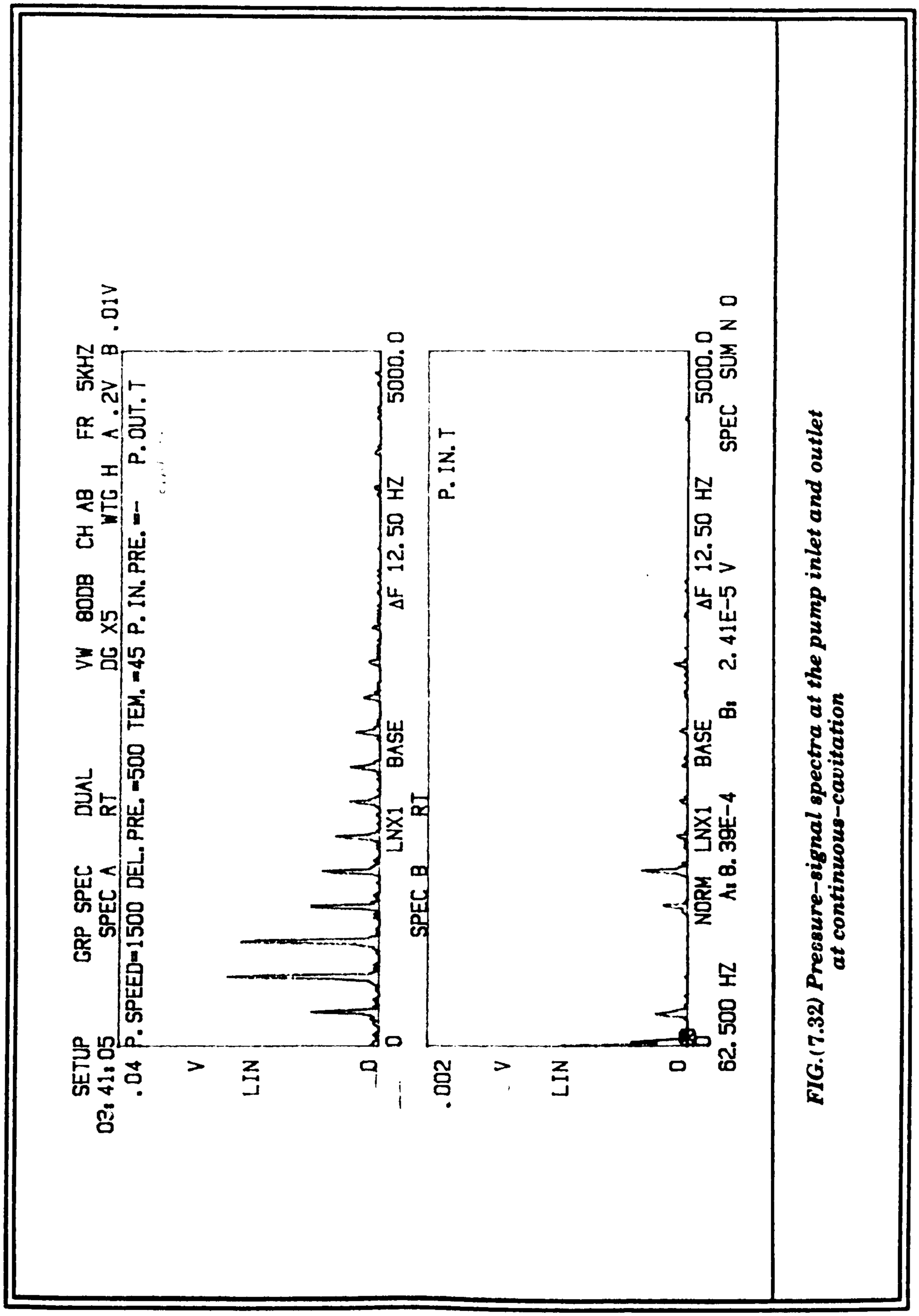

FIG.(7.32) Pressure-signal spectra at the pump inlet and outlet at continuous-cavitation

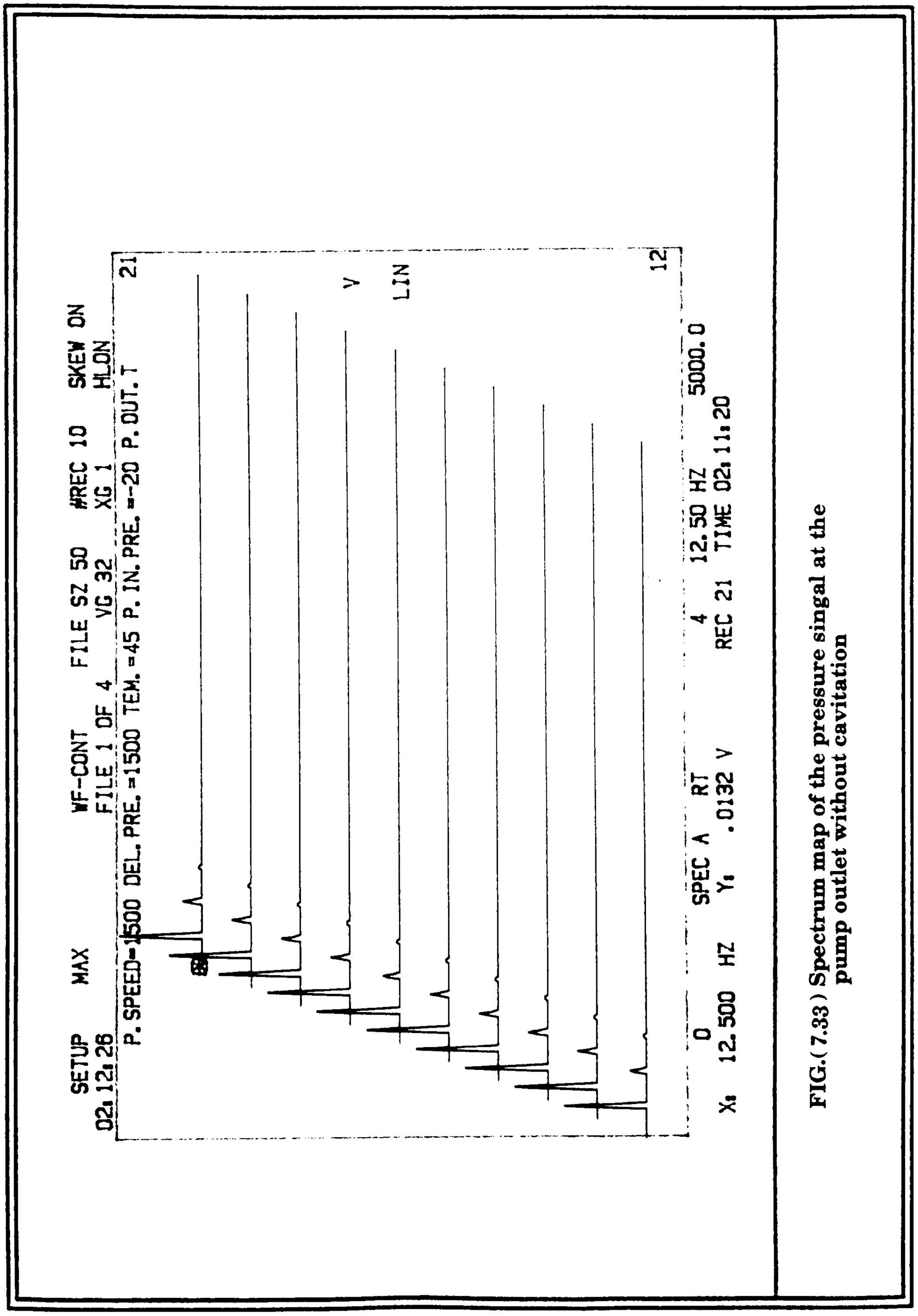

FIG.(7.33) Spectrum map of the pressure singal at the pump outlet without cavitation

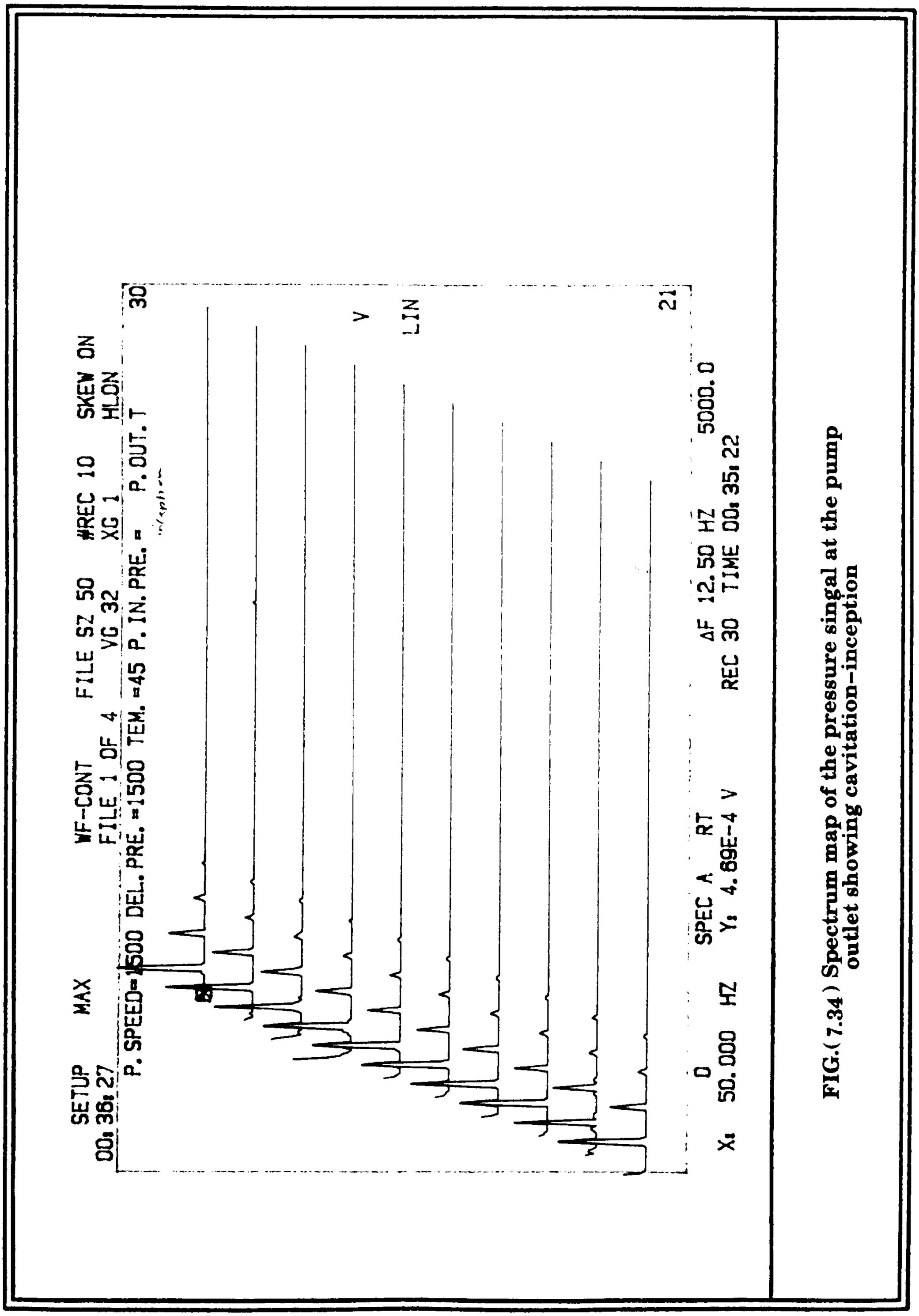

FIG.(7.34) Spectrum map of the pressure singal at the pump outlet showing cavitation-inception

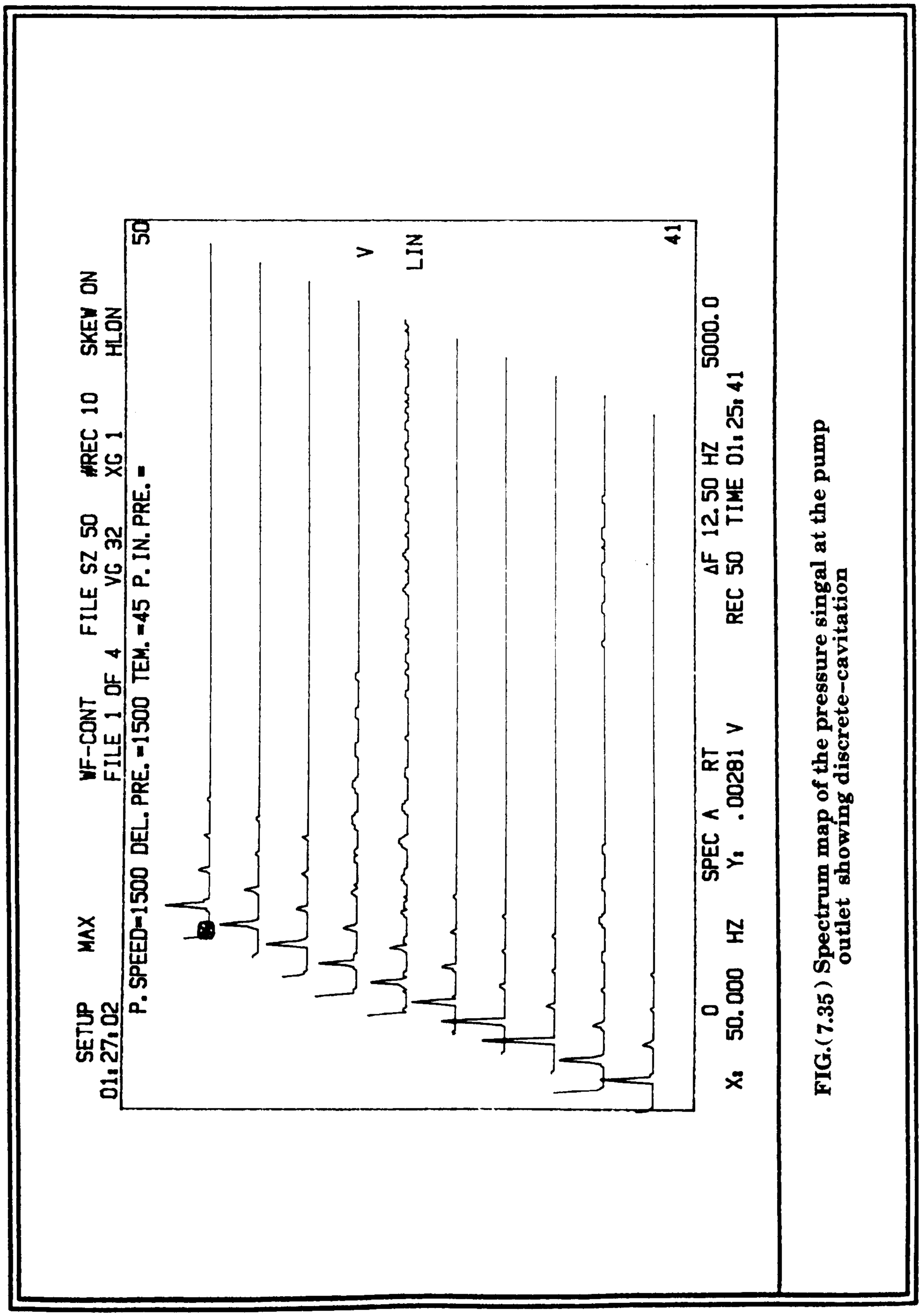

FIG.(7.35) Spectrum map of the pressure singal at the outlet showing discrete-cavitation

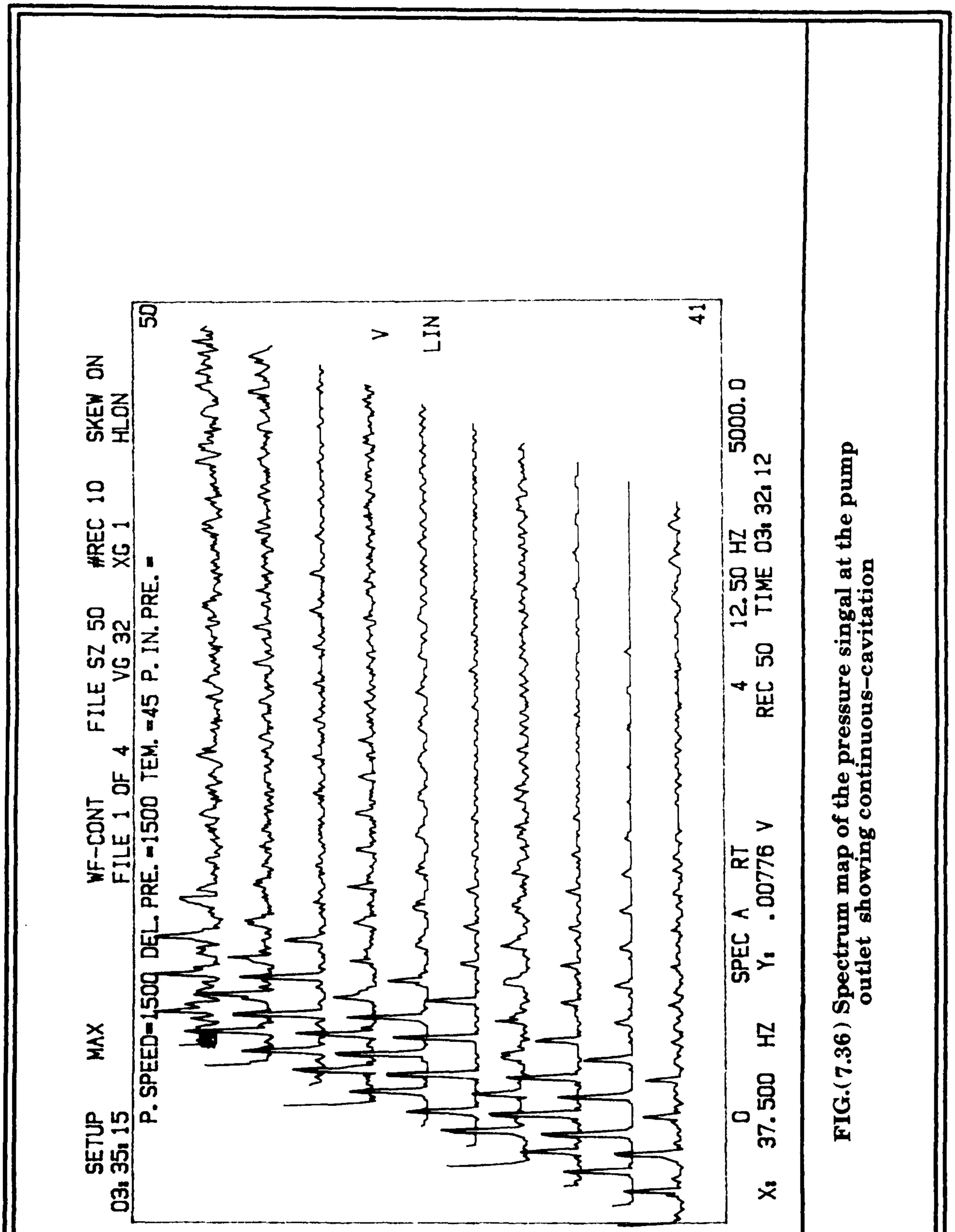

FIG.(7.36) Spectrum map of the pressure singal at the pump outlet showing continuous-cavitation

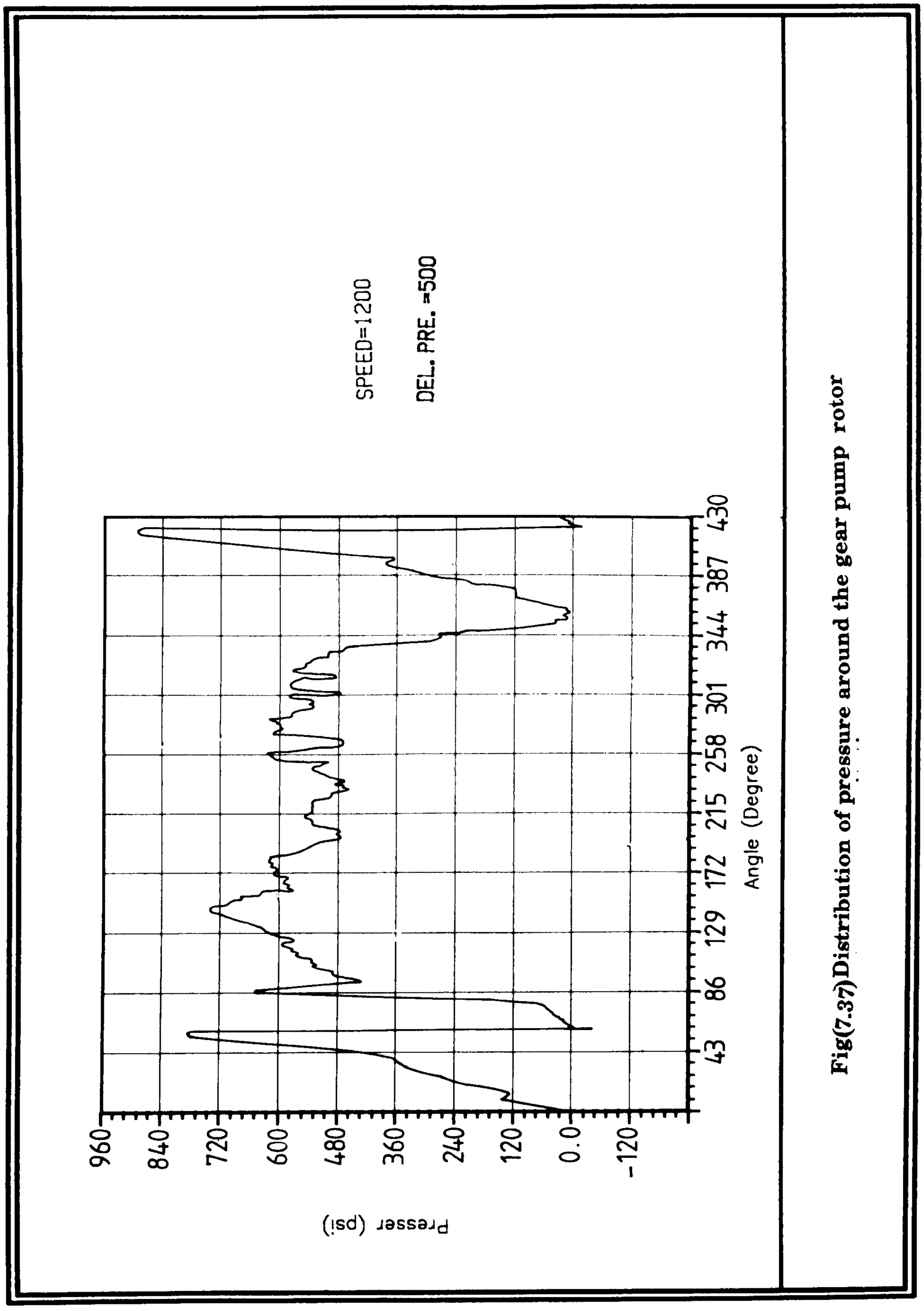

Fig(7.37)Distribution of pressure around the gear pump rotor

ME945P

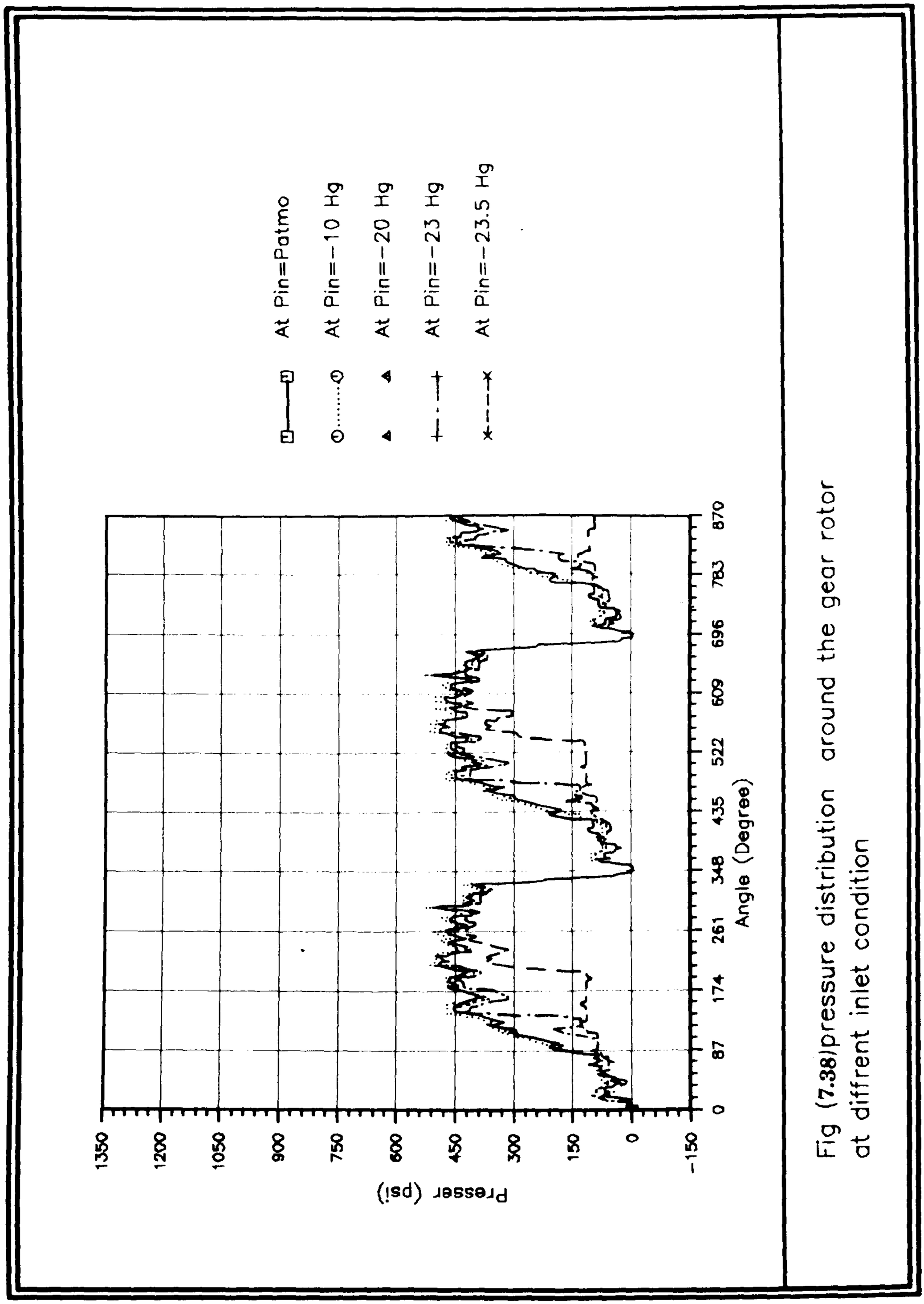

Fig (7.38) pressure distribution around the gear rotor at different inlet condition

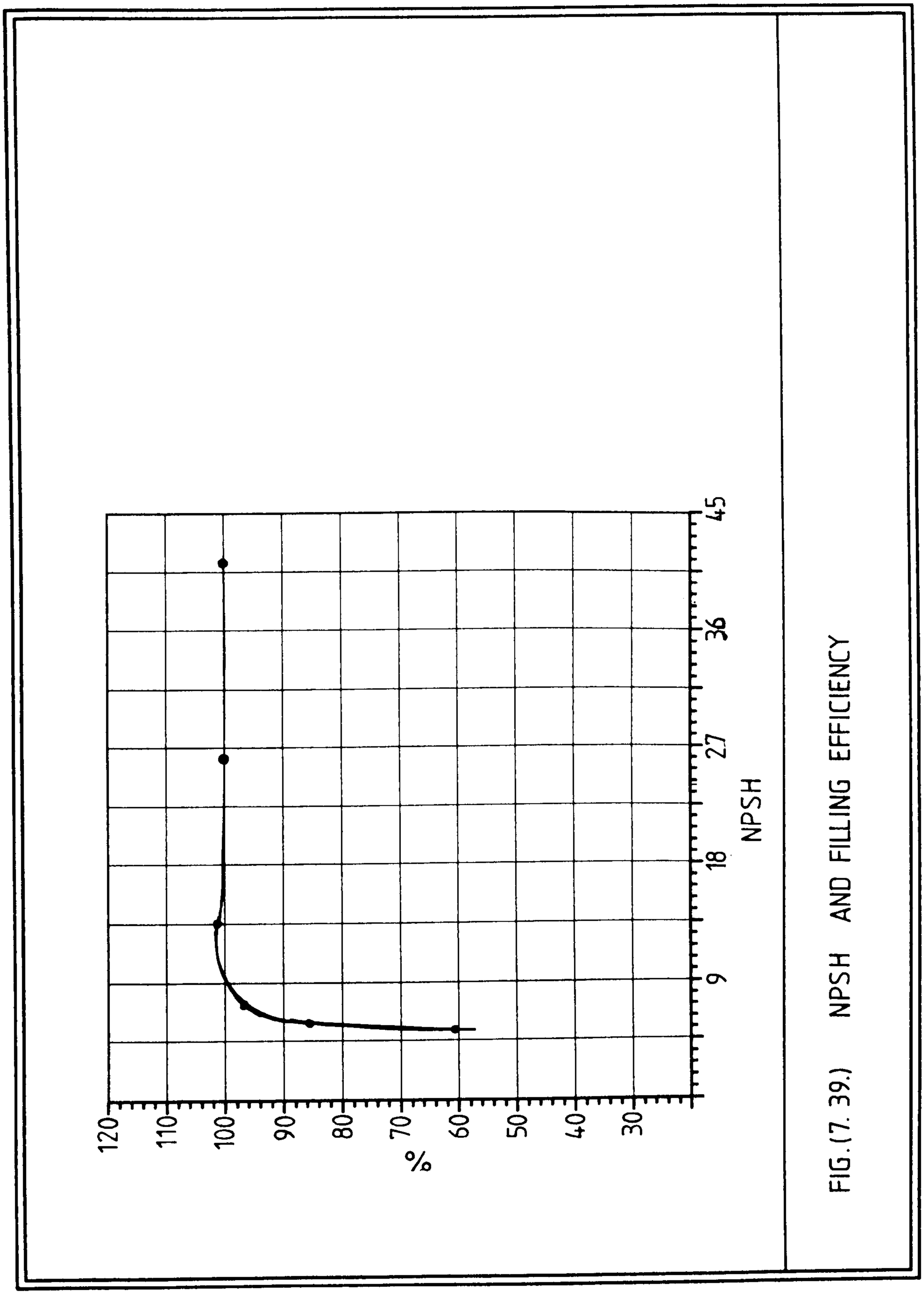

FIG.(7. 39.) NPSH AND FILLING EFFICIENCY

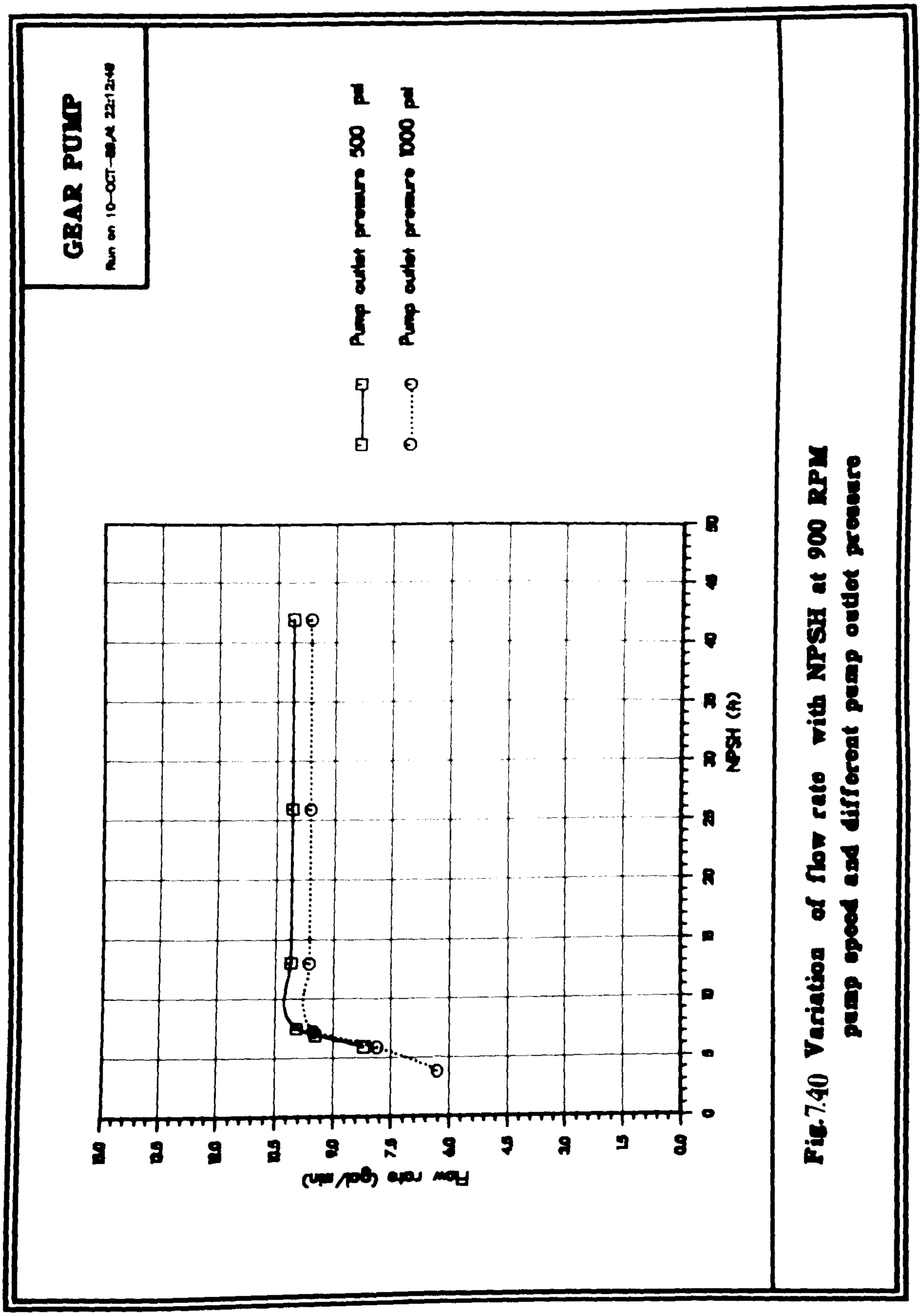

Fig.7.40 Variation of flow rate with NPSH at 900 RPM pump speed and different pump outlet pressure

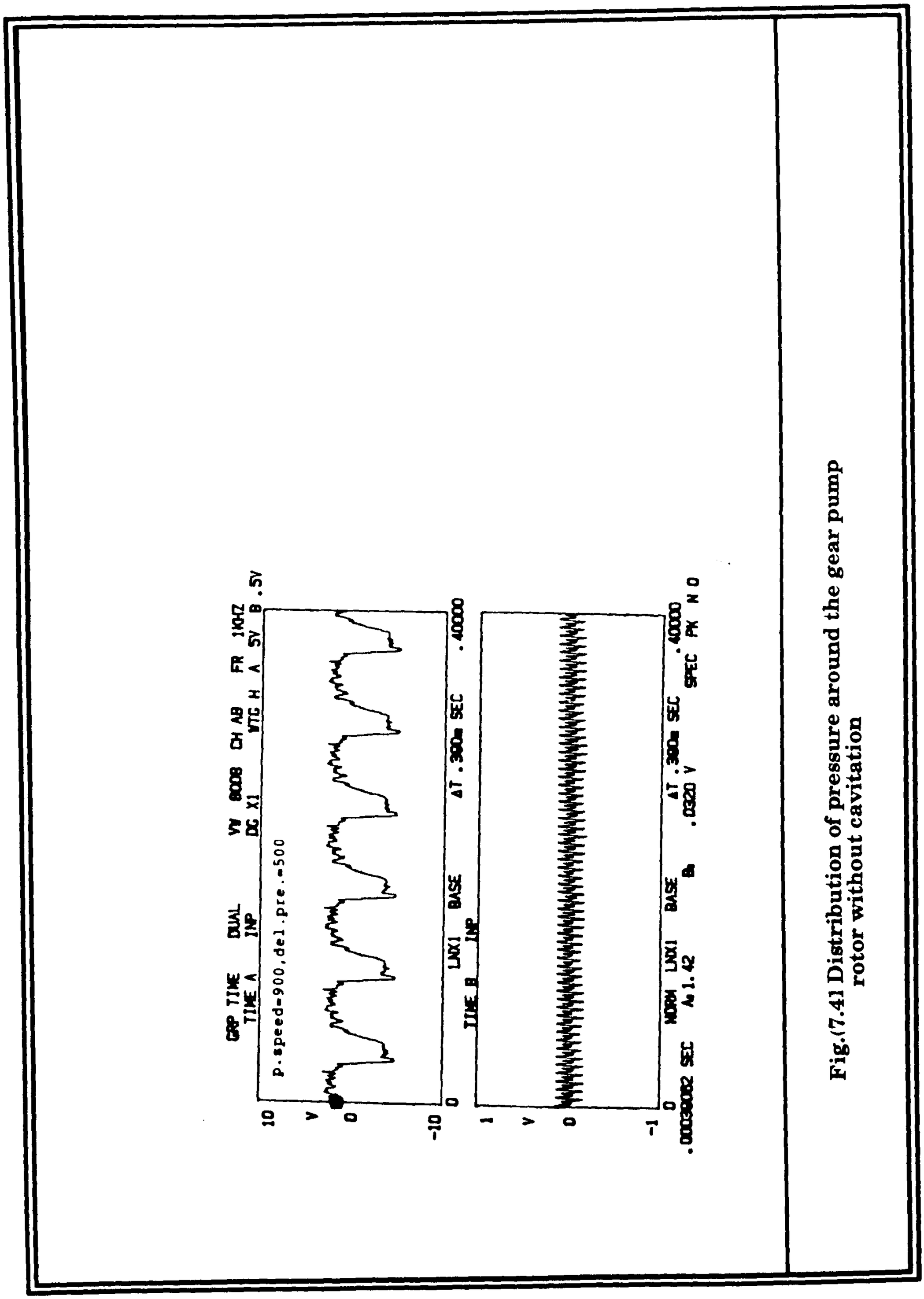

Fig.(7.41 Distribution of pressure around the gear pump rotor without cavitation

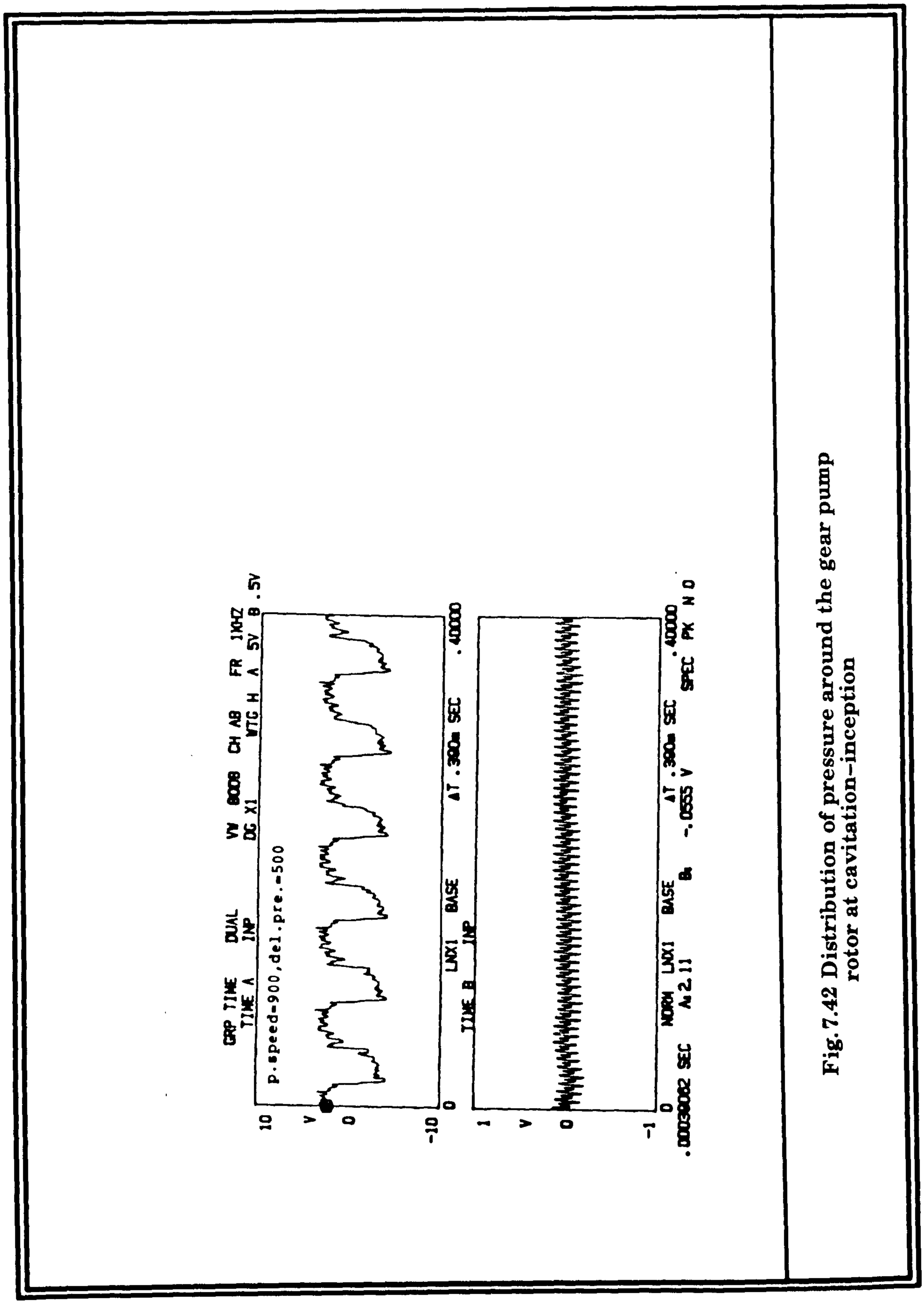

Fig. 7.42 Distribution of pressure around the gear pump rotor at cavitation–inception

ME945P

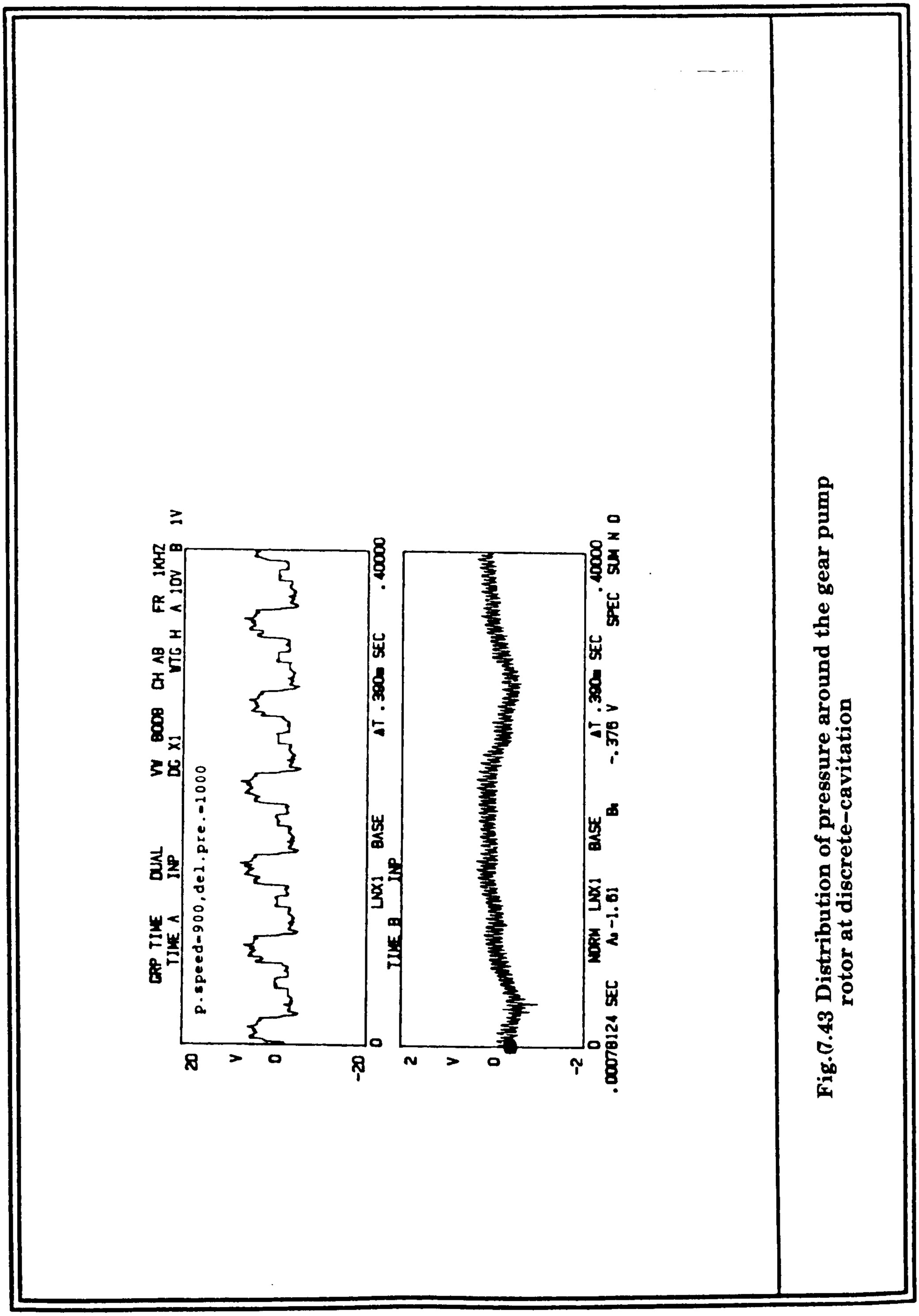

Fig.7.43 Distribution of pressure around the gear pump rotor at discrete-cavitation

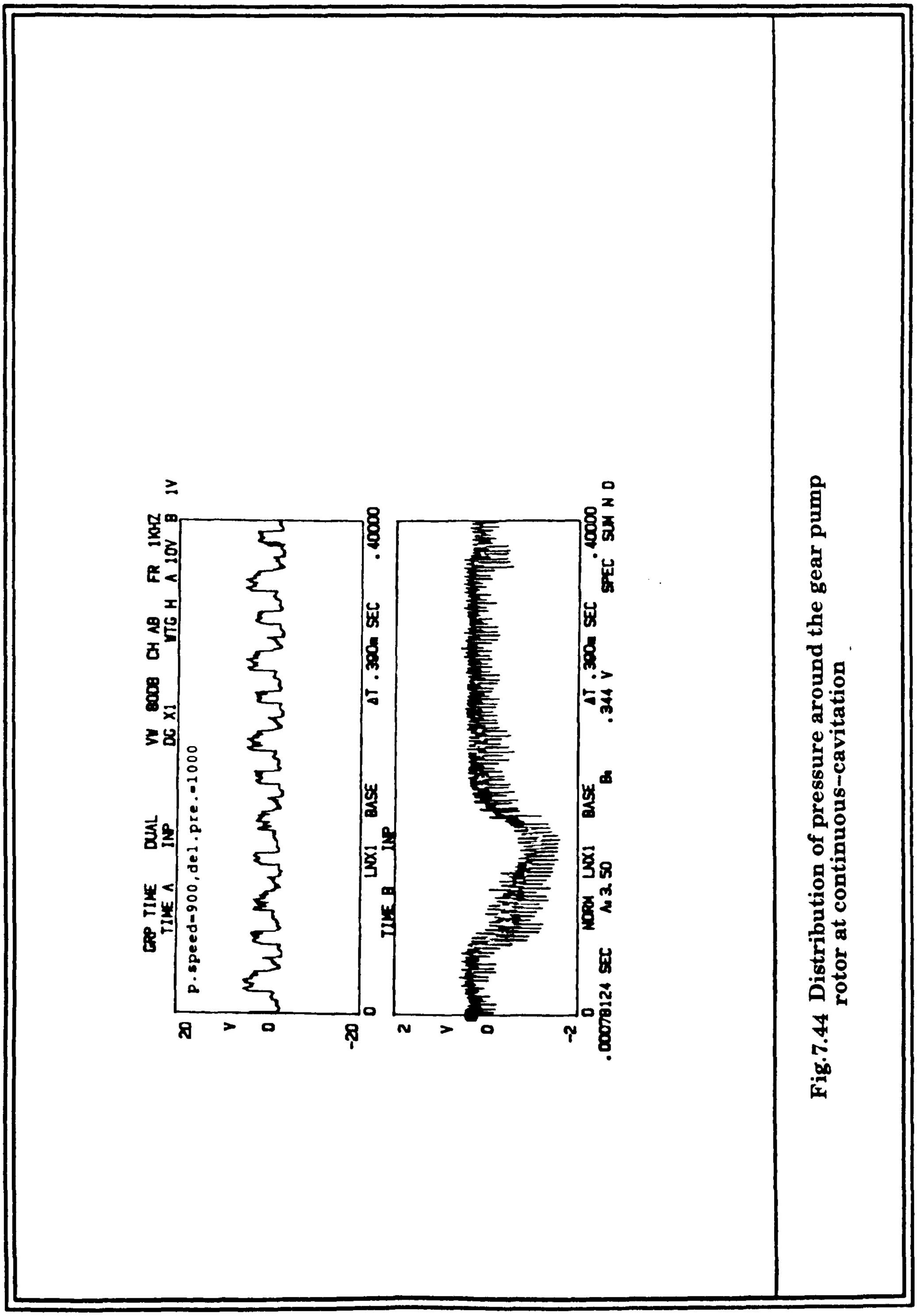

Fig.7.44 Distribution of pressure around the gear pump rotor at continuous-cavitation

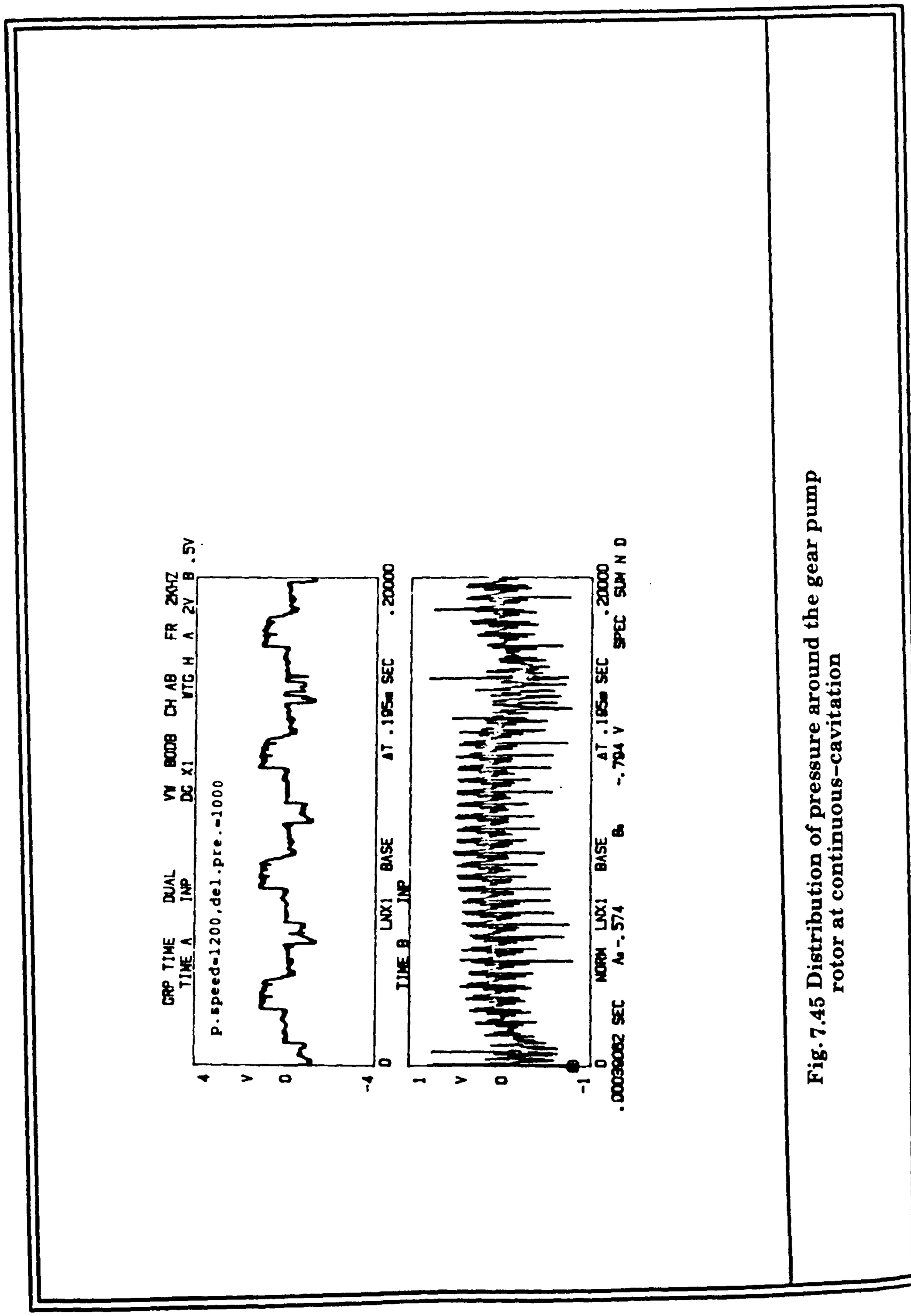

Fig. 7.45 Distribution of pressure around the gear pump rotor at continuous-cavitation

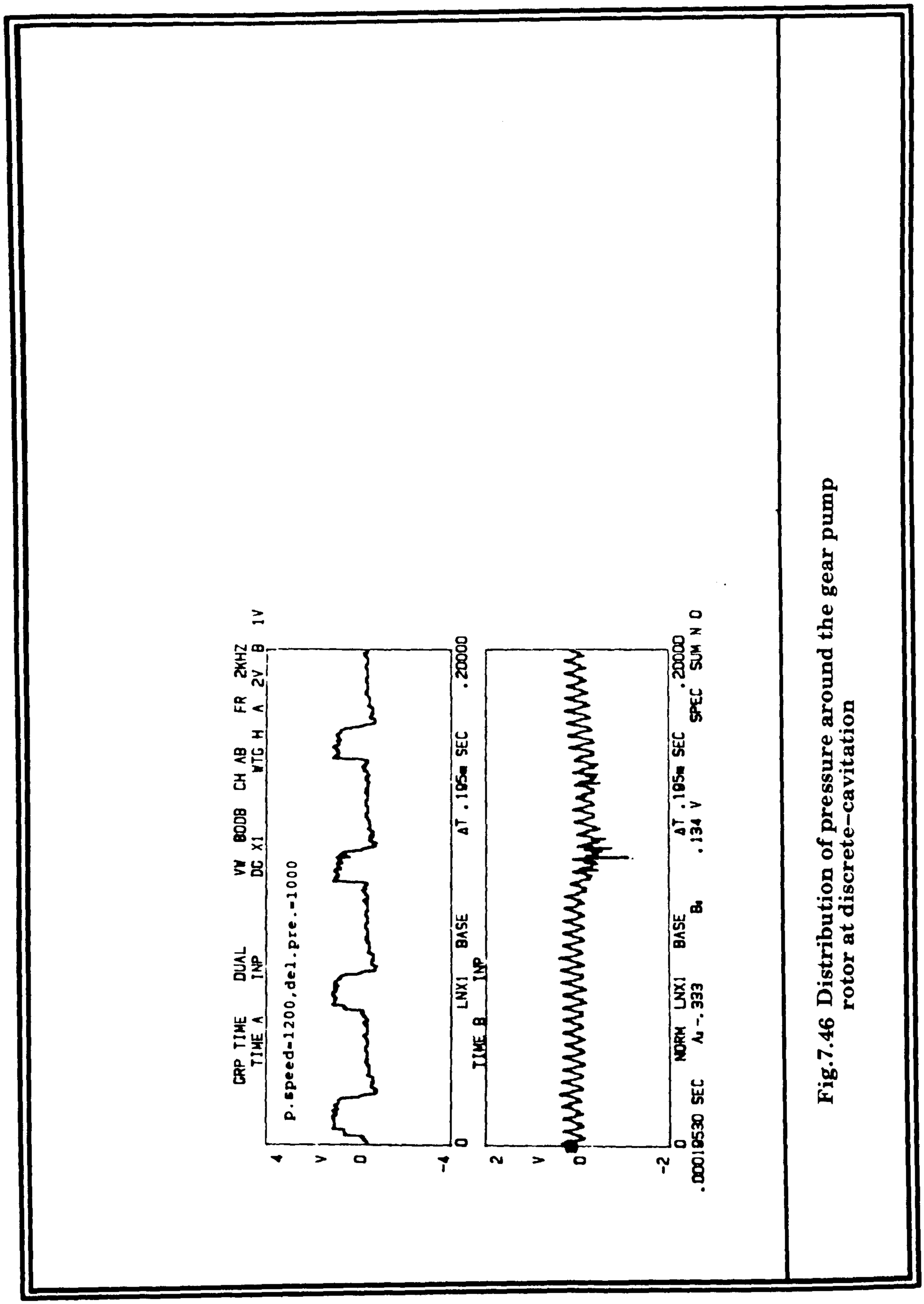

Fig.7.46 Distribution of pressure around the gear pump rotor at discrete-cavitation

ME945P

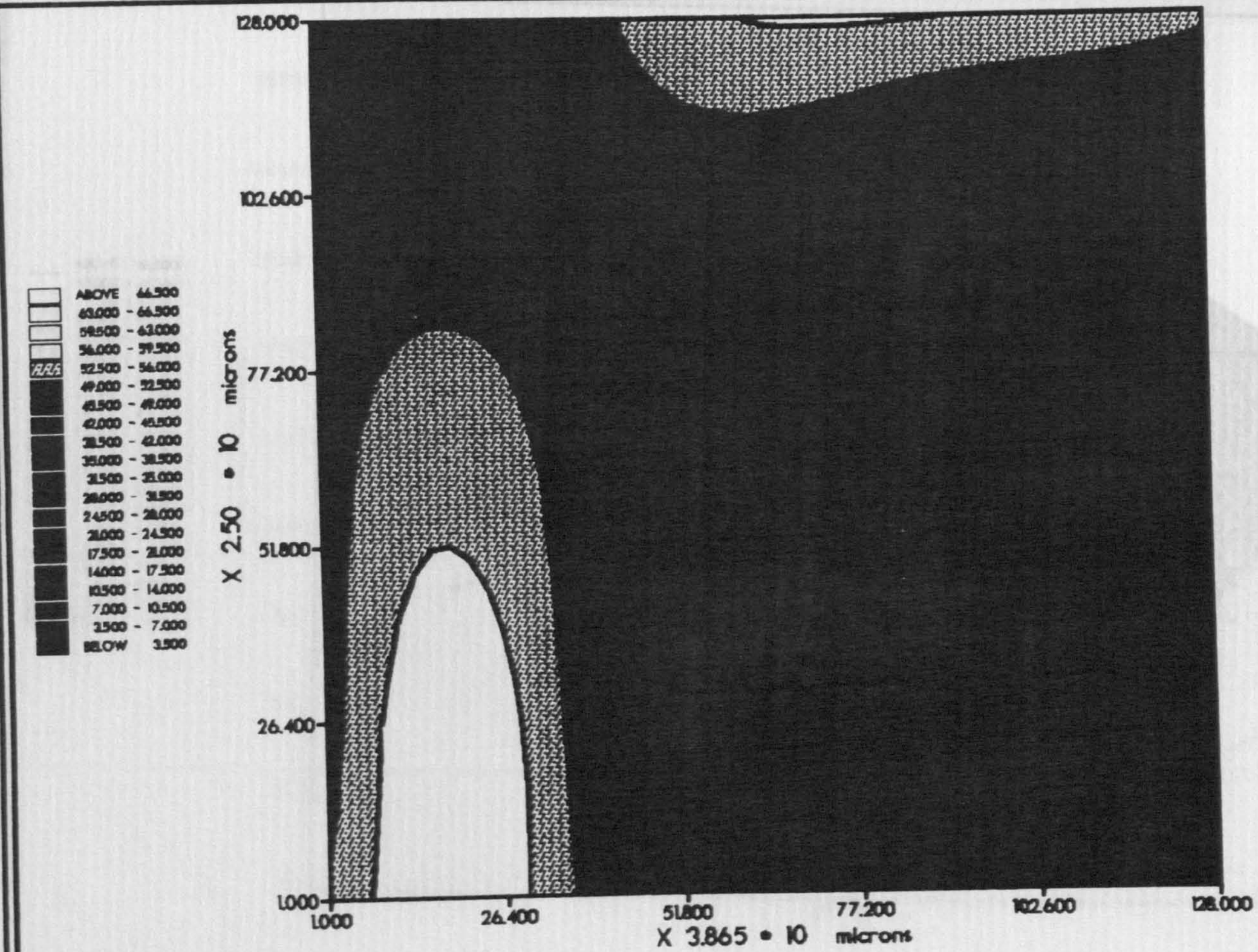

FIG(7.47) **CAVITATION EROSION**

SIDE PLATE

Run on 22-MAR-88, At 12:43:09

ME945P

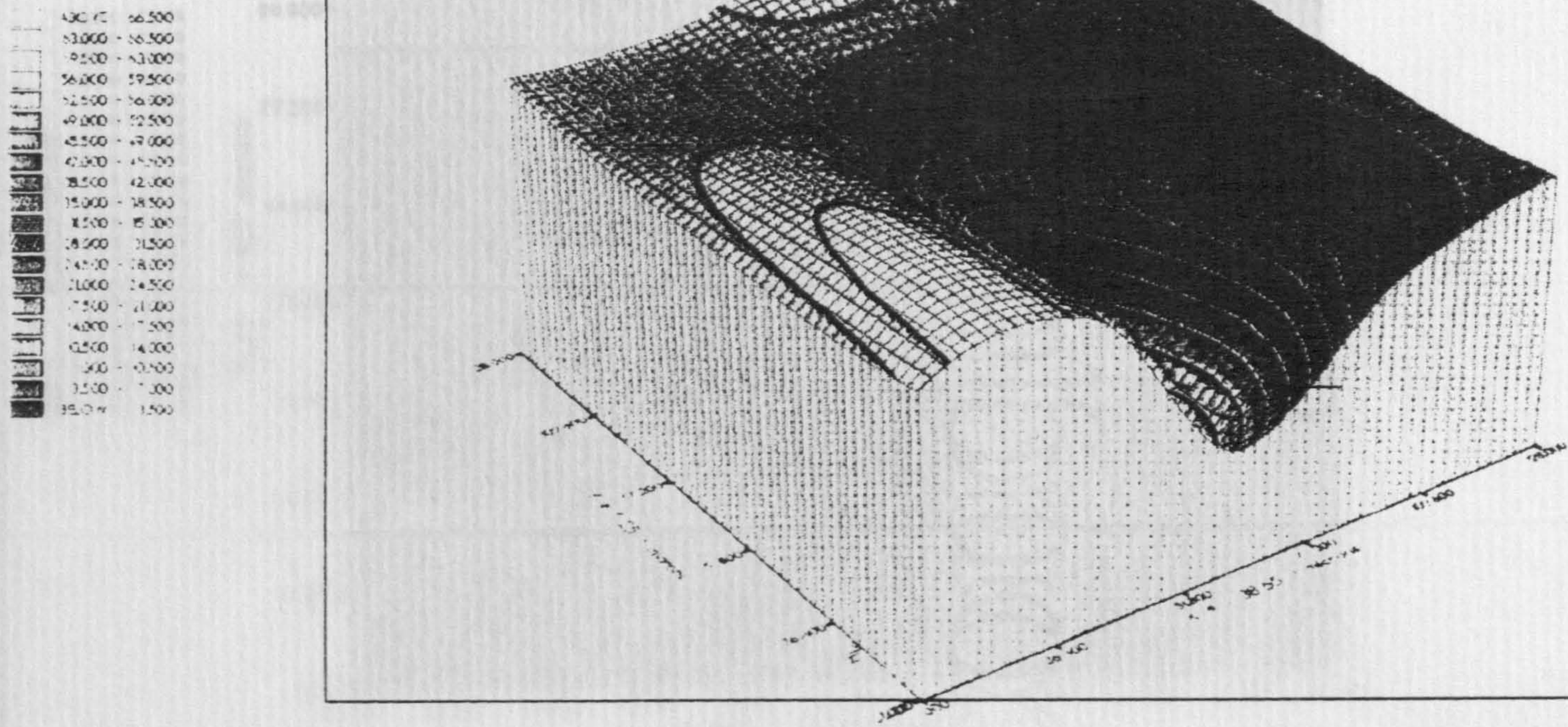

FIG 7.48 : CAVITATION EROSION ON THE SIDE PLATE
TACEM. DEP. (S.M.E.)

BY(K.H.A.L.)

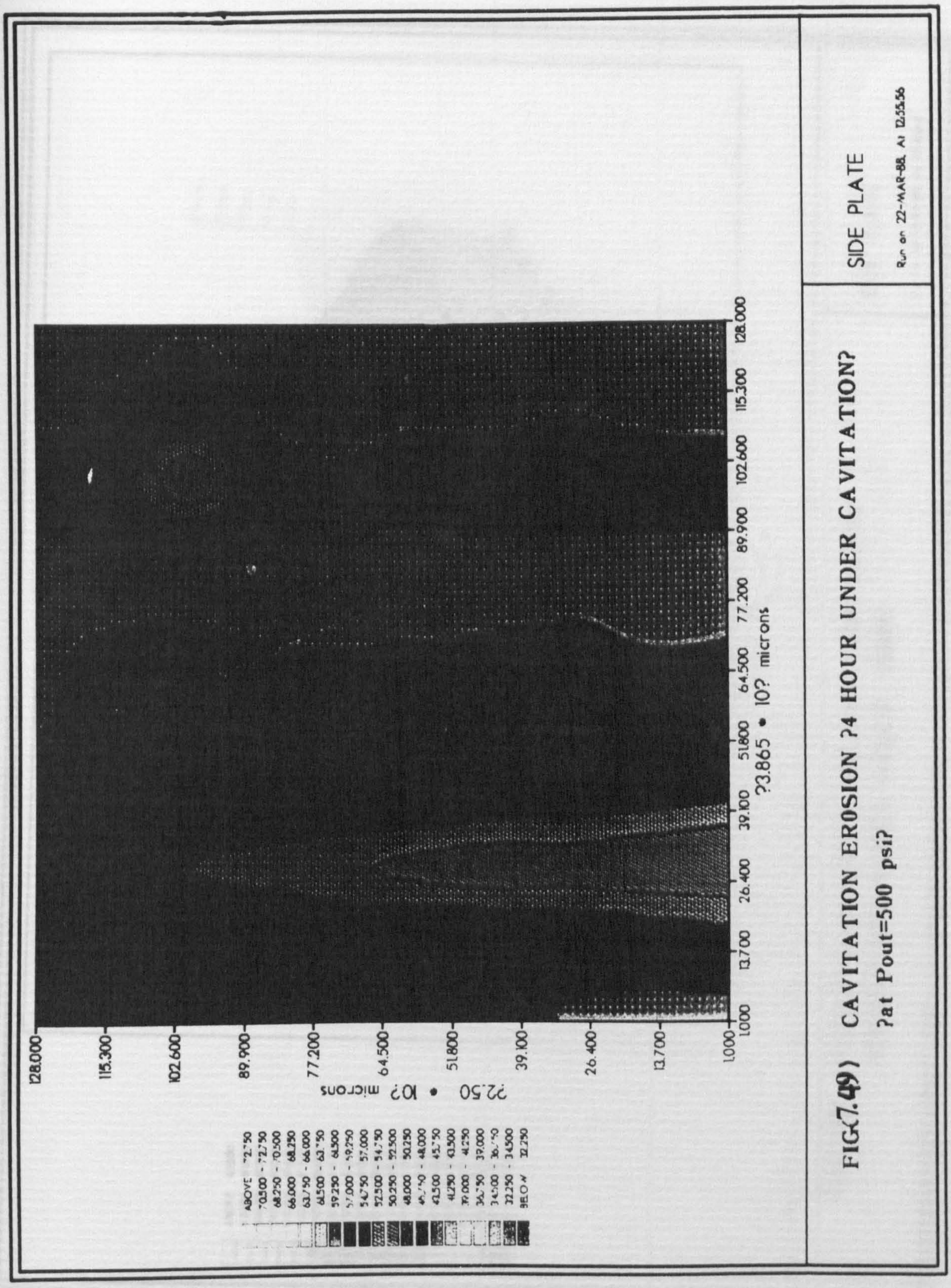

FIG(7.49) C
?at Pout=500 psi?

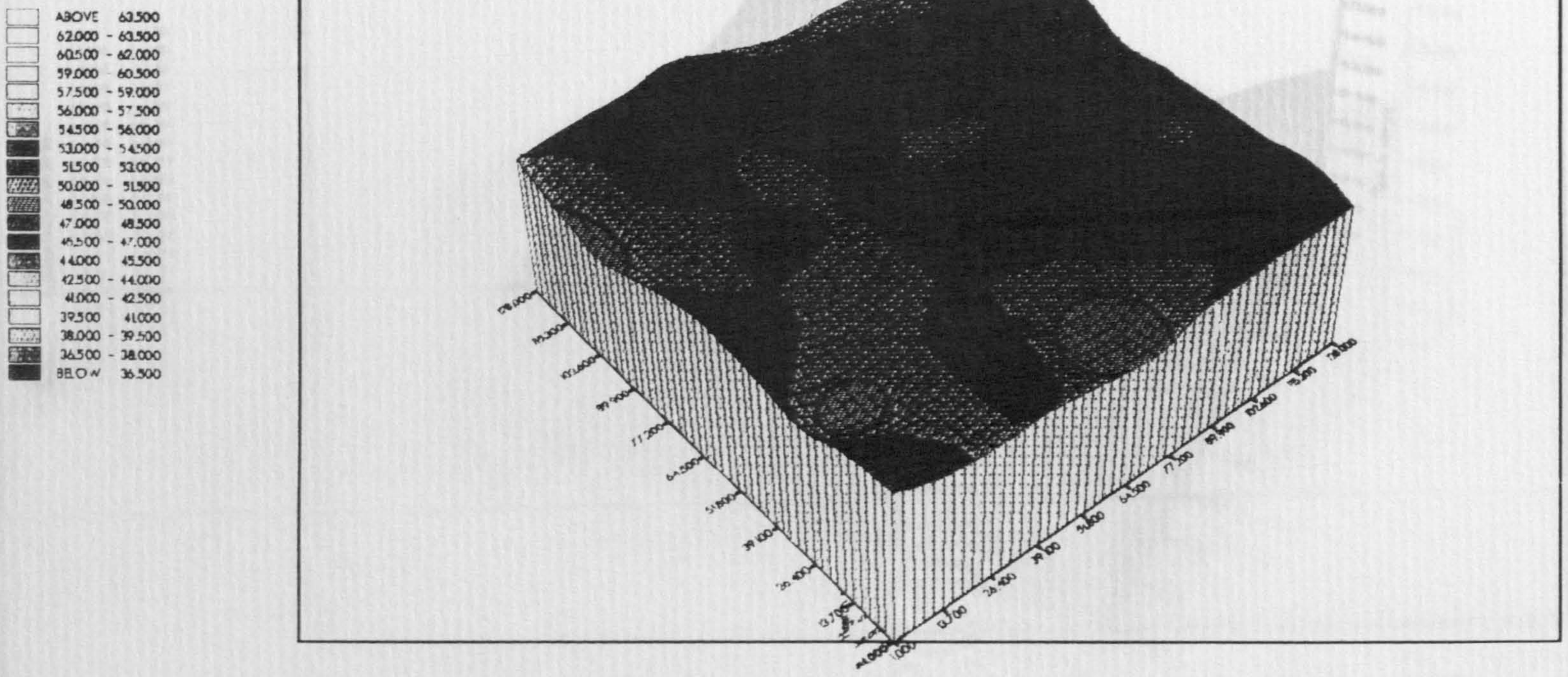

FIG(7.50) SURFACE ANALYSIS FOR NEW SIDE PLATE
APPLIED MECHANICS GROUP (SME)

SIDE PLATE

Run on 24-MAR-88, At 15:40:45

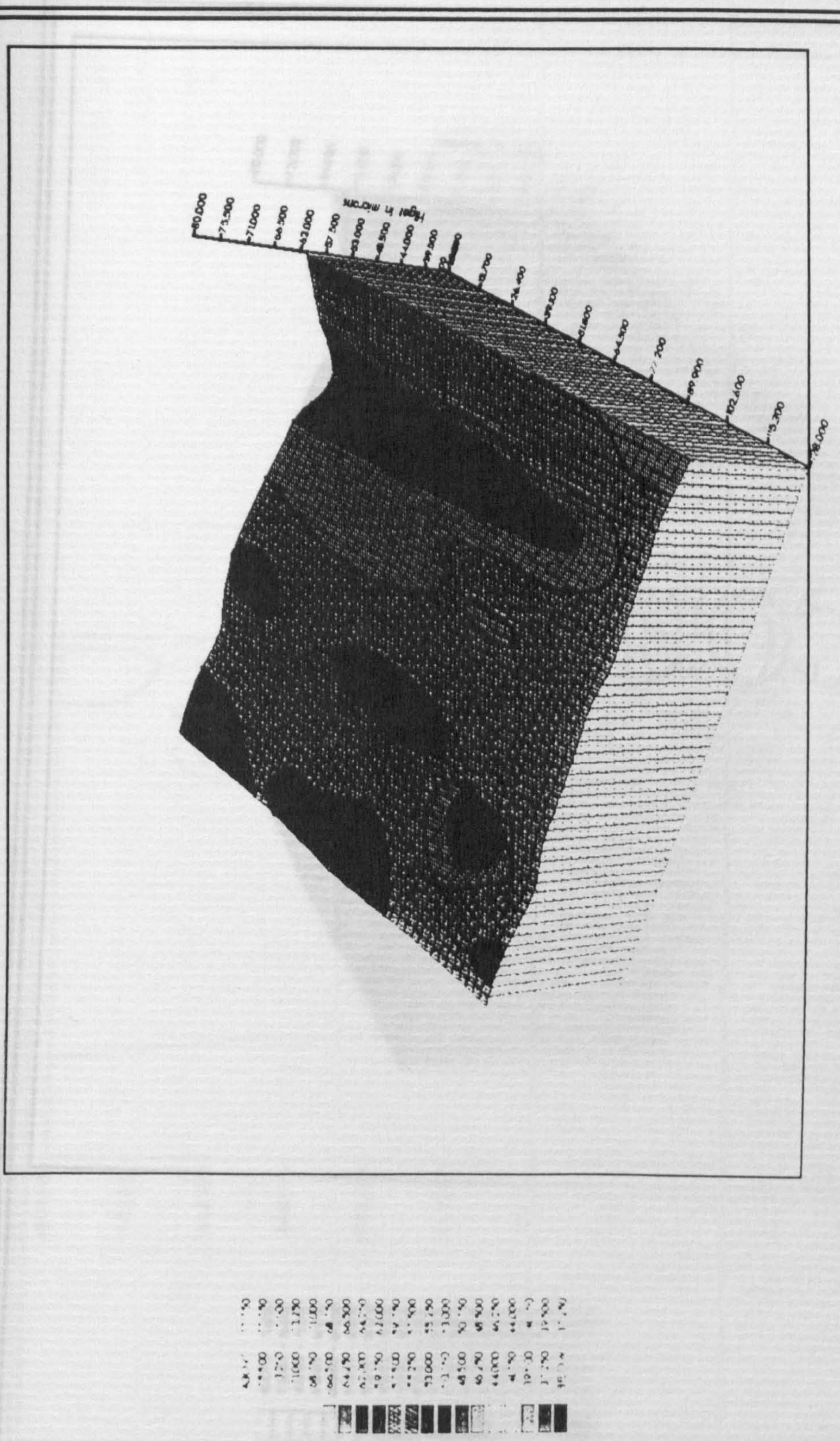

SIDE PLATE

Run on 24-MAR-88, A1 16x12.54

CAVITATION EROSION 1/4 HOUR UNDER CAVITATION)
(at Pout=500 psi) APPLIED MCH. GROUP (SME)

FIG 7.51

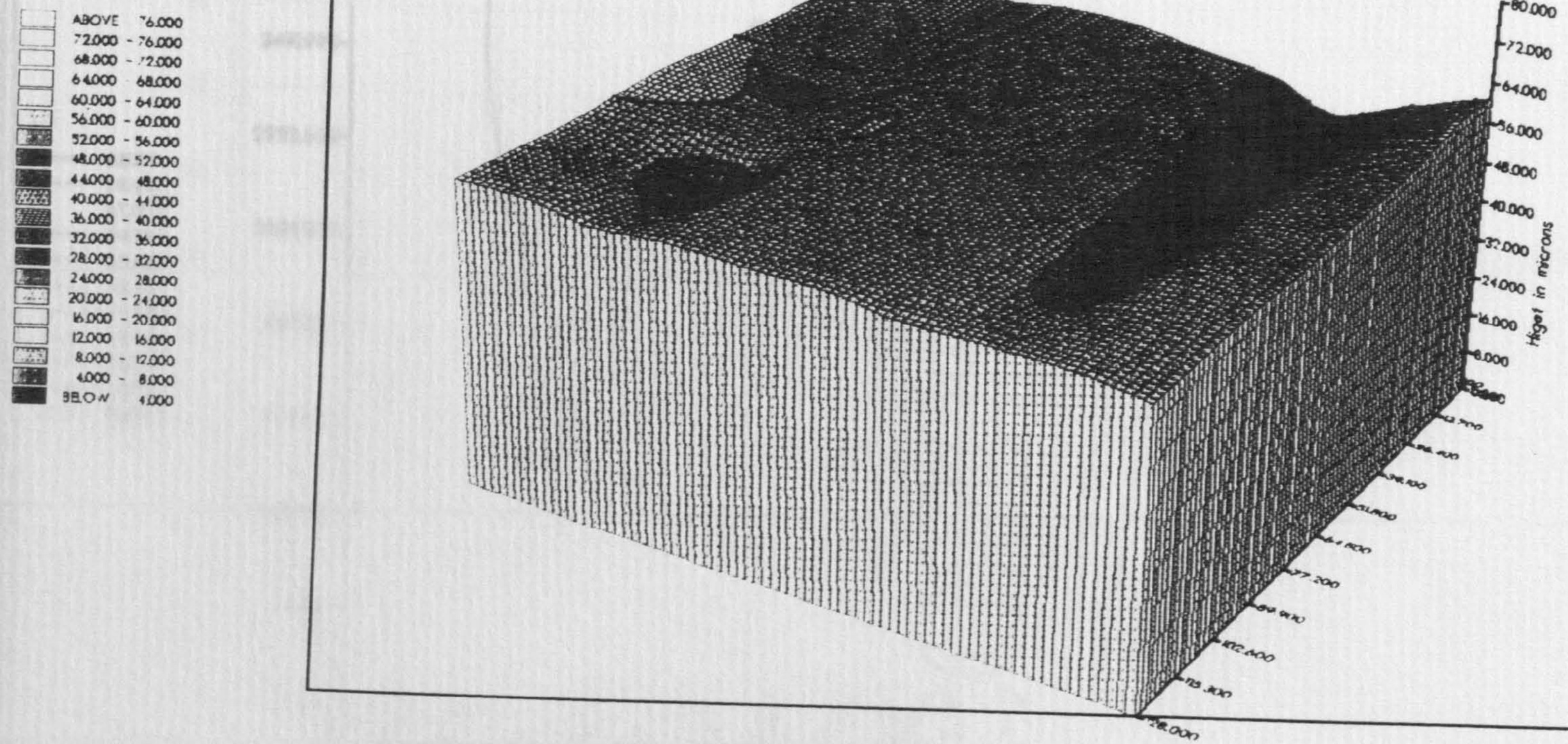

FIG 7.52 **CAVITATION EROSION (4 HOUR UNDER CAVITATION)**
(at Pout=500 psi) APPLIED MCH. GROUP (SME)

SIDE PLATE

Run on 20-APR-88 At 13:00:43

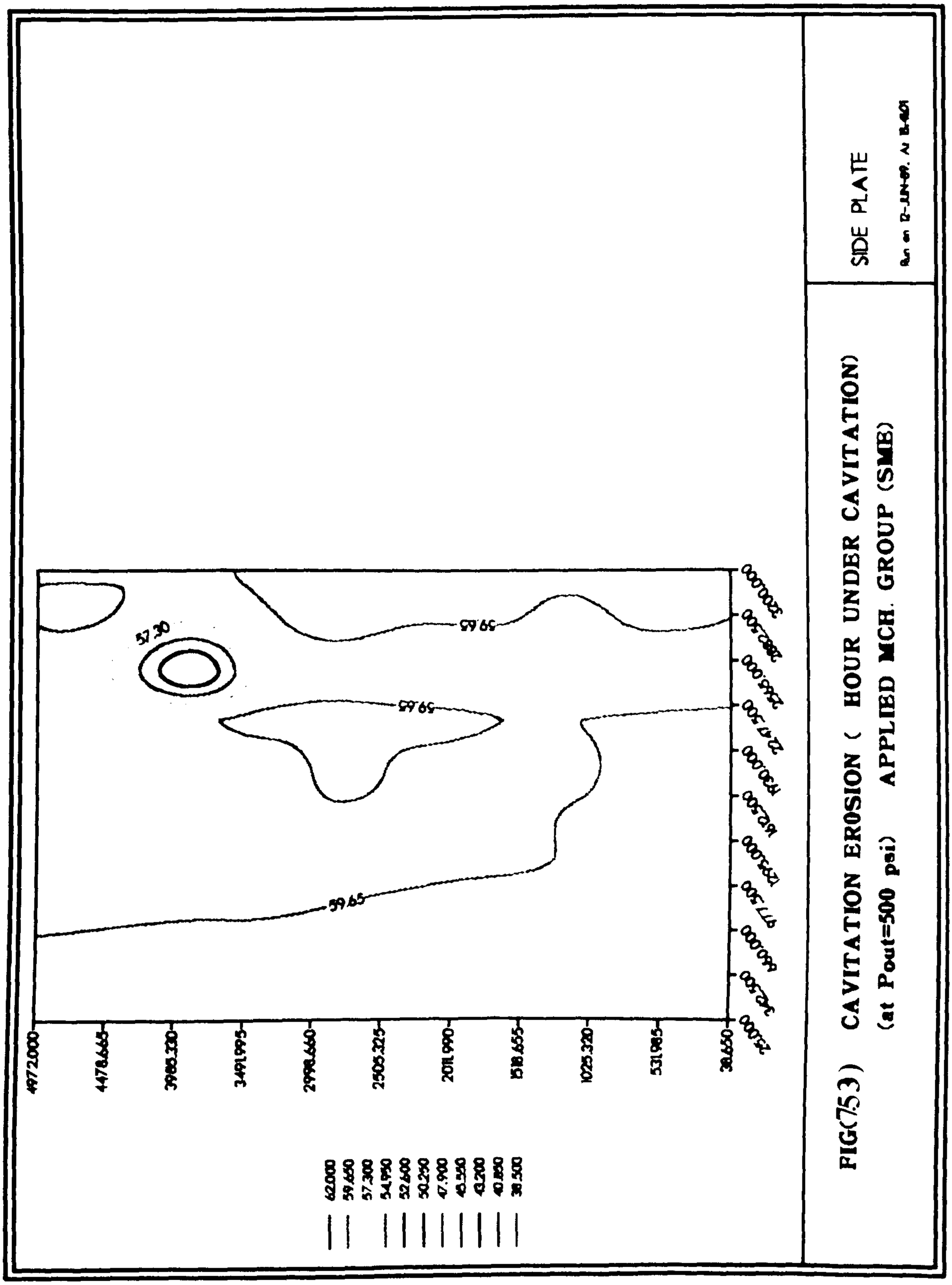

FIG(753) CAVITATION EROSION (HOUR UNDER CAVITATION)
(at Pout=500 psi) APPLIED MCH. GROUP (SMB)

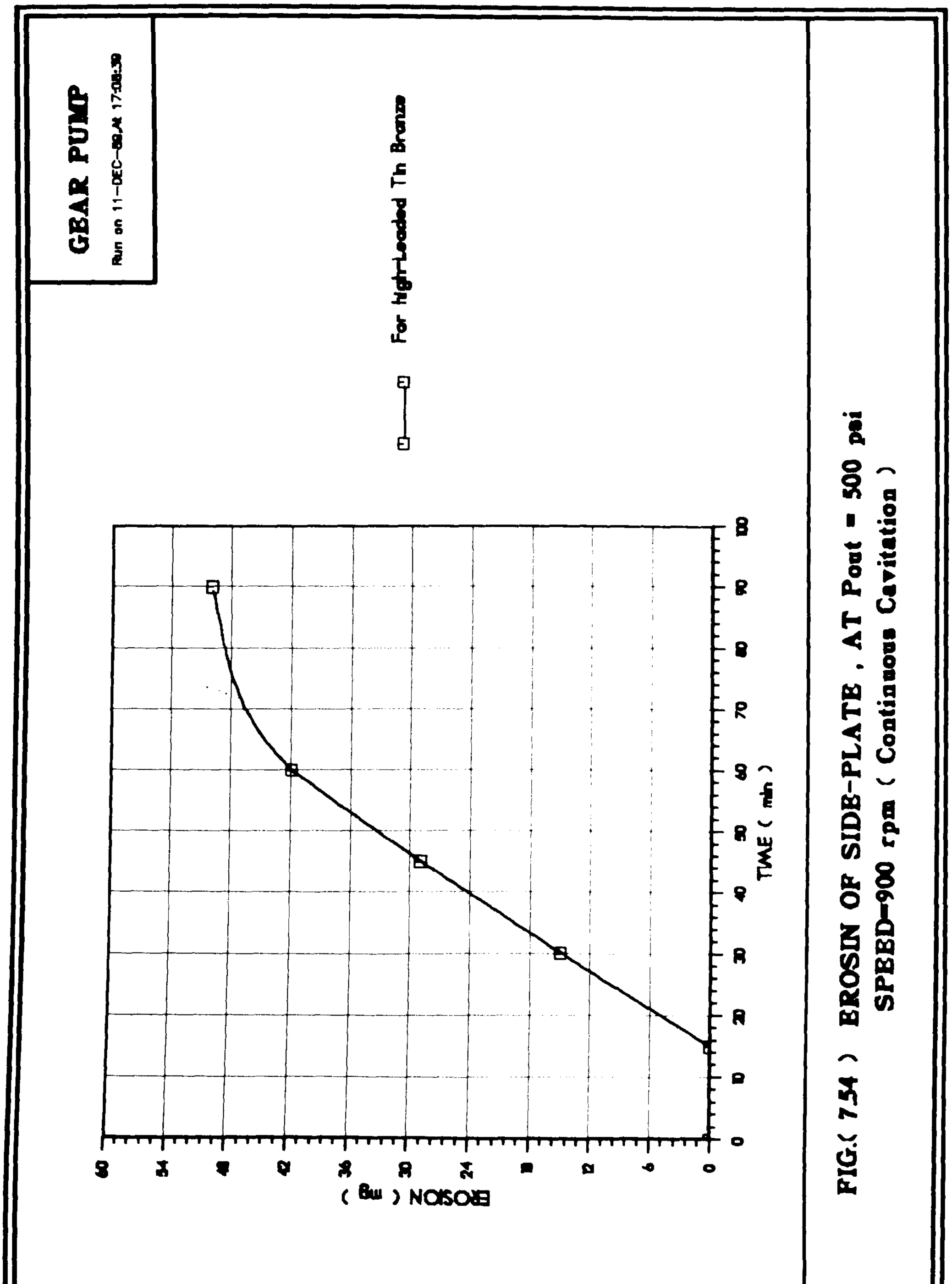

FIG.(7.54) EROSIN OF SIDE-PLATE , AT Pout = 500 psi
SPBBD-900 rpm (Continuous Cavitation)

CHAPTER EIGHT

CONCLUSIONS

It is clear that the major objective of this work has been achieved. A test rig has been designed and built using a new technique for cavitation detection which has proved to be capable of performing a variety of cavitation experiments efficiently.

The theoretical equations describing the ideal discharge flowrate of involute profile external gear pumps with spur gears have been clarified and become well established.

The leakage inside the gear pump has carefully been studied and due to the absence of complete measurements of the tip losses, an analytical expression for the losses efficiency, η_L, considering tip leakage and drag force has been presented in a way which is useful for the calculation of the optimum design of gear pumps as a function of the gear operating conditions and gear tip clearances.

A full investigation of the effect of the trapped oil on the pressure generated in the inter-tooth spaces, has been carried out for the first time through the derivation of an expression to calculate the pressure in terms of gear geometry and operating conditions and it gives good results compared with published work.

Computer programs capable of designing and modelling the performance of gear pumps has been developed and they provide a simple and quick way of obtaining the optimum design of a gear pump for a specified service.

It is clear from the experimental investigation that three types of cavitation can be observed; one at the teeth of meshing gear due to trapped pressure, the second between a tooth and casing due to high shear stress in the oil film, the third being the inlet cavitation at which the released dissolved gas and vapour accumulate at the tooth space cavity in the form of bubbles, concentrated at the root of the teeth due to centrifugal effects. The last type of cavitation occurs in three stages, first cavitation inception which allows the pressure

ripple to modulate by frequency approximately equal to the frequency of the main pump shaft and no collapse can be reported. The second stage is the discrete-cavitation at which a bubble collapse may be observed in one or two pressure ripples and the rest of the ripples are not disturbed. The last stage is the stage of continuous-cavitation when the cavitation can be seen in the whole pressure ripple. This can be detected from the time domain of the pressure signal. As the output pressure increases, the leakage towards the suction side increases resulting in a delay to cavitation occurrence but with the increase of pump speed the cavitation appearance in the pump may be accelerated.

These three stages of cavitation were investigated by means of the pressure distribution around the rotor, and the failure of the filling efficiency of the tooth space due to cavitation was monitored, and provided a reasonable explanation of the pump performance charateristics at different inlet conditions. The waveform of trapped pressure, which may cause damage to gear pump bearings due to its high frequency and amplitude, has also been detected.

It is clear that the surface analysis technique employed in this work has led to an accurate estimation for material erosion of the side plate due to cavitation, and the results obtained are in good agreement with those published by NEL.

Recommendations for Future Work

Although the present work provides a thorough investigation of cavitation phenomenon in gear pumps, it is advantageous if the following relevant areas of research could be investigated.

1. A study of the effect of excentricity on the pressure build up around the gear rotor.

2. A theoretical modelling of cavitation fluid borne noise in terms of frequency and amplitude using fast Fourier technique.

3. A flow visualisation study for the cavitation bubble behaviour inside the tooth space.

4. The effect of pressure delivery and speed on the cavitation erosion rate in gear pumps.